14

DC/DC Conversion Technique and Twelve Series Luo-converters

Fang Lin Luo, Ph.D.
School of EEE, Block S1, Nanyang Technological University, Nanyang Avenue, Singapore

Hong Ye, Ph.D.
School of Biological Sciences, Block SBS, Nanyang Technological University, Nanyang Avenue, Singapore

14.1 Introduction

DC/DC converters are widely used in industrial applications and computer hardware circuits. DC/DC conversion technique has been developed very quickly. Since 1920s there have been more than 500 DC/DC converters' topologies developed. Professor Luo and Dr. Ye have systematically sorted them in six generations in 2001. They are the first-generation (classical) converters, second-generation (multi-quadrant) converters, third-generation (switched-component) converters, fourth-generation (soft-switching) converters, fifth-generation (synchronous-rectifier) converters and sixth-generation (multi-element resonant power) converters.

The first-generation converters perform in a single quadrant mode with low power range (up to around 100 W), such as buck converter, boost converter and buck–boost converter. Because of the effects of parasitic elements, the output voltage and power transfer efficiency of all these converters are restricted.

The voltage-lift (VL) technique is a popular method that is widely applied in electronic circuit design. Applying this technique effectively overcomes the effects of parasitic elements and greatly increases the output voltage. Therefore, these DC/DC converters can convert the source voltage into a higher output voltage with high power efficiency, high power density, and a simple structure.

The VL converters have high voltage transfer gains, which increase in arithmetical series stage-by-stage. Super-lift (SL) technique is more powerful to increase the converters voltage transfer gains in geometric series stage-by-stage. Even higher, ultra-lift (UL) technique is most powerful to increase the converters voltage transfer gain.

The second-generation converters perform in two- or four-quadrant operation with medium output power range (say hundreds watts or higher). Because of high power conversion, these converters are usually applied in industrial applications with high power transmission. For example, DC motor drives with multi-quadrant operation. Since most of second-generation converters are still made of capacitors and inductors, they are large.

The third-generation converters are called switched-component DC/DC converters, and made of either inductor or capacitors, which are so-called switched-inductor and switched-capacitors. They usually perform in two- or four-quadrant operation with high output power range (say thousands watts). Since they are made of only inductor or capacitors, they are small.

Switched-capacitor (SC) DC/DC converters are made of only switched-capacitors. Since switched-capacitors can be integrated into power semiconductor integrated circuits (IC) chips, they have limited size and work in high switching frequency. They have been successfully employed in the inductorless DC/DC converters and opened the way to build the converters with high power density. Therefore, they have drawn much attention from the research workers and manufacturers. However, most of these converters in the literature perform single-quadrant operation. Some of them work in the push–pull status. In addition, their control circuit and topologies are very complex, especially, for the large difference between input and output voltages.

Switched-inductor (SI) DC/DC converters are made of only inductor, and have been derived from four-quadrant choppers. They usually perform multi-quadrant operation with very simple structure. The significant advantage of these converters is its simplicity and high power density. No matter how large the difference between the input and output voltages, only one inductor is required for each SI DC/DC converter. Therefore, they are widely required for industrial applications.

The fourth-generation converters are called soft-switching converters. Soft-switching technique involves many methods implementing resonance characteristics. Popular method is resonant-switching. There are three main groups: zero-current-switching (ZCS), zero-voltage-switching (ZVS), and zero-transition (ZT) converters. They usually perform in single quadrant operation in the literature. We have developed this technique in two- and four-quadrant operation with high output power range (say thousands watts).

Multi-quadrant ZCS/ZVS/ZT converters implement ZCS/ZVS technique in four-quadrant operation. Since switches turn on and off at the moment that the current/voltage is equal to zero, the power losses during switching on and off become zero. Consequently, these converters have high power density and transfer efficiency. Usually, the repeating frequency is not very high and the converters work in a mono-resonance frequency, the components of higher order harmonics is very low. Using fast fourier transform (FFT) analysis, we obtain that the total harmonic distortion (THD) is very small. Therefore, the electromagnetic interference (EMI) is weaker, electromagnetic sensitivity (EMS) and electromagnetic compatibility (EMC) are reasonable.

The fifth-generation converters are called synchronous rectifier (SR) DC/DC Converters. Corresponding to the development of the microelectronics and computer science, the power supplies with low output voltage (5 V, 3.3 V, and $1.8 \sim 1.5$ V) and strong output current (30 A, 50 A, 100 A up to 200 A) are widely required in industrial applications and computer peripheral equipment. Traditional diode bridge rectifiers are not available for this requirement. Many prototypes of SR DC/DC converters with soft-switching technique have been developed. The SR DC/DC converters possess the technical feathers with very low voltage and strong current and high power transfer efficiency η (90%, 92% up to 95%) and high power density (22–25 W/in^3).

The sixth-generation converters are called multi-element resonant power converters (RPCs). There are eight topologies of 2-E RPC, 38 topologies of 3-E RPC, and 98 topologies of 4-E RPC. The RPCs have very high current transfer gain, purely harmonic waveform, low power losses and EMI since

they are working in resonant operation. Usually, the sixth-generation RPCs used in large power industrial applications with high output power range (say thousands watts).

The DC/DC converter family tree is shown in Fig. 14.1.

Professor F. L. Luo and Dr. H. Ye have devoted in the subject area of DC/DC conversion technique for a long time and harvested outstanding achievements. They have created **twelve** (12) series converters namely **Luo-converters** and more knowledge which are listed below:

Positive output Luo-converters;
Negative output Luo-converters;
Double output Luo-converters;
Positive/Negative output super-lift Luo-converters;
Ultra-lift Luo-converter;
Multiple-quadrant Luo-converters;
Switched capacitor multi-quadrant Luo-converters;
Multiple-lift push-pull switched-capacitor Luo-converters;
Switched-inductor multi-quadrant Luo-converters;
Multi-quadrant ZCS quasi-resonant Luo-converters;
Multi-quadrant ZVS quasi-resonant Luo-converters;
Synchronous-rectifier DC/DC Luo-converters;
Multi-element resonant power converters;
Energy factor and mathematical modeling for power DC/DC converters.

All of their research achievements have been published in the international top-journals and conferences. Many experts, including Prof. Rashid of West Florida University, Prof. Kassakian of MIT, and Prof. Rahman of Memorial University of Newfoundland are very interested in their work, and acknowledged their outstanding achievements.

In this handbook, we only show the circuit diagram and list a few parameters of each converter for readers, such as the output voltage and current, voltage transfer gain and output voltage variation ratio, and the discontinuous condition and output voltage.

After a well discussion of steady-state operation, we prepare one section to investigate the dynamic transient process of DC/DC converters. Energy storage in DC/DC converters have been paid attention long time ago, but it was not well investigated and defined. Professor Fang Lin Luo and Dr. Hong Ye have theoretically defined it and introduced new parameters: energy factor (*EF*) and other variables. They have also fundamentally established the mathematical modeling and discussed the characteristics of all power DC/DC converters. They have successfully solved the traditional problems.

In this chapter, the input voltage is V_I or V_1 and load voltage is V_O or V_2. Pulse width modulated (PWM) pulse train has repeating frequency f, the repeating period is $T = 1/f$. Conduction duty is k, the switching-on period is kT, and switching-off period is $(1 - k)T$. All average values are in capital letter, and instantaneous values in small letter, e.g. V_1 and $v_1(t)$ or v_1. The variation ratio of the free-wheeling diode's current is ζ. Voltage transfer gain is M and power transfer efficiency is η.

14.2 Fundamental, Developed, Transformer-type, and Self-lift Converters

The first-generation converters are called classical converters which perform in a single-quadrant mode and in low. Historically, the development of the first generation converters covers very long time. Many prototypes of these converters have been created. We can sort them in six categories:

- Fundamental topologies: buck converter, boost converter, and buck–boost converter.
- Developed topologies: positive output Luo-converter, negative output Luo-converter, double output Luo-converter, Cúk-converter, and single-ended primary inductance converter (SEPIC).
- Transformer-type topologies: forward converter, push–pull converter, fly-back converter, half-bridge converter, bridge converter, and ZETA.
- Voltage-lift topologies: self-lift converters, positive output Luo-converters, negative output Luo-converters, double output Luo-converters.
- Super-lift topologies: positive/negative output super-lift Luo-converters, positive/negative output cascade boost-converters.
- Ultra-lift topologies: ultra-lift Luo-converter.

14.2.1 Fundamental Topologies

Buck converter is a step-down converter, which is shown in Fig. 14.2a, the equivalent circuits during switch-on and -off periods are shown in Figs. 14.2b and c. Its output voltage and output current are

$$V_2 = kV_1 \tag{14.1}$$

and

$$I_2 = \frac{1}{k} I_1 \tag{14.2}$$

This converter may work in discontinuous mode if the frequency f is small, conduction duty k is small, inductance L is small, and load current is high.

Boost converter is a step-up converter, which is shown in Fig. 14.3a, the equivalent circuits during switch-on and -off periods are shown in Figs. 14.3b and c. Its output voltage and current are

$$V_2 = \frac{1}{1 - k} V_1 \tag{14.3}$$

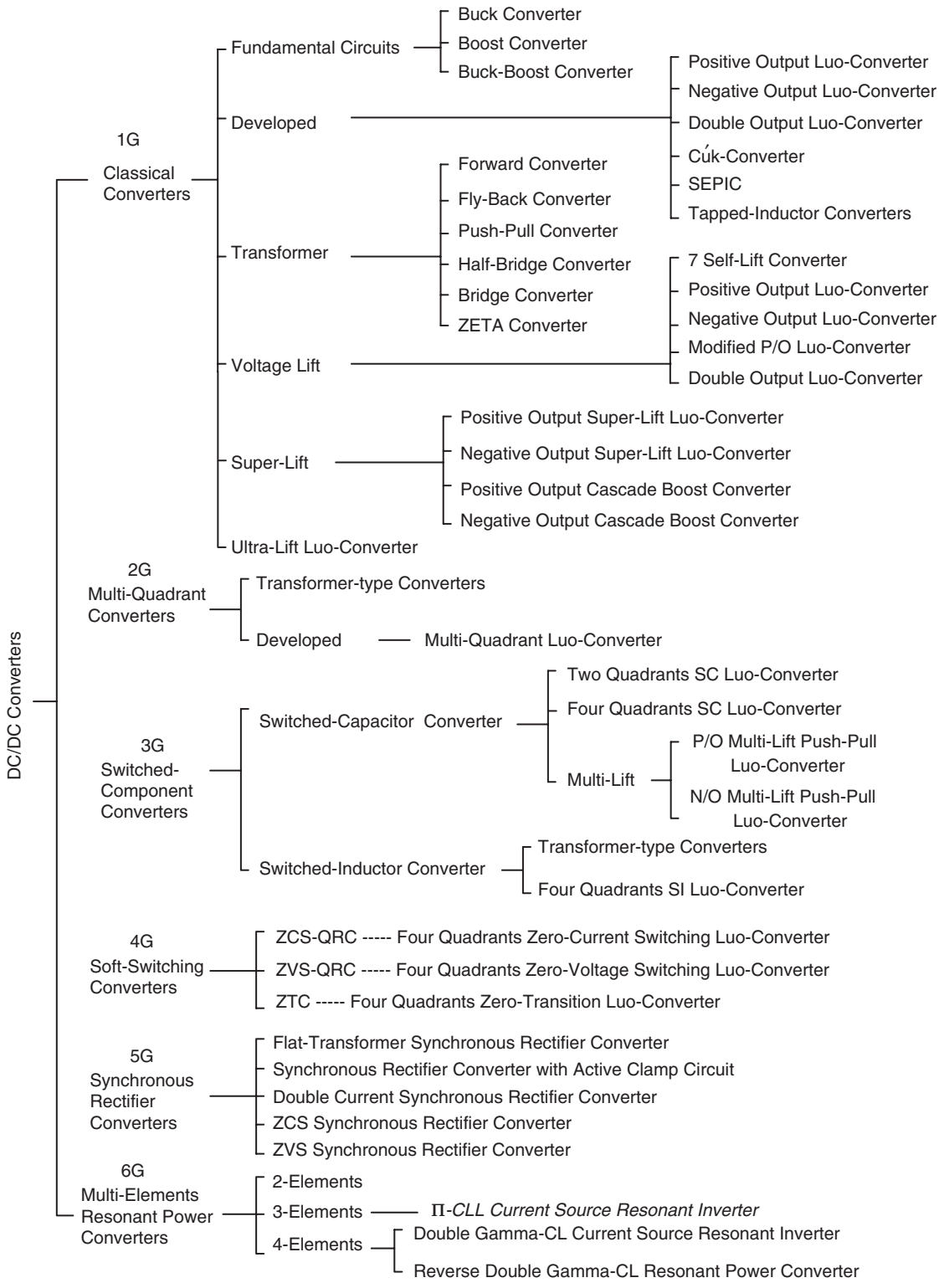

FIGURE 14.1 DC/DC converter family tree.

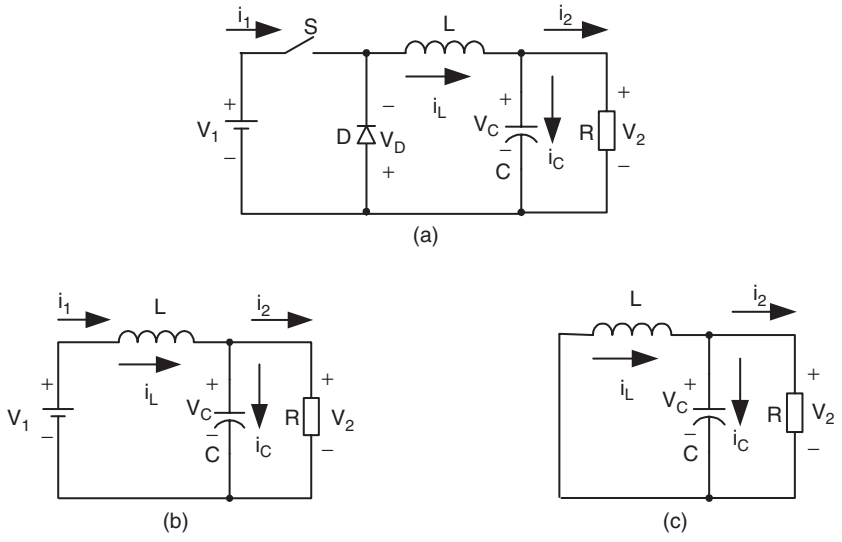

FIGURE 14.2 Buck converter: (a) circuit diagram; (b) switch-on equivalent circuit; and (c) switch-off equivalent circuit.

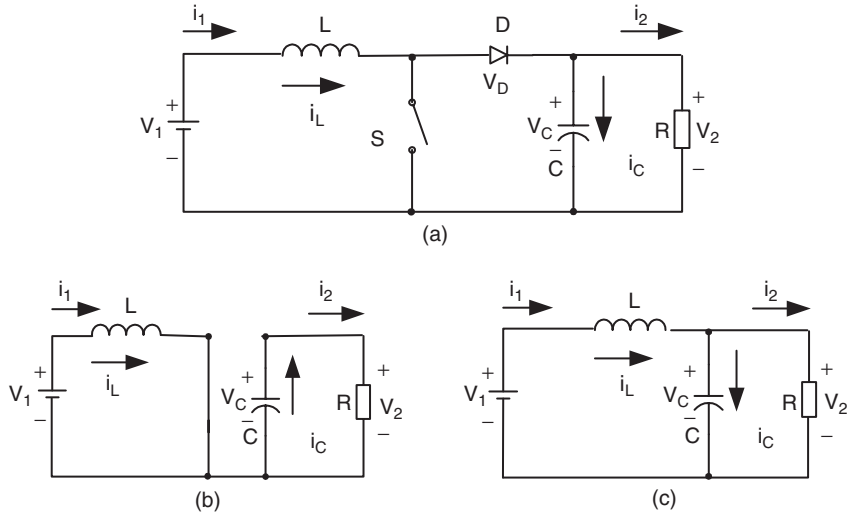

FIGURE 14.3 Boost converter: (a) circuit diagram; (b) switch-on equivalent circuit; and (c) switch-off equivalent circuit.

and

$$I_2 = (1 - k)I_1 \tag{14.4}$$

The output voltage is higher than the input voltage. This converter may work in discontinuous mode if the frequency f is small, conduction duty k is small, inductance L is small, and load current is high.

Buck–boost converter is a step–down/up converter, which is shown in Fig. 14.4a, the equivalent circuits during switch-on and -off periods are shown in Figs. 14.4b and c. Its output voltage and current are

$$V_2 = \frac{k}{1 - k} V_1 \tag{14.5}$$

and

$$I_2 = \frac{1 - k}{k} I_1 \tag{14.6}$$

When k is greater than 0.5, the output voltage can be higher than the input voltage. This converter may work in

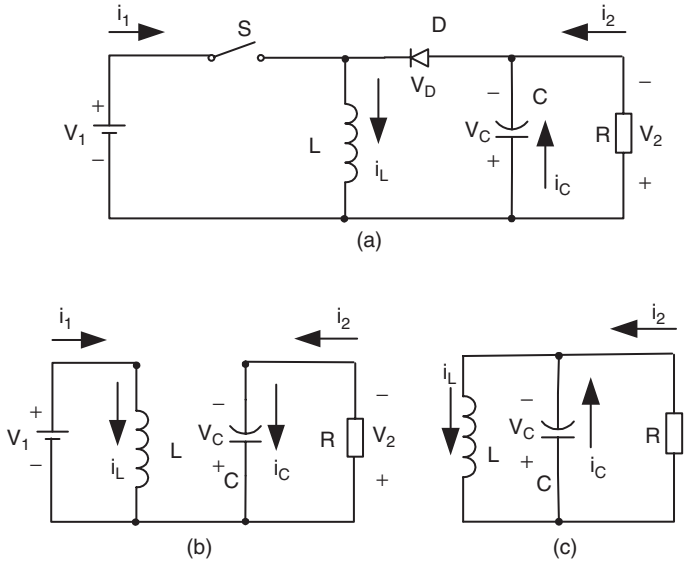

FIGURE 14.4 Buck-boost converter: (a) circuit diagram; (b) switch-on equivalent circuit; and (c) switch-off equivalent circuit.

discontinuous mode if the frequency f is small, conduction duty k is small, inductance L is small, and load current is high.

14.2.2 Developed Topologies

For convenient applications, all developed converters have output voltage and current as

$$V_2 = \frac{k}{1-k} V_1 \tag{14.7}$$

and

$$I_2 = \frac{1-k}{k} I_1 \tag{14.8}$$

Positive output (P/O) Luo-converter is a step-down/up converter, and is shown in Fig. 14.5. This converter may work in discontinuous mode if the frequency f is small, k is small, and inductance L is small.

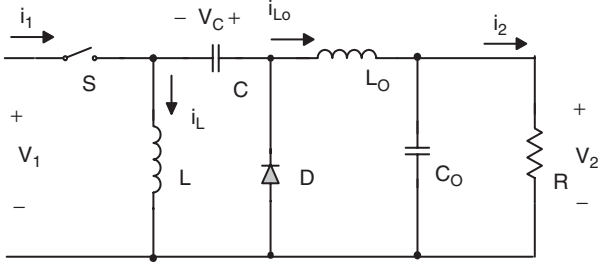

FIGURE 14.5 Positive output Luo-converter.

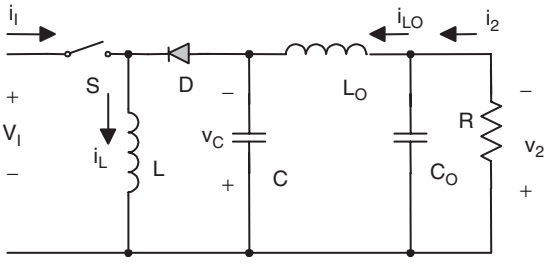

FIGURE 14.6 Negative output Luo-converter.

Negative output (N/O) Luo-converter is shown in Fig. 14.6. This converter may work in discontinuous mode if the frequency f is small, k is small, inductance L is small, and load current is high.

Double output Luo-converter is a double output step-down/up converter, which is derived from **P/O Luo-converter** and **N/O Luo-converter**. It has two conversion paths and two output voltages V_{O+} and V_{O-}. It is shown in Fig. 14.7. If the components are carefully selected the output voltages and currents (concentrate the absolute value) obtained are

$$V_2^+ = |V_2^-| = \frac{k}{1-k} V_1 \tag{14.9}$$

and

$$I_2^+ = \frac{1-k}{k} I_1^+ \quad \text{and} \quad I_2^- = \frac{1-k}{k} I_1^- \tag{14.10}$$

When k is greater than 0.5, the output voltage can be higher than the input voltage. This converter may work in discontinuous mode if the frequency f is small, k is small, inductance L is small, and load current is high.

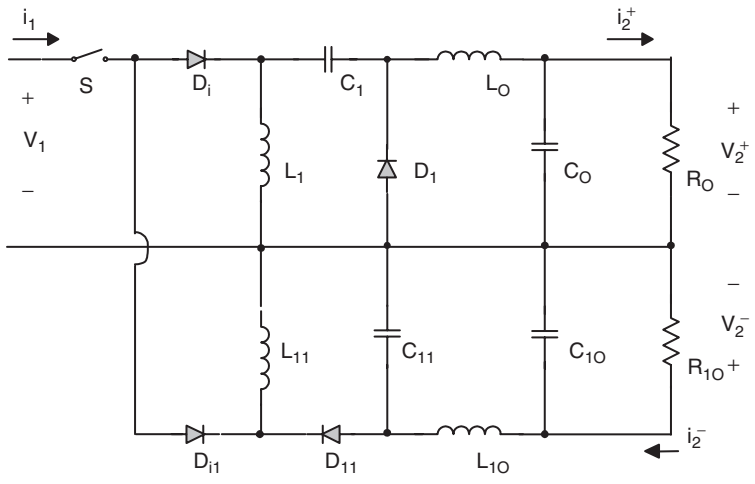

FIGURE 14.7 Double output Luo-converter.

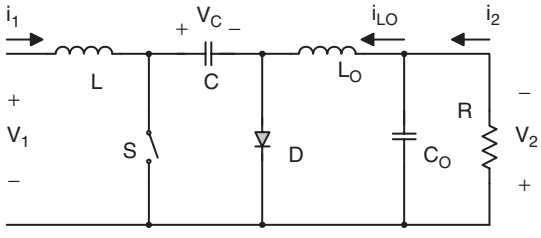

FIGURE 14.8 Cúk converter.

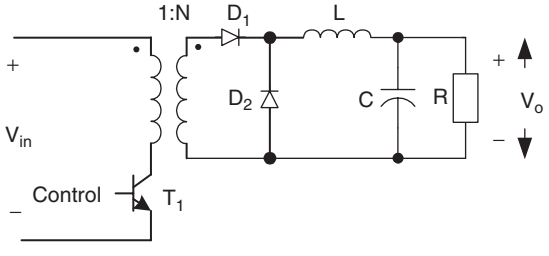

FIGURE 14.10 Forward converter.

Cúk-converter is a negative output step-down/up converter, which is derived from boost and buck converters. It is shown in Fig. 14.8.

Single-ended primary inductance converter is a positive output step-down/up converter, which is derived from boost converters. It is shown in Fig. 14.9.

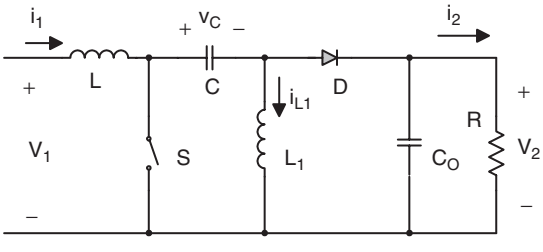

FIGURE 14.9 SEPIC.

14.2.3 Transformer-type Topologies

All transformer-type converters have transformer(s) to isolate the input and output voltages. Therefore, it is easy to obtain the high or low output voltage by changing the turns ratio N, the positive or negative polarity by changing the winding direction, and multiple output voltages by setting multiple secondary windings.

Forward converter is a step-up/down converter, which is shown in Fig. 14.10. The transformer turns ratio is N (usually $N > 1$). If the transformer has never been saturated during operation, it works as a buck converter. The output voltage and current are

$$V_O = kNV_I \tag{14.11}$$

and

$$I_O = \frac{1}{kN} I_I \tag{14.12}$$

This converter may work in discontinuous mode if the frequency f is small, conduction duty k is small, inductance L is small, and load current is high.

To avoid the saturation of transformer applied in forward converters, a tertiary winding is applied. The corresponding circuit diagram is shown in Fig. 14.11.

To obtain multiple output voltages we can set multiple secondary windings. The corresponding circuit diagram is shown in Fig. 14.12.

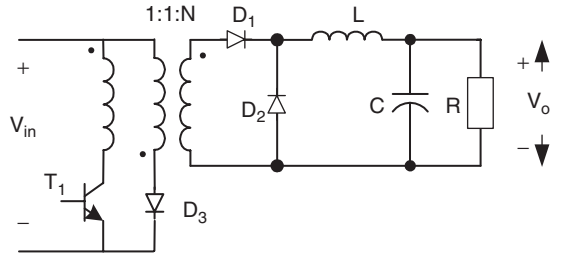

FIGURE 14.11 Forward converter with tertiary winding.

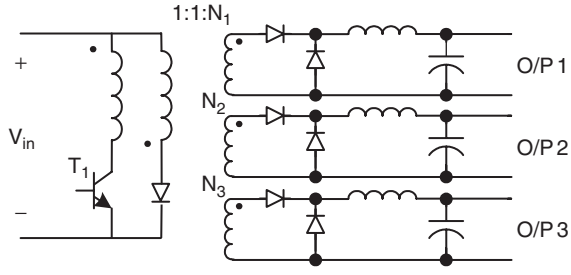

FIGURE 14.12 Forward converter with multiple secondary windings.

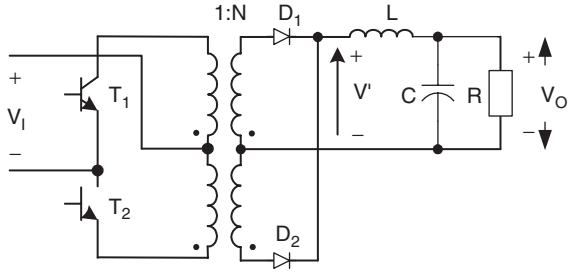

FIGURE 14.13 Push–pull converter.

Push–pull converter is a step-up/down converter, which is shown in Fig. 14.13. It is not necessary to set the tertiary winding. The transformer turns ratio is N (usually $N > 1$). If the transformer has never been saturated during operation, it works as a buck converter with the conduction duty cycle $k < 0.5$. The output voltage and current are

$$V_O = 2kNV_I \tag{14.13}$$

and

$$I_O = \frac{1}{2kN} I_I \tag{14.14}$$

This converter may work in discontinuous mode if the frequency f is small, conduction duty k is small, inductance L is small, and load current is high.

Fly-back converter is a high step-up converter, which is shown in Fig. 14.14. The transformer turns ratio is N (usually $N > 1$). It effectively uses the transformer leakage inductance

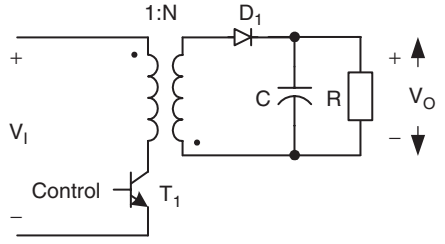

FIGURE 14.14 Fly-back converter.

in fly-back operation to obtain high surge voltage induced, then get high output voltage. It works likely in buck–boost operation as a buck–boost converter. Its output voltage and current are

$$V_O = \frac{kN}{1-k} V_I \tag{14.15}$$

and

$$I_O = \frac{1-k}{kN} I_I \tag{14.16}$$

Half-bridge converter is a step-up converter, which is shown in Fig. 14.15. There are two switches and one double secondary coils transformer required. The transformer turns ratio is N. It works as a half-bridge rectifier (half of V_1 inputs to primary winding) plus a buck converter circuit in secondary side. The conduction duty cycle k is set in $0.1 < k < 0.5$. Its output voltage and current are

$$V_O = 2kN\frac{V_I}{2} = kNV_I \tag{14.17}$$

and

$$I_O = \frac{1}{kN} I_I \tag{14.18}$$

This converter may work in discontinuous mode if the frequency f is small, conduction duty k is small, inductance L is small, and load current is high.

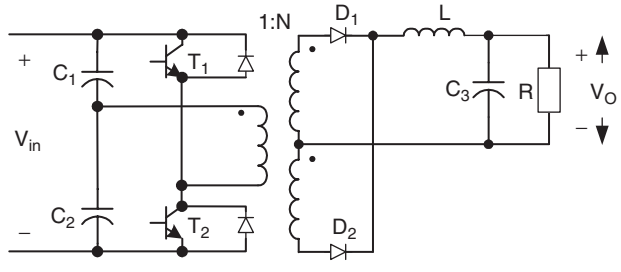

FIGURE 14.15 Half-bridge converter.

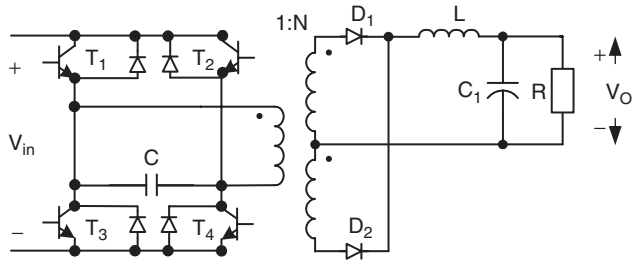

FIGURE 14.16 Bridge converter.

Bridge converter is a step-up converter, which is shown in Fig. 14.16. There are four switches and one double secondary coils transformer required. The transformer turns ratio is N. It works as a full-bridge rectifier (full V_1 inputs to primary winding) plus a buck-converter circuit in secondary side. The conduction duty cycle k is set in $0.1 < k < 0.5$. Its output voltage and current are

$$V_O = 2kNV_I \tag{14.19}$$

and

$$I_O = \frac{1}{2kN} I_I \tag{14.20}$$

ZETA (zeta) converter is a step-up converter, which is shown in Fig. 14.17. The transformer turns ratio is N. The transformer functions as a inductor (L_1) plus a buck–boost converter plus a low-pass filter (L_2–C_2). Its output voltage and current are

$$V_O = \frac{k}{1-k} NV_I \tag{14.21}$$

and

$$I_O = \frac{1-k}{kN} I_I \tag{14.22}$$

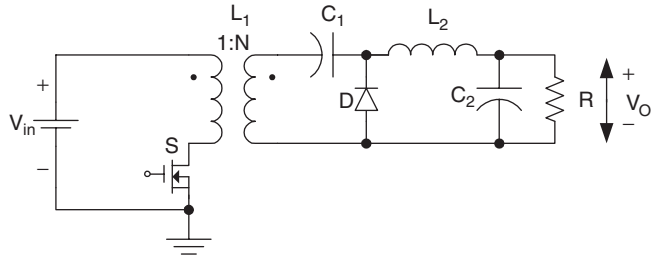

FIGURE 14.17 ZETA (zeta) converter.

14.2.4 Seven (7) Self-lift DC/DC Converters

Because of the effect of the parasitic elements, the voltage conversion gain is limited. Especially, when the conduction duty k is towards unity, the output voltage is sharply reduced. Voltage-lift technique is a popular method used in electronic circuit design. Applying this technique can effectively overcome the effect of the parasitic elements, and largely increase the voltage transfer gain. In this section, we introduce seven self-lift converters which are working in continuous mode.

- Positive output (P/O) self-lift Luo-converter;
- Reverse P/O self-lift Luo-converter;
- Negative output (N/O) self-lift Luo-converter;
- Reverse N/O self-lift Luo-converter;
- Self-lift Cúk-converter;
- Self-lift SEPIC;
- Enhanced self-lift Luo-converter.

All self-lift converters (except enhanced self-lift circuit) have the output voltage and current to be

$$V_O = \frac{1}{1-k} V_I \tag{14.23}$$

and

$$I_O = (1-k) I_I \tag{14.24}$$

The voltage transfer gain in continuous mode is

$$M_S = \frac{V_O}{V_I} = \frac{I_I}{I_O} = \frac{1}{1-k} \tag{14.25}$$

P/O self-lift Luo-converter is shown in Fig. 14.18. The variation ratio of the output voltage v_O in continuous conduction mode (CCM) is

$$\varepsilon = \frac{\Delta v_O/2}{V_O} = \frac{k}{8M_S} \frac{1}{f^2 C_O L_2} \tag{14.26}$$

Reverse P/O self-lift Luo-converter is shown in Fig. 14.19. The variation ratio of the output voltage v_O in CCM is

$$\varepsilon = \frac{\Delta v_O/2}{V_O} = \frac{k}{16M_S} \frac{1}{f^2 C_O L_2} \tag{14.27}$$

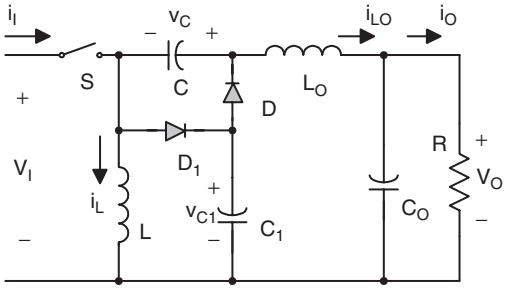

FIGURE 14.18 P/O self-lift Luo-converter.

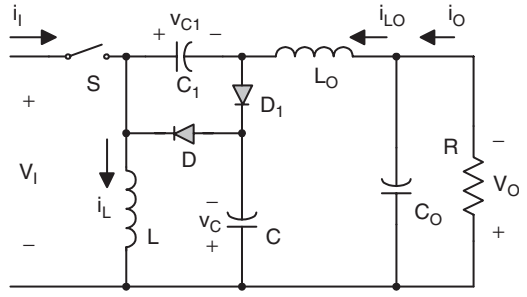

FIGURE 14.19 Reverse P/O self-lift Luo-converter.

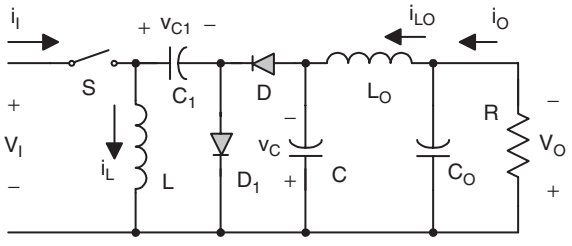

FIGURE 14.20 N/O self-lift Luo-converter.

N/O self-lift Luo-converter is shown in Fig. 14.20. The variation ratio of the output voltage v_O in CCM is

$$\varepsilon = \frac{\Delta v_O/2}{V_O} = \frac{k}{128}\frac{1}{f^3 L_O C_1 C_O R} \tag{14.28a}$$

Reverse N/O self-lift Luo-converter is shown in Fig. 14.21. The variation ratio of the output voltage v_O in CCM is

$$\varepsilon = \frac{\Delta v_O/2}{V_O} = \frac{k}{128}\frac{1}{f^3 L_O C_1 C_O R} \tag{14.28b}$$

Self-lift Cúk-converter is shown in Fig. 14.22. The variation ratio of the output voltage v_O in CCM is

$$\varepsilon = \frac{\Delta v_O/2}{V_O} = \frac{k}{128}\frac{1}{f^3 L_O C_1 C_O R} \tag{14.28c}$$

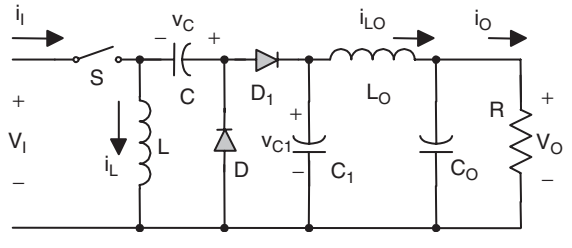

FIGURE 14.21 Reverse N/O self-lift Luo-converter.

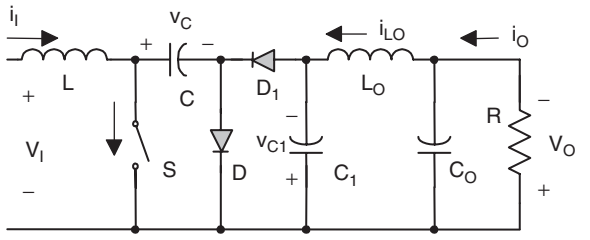

FIGURE 14.22 Self-lift Cúk-converter.

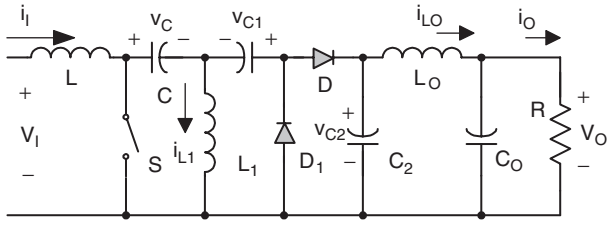

FIGURE 14.23 Self-lift SEPIC.

Self-lift SEPIC is shown in Fig. 14.23. The variation ratio of the output voltage v_O in CCM is

$$\varepsilon = \frac{\Delta v_O/2}{V_O} = \frac{k}{128}\frac{1}{f^3 L_O C_1 C_O R} \tag{14.28d}$$

Enhanced self-lift Luo-converter is shown in Fig. 14.24. Its output voltage and current are

$$V_O = \frac{2-k}{1-k} V_I \tag{14.29}$$

and

$$I_O = \frac{1-k}{2-k} I_I \tag{14.30}$$

The voltage transfer gain in continuous mode is

$$M_S = \frac{V_O}{V_I} = \frac{I_I}{I_O} = \frac{1}{1-k} + 1 = \frac{2-k}{1-k} \tag{14.31}$$

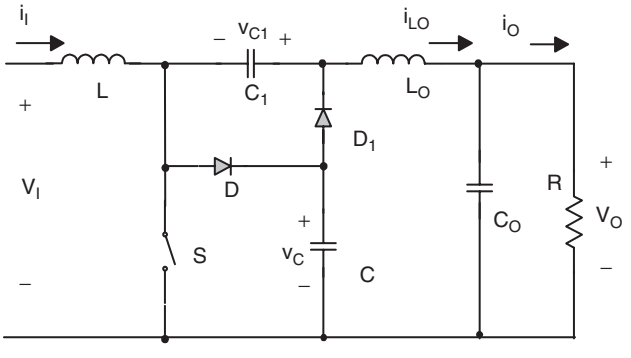

FIGURE 14.24 Enhanced self-lift Luo-converter.

TABLE 14.1 The circuit diagrams of the tapped inductor fundamental converters

	Standard converter	Switch tap	Diode to tap	Rail to tap
Buck	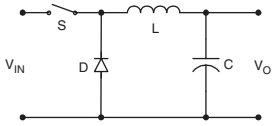	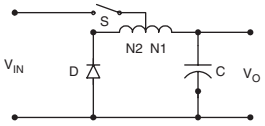	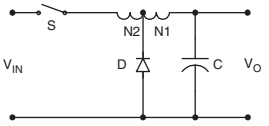	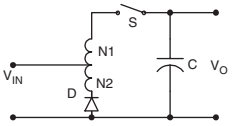
Boost	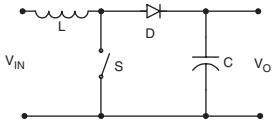	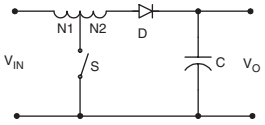	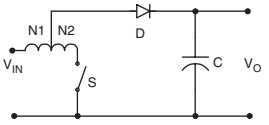	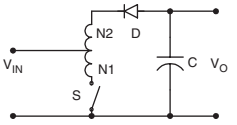
Buck–Boost	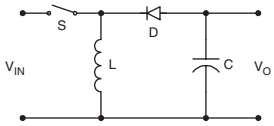	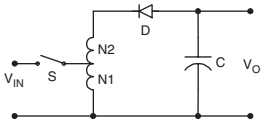	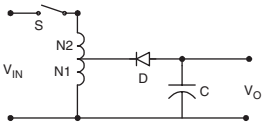	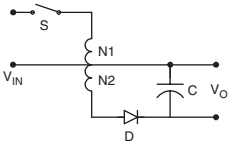

The variation ratio of the output voltage v_O in CCM is as in Eq. (14.26)

$$\varepsilon = \frac{\Delta v_O/2}{V_O} = \frac{k}{8M_S} \frac{1}{f^2 C_O L_2}$$

14.2.5 Tapped Inductor (Watkins–Johnson) Converters

Tapped inductor (Watkins–Johnson) converters have been derived from fundamental converters, which circuit diagrams are shown in Table 14.1. The voltage transfer gains are shown in Table 14.2. Here the tapped inductor ratio is $n = n1/(n1 + n2)$.

14.3 Voltage-lift Luo-converters

Voltage-lift (**VL**) technique is very popular for electronic circuit design. Professor Luo and Dr. Ye have successfully applied this technique in the design of DC/DC converters, and created a number of up-to-date converters. There are three series of Luo-converters introduced in this section:

- Positive output Luo-converters;
- Simplified positive output Luo-converters;
- Negative output Luo-converters.

TABLE 14.2 The voltage transfer gains of the tapped inductor fundamental converters

Converter	No tap	Switched to tap	Diode to tap	Rail to tap
Buck	k	$\frac{k}{n+k(1-n)}$	$\frac{nk}{1+k(n-1)}$	$\frac{k-n}{k(1-n)}$
Boost	$\frac{1}{1-k}$	$\frac{n+k(1-n)}{n(1-k)}$	$\frac{1+k(n-1)}{1-k}$	$\frac{n-k}{n(1-k)}$
Buck–Boost	$\frac{k}{1-k}$	$\frac{k}{n(1-k)}$	$\frac{nk}{1-k}$	$\frac{k}{1-k}$

14.3.1 Positive Output Luo-converters

Positive output (P/O) Luo-converters perform the voltage conversion from positive to positive voltages using the voltage lift technique. They work in the first-quadrant with large voltage amplification. Their voltage transfer gains are high. Five circuits are introduced in the literature. They are:

- Elementary circuit;
- Self-lift circuit;
- Re-lift circuit;
- Triple-lift circuit;
- Quadruple-lift circuit.

Further lift circuits can be derived from the above circuits. In all P/O Luo-Converters, we define normalized inductance $L = L_1 L_2/(L_1 + L_2)$ and normalized impedance $z_N = R/fL$.

P/O Luo-converter elementary circuit is shown in Fig. 14.25a. The equivalent circuits during switch-on and -off periods are shown in Figs. 14.25b and c. Its output voltage and current are

$$V_O = \frac{k}{1-k} V_I$$

and

$$I_O = \frac{1-k}{k} I_I$$

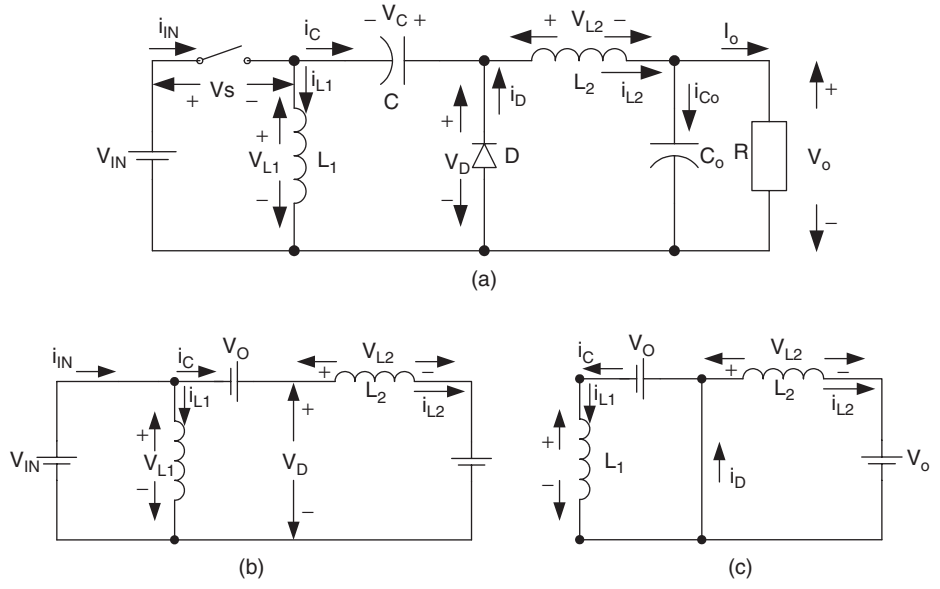

FIGURE 14.25 P/O Luo-converter elementary circuit; (a) circuit diagram; (b) switch on; and (c) switch off.

The voltage transfer gain in continuous mode is

$$M_E = \frac{V_O}{V_I} = \frac{I_I}{I_O} = \frac{k}{1-k} \tag{14.32}$$

The variation ratio of the output voltage v_O in CCM is

$$\varepsilon = \frac{\Delta v_O/2}{V_O} = \frac{k}{16M_E}\frac{1}{f^2 C_O L_2} \tag{14.33}$$

This converter may work in discontinuous conduction mode if the frequency f is small, conduction duty k is small, inductance L is small, and load current is high. The condition for discontinuous conduction mode (DCM) is

$$M_E \le k\sqrt{\frac{z_N}{2}} \tag{14.34}$$

The output voltage in DCM is

$$V_O = k(1-k)\frac{R}{2fL}V_I \quad \text{with} \quad \sqrt{\frac{R}{2fL}} \ge \frac{1}{1-k} \tag{14.35}$$

P/O Luo-converter self-lift circuit is shown in Fig. 14.26a. The equivalent circuits during switch-on and -off periods are shown in Figs. 14.26b and c. Its output voltage and current are

$$V_O = \frac{1}{1-k}V_I$$

and

$$I_O = (1-k)I_I$$

The voltage transfer gain in continuous mode is

$$M_S = \frac{V_O}{V_I} = \frac{I_I}{I_O} = \frac{1}{1-k} \tag{14.36}$$

The variation ratio of the output voltage v_O in CCM is

$$\varepsilon = \frac{\Delta v_O/2}{V_O} = \frac{k}{16M_S}\frac{1}{f^2 C_O L_2} \tag{14.37}$$

This converter may work in discontinuous conduction mode if the frequency f is small, conduction duty k is small, inductance L is small, and load current is high. The condition for DCM is

$$M_S \le \sqrt{k}\sqrt{\frac{z_N}{2}} \tag{14.38}$$

The output voltage in DCM is

$$V_O = \left[1 + k^2(1-k)\frac{R}{2fL}\right]V_I \quad \text{with} \quad \sqrt{k}\sqrt{\frac{R}{2fL}} \ge \frac{1}{1-k} \tag{14.39}$$

P/O Luo-converter re-lift circuit is shown in Fig. 14.27a. The equivalent circuits during switch-on and -off periods are shown in Figs. 14.27b and c. Its output voltage and current are

$$V_O = \frac{2}{1-k}V_I$$

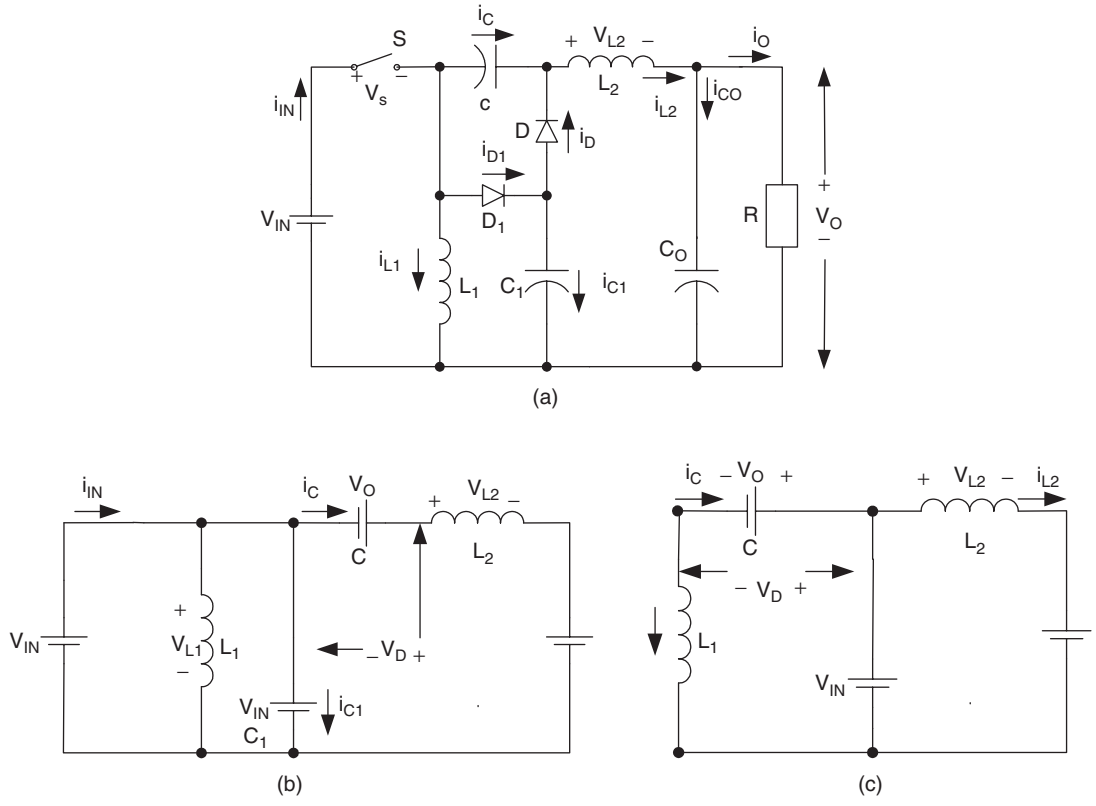

FIGURE 14.26 P/O Luo-converter self-lift circuit: (a) circuit diagram; (b) switch on; and (c) switch off.

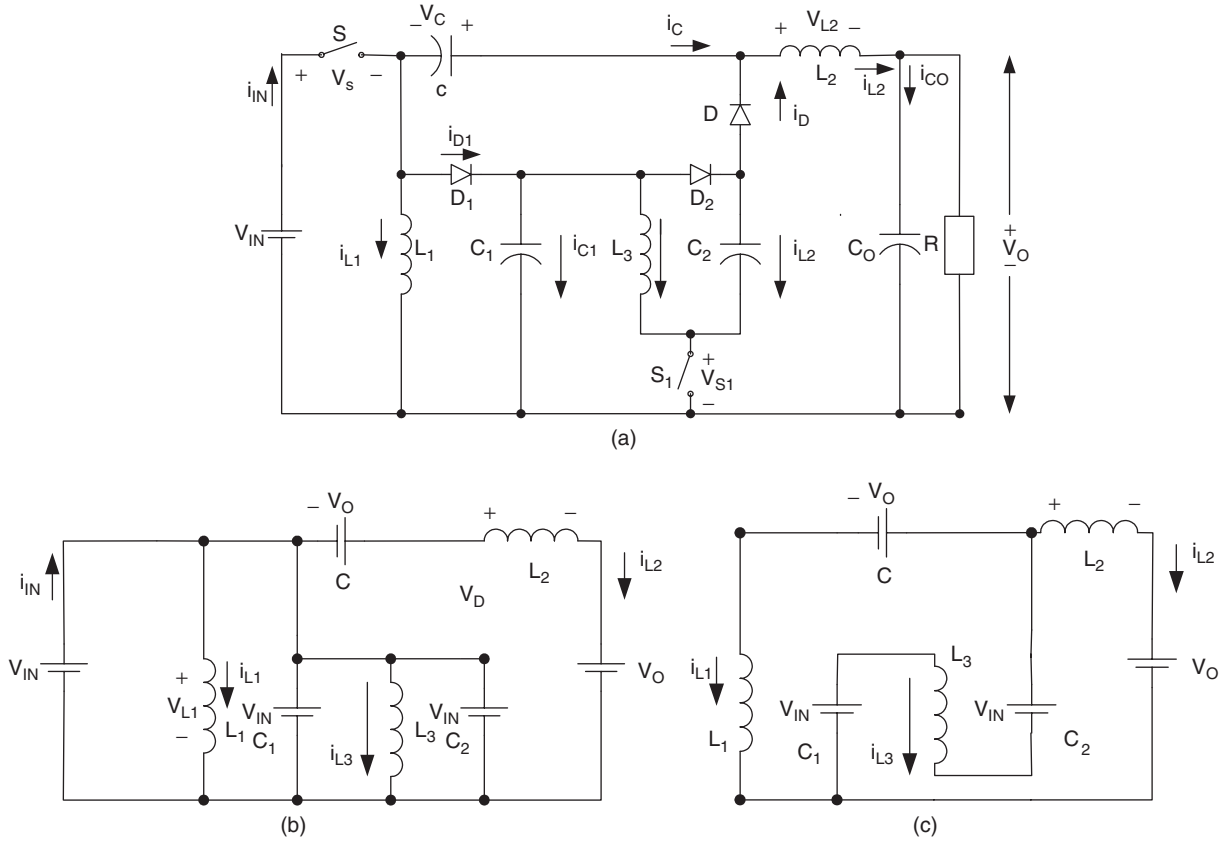

FIGURE 14.27 P/O Luo-converter re-lift circuit: (a) circuit diagram; (b) switch on; and (c) switch off.

and

$$I_O = \frac{1-k}{2} I_I$$

The voltage transfer gain in CCM is

$$M_R = \frac{V_O}{V_I} = \frac{I_I}{I_O} = \frac{2}{1-k} \tag{14.40}$$

The variation ratio of the output voltage v_O in CCM is

$$\varepsilon = \frac{\Delta v_O/2}{V_O} = \frac{k}{16 M_R} \frac{1}{f^2 C_O L_2} \tag{14.41}$$

This converter may work in discontinuous conduction mode if the frequency f is small, conduction duty k is small, inductance L is small, and load current is high. The condition for DCM is

$$M_R \le \sqrt{k z_N} \tag{14.42}$$

The output voltage in DCM is

$$V_O = \left[2 + k^2 (1-k) \frac{R}{2fL} \right] V_I \quad \text{with} \quad \sqrt{k} \sqrt{\frac{R}{fL}} \ge \frac{2}{1-k} \tag{14.43}$$

P/O Luo-converter triple-lift circuit is shown in Fig. 14.28a. The equivalent circuits during switch-on and -off periods are shown in Figs. 14.28b and c. Its output voltage and current are

$$V_O = \frac{3}{1-k} V_I$$

and

$$I_O = \frac{1-k}{3} I_I$$

The voltage transfer gain in CCM is

$$M_T = \frac{V_O}{V_I} = \frac{I_I}{I_O} = \frac{3}{1-k} \tag{14.44}$$

The variation ratio of the output voltage v_O in CCM is

$$\varepsilon = \frac{\Delta v_O/2}{V_O} = \frac{k}{16 M_T} \frac{1}{f^2 C_O L_2} \tag{14.45}$$

This converter may work in discontinuous conduction mode if the frequency f is small, conduction duty k is small, inductance L is small, and load current is high. The condition for DCM is

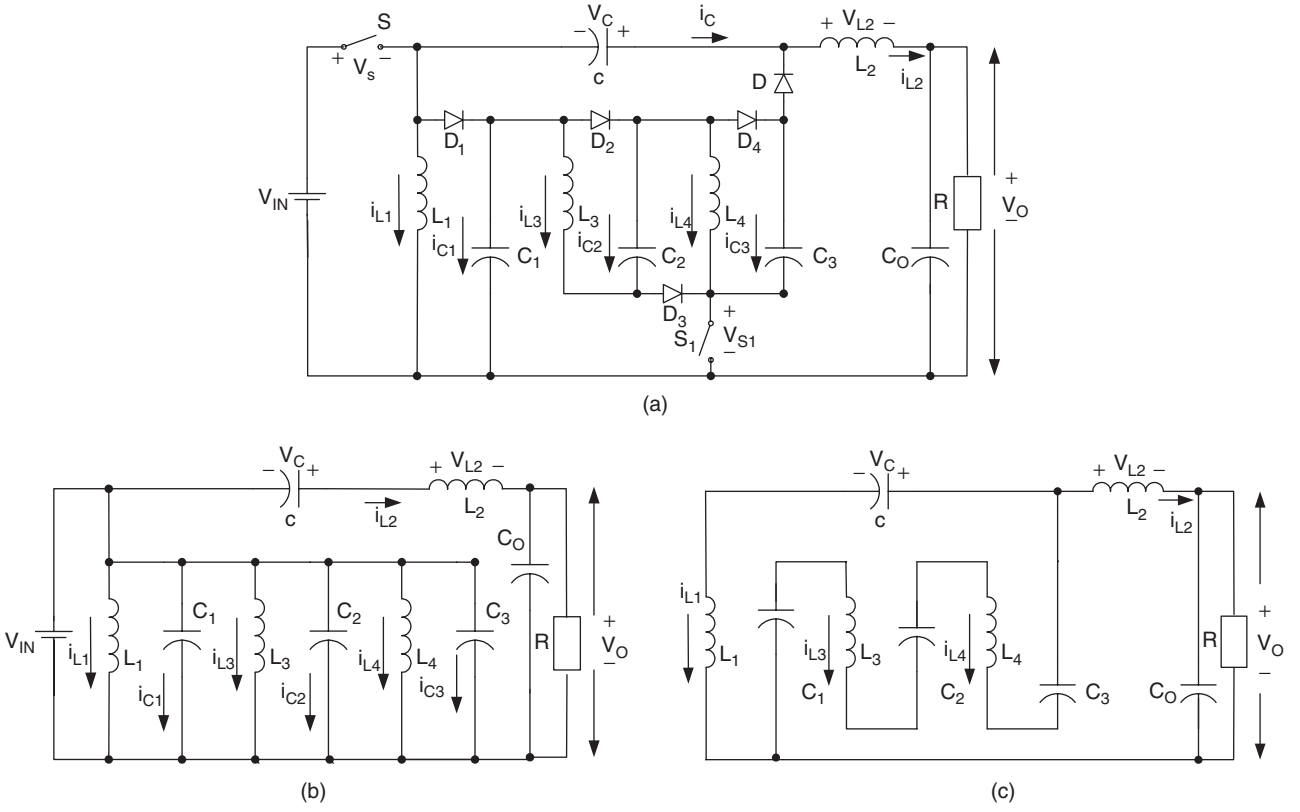

FIGURE 14.28 P/O Luo-converter triple-lift circuit: (a) circuit diagram; (b) switch on; and (c) switch off.

$$M_T \le \sqrt{\frac{3kz_N}{2}} \tag{14.46}$$

The output voltage in DCM is

$$V_O = \left[3 + k^2(1-k)\frac{R}{2fL}\right] V_I \quad \text{with} \quad \sqrt{k}\sqrt{\frac{3R}{2fL}} \ge \frac{3}{1-k} \tag{14.47}$$

P/O Luo-converter quadruple-lift circuit is shown in Fig. 14.29a. The equivalent circuits during switch-on and -off periods are shown in Figs. 14.29b and c. Its output voltage and current are

$$V_O = \frac{4}{1-k} V_I$$

and

$$I_O = \frac{1-k}{4} I_I$$

The voltage transfer gain in CCM is

$$M_Q = \frac{V_O}{V_I} = \frac{I_I}{I_O} = \frac{4}{1-k} \tag{14.48}$$

The variation ratio of the output voltage v_O in CCM is

$$\varepsilon = \frac{\Delta v_O/2}{V_O} = \frac{k}{16M_Q}\frac{1}{f^2 C_O L_2} \tag{14.49}$$

This converter may work in discontinuous conduction mode if the frequency f is small, conduction duty k is small, inductance L is small, and load current is high. The condition for DCM is

$$M_Q \le \sqrt{2kz_N} \tag{14.50}$$

The output voltage in DCM is

$$V_O = \left[4 + k^2(1-k)\frac{R}{2fL}\right] V_I \quad \text{with} \quad \sqrt{k}\sqrt{\frac{2R}{fL}} \ge \frac{4}{1-k} \tag{14.51}$$

Summary for all P/O Luo-converters:

$$M = \frac{V_O}{V_I} = \frac{I_I}{I_O}; \quad L = \frac{L_1 L_2}{L_1 + L_2}; \quad z_N = \frac{R}{fL}; \quad R = \frac{V_O}{I_O}$$

To write common formulas for all circuits parameters, we define that subscript $j = 0$ for the elementary circuit, $j = 1$

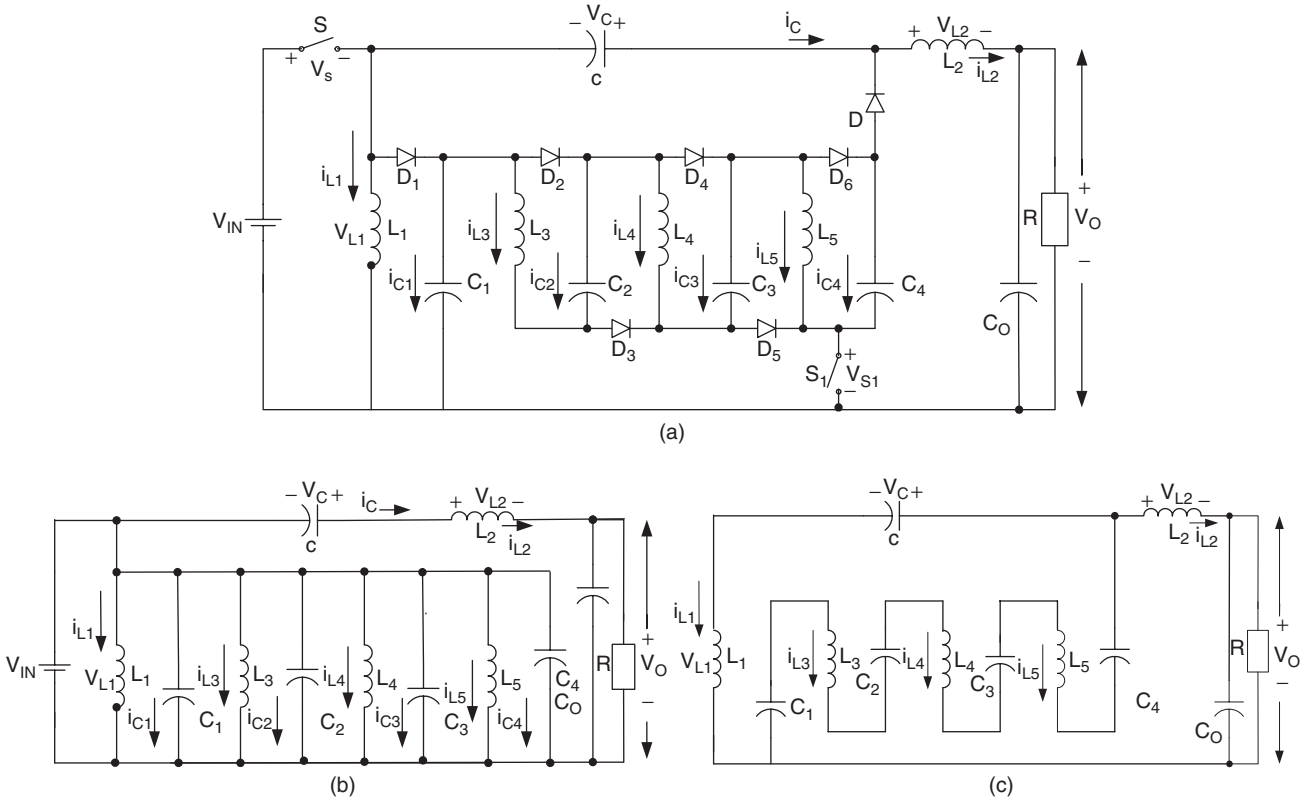

FIGURE 14.29 P/O Luo-converter quadruple-lift circuit: (a) circuit diagram; (b) switch on; and (c) switch off.

for the self-lift circuit, $j = 2$ for the re-lift circuit, $j = 3$ for the triple-lift circuit, $j = 4$ for the quadruple-lift circuit, and so on. The voltage transfer gain is

$$M_j = \frac{k^{h(j)}[j + h(j)]}{1 - k} \tag{14.52}$$

The variation ratio of the output voltage is

$$\varepsilon_j = \frac{\Delta v_O/2}{V_O} = \frac{k}{16M_j} \frac{1}{f^2 C_O L_2} \tag{14.53}$$

The condition for discontinuous conduction mode is

$$\frac{k^{[1+h(j)]}}{M_j^2} \frac{j + h(j)}{2} z_N \geq 1 \tag{14.54}$$

The output voltage in discontinuous conduction mode is

$$V_{O-j} = \left\{ j + k^{[2-h(j)]} \frac{1 - k}{2} z_N \right\} V_I \tag{14.55}$$

where

$$h(j) = \begin{cases} 0 & if \quad j \geq 1 \\ 1 & if \quad j = 0 \end{cases} \tag{14.56}$$

is the **Hong** function.

14.3.2 Simplified Positive Output (S P/O) Luo-converters

Carefully check P/O Luo-converters, we can see that there are two switches required from re-lift circuit. In order to use only one switch in all P/O Luo-converters, we modify the circuits. In this section we introduce following four circuits:

- Simplified self-lift circuit;
- Simplified re-lift circuit;
- Simplified triple-lift circuit;
- Simplified quadruple-lift circuit.

Further lift circuits can be derived from the above circuits. In all S P/O Luo-converters, we define normalized impedance $z_N = R/fL$.

S P/O Luo-converter self-lift circuit is shown in Fig. 14.30a. The equivalent circuits during switch-on and -off periods are shown in Figs. 14.30b and c. Its output voltage and current are

$$V_O = \frac{1}{1 - k} V_I$$

and

$$I_O = (1 - k) I_I$$

The voltage transfer gain in CCM is

$$M_S = \frac{V_O}{V_I} = \frac{I_I}{I_O} = \frac{1}{1 - k} \tag{14.57}$$

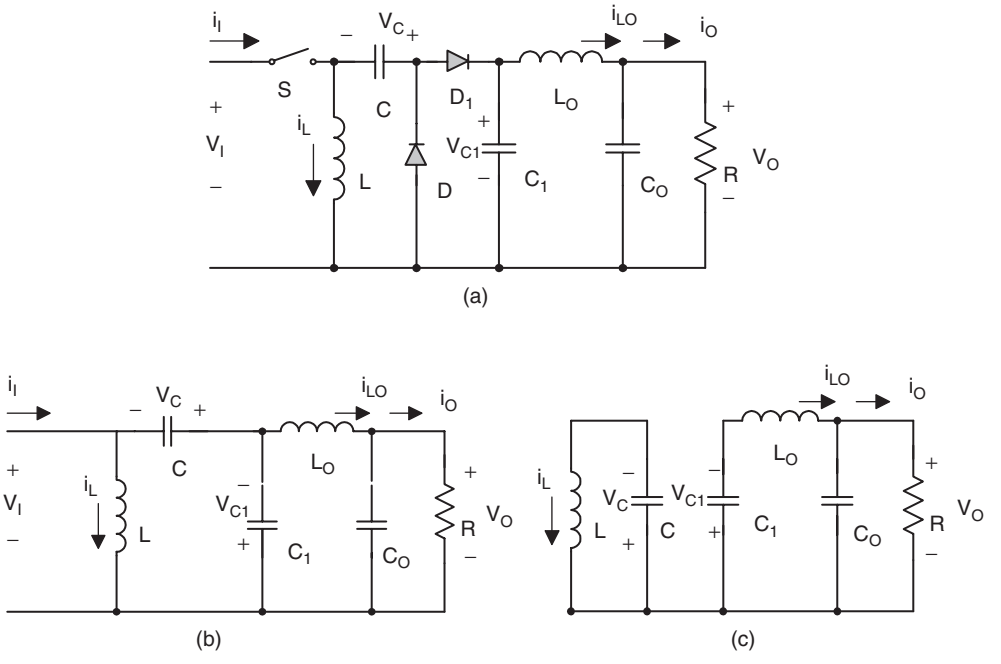

FIGURE 14.30 S P/O Luo-converter self-lift circuit: (a) circuit diagram; (b) switch on; and (c) switch off.

The variation ratio of the output voltage v_O in CCM is

$$\varepsilon = \frac{\Delta v_O/2}{V_O} = \frac{k}{128} \frac{1}{f^3 L_O C_1 C_O R} \tag{14.58}$$

This converter may work in discontinuous conduction mode if the frequency f is small, conduction duty k is small, inductance L is small, and load current is high. The condition for DCM is

$$M_S \le \sqrt{k}\sqrt{\frac{z_N}{2}} \tag{14.59}$$

The output voltage in DCM is

$$V_O = \left[1 + k^2(1-k)\frac{R}{2fL}\right] V_I \quad \text{with} \quad \sqrt{k}\sqrt{\frac{R}{2fL}} \ge \frac{1}{1-k} \tag{14.60}$$

S P/O Luo-converter re-lift circuit is shown in Fig. 14.31a. The equivalent circuits during switch-on and -off periods are shown in Figs. 14.31b and c. Its output voltage and current are

$$V_O = \frac{2}{1-k} V_I$$

and

$$I_O = \frac{1-k}{2} I_I$$

The voltage transfer gain in CCM is

$$M_R = \frac{V_O}{V_I} = \frac{I_I}{I_O} = \frac{2}{1-k} \tag{14.61}$$

The variation ratio of the output voltage v_O in CCM is

$$\varepsilon = \frac{\Delta v_O/2}{V_O} = \frac{k}{128} \frac{1}{f^3 L_O C_1 C_O R} \tag{14.62}$$

This converter may work in discontinuous conduction mode if the frequency f is small, conduction duty k is small, inductance L is small, and load current is high. The condition for DCM is

$$M_R \le \sqrt{k z_N} \tag{14.63}$$

The output voltage in DCM is

$$V_O = \left[2 + k^2(1-k)\frac{R}{2fL}\right] V_I \quad \text{with} \quad \sqrt{k}\sqrt{\frac{R}{fL}} \ge \frac{2}{1-k} \tag{14.64}$$

S P/O Luo triple-lift circuit is shown in Fig. 14.32a. The equivalent circuits during switch-on and -off periods are shown in Figs. 14.32b and c. Its output voltage and current are

$$V_O = \frac{3}{1-k} V_I$$

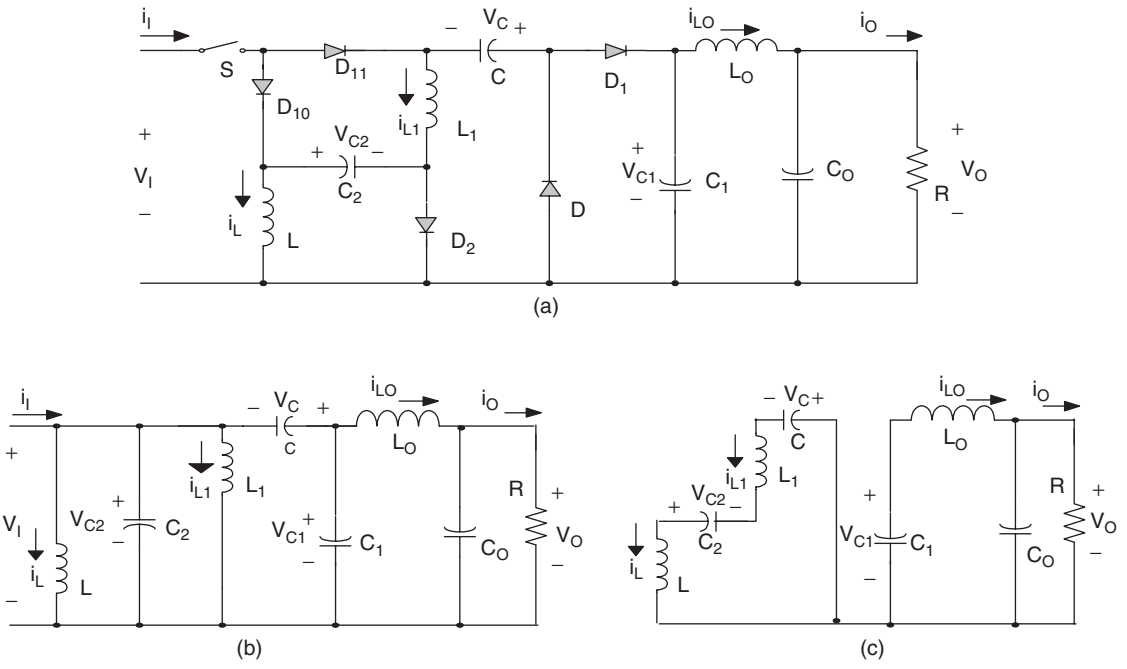

FIGURE 14.31 S P/O Luo-converter re-lift circuit: (a) circuit diagram; (b) switch on; and (c) switch off.

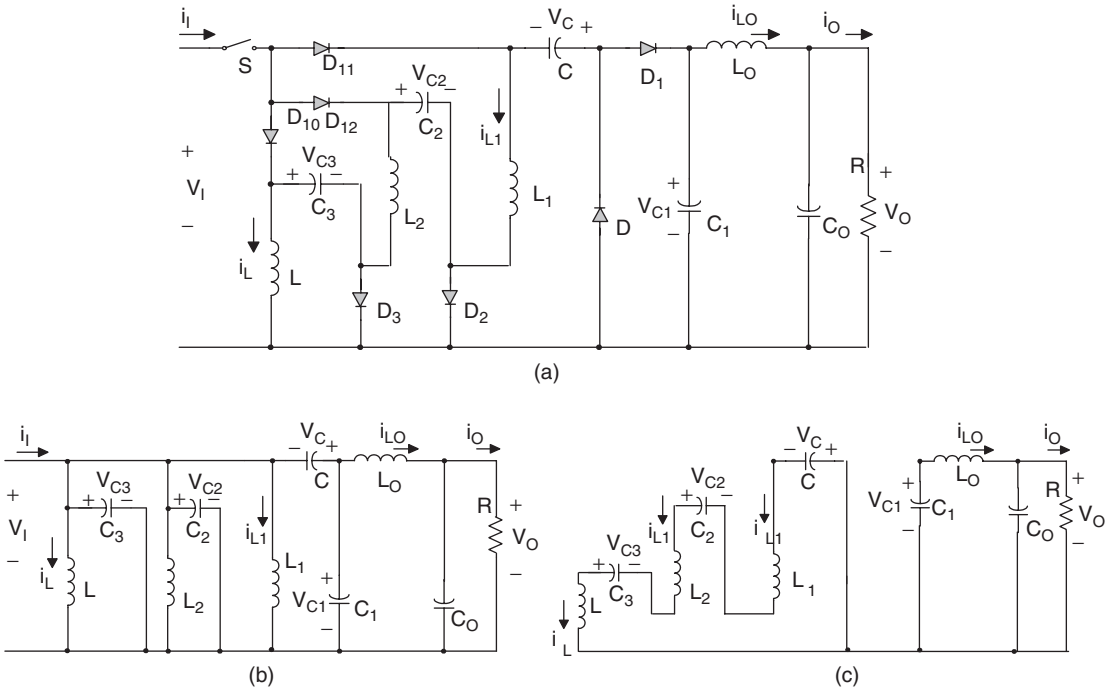

FIGURE 14.32 S P/O Luo-converter triple-lift circuit: (a) circuit diagram; (b) switch on; and (c) switch off.

and

$$I_O = \frac{1-k}{3} I_I$$

The voltage transfer gain in CCM is

$$M_T = \frac{V_O}{V_I} = \frac{I_I}{I_O} = \frac{3}{1-k} \tag{14.65}$$

The variation ratio of the output voltage v_O in CCM is

$$\varepsilon = \frac{\Delta v_O/2}{V_O} = \frac{k}{128} \frac{1}{f^3 L_O C_1 C_O R} \tag{14.66}$$

This converter may work in discontinuous conduction mode if the frequency f is small, conduction duty k is small, inductance L is small, and load current is high. The condition for DCM is

$$M_T \le \sqrt{\frac{3kz_N}{2}} \tag{14.67}$$

The output voltage in DCM is

$$V_O = \left[3 + k^2(1-k)\frac{R}{2fL}\right] V_I \quad \text{with} \quad \sqrt{k}\sqrt{\frac{3R}{2fL}} \ge \frac{3}{1-k} \tag{14.68}$$

S P/O Luo quadruple-lift circuit is shown in Fig. 14.33a. The equivalent circuits during switch-on and -off periods are shown in Figs. 14.33b and c. Its output voltage and current are

$$V_O = \frac{4}{1-k} V_I$$

and

$$I_O = \frac{1-k}{4} I_I$$

The voltage transfer gain in CCM is

$$M_Q = \frac{V_O}{V_I} = \frac{I_I}{I_O} = \frac{4}{1-k} \tag{14.69}$$

The variation ratio of the output voltage v_O in CCM is

$$\varepsilon = \frac{\Delta v_O/2}{V_O} = \frac{k}{128} \frac{1}{f^3 L_O C_1 C_O R} \tag{14.70}$$

This converter may work in discontinuous conduction mode if the frequency f is small, conduction duty k is small, inductance L is small, and load current is high. The condition for DCM is

$$M_Q \le \sqrt{2kz_N} \tag{14.71}$$

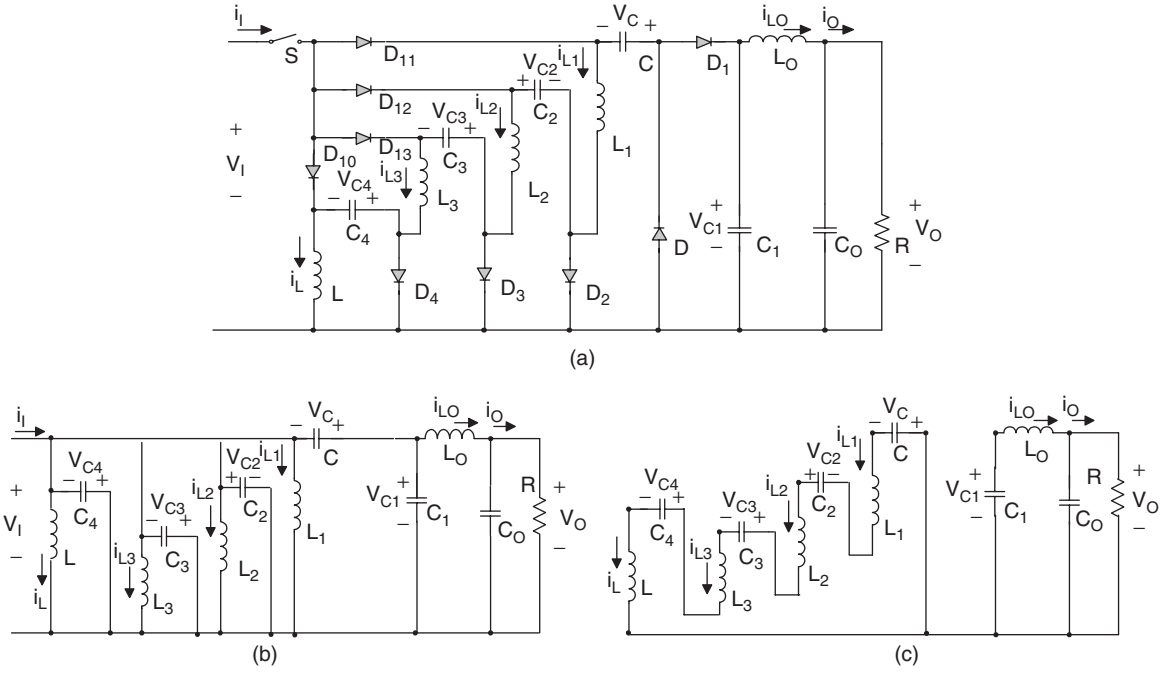

FIGURE 14.33 S P/O Luo-converter quadruple-lift circuit: (a) circuit diagram; (b) switch on; and (c) switch off.

The output voltage in DCM is

$$V_O = \left[4 + k^2(1-k)\frac{R}{2fL}\right] V_I \quad \text{with} \quad \sqrt{k}\sqrt{\frac{2R}{fL}} \geq \frac{4}{1-k} \tag{14.72}$$

Summary for all S P/O Luo-converters:

$$M = \frac{V_O}{V_I} = \frac{I_I}{I_O}; \quad z_N = \frac{R}{fL}; \quad R = \frac{V_O}{I_O}$$

To write common formulas for all circuits parameters, we define that subscript $j = 1$ for the self-lift circuit, $j = 2$ for the re-lift circuit, $j = 3$ for the triple-lift circuit, $j = 4$ for the quadruple-lift circuit, and so on. The voltage transfer gain is

$$M_j = \frac{j}{1-k} \tag{14.73}$$

The variation ratio of the output voltage is

$$\varepsilon_j = \frac{\Delta v_O/2}{V_O} = \frac{k}{128}\frac{1}{f^3 L_O C_1 C_O R} \tag{14.74}$$

The condition for discontinuous mode is

$$M_j \leq \sqrt{\frac{jkz_N}{2}} \tag{14.75}$$

The output voltage in discontinuous mode is

$$V_{O-j} = \left[j + k^2(1-k)\frac{z_N}{2}\right] V_I \tag{14.76}$$

14.3.3 Negative Output Luo-converters

Negative output (N/O) Luo-converters perform the voltage conversion from positive to negative voltages using the voltage-lift technique. They work in the third-quadrant with large voltage amplification. Their voltage transfer gains are high. Five circuits are introduced in the literature. They are:

- Elementary circuit;
- Self-lift circuit;
- Re-lift circuit;
- Triple-lift circuit;
- Quadruple-lift circuit.

Further lift circuits can be derived from above circuits. In all N/O Luo-converters, we define normalized impedance $z_N = R/fL$.

N/O Luo-converter elementary circuit is shown in Fig. 14.34a. The equivalent circuits during switch-on and -off periods are shown in Figs. 14.34b and c. Its output voltage and current (the absolute value) are

$$V_O = \frac{k}{1-k} V_I$$

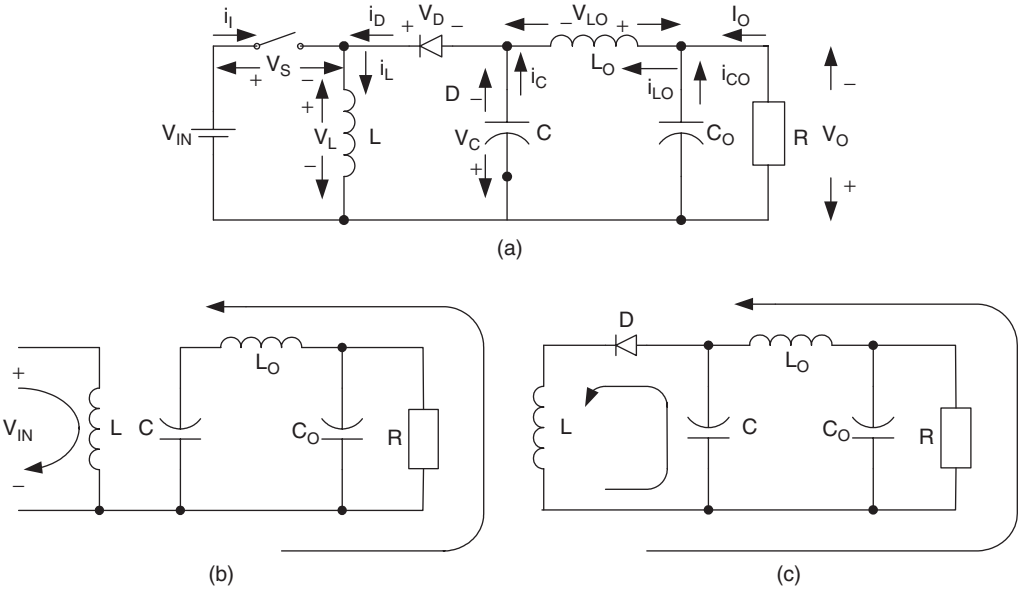

FIGURE 14.34 N/O Luo-converter elementary circuit: (a) circuit diagram; (b) switch on; and (c) switch off.

and

$$I_O = \frac{1-k}{k} I_I$$

When k is greater than 0.5, the output voltage can be higher than the input voltage.

The voltage transfer gain in CCM is

$$M_E = \frac{V_O}{V_I} = \frac{I_I}{I_O} = \frac{k}{1-k} \tag{14.77}$$

The variation ratio of the output voltage v_O in CCM is

$$\varepsilon = \frac{\Delta v_O/2}{V_O} = \frac{k}{128} \frac{1}{f^3 C C_O L_O R} \tag{14.78}$$

This converter may work in discontinuous conduction mode if the frequency f is small, conduction duty k is small, inductance L is small, and load current is high. The condition for DCM is

$$M_E \le k\sqrt{\frac{z_N}{2}} \tag{14.79}$$

The output voltage in DCM is

$$V_O = k(1-k)\frac{R}{2fL} V_I \quad \text{with} \quad \sqrt{\frac{R}{2fL}} \ge \frac{1}{1-k} \tag{14.80}$$

N/O Luo-converter self-lift circuit is shown in Fig. 14.35a. The equivalent circuits during switch-on and -off periods are shown in Figs. 14.35b and c. Its output voltage and current (the absolute value) are

$$V_O = \frac{1}{1-k} V_I$$

and

$$I_O = (1-k) I_I$$

The voltage transfer gain in CCM is

$$M_S = \frac{V_O}{V_I} = \frac{I_I}{I_O} = \frac{1}{1-k} \tag{14.81}$$

The variation ratio of the output voltage v_O in CCM is

$$\varepsilon = \frac{\Delta v_O/2}{V_O} = \frac{k}{128} \frac{1}{f^3 C C_O L_O R} \tag{14.82}$$

This converter may work in discontinuous conduction mode if the frequency f is small, conduction duty k is small, inductance L is small, and load current is high. The condition for DCM is

$$M_S \le \sqrt{k}\sqrt{\frac{z_N}{2}} \tag{14.83}$$

The output voltage in DCM is

$$V_O = \left[1 + k^2(1-k)\frac{R}{2fL}\right] V_I \quad \text{with} \quad \sqrt{k}\sqrt{\frac{R}{2fL}} \ge \frac{1}{1-k} \tag{14.84}$$

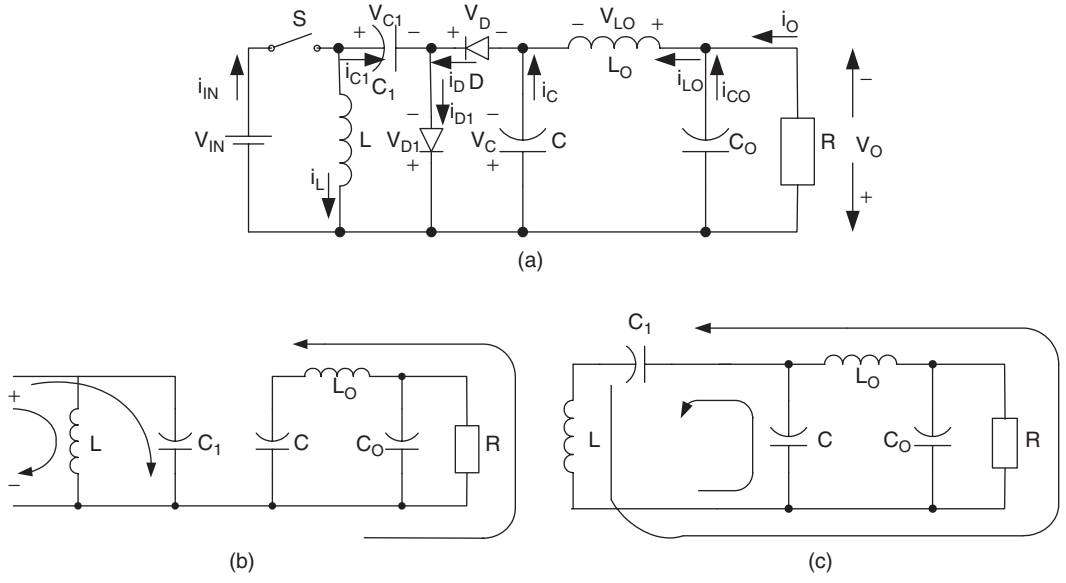

FIGURE 14.35 N/O Luo-converter self-lift circuit: (a) circuit diagram; (b) switch on; and (c) switch off.

N/O Luo-converter re-lift circuit is shown in Fig. 14.36a. The equivalent circuits during switch-on and -off periods are shown in Figs. 14.36b and c. Its output voltage and current (the absolute value) are

$$V_O = \frac{2}{1-k} V_I$$

and

$$I_O = \frac{1-k}{2} I_I$$

The voltage transfer gain in CCM is

$$M_R = \frac{V_O}{V_I} = \frac{I_I}{I_O} = \frac{2}{1-k} \tag{14.85}$$

The variation ratio of the output voltage v_O in CCM is

$$\varepsilon = \frac{\Delta v_O/2}{V_O} = \frac{k}{128} \frac{1}{f^3 C C_O L_O R} \tag{14.86}$$

This converter may work in discontinuous conduction mode if the frequency f is small, conduction duty k is small, inductance L is small, and load current is high. The condition for DCM is

$$M_R \le \sqrt{k z_N} \tag{14.87}$$

The output voltage in DCM is

$$V_O = \left[2 + k^2(1-k)\frac{R}{2fL}\right] V_I \quad \text{with} \quad \sqrt{k}\sqrt{\frac{R}{fL}} \ge \frac{2}{1-k} \tag{14.88}$$

N/O Luo-converter triple-lift circuit is shown in Fig. 14.37a. The equivalent circuits during switch-on and -off periods are shown in Figs. 14.37b and c. Its output voltage and current (the absolute value) are

$$V_O = \frac{3}{1-k} V_I$$

and

$$I_O = \frac{1-k}{3} I_I$$

The voltage transfer gain in CCM is

$$M_T = \frac{V_O}{V_I} = \frac{I_I}{I_O} = \frac{3}{1-k} \tag{14.89}$$

The variation ratio of the output voltage v_O in CCM is

$$\varepsilon = \frac{\Delta v_O/2}{V_O} = \frac{k}{128} \frac{1}{f^3 C C_O L_O R} \tag{14.90}$$

This converter may work in discontinuous conduction mode if the frequency f is small, conduction duty k is small,

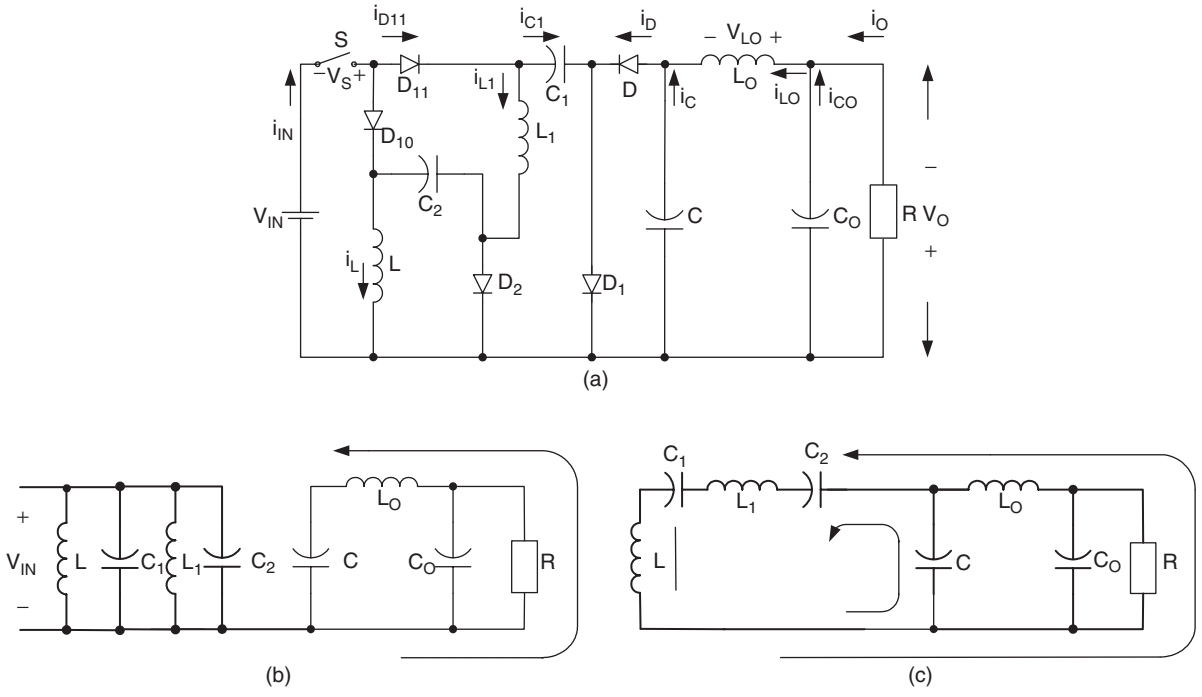

FIGURE 14.36 N/O Luo-converter re-lift circuit: (a) circuit diagram; (b) switch on; and (c) switch off.

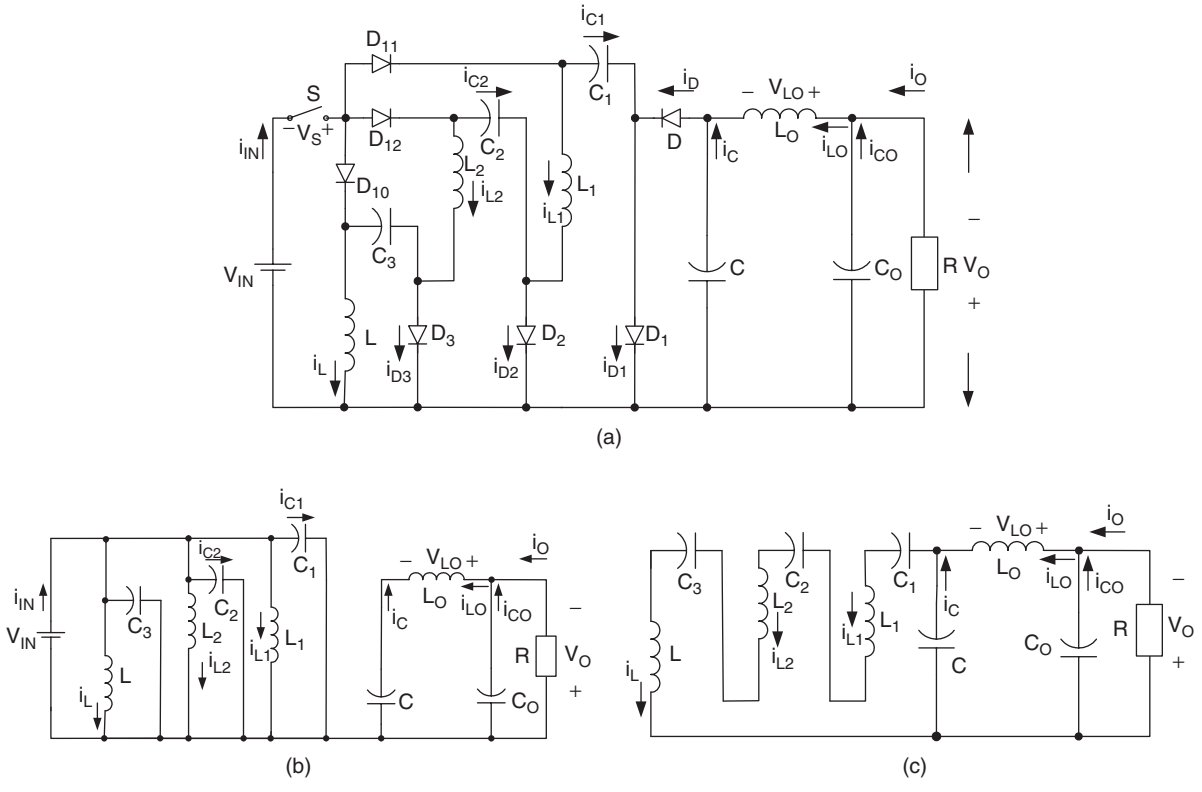

FIGURE 14.37 N/O Luo-converter triple-lift circuit: (a) circuit diagram; (b) switch on; and (c) switch off.

inductance L is small, and load current is high. The condition for DCM is

$$M_T \le \sqrt{\frac{3kz_N}{2}} \tag{14.91}$$

The output voltage in DCM is

$$V_O = \left[3 + k^2(1-k)\frac{R}{2fL}\right] V_I \quad \text{with} \quad \sqrt{k}\sqrt{\frac{3R}{2fL}} \ge \frac{3}{1-k} \tag{14.92}$$

N/O Luo-converter quadruple-lift circuit is shown in Fig. 14.38a. The equivalent circuits during switch-on and -off periods are shown in Figs. 14.38b and c. Its output voltage and current (the absolute value) are

$$V_O = \frac{4}{1-k} V_I$$

and

$$I_O = \frac{1-k}{4} I_I$$

The voltage transfer gain in CCM is

$$M_Q = \frac{V_O}{V_I} = \frac{I_I}{I_O} = \frac{4}{1-k} \tag{14.93}$$

The variation ratio of the output voltage v_O in CCM is

$$\varepsilon = \frac{\Delta v_O/2}{V_O} = \frac{k}{128} \frac{1}{f^3 C C_O L_O R} \tag{14.94}$$

This converter may work in discontinuous conduction mode if the frequency f is small, conduction duty k is small, inductance L is small, and load current is high. The condition for DCM is

$$M_Q \le \sqrt{2kz_N} \tag{14.95}$$

The output voltage in DCM is

$$V_O = \left[4 + k^2(1-k)\frac{R}{2fL}\right] V_I \quad \text{with} \quad \sqrt{k}\sqrt{\frac{2R}{fL}} \ge \frac{4}{1-k} \tag{14.96}$$

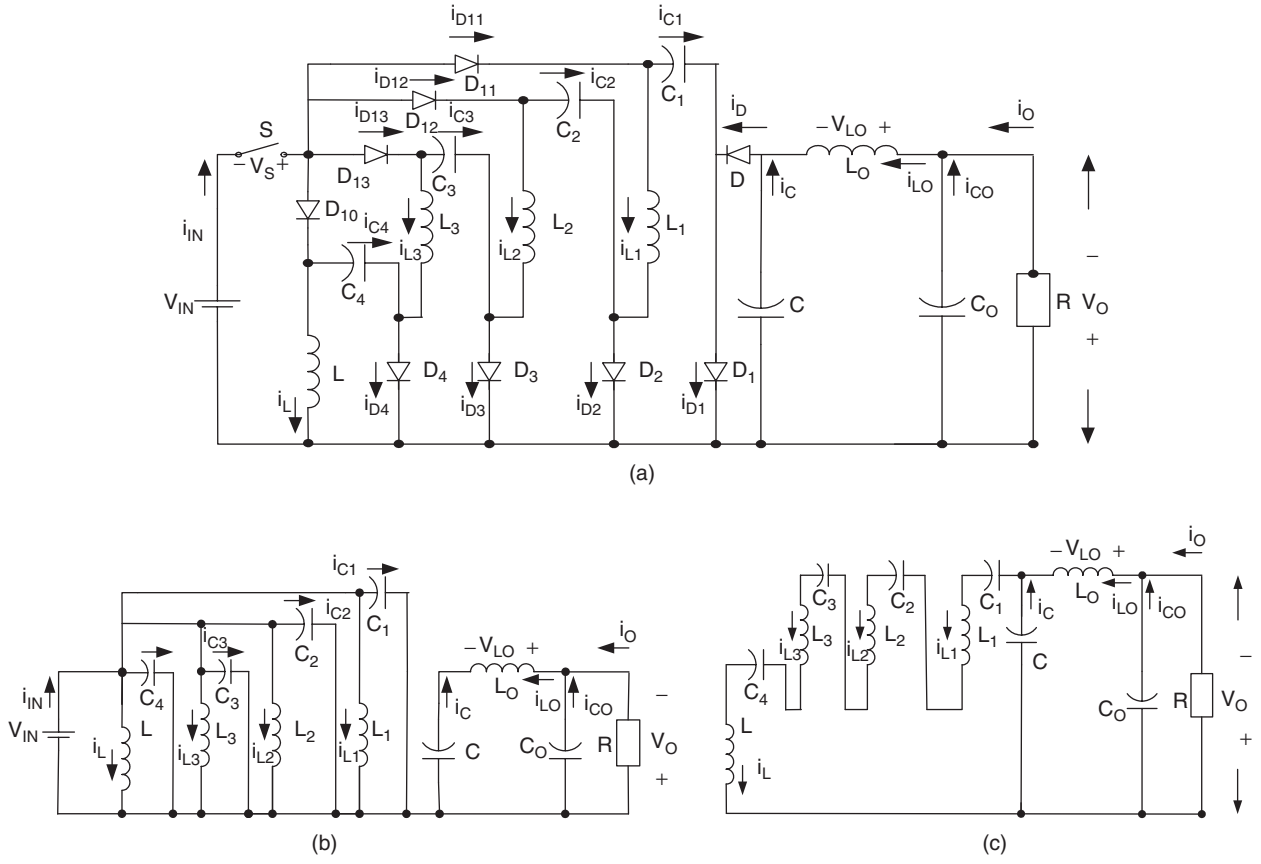

FIGURE 14.38 N/O Luo-converter quadruple-lift circuit: (a) circuit diagram; (b) switch on; and (c) switch off.

Summary for all N/O Luo-converters:

$$M = \frac{V_O}{V_I} = \frac{I_I}{I_O}; \quad z_N = \frac{R}{fL}; \quad R = \frac{V_O}{I_O}$$

To write common formulas for all circuits parameters, we define that subscript $j = 0$ for the elementary circuit, $j = 1$ for the self-lift circuit, $j = 2$ for the re-lift circuit, $j = 3$ for the triple-lift circuit, $j = 4$ for the quadruple-lift circuit, and so on. The voltage transfer gain is

$$M_j = \frac{k^{h(j)}[j + h(j)]}{1 - k} \tag{14.97}$$

The variation ratio of the output voltage is

$$\varepsilon = \frac{\Delta v_O/2}{V_O} = \frac{k}{128} \frac{1}{f^3 C C_O L_O R} \tag{14.98}$$

The condition for discontinuous conduction mode is

$$\frac{k^{[1+h(j)]}}{M_j^2} \frac{j + h(j)}{2} z_N \geq 1 \tag{14.99}$$

The output voltage in discontinuous conduction mode is

$$V_{O-j} = \left\{ j + k^{[2-h(j)]} \frac{1 - k}{2} z_N \right\} V_I \tag{14.100}$$

where

$$h(j) = \begin{cases} 0 & if \quad j \geq 1 \\ 1 & if \quad j = 0 \end{cases}$$

is the **Hong** function.

14.4 Double Output Luo-converters

Double output (D/O) Luo-converters perform the voltage conversion from positive to positive and negative voltages simultaneously using the voltage-lift technique. They work in the first- and third-quadrants with high voltage transfer gain. There are five circuits introduced in this section:

- D/O Luo-converter elementary circuit;
- D/O Luo-converter self-lift circuit;
- D/O Luo-converter re-lift circuit;
- D/O Luo-converter triple-lift circuit;
- D/O Luo-converter quadruple-lift circuit.

Further lift circuits can be derived from above circuits. In all D/O Luo-converters, each circuit has two conversion paths – positive conversion path and negative conversion path. The positive path likes P/O Luo-converters, and the negative path likes N/O Luo-converters. We define normalized impedance $z_{N+} = R/fL$ for positive path, and normalized impedance $z_{N-} = R_1/fL_{11}$. We usually purposely select $R = R_1$ and $L = L_{11}$, so that we have $z_N = z_{N+} = z_{N-}$.

D/O Luo-converter elementary circuit is shown in Fig. 14.7. Its output voltages and currents (absolute values) are

$$V_{O+} = |V_{O-}| = \frac{k}{1 - k} V_I$$

$$I_{O+} = \frac{1 - k}{k} I_{I+}$$

and

$$I_{O-} = \frac{1 - k}{k} I_{I-}$$

When k is greater than 0.5, the output voltage can be higher than the input voltage.

The voltage transfer gain in CCM is

$$M_E = \frac{V_{O+}}{V_I} = \frac{|V_{O-}|}{V_I} = \frac{k}{1 - k} \tag{14.101}$$

The variation ratio of the output voltage v_{O+} in CCM is

$$\varepsilon_+ = \frac{\Delta v_{O+}/2}{V_{O+}} = \frac{k}{16 M_E} \frac{1}{f^2 C_O L_2} \tag{14.102}$$

The variation ratio of the output voltage v_{O-} in CCM is

$$\varepsilon_- = \frac{\Delta v_{O-}/2}{V_{O-}} = \frac{k}{128} \frac{1}{f^3 C_{11} C_{10} L_{12} R_1} \tag{14.103}$$

This converter may work in discontinuous conduction mode if the frequency f is small, conduction duty k is small, inductance L is small, and load current is high. The condition for DCM is

$$M_E \leq k \sqrt{\frac{z_N}{2}} \tag{14.104}$$

The output voltages in DCM are

$$V_O = V_{O+} = |V_{O-}| = k(1 - k) \frac{z_N}{2} V_I \quad \text{with} \quad \sqrt{\frac{z_N}{2}} \geq \frac{1}{1 - k} \tag{14.105}$$

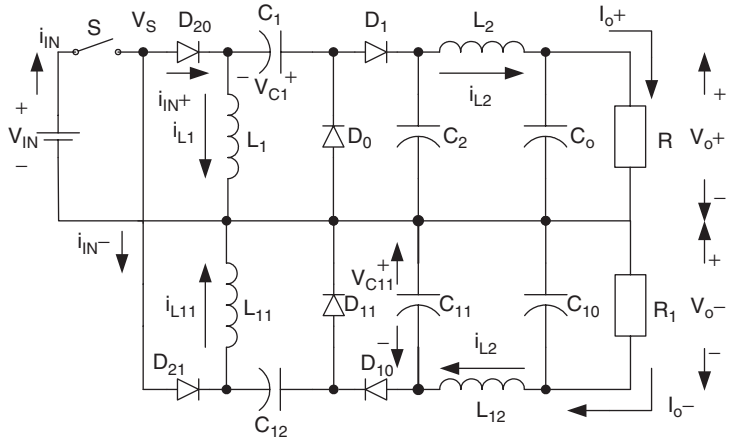

FIGURE 14.39 Double output Luo-converter self-lift circuit.

D/O Luo-converter self-lift circuit is shown in Fig. 14.39. Its output voltages and currents (absolute values) are

$$V_{O+} = |V_{O-}| = \frac{1}{1-k} V_I$$

$$I_{O+} = (1-k) I_{I+}$$

and

$$I_{O-} = (1-k) I_{I-}$$

The voltage transfer gain in CCM is

$$M_S = \frac{V_{O+}}{V_I} = \frac{|V_{O-}|}{V_I} = \frac{1}{1-k} \tag{14.106}$$

The variation ratio of the output voltage v_{O+} in CCM is

$$\varepsilon_+ = \frac{\Delta v_{O+}/2}{V_{O+}} = \frac{k}{128} \frac{1}{f^3 L_2 C_O C_2 R} \tag{14.107}$$

The variation ratio of the output voltage v_{O-} in CCM is

$$\varepsilon_- = \frac{\Delta v_{O-}/2}{V_{O-}} = \frac{k}{128} \frac{1}{f^3 C_{11} C_{10} L_{12} R_1} \tag{14.108}$$

This converter may work in discontinuous conduction mode if the frequency f is small, conduction duty k is small, inductance L is small, and load current is high. The condition for DCM is

$$M_S \le \sqrt{k} \sqrt{\frac{z_N}{2}} \tag{14.109}$$

The output voltages in DCM are

$$V_O = V_{O+} = |V_{O-}| = \left[1 + k^2 (1-k) \frac{z_N}{2}\right] V_I$$

$$\text{with} \quad \sqrt{\frac{k z_N}{2}} \ge \frac{1}{1-k} \tag{14.110}$$

D/O Luo-converter re-lift circuit is shown in Fig. 14.40. Its output voltages and currents (absolute values) are

$$V_{O+} = |V_{O-}| = \frac{2}{1-k} V_I$$

$$I_{O+} = \frac{1-k}{2} I_{I+}$$

and

$$I_{O-} = \frac{1-k}{2} I_{I-}$$

The voltage transfer gain in CCM is

$$M_R = \frac{V_{O+}}{V_I} = \frac{|V_{O-}|}{V_I} = \frac{2}{1-k} \tag{14.111}$$

The variation ratio of the output voltage v_{O+} in CCM is

$$\varepsilon_+ = \frac{\Delta v_{O+}/2}{V_{O+}} = \frac{k}{128} \frac{1}{f^3 L_2 C_O C_2 R} \tag{14.112}$$

The variation ratio of the output voltage v_{O-} in CCM is

$$\varepsilon_- = \frac{\Delta v_{O-}/2}{V_{O-}} = \frac{k}{128} \frac{1}{f^3 C_{11} C_{10} L_{12} R_1} \tag{14.113}$$

This converter may work in discontinuous conduction mode if the frequency f is small, conduction duty k is small,

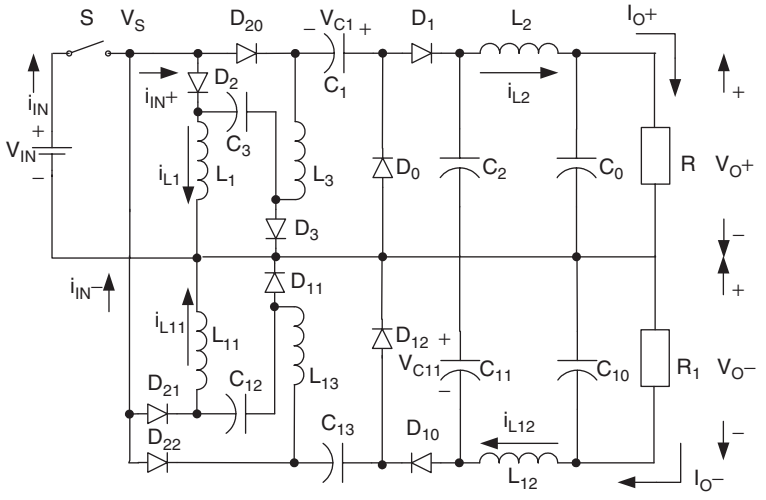

FIGURE 14.40 D/O Luo-converter re-lift circuit.

inductance L is small, and load current is high. The condition for DCM is

$$M_R \le \sqrt{kz_N} \tag{14.114}$$

The output voltages in DCM are

$$V_O = V_{O+} = |V_{O-}| = \left[2 + k^2(1-k)\frac{z_N}{2}\right] V_I \quad \text{with} \quad \sqrt{kz_N} \ge \frac{2}{1-k} \tag{14.115}$$

D/O Luo-converter triple-lift circuit is shown in Fig. 14.41. Its output voltages and currents (absolute values) are

$$V_{O+} = |V_{O-}| = \frac{3}{1-k} V_I$$

$$I_{O+} = \frac{1-k}{3} I_{I+}$$

and

$$I_{O-} = \frac{1-k}{3} I_{I-}$$

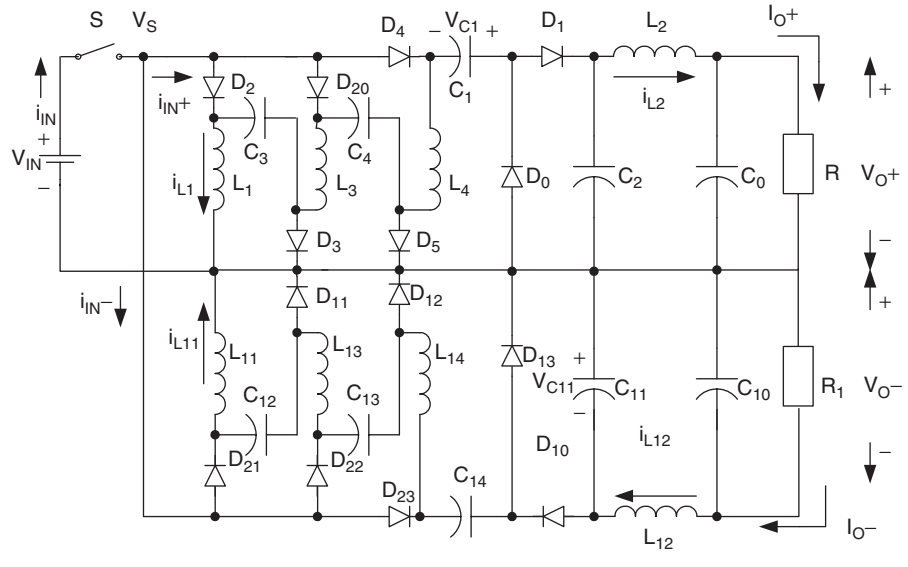

FIGURE 14.41 D/O Luo-converter triple-lift circuit.

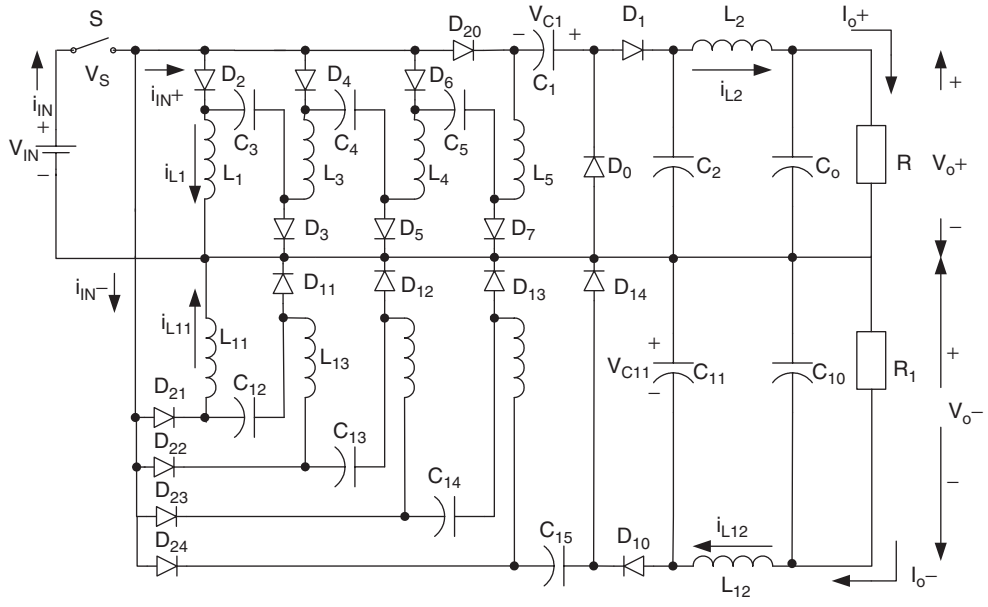

FIGURE 14.42 D/O Luo-converter quadruple-lift circuit.

The voltage transfer gain in CCM is

$$M_T = \frac{V_{O+}}{V_I} = \frac{|V_{O-}|}{V_I} = \frac{3}{1-k} \tag{14.116}$$

The variation ratio of the output voltage v_{O+} in CCM is

$$\varepsilon_+ = \frac{\Delta v_{O+}/2}{V_{O+}} = \frac{k}{128}\frac{1}{f^3 L_2 C_O C_2 R} \tag{14.117}$$

The variation ratio of the output voltage v_{O-} in CCM is

$$\varepsilon_- = \frac{\Delta v_{O-}/2}{V_{O-}} = \frac{k}{128}\frac{1}{f^3 C_{11} C_{10} L_{12} R_1} \tag{14.118}$$

This converter may work in discontinuous conduction mode if the frequency f is small, conduction duty k is small, inductance L is small, and load current is high. The condition for DCM is

$$M_T \le \sqrt{\frac{3kz_N}{2}} \tag{14.119}$$

The output voltages in DCM are

$$V_O = V_{O+} = |V_{O-}| = \left[3 + k^2(1-k)\frac{z_N}{2}\right] V_I$$

$$\text{with} \quad \sqrt{\frac{3kz_N}{2}} \ge \frac{3}{1-k} \tag{14.120}$$

D/O Luo-converter quadruple-lift circuit is shown in Fig. 14.42. Its output voltages (absolute values) are

$$V_{O+} = |V_{O-}| = \frac{4}{1-k} V_I$$

$$I_{O+} = \frac{1-k}{4} I_{I+}$$

and

$$I_{O-} = \frac{1-k}{4} I_{I-}$$

The voltage transfer gain in CCM is

$$M_Q = \frac{V_{O+}}{V_I} = \frac{|V_{O-}|}{V_I} = \frac{4}{1-k} \tag{14.121}$$

The variation ratio of the output voltage v_{O+} in CCM is

$$\varepsilon_+ = \frac{\Delta v_{O+}/2}{V_{O+}} = \frac{k}{128}\frac{1}{f^3 L_2 C_O C_2 R} \tag{14.122}$$

The variation ratio of the output voltage v_{O-} in CCM is

$$\varepsilon_- = \frac{\Delta v_{O-}/2}{V_{O-}} = \frac{k}{128}\frac{1}{f^3 C_{11} C_{10} L_{12} R_1} \tag{14.123}$$

This converter may work in discontinuous conduction mode if the frequency f is small, conduction duty k is small,

inductance L is small, and load current is high. The condition for DCM is

$$M_Q \le \sqrt{2kz_N} \tag{14.124}$$

The output voltages in DCM are

$$V_O = V_{O+} = |V_{O-}| = \left[4 + k^2(1-k)\frac{z_N}{2}\right] V_I$$

$$\text{with} \quad \sqrt{2kz_N} \ge \frac{4}{1-k} \tag{14.125}$$

Summary for all D/O Luo-converters:

$$M = \frac{V_{O+}}{V_I} = \frac{|V_{O-}|}{V_I}; \quad L = \frac{L_1 L_2}{L_1 + L_2}; \quad L = L_{11}; \quad R = R_1;$$

$$z_{N+} = \frac{R}{fL}; \quad z_{N-} = \frac{R_1}{fL_{11}}$$

so that

$$z_N = z_{N+} = z_{N-}$$

To write common formulas for all circuits parameters, we define that subscript $j = 0$ for the elementary circuit, $j = 1$ for the self-lift circuit, $j = 2$ for the re-lift circuit, $j = 3$ for the triple-lift circuit, $j = 4$ for the quadruple-lift circuit, and so on. The voltage transfer gain is

$$M_j = \frac{k^{h(j)}[j + h(j)]}{1-k} \tag{14.126}$$

The variation ratio of the output voltage v_{O+} in CCM is

$$\varepsilon_{+j} = \frac{\Delta v_{O+}/2}{V_{O+}} = \frac{k}{128}\frac{1}{f^3 L_2 C_O C_2 R} \tag{14.127}$$

The variation ratio of the output voltage v_{O-} in CCM is

$$\varepsilon_{-j} = \frac{\Delta v_{O-}/2}{V_{O-}} = \frac{k}{128}\frac{1}{f^3 C_{11} C_{10} L_{12} R_1} \tag{14.128}$$

The condition for DCM is

$$\frac{k^{[1+h(j)]}}{M_j^2}\frac{j + h(j)}{2} z_N \ge 1 \tag{14.129}$$

The output voltage in DCM is

$$V_{O-j} = \left\{ j + k^{[2-h(j)]}\frac{1-k}{2} z_N \right\} V_I \tag{14.130}$$

where

$$h(j) = \begin{cases} 0 & if \quad j \ge 1 \\ 1 & if \quad j = 0 \end{cases}$$

is the **Hong** function.

14.5 Super-lift Luo-converters

Voltage-lift (VL) technique has been successfully applied in DC/DC converter's design. However, the output voltage of all VL converters increases in arithmetic progression stage-by-stage. Super-lift (SL) technique is more powerful than VL technique. The output voltage of all SL converters increases in geometric progression stage-by-stage. All super-lift converters are outstanding contributions in DC/DC conversion technology, and invented by Professor Luo and Dr. Ye in 2000–2003. There are four series SL Converters introduced in this section:

1. Positive output (P/O) super-lift Luo-converters;
2. Negative output (N/O) super-lift Luo-converters;
3. Positive output (P/O) cascade boost-converter;
4. Negative output (N/O) cascade boost-converter;

14.5.1 P/O Super-lift Luo-converters

There are several sub-series of P/O super-lift Luo-converters:

- Main series;
- Additional series;
- Enhanced series;
- Re-enhanced series;
- Multi-enhanced series.

We only introduce three circuits of main series and additional series.

P/O SL Luo-converter elementary circuit is shown in Fig. 14.43a. The equivalent circuits during switch on and switch off are shown in Figs. 14.43b and c. Its output voltage and current are

$$V_O = \frac{2-k}{1-k} V_I$$

and

$$I_O = \frac{1-k}{2-k} I_I$$

The voltage transfer gain is

$$M_E = \frac{V_O}{V_I} = \frac{2-k}{1-k} \tag{14.131}$$

The variation ratio of the output voltage v_O is

$$\varepsilon = \frac{\Delta v_O/2}{V_O} = \frac{k}{2RfC_2} \tag{14.132}$$

P/O SL Luo-converter re-lift circuit is shown in Fig. 14.44a. The equivalent circuits during switch on and switch off are

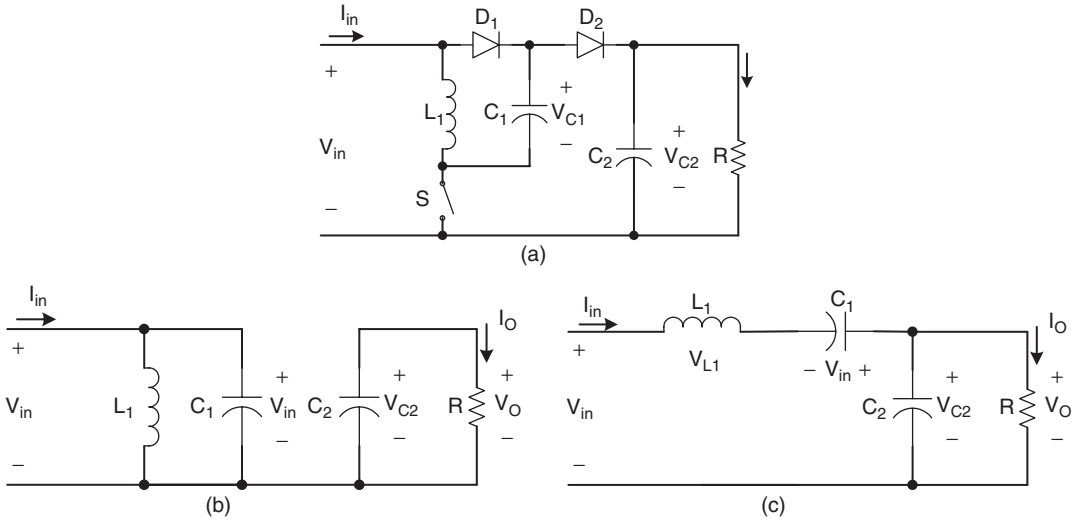

FIGURE 14.43 P/O SL Luo-converter elementary circuit: (a) circuit diagram; (b) switch on; and (c) switch off.

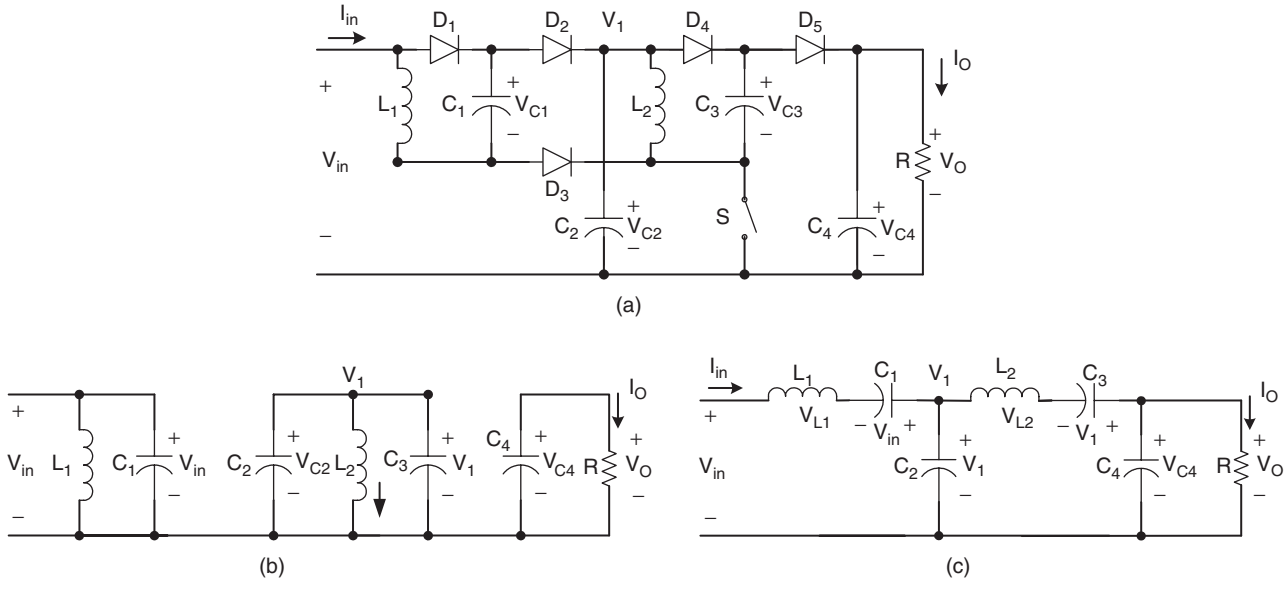

FIGURE 14.44 P/O SL Luo-converter re-lift circuit: (a) circuit diagram; (b) switch on; and (c) switch off.

shown in Figs. 14.44b and c. Its output voltage and current are

$$V_O = \left(\frac{2-k}{1-k}\right)^2 V_I$$

and

$$I_O = \left(\frac{1-k}{2-k}\right)^2 I_I$$

The voltage transfer gain is

$$M_R = \frac{V_O}{V_I} = \left(\frac{2-k}{1-k}\right)^2 \tag{14.133}$$

The variation ratio of the output voltage v_O is

$$\varepsilon = \frac{\Delta v_O/2}{V_O} = \frac{k}{2RfC_4} \tag{14.134}$$

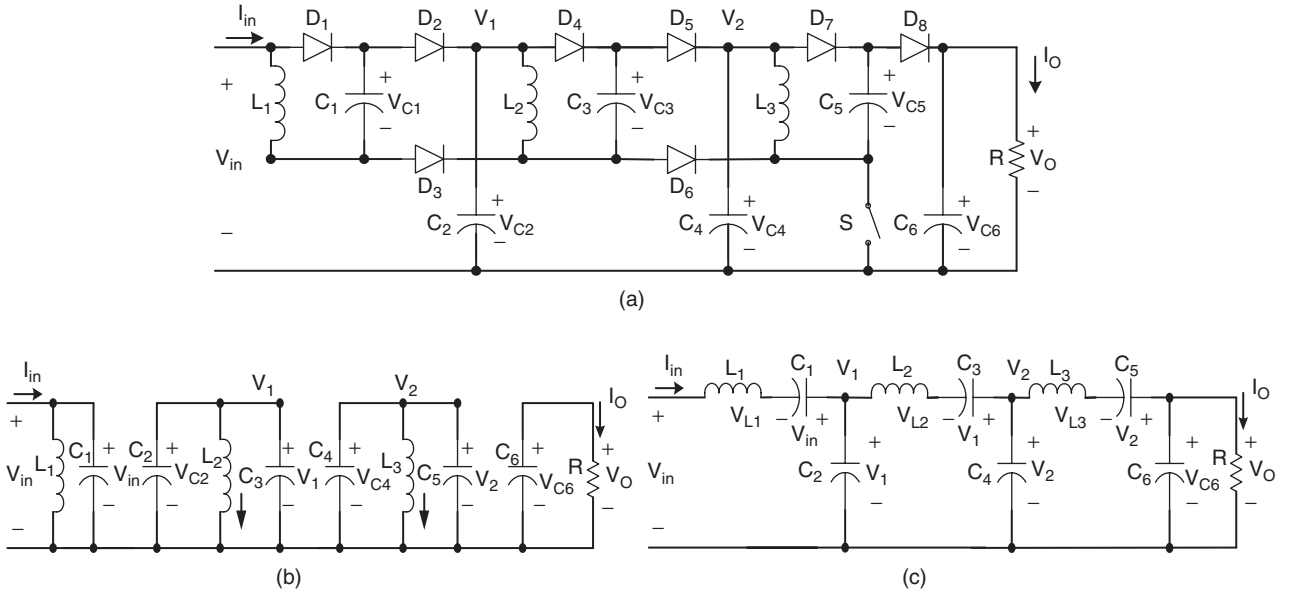

FIGURE 14.45 P/O SL Luo-converter triple-lift circuit: (a) circuit diagram; (b) switch on; and (c) switch off.

P/O SL Luo-converter triple-lift circuit is shown in Fig. 14.45a. The equivalent circuits during switch on and switch off are shown in Figs. 14.45b and c. Its output voltage and current are

$$V_O = \left(\frac{2-k}{1-k}\right)^3 V_I$$

and

$$I_O = \left(\frac{1-k}{2-k}\right)^3 I_I$$

The voltage transfer gain is

$$M_T = \frac{V_O}{V_I} = \left(\frac{2-k}{1-k}\right)^3 \tag{14.135}$$

The variation ratio of the output voltage v_O is

$$\varepsilon = \frac{\Delta v_O/2}{V_O} = \frac{k}{2RfC_6} \tag{14.136}$$

P/O SL Luo-converter additional circuit is shown in Fig. 14.46a. The equivalent circuits during switch on and switch off are shown in Figs. 14.46b and c. Its output voltage and current are

$$V_O = \frac{3-k}{1-k} V_I$$

and

$$I_O = \frac{1-k}{3-k} I_I$$

The voltage transfer gain is

$$M_A = \frac{V_O}{V_I} = \frac{3-k}{1-k} \tag{14.137}$$

The variation ratio of the output voltage v_O is

$$\varepsilon = \frac{\Delta v_O/2}{V_O} = \frac{k}{2RfC_{12}} \tag{14.138}$$

P/O SL Luo-converter additional re-lift circuit is shown in Fig. 14.47a. The equivalent circuits during switch on and switch off are shown in Figs. 14.47b and c. Its output voltage and current are

$$V_O = \frac{2-k}{1-k}\frac{3-k}{1-k} V_I$$

and

$$I_O = \frac{1-k}{2-k}\frac{1-k}{3-k} I_I$$

The voltage transfer gain is

$$M_{AR} = \frac{V_O}{V_I} = \frac{2-k}{1-k}\frac{3-k}{1-k} \tag{14.139}$$

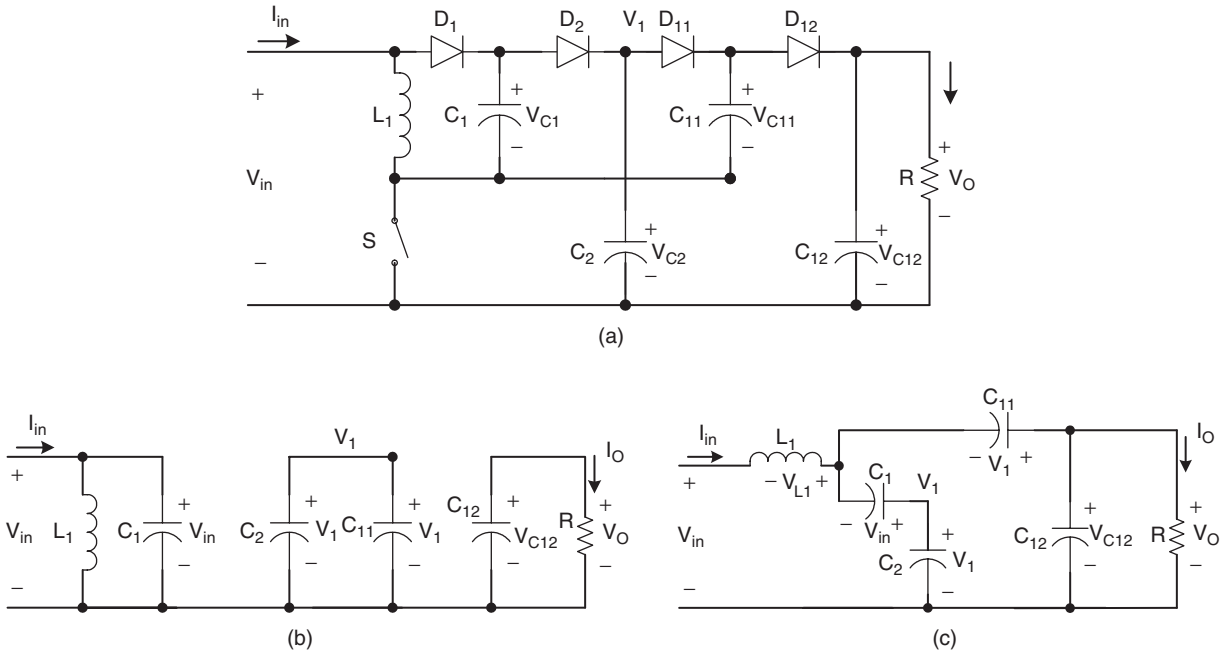

FIGURE 14.46 P/O SL Luo-converter additional circuit: (a) circuit diagram; (b) switch on; and (c) switch off.

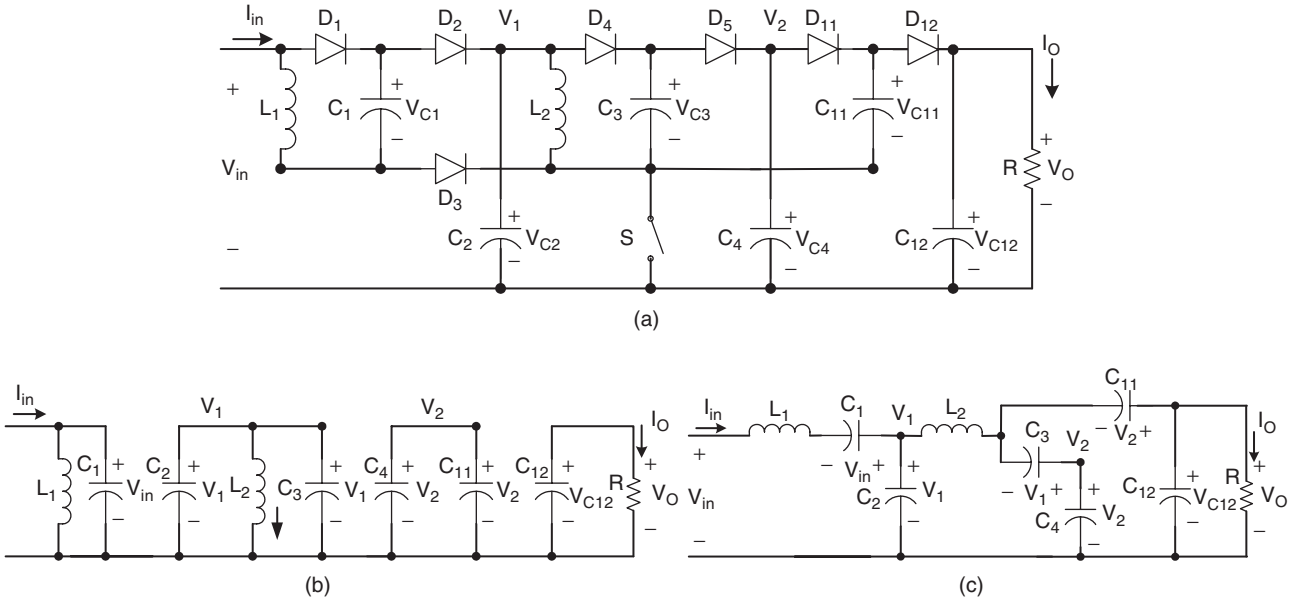

FIGURE 14.47 P/O SL Luo-converter additional re-lift circuit: (a) circuit diagram; (b) switch on; and (c) switch off.

The variation ratio of the output voltage v_O is

$$\varepsilon = \frac{\Delta v_O/2}{V_O} = \frac{k}{2RfC_{12}} \tag{14.140}$$

P/O SL Luo-converter additional triple-lift circuit is shown in Fig. 14.48a. The equivalent circuits during switch on and switch off are shown in Figs. 14.48b and c. Its output voltage and current are

$$V_O = \left(\frac{2-k}{1-k}\right)^2 \frac{3-k}{1-k} V_I$$

and

$$I_O = \left(\frac{1-k}{2-k}\right)^2 \frac{1-k}{3-k} I_I$$

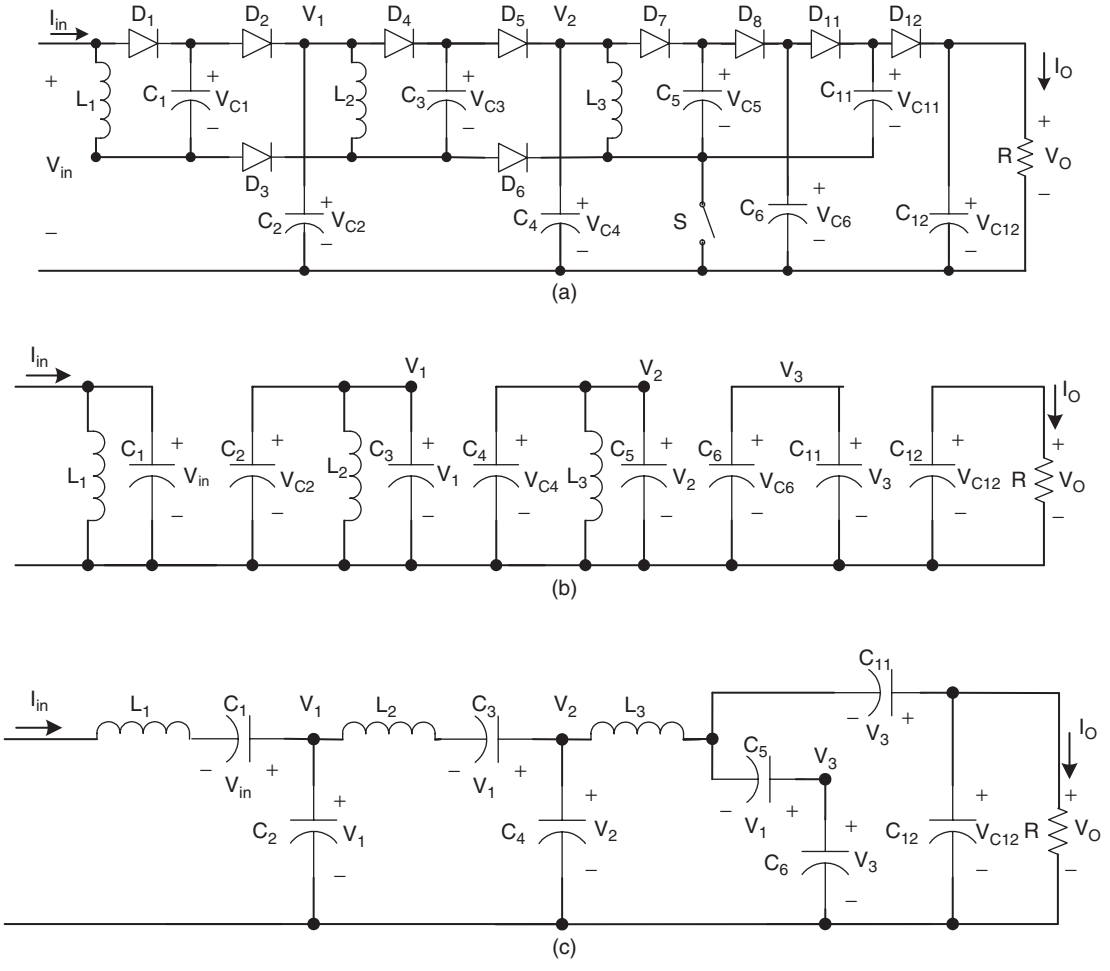

FIGURE 14.48 P/O SL Luo-converter additional triple-lift circuit: (a) circuit diagram; (b) switch on; and (c) switch off.

The voltage transfer gain is

$$M_{AT} = \frac{V_O}{V_I} = \left(\frac{2-k}{1-k}\right)^2 \frac{3-k}{1-k} \tag{14.141}$$

The variation ratio of the output voltage v_O is

$$\varepsilon = \frac{\Delta v_O/2}{V_O} = \frac{k}{2RfC_{12}} \tag{14.142}$$

14.5.2 N/O Super-lift Luo-converters

There are several subseries of N/O Super-lift Luo-converters:

- Main series;
- Additional series;
- Enhanced series;
- Re-enhanced series;
- Multi-enhanced series.

We only introduce three circuits of main series and additional series.

N/O SL Luo-converter elementary circuit is shown in Fig. 14.49. Its output voltage and current are

$$V_O = \left[\frac{2-k}{1-k} - 1\right] = \frac{1}{1-k} V_I$$

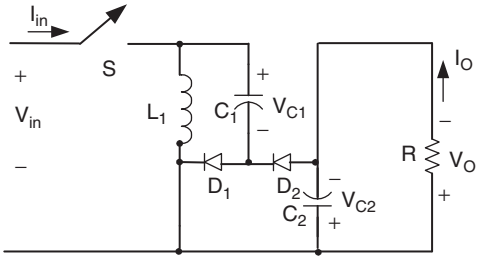

FIGURE 14.49 N/O SL Luo-converter elementary circuit.

and

$$I_O = (1-k)I_I$$

The voltage transfer gain is

$$M_E = \frac{V_O}{V_I} = \frac{1}{1-k} \tag{14.143}$$

The variation ratio of the output voltage v_O is

$$\varepsilon = \frac{\Delta v_O/2}{V_O} = \frac{k}{2RfC_2} \tag{14.144}$$

N/O SL Luo-converter re-lift circuit is shown in Fig. 14.50. Its output voltage and current are

$$V_O = \left[\left(\frac{2-k}{1-k}\right)^2 - 1\right] V_I$$

and

$$I_O = \frac{I_I}{\left((2-k)/(1-k)\right)^2 - 1}$$

The voltage transfer gain is

$$M_R = \frac{V_O}{V_I} = \left(\frac{2-k}{1-k}\right)^2 - 1 \tag{14.145}$$

The variation ratio of the output voltage v_O is

$$\varepsilon = \frac{\Delta v_O/2}{V_O} = \frac{k}{2RfC_4} \tag{14.146}$$

N/O SL Luo-converter triple-lift circuit is shown in Fig. 14.51. Its output voltage and current are

$$V_O = \left[\left(\frac{2-k}{1-k}\right)^3 - 1\right] V_I$$

and

$$I_O = \frac{I_I}{\left((2-k)/(1-k)\right)^3 - 1}$$

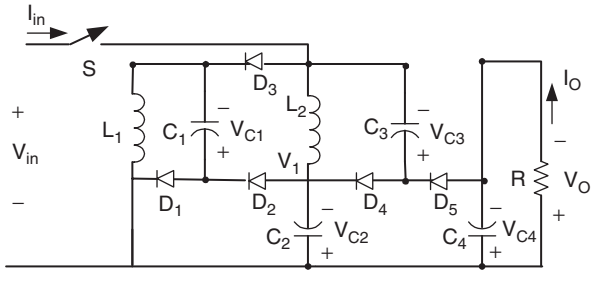

FIGURE 14.50 N/O SL Luo-converter re-lift circuit.

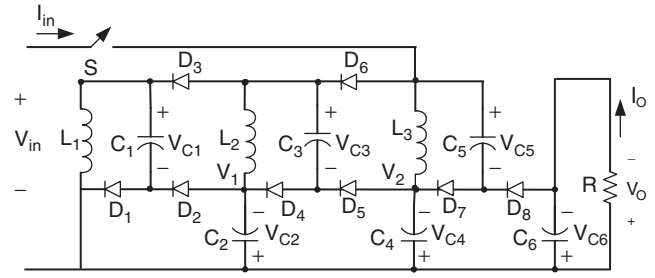

FIGURE 14.51 N/O SL Luo-converter triple-lift circuit.

The voltage transfer gain is

$$M_T = \frac{V_O}{V_I} = \left(\frac{2-k}{1-k}\right)^3 - 1 \tag{14.147}$$

The variation ratio of the output voltage v_O is

$$\varepsilon = \frac{\Delta v_O/2}{V_O} = \frac{k}{2RfC_6} \tag{14.148}$$

N/O SL Luo-converter additional circuit is shown in Fig. 14.52. Its output voltage and current are

$$V_O = \left[\frac{3-k}{1-k} - 1\right] V_I = \frac{2}{1-k} V_I$$

and

$$I_O = \frac{1-k}{2} I_I$$

The voltage transfer gain is

$$M_A = \frac{V_O}{V_I} = \frac{3-k}{1-k} - 1 = \frac{2}{1-k} \tag{14.149}$$

The variation ratio of the output voltage v_O is

$$\varepsilon = \frac{\Delta v_O/2}{V_O} = \frac{k}{2RfC_{12}} \tag{14.150}$$

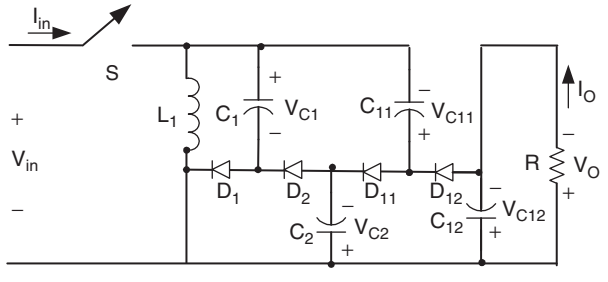

FIGURE 14.52 N/O SL Luo-converter additional circuit.

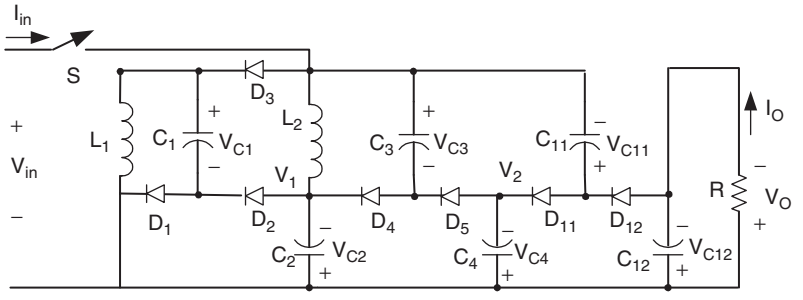

FIGURE 14.53 N/O SL Luo-converter additional re-lift circuit.

NO SL Luo-converter additional re-lift circuit is shown in Fig. 14.53. Its output voltage and current are

$$V_O = \left[\frac{2-k}{1-k}\frac{3-k}{1-k} - 1\right] V_I$$

and

$$I_O = \frac{I_I}{\big((2-k)/(1-k)\big)\big((3-k)/(1-k)\big) - 1}$$

The voltage transfer gain is

$$M_{AR} = \frac{V_O}{V_I} = \frac{2-k}{1-k}\frac{3-k}{1-k} - 1 \tag{14.151}$$

The variation ratio of the output voltage v_O is

$$\varepsilon = \frac{\Delta v_O/2}{V_O} = \frac{k}{2RfC_{12}} \tag{14.152}$$

N/O SL Luo-converter additional triple-lift circuit is shown in Fig. 14.54. Its output voltage and current are

$$V_O = \left[\left(\frac{2-k}{1-k}\right)^2 \frac{3-k}{1-k} - 1\right] V_I$$

and

$$I_O = \frac{I_I}{\big((2-k)/(1-k)\big)^2\big((3-k)/(2-k)\big) - 1}$$

The voltage transfer gain is

$$M_{AT} = \frac{V_O}{V_I} = \left(\frac{2-k}{1-k}\right)^2 \frac{3-k}{1-k} - 1 \tag{14.153}$$

The variation ratio of the output voltage v_O is

$$\varepsilon = \frac{\Delta v_O/2}{V_O} = \frac{k}{2RfC_{12}} \tag{14.154}$$

14.5.3 P/O Cascade Boost-converters

There are several subseries of P/O cascade boost-converters (CBC):

- Main series;
- Additional series;
- Double series;
- Triple series;
- Multiple series.

We only introduce three circuits of main series and additional series.

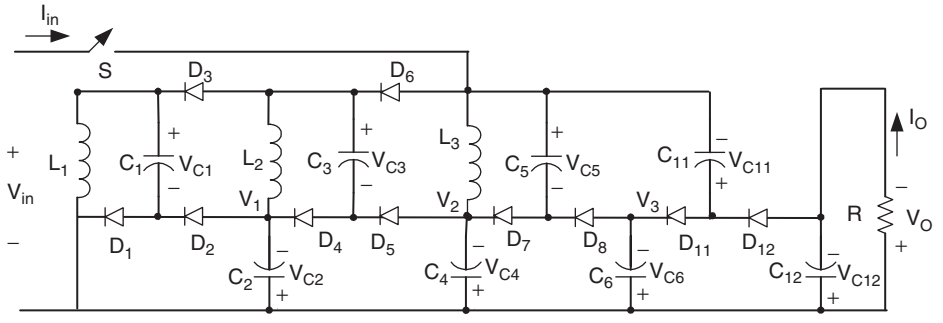

FIGURE 14.54 N/O SL Luo-converter additional triple-lift circuit.

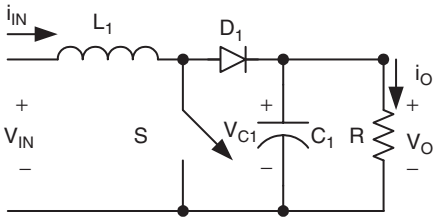

FIGURE 14.55 P/O CBC elementary circuit.

P/O CBC elementary circuit is shown in Fig. 14.55. Its output voltage and current are

$$V_O = \frac{1}{1-k} V_I$$

and

$$I_O = (1-k) I_I$$

The voltage transfer gain is

$$M_E = \frac{V_O}{V_I} = \frac{1}{1-k} \tag{14.155}$$

The variation ratio of the output voltage v_O is

$$\varepsilon = \frac{\Delta v_O/2}{V_O} = \frac{k}{2RfC_1} \tag{14.156}$$

P/O CBC two-stage circuit is shown in Fig. 14.56. Its output voltage and current are

$$V_O = \left(\frac{1}{1-k}\right)^2 V_I$$

and

$$I_O = (1-k)^2 I_I$$

The voltage transfer gain is

$$M_2 = \frac{V_O}{V_I} = \left(\frac{1}{1-k}\right)^2 \tag{14.157}$$

The variation ratio of the output voltage v_O is

$$\varepsilon = \frac{\Delta v_O/2}{V_O} = \frac{k}{2RfC_2} \tag{14.158}$$

P/O CBC three-stage circuit is shown in Fig. 14.57. Its output voltage and current are

$$V_O = \left(\frac{1}{1-k}\right)^3 V_I$$

and

$$I_O = (1-k)^3 I_I$$

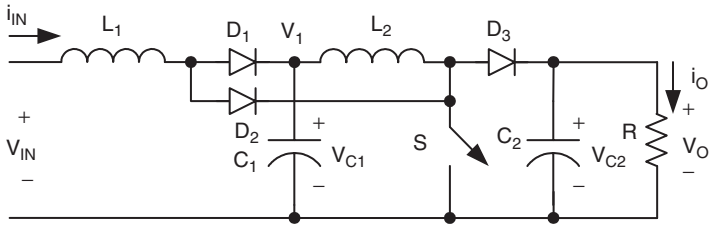

FIGURE 14.56 P/O CBC two-stage circuit.

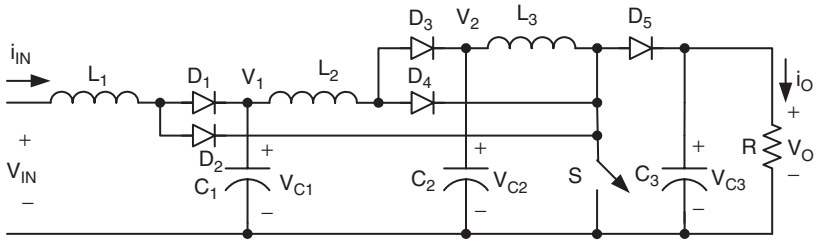

FIGURE 14.57 P/O CBC three-stage circuit.

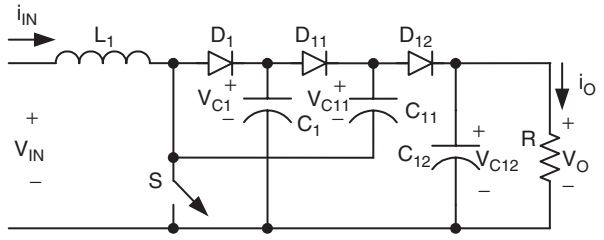

FIGURE 14.58 P/O CBC additional circuit.

The voltage transfer gain is

$$M_3 = \frac{V_O}{V_I} = \left(\frac{1}{1-k}\right)^3 \tag{14.159}$$

The variation ratio of the output voltage v_O is

$$\varepsilon = \frac{\Delta v_O/2}{V_O} = \frac{k}{2RfC_3} \tag{14.160}$$

P/O CBC additional circuit is shown in Fig. 14.58. Its output voltage and current are

$$V_O = \frac{2}{1-k} V_I$$

and

$$I_O = \frac{1-k}{2} I_I$$

The voltage transfer gain is

$$M_A = \frac{V_O}{V_I} = \frac{2}{1-k} \tag{14.161}$$

The variation ratio of the output voltage v_O is

$$\varepsilon = \frac{\Delta v_O/2}{V_O} = \frac{k}{2RfC_{12}} \tag{14.162}$$

P/O CBC additional two-stage circuit is shown in Fig. 14.59. Its output voltage and current are

$$V_O = 2\left(\frac{1}{1-k}\right)^2 V_I$$

and

$$I_O = \frac{(1-k)^2}{2} I_I$$

The voltage transfer gain is

$$M_{A2} = \frac{V_O}{V_I} = 2\left(\frac{1}{1-k}\right)^2 \tag{14.163}$$

The variation ratio of the output voltage v_O is

$$\varepsilon = \frac{\Delta v_O/2}{V_O} = \frac{k}{2RfC_{12}} \tag{14.164}$$

P/O CBC additional three-stage circuit is shown in Fig. 14.60. Its output voltage and current are

$$V_O = 2\left(\frac{1}{1-k}\right)^3 V_I$$

and

$$I_O = \frac{(1-k)^3}{2} I_I$$

The voltage transfer gain is

$$M_{A3} = \frac{V_O}{V_I} = 2\left(\frac{1}{1-k}\right)^3 \tag{14.165}$$

The variation ratio of the output voltage v_O is

$$\varepsilon = \frac{\Delta v_O/2}{V_O} = \frac{k}{2RfC_{12}} \tag{14.166}$$

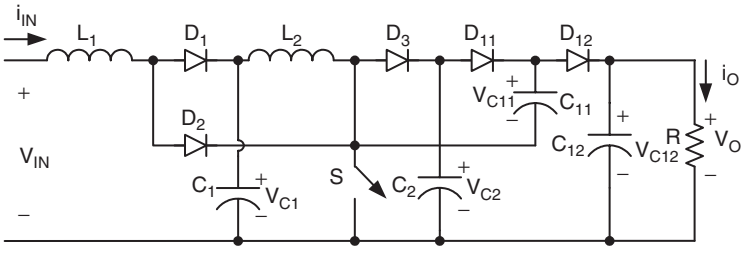

FIGURE 14.59 P/O CBC additional two-stage circuit.

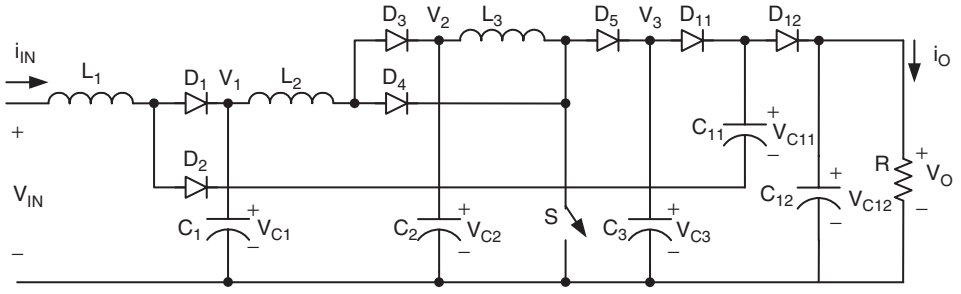

FIGURE 14.60 P/O CBC additional three-stage circuit.

14.5.4 N/O Cascade Boost-converters

There are several subseries of N/O CBC:

- Main series;
- Additional series;
- Double series;
- Triple series;
- Multiple series.

We only introduce three circuits of main series and additional series.

N/O CBC elementary circuit is shown in Fig. 14.61. Its output voltage and current are

$$V_O = \left[\frac{1}{1-k} - 1\right] V_I = \frac{k}{1-k} V_I$$

and

$$I_O = \frac{1-k}{k} I_I$$

The voltage transfer gain is

$$M_E = \frac{V_O}{V_I} = \frac{k}{1-k} \tag{14.167}$$

The variation ratio of the output voltage v_O is

$$\varepsilon = \frac{\Delta v_O/2}{V_O} = \frac{k}{2RfC_1} \tag{14.168}$$

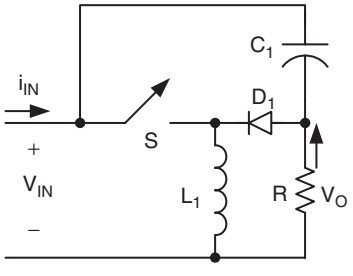

FIGURE 14.61 N/O CBC elementary circuit.

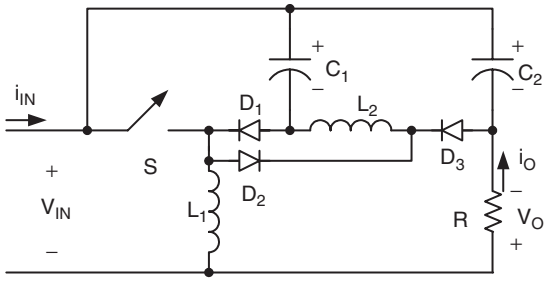

FIGURE 14.62 N/O CBC two-stage circuit.

N/O CBC two-stage circuit is shown in Fig. 14.62. Its output voltage and current are

$$V_O = \left[\left(\frac{1}{1-k}\right)^2 - 1\right] V_I$$

and

$$I_O = \frac{I_I}{\left(1/(1-k)\right)^2 - 1}$$

The voltage transfer gain is

$$M_2 = \frac{V_O}{V_I} = \left(\frac{1}{1-k}\right)^2 - 1 \tag{14.169}$$

The variation ratio of the output voltage v_O is

$$\varepsilon = \frac{\Delta v_O/2}{V_O} = \frac{k}{2RfC_2} \tag{14.170}$$

N/O CBC three-stage circuit is shown in Fig. 14.63. Its output voltage and current are

$$V_O = \left[\left(\frac{1}{1-k}\right)^3 - 1\right] V_I$$

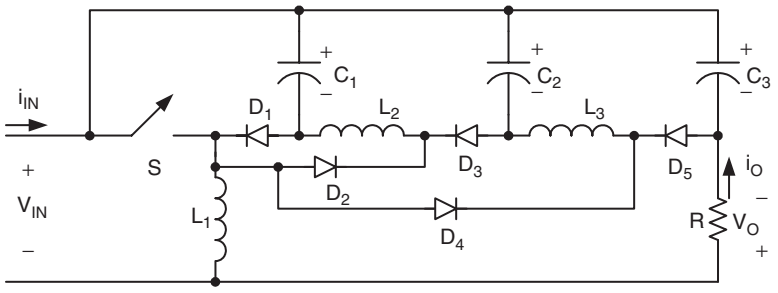

FIGURE 14.63 N/O CBC three-stage circuit.

and

$$I_O = \frac{I_I}{\left(1/(1-k)\right)^3 - 1}$$

The voltage transfer gain is

$$M_3 = \frac{V_O}{V_I} = \left(\frac{1}{1-k}\right)^3 - 1 \tag{14.171}$$

The variation ratio of the output voltage v_O is

$$\varepsilon = \frac{\Delta v_O/2}{V_O} = \frac{k}{2RfC_3} \tag{14.172}$$

N/O CBC additional circuit is shown in Fig. 14.64. Its output voltage and current are

$$V_O = \left[\frac{2}{1-k} - 1\right] V_I = \frac{1+k}{1-k} V_I$$

and

$$I_O = \frac{1-k}{1+k} I_I$$

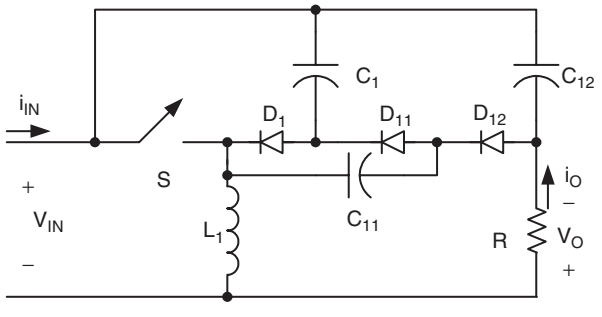

FIGURE 14.64 N/O CBC additional circuit.

The voltage transfer gain is

$$M_A = \frac{V_O}{V_I} = \frac{1+k}{1-k} \tag{14.173}$$

The variation ratio of the output voltage v_O is

$$\varepsilon = \frac{\Delta v_O/2}{V_O} = \frac{k}{2RfC_{12}} \tag{14.174}$$

N/O CBC additional two-stage circuit is shown in Fig. 14.65. Its output voltage and current are

$$V_O = \left[2\left(\frac{1}{1-k}\right)^2 - 1\right] V_I$$

and

$$I_O = \frac{I_I}{2\left(1/(1-k)\right)^2 - 1}$$

The voltage transfer gain is

$$M_{A2} = \frac{V_O}{V_I} = 2\left(\frac{1}{1-k}\right)^2 - 1 \tag{14.175}$$

The variation ratio of the output voltage v_O is

$$\varepsilon = \frac{\Delta v_O/2}{V_O} = \frac{k}{2RfC_{12}} \tag{14.176}$$

N/O CBC additional three-stage circuit is shown in Fig. 14.66. Its output voltage and current are

$$V_O = \left[2\left(\frac{1}{1-k}\right)^3 - 1\right] V_I$$

and

$$I_O = \frac{I_I}{2\left(1/(1-k)\right)^3 - 1}$$

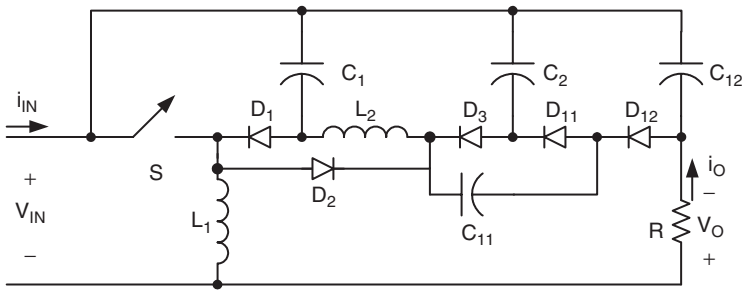

FIGURE 14.65 N/O CBC additional two-stage circuit.

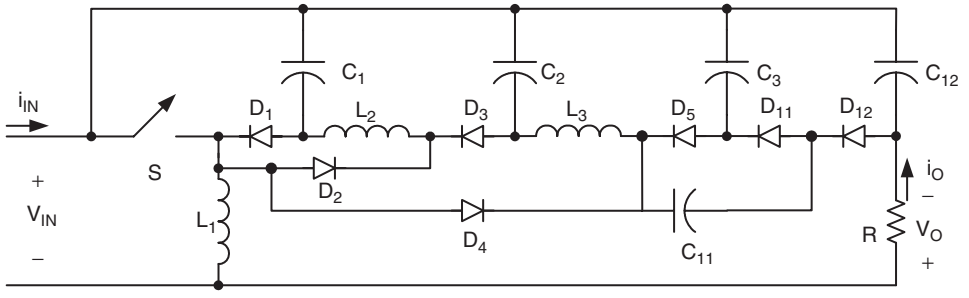

FIGURE 14.66 N/O CBC additional three-stage circuit.

The voltage transfer gain is

$$M_{A3} = \frac{V_O}{V_I} = 2\left(\frac{1}{1-k}\right)^3 - 1 \tag{14.177}$$

The variation ratio of the output voltage v_O is

$$\varepsilon = \frac{\Delta v_O/2}{V_O} = \frac{k}{2RfC_{12}} \tag{14.178}$$

14.6 Ultra-lift Luo-converters

Ultra-lift (UL) Luo-converter performs very high voltage transfer gain conversion. Its voltage transfer gain is the product of those of VL Luo-converter and SL Luo-converter.

We know that the gain of P/O VL Luo-converters (as in Eq. (14.52)) is

$$M = \frac{V_O}{V_I} = \frac{k^{h(n)}[n + h(n)]}{1-k}$$

where n is the stage number, $h(n)$ (as in Eq. (14.56)) is the Hong function.

$$h(n) = \begin{cases} 1 & n = 0 \\ 0 & n > 0 \end{cases}$$

(from Eq. (14.32)) $n = 0$ for the elementary circuit with the voltage transfer gain

$$M_E = \frac{V_O}{V_I} = \frac{k}{1-k}$$

The voltage transfer gain of P/O SL Luo-converters is

$$M = \frac{V_O}{V_I} = \left(\frac{j+2-k}{1-k}\right)^n \tag{14.179}$$

where n is the stage number, j is the multiple-enhanced number. $n = 1$ and $j = 0$ for the elementary circuit with gain (as in Eq. (14.131))

$$M_E = \frac{V_O}{V_I} = \frac{2-k}{1-k}$$

The circuit diagram of UL Luo-converter is shown in Fig. 14.67a, which consists of one switch S, two inductors L_1 and L_2, two capacitors C_1 and C_2, three diodes, and the load R. Its switch-on equivalent circuit is shown in Fig. 14.67b. Its switch-off equivalent circuit for the continuous conduction mode is shown in Fig. 14.67c and switch-off equivalent circuit for the discontinuous conduction mode is shown in Fig. 14.67d.

14.6.1 Continuous Conduction Mode

Referring to Figs. 14.67b and c, we have got the current i_{L1} increases with the slope $+V_I/L_1$ during switch on, and

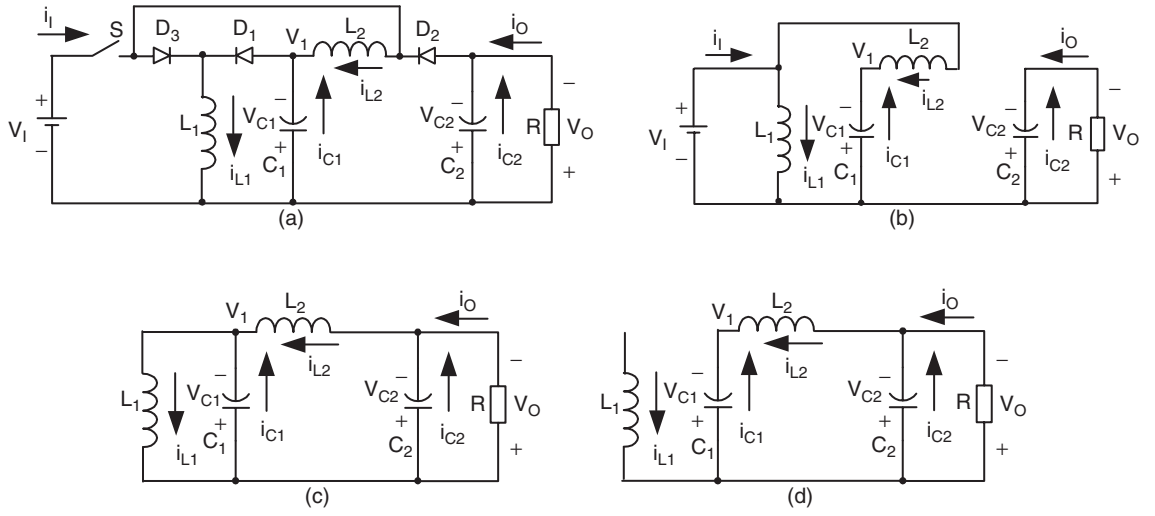

FIGURE 14.67 Ultra-lift (UL) Luo-converter: (a) circuit diagram; (b) switch on; (c) switch off in CCM; and (d) switch off in DCM.

decreases with the slope $-V_1/L_1$ during switch off. In the steady state, the current increment is equal to the decrement in a whole period T. The relation below is obtained

$$kT\frac{V_I}{L_1} = (1-k)T\frac{V_1}{L_1} \tag{14.180}$$

Thus,

$$V_{C1} = V_1 = \frac{k}{1-k}V_I \tag{14.181}$$

The current i_{L2} increases with the slope $+(V_I - V_1)/L_2$ during switch on, and decreases with the slope $-(V_1 - V_O)/L_2$ during switch off. In the steady state, the current increment is equal to the decrement in a whole period T. We obtain the relation below

$$kT\frac{V_I + V_1}{L_2} = (1-k)T\frac{V_O - V_1}{L_2} \tag{14.182}$$

$$V_O = V_{C2} = \frac{2-k}{1-k}V_1 = \frac{k}{1-k}\frac{2-k}{1-k}V_I = \frac{k(2-k)}{(1-k)^2}V_I \tag{14.183}$$

$$I_O = \frac{(1-k)^2}{k(2-k)}I_I \tag{14.184}$$

The voltage transfer gain is

$$M = \frac{V_O}{V_I} = \frac{k(2-k)}{(1-k)^2} = \frac{k}{1-k}\frac{2-k}{1-k} = M_{E-VL} \times M_{E-SL} \tag{14.185}$$

From Eq. (14.185) we can see that the voltage transfer gain of UL Luo-converter is very high which is the product of those of VL Luo-converter and SL Luo-converter. We list the transfer gains of various converters in Table 14.3 for reference.

TABLE 14.3 Comparison of various converters gains

k	0.2	0.33	0.5	0.67	0.8	0.9
Buck	0.2	0.33	0.5	0.67	0.8	0.9
Boost	1.25	1.5	2	3	5	10
Buck–Boost	0.25	0.5	1	2	4	9
VL Luo-converter	0.25	0.5	1	2	4	9
SL Luo-converter	2.25	2.5	3	4	6	11
UL Luo-converter	0.56	1.25	3	8	24	99

The variation of inductor current i_{L1} is

$$\Delta i_{L1} = kT\frac{V_I}{L_1} \tag{14.186}$$

and its variation ratio is

$$\xi_1 = \frac{\Delta i_{L1}/2}{I_{L1}} = \frac{k(1-k)^2 TV_I}{2L_1 I_2} = \frac{k(1-k)^2 TR}{2L_1 M} = \frac{(1-k)^4 TR}{2(2-k)fL_1} \tag{14.187}$$

The variation of inductor current i_{L2} is

$$\Delta i_{L2} = \frac{kTV_I}{(1-k)L_2} \tag{14.188}$$

and its variation ratio is

$$\xi_2 = \frac{\Delta i_{L2}/2}{I_{L2}} = \frac{kTV_I}{2L_2 I_2} = \frac{kTR}{2L_2 M} = \frac{(1-k)^2 TR}{2(2-k)fL_2} \tag{14.189}$$

The variation of capacitor voltage v_{C1} is

$$\Delta v_{C1} = \frac{\Delta Q_{C1}}{C_1} = \frac{kTI_{L2}}{C_1} = \frac{kTI_O}{(1-k)C_1} \tag{14.190}$$

and its variation ratio is

$$\sigma_1 = \frac{\Delta v_{C1}/2}{V_{C1}} = \frac{kTI_O}{2(1-k)V_1C_1} = \frac{k(2-k)}{2(1-k)^2 fC_1R} \tag{14.191}$$

The variation of capacitor voltage v_{C2} is

$$\Delta v_{C2} = \frac{\Delta Q_{C2}}{C_2} = \frac{kTI_O}{C_2} \tag{14.192}$$

and its variation ratio is

$$\varepsilon = \sigma_2 = \frac{\Delta v_{C2}/2}{V_{C2}} = \frac{kTI_O}{2V_OC_2} = \frac{k}{2fC_2R} \tag{14.193}$$

From the analysis and calculations, we can see that all variations are very small. A design example is that $V_I = 10\,\text{V}$, $L_1 = L_2 = 1\,\text{mH}$, $C_1 = C_2 = 1\,\mu\text{F}$, $R = 3000\,\Omega$, $f = 50\,\text{kHz}$, and conduction duty cycle k varies from 0.1 to 0.9. We then obtain the output voltage variation ratio $\boldsymbol{\varepsilon}$, which is less than 0.003. The output voltage is very smooth DC voltage nearly no ripple.

14.6.2 Discontinuous Conduction Mode

Referring to Fig. 14.67d, we have got the current i_{L1} decreases to zero before $t = T$, i.e. the current becomes zero before next time the switch turns on. The DCM operation condition is defined as

$$\xi \geq 1$$

or

$$\xi_1 = \frac{k(1-k)^2TR}{2L_1M} = \frac{(1-k)^4TR}{2(2-k)fL_1} \geq 1 \tag{14.194}$$

The normalized impedance Z_N is,

$$Z_N = \frac{R}{fL_1} \tag{14.195}$$

We define the filling factor $\boldsymbol{m}$ to describe the current exists time. For DCM operation, $0 < m \leq 1$,

$$m = \frac{1}{\xi_1} = \frac{2L_1G}{k(1-k)^2TR} = \frac{2(2-k)}{(1-k)^4Z_N} \tag{14.196}$$

$$kT\frac{V_I}{L_1} = (1-k)mT\frac{V_1}{L_1}$$

Thus,

$$V_{C1} = V_1 = \frac{k}{(1-k)m}V_I \tag{14.197}$$

We finally obtain the relation below

$$kT\frac{V_I + V_1}{L_2} = (1-k)T\frac{V_O - V_1}{L_2} \tag{14.198}$$

$$V_O = V_{C2} = \frac{2-k}{1-k}V_1 = \frac{k(2-k)}{m(1-k)^2}V_I \tag{14.199}$$

The voltage transfer gain in DCM is higher than that in CCM.

$$M_{DCM} = \frac{V_O}{V_I} = \frac{k(2-k)}{m(1-k)^2} = \frac{M_{CCM}}{m} \quad \text{with } m < 1 \tag{14.200}$$

14.7 Multiple-quadrant Operating Luo-converters

Multiple-quadrant operating converters are the second-generation converters. These converters usually perform between two voltage sources: V_1 and V_2. Voltage source V_1 is proposed positive voltage and voltage V_2 is the load voltage. In the investigation both voltages are proposed constant voltage. Since V_1 and V_2 are constant values, voltage transfer gain is constant. Our interesting research will concentrate the working current, minimum conduction duty k_{min}, and the power transfer efficiency η.

Multiple-quadrant operating Luo-converters are the second-generation converters and they have three modes:

- Two-quadrant DC/DC Luo-converter in forward operation;
- Two-quadrant DC/DC Luo-converter in reverse operation;
- Four-quadrant DC/DC Luo-converter.

The two-quadrant DC/DC Luo-converter in forward operation has been derived from the positive output Luo-converter. It performs in the first-quadrant Q_I and the second-quadrant Q_{II} corresponding to the DC motor forward operation in motoring and regenerative braking states.

The two-quadrant DC/DC Luo-converter in reverse operation has been derived from the N/O Luo-converter. It performs in the third-quadrant Q_{III} and the fourth-quadrant Q_{IV} corresponding to the DC motor reverse operation in motoring and regenerative braking states.

The four-quadrant DC/DC Luo-converter has been derived from the double output Luo-converter. It performs four-quadrant operation corresponding to the DC motor forward

and reverse operation in motoring and regenerative braking states.

In the following analysis the input source and output load are usually constant voltages as shown, V_1 and V_2. Switches S_1 and S_2 in this diagram are power metal oxide semiconductor field effect transistor (MOSFET) devices, and they are driven by a PWM switching signal with repeating frequency $\boldsymbol{f}$ and conduction duty $\boldsymbol{k}$. In this paper the switch repeating period is $T = 1/f$, so that the switch-on period is kT and switch-off period is $(1-k)T$. The equivalent resistance is R for each inductor. During switch-on the voltage drop across the switches and diodes are V_S and V_D respectively.

14.7.1 Forward Two-quadrant DC/DC Luo-converter

Forward Two-quadrant (F 2Q) Luo-converter is shown in Fig. 14.68. The source voltage (V_1) and load voltage (V_2) are usually considered as constant voltages. The load can be a battery or motor back electromotive force (EMF). For example, the source voltage is 42 V and load voltage is +14 V. There are two modes of operation:

1. Mode A (Quadrant I): electrical energy is transferred from source side V_1 to load side V_2;
2. Mode B (Quadrant II): electrical energy is transferred from load side V_2 to source side V_1.

Mode A: The equivalent circuits during switch-on and -off periods are shown in Figs. 14.69a and b. The typical output voltage and current waveforms are shown in Fig. 14.69c. We have the output current I_2 as

$$I_2 = \frac{1-k}{k} I_1 \tag{14.201}$$

and

$$I_2 = \frac{V_1 - V_S - V_D - V_2((1-k)/k)}{R\left((k/(1-k)) + ((1-k)/k)\right)} \tag{14.202}$$

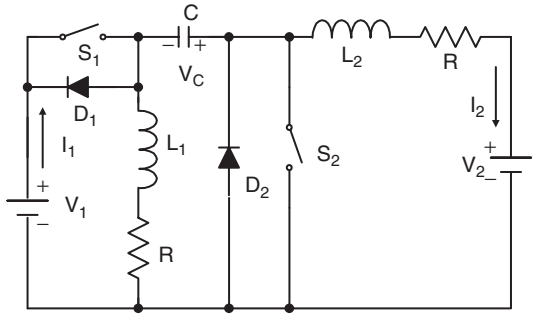

FIGURE 14.68 Forward two-quadrant operating Luo-converter.

The minimum conduction duty k corresponding to $I_2 = 0$ is

$$k_{min} = \frac{V_2}{V_1 + V_2 - V_S - V_D} \tag{14.203}$$

The power transfer efficiency is

$$\eta_A = \frac{P_O}{P_I} = \frac{V_2 I_2}{V_1 I_1}$$

$$= \frac{1}{1 + \left((V_S + V_D)/V_2\right)(k/(1-k)) + (RI_2/V_2)\left[1 + ((1-k)/k)^2\right]} \tag{14.204}$$

The variation ratio of capacitor voltage v_C is

$$\rho = \frac{\Delta v_C/2}{V_C} = \frac{(1-k)I_2}{2fC(V_1 - RI_2(1/(1-k)))} \tag{14.205}$$

The variation ratio of inductor current i_{L1} is

$$\xi_1 = \frac{\Delta i_{L1}/2}{I_{L1}} = k\frac{V_1 - V_S - RI_1}{2fL_1 I_1} \tag{14.206}$$

The variation ratio of inductor current i_{L2} is

$$\xi_2 = \frac{\Delta i_{L2}/2}{I_{L2}} = k\frac{V_1 - V_S - RI_1}{2fL_2 I_2} \tag{14.207}$$

The variation ratio of diode current i_{D2} is

$$\zeta_{D2} = \frac{\Delta i_{D2}/2}{I_{L1} + I_{L2}} = k\frac{V_1 - V_S - RI_1}{2fL(I_1 + I_2)} = k^2\frac{V_1 - V_S - RI_1}{2fLI_1} \tag{14.208}$$

If the diode current becomes zero before S_1 switch on again, the converter works in discontinuous region. The condition is

$$\zeta_{D2} = 1, \quad \text{i.e.} \quad k^2 = \frac{2fLI_1}{V_1 - V_S - RI_1} \tag{14.209}$$

Mode B: The equivalent circuits during switch-on and -off periods are shown in Figs. 14.70a and b. The typical output voltage and current waveforms are shown in Fig. 14.70c. We have the output current I_1 as

$$I_1 = \frac{1-k}{k} I_2 \tag{14.210}$$

and

$$I_1 = \frac{V_2 - (V_1 + V_S + V_D)((1-k)/k)}{R\left((k/(1-k)) + ((1-k)/k)\right)} \tag{14.211}$$

The minimum conduction duty k corresponding to $I_1 = 0$ is

$$k_{min} = \frac{V_1 + V_S + V_D}{V_1 + V_2 + V_S + V_D} \tag{14.212}$$

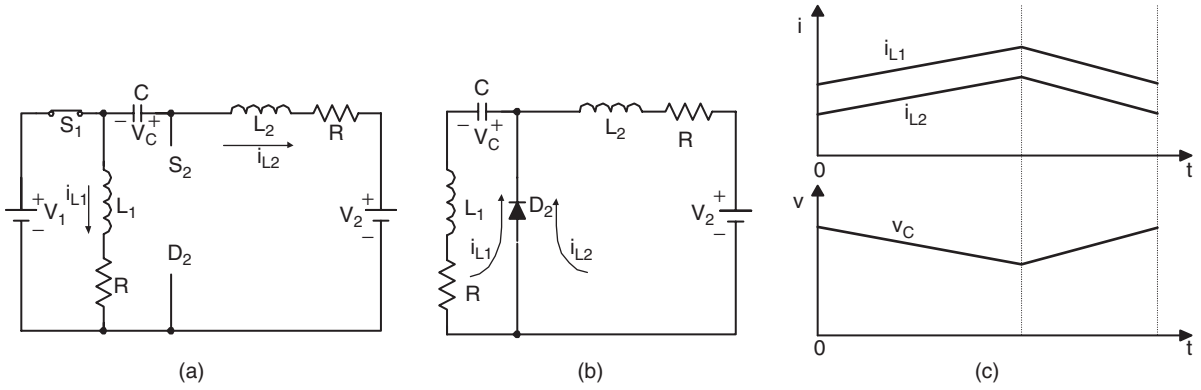

FIGURE 14.69 Mode A: (a) switch on; (b) switch off; and (c) waveforms.

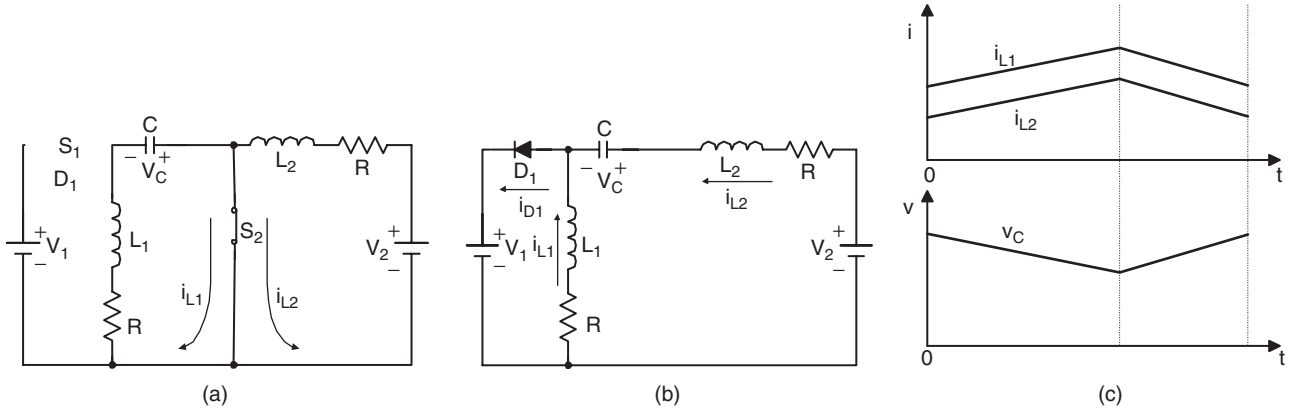

FIGURE 14.70 Mode B: (a) switch on; (b) switch off; and (c) waveforms.

The power transfer efficiency

$$\eta_B = \frac{P_O}{P_I} = \frac{V_1 I_1}{V_2 I_2}$$

$$= \frac{1}{1 + ((V_S + V_D)/V_1) + (RI_1/V_1)[1 + ((1-k)/k)^2]} \tag{14.213}$$

The variation ratio of capacitor voltage v_C is

$$\rho = \frac{\Delta v_C/2}{V_C} = \frac{kI_1}{2fC[(V_2/(1-k)) - V_1 - RI_1(k/(1-k)^2)]} \tag{14.214}$$

The variation ratio of inductor current i_{L1} is

$$\xi_1 = \frac{\Delta i_{L1}/2}{I_{L1}} = k\frac{V_2 - V_S - RI_2}{2fL_1 I_1} \tag{14.215}$$

The variation ratio of inductor current i_{L2} is

$$\xi_2 = \frac{\Delta i_{L2}/2}{I_{L2}} = k\frac{V_2 - V_S - RI_2}{2fL_2 I_2} \tag{14.216}$$

The variation ratio of diode current i_{D1} is

$$\zeta_{D1} = \frac{\Delta i_{D2}/2}{I_{L1} + I_{L2}} = k\frac{V_2 - V_S - RI_2}{2fL(I_1 + I_2)} = k^2\frac{V_2 - V_S - RI_2}{2fLI_2} \tag{14.217}$$

If the diode current becomes zero before S_2 switch on again, the converter works in discontinuous region. The condition is

$$\zeta_{D1} = 1, \quad \text{i.e.} \quad k^2 = \frac{2fLI_2}{V_2 - V_S - RI_2} \tag{14.218}$$

14.7.2 Two-quadrant DC/DC Luo-converter in Reverse Operation

Reverse two-quadrant operating (R 2Q) Luo-converter is shown in Fig. 14.71, and it consists of two switches with two passive diodes, two inductors and one capacitor. The source voltage (V_1) and load voltage (V_2) are usually considered as constant voltages. The load can be a battery or motor back EMF. For example, the source voltage is 42 V and load voltage

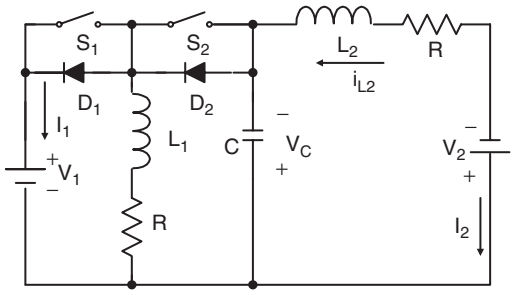

FIGURE 14.71 Reverse two-quadrant operating Luo-converter.

is −14 V. There are two modes of operation:

1. Mode C (Quadrant III): electrical energy is transferred from source side V_1 to load side $-V_2$;
2. Mode D (Quadrant IV): electrical energy is transferred from load side $-V_2$ to source side V_1.

Mode C: The equivalent circuits during switch-on and -off periods are shown in Figs. 14.72a and b. The typical output voltage and current waveforms are shown in Fig. 14.72c. We have the output current I_2 as

$$I_2 = \frac{1-k}{k} I_1 \tag{14.219}$$

and

$$I_2 = \frac{V_1 - V_S - V_D - V_2((1-k)/k)}{R\left[(1/(k(1-k))) + ((1-k)/k)\right]} \tag{14.220}$$

The minimum conduction duty k corresponding to $I_2 = 0$ is

$$k_{min} = \frac{V_2}{V_1 + V_2 - V_S - V_D} \tag{14.221}$$

The power transfer efficiency is

$$\eta_C = \frac{P_O}{P_I} = \frac{V_2 I_2}{V_1 I_1}$$

$$= \frac{1}{1 + ((V_S + V_D)/V_2)(k/(1-k)) + (RI_2/V_2)[1 + (1/(1-k))^2]} \tag{14.222}$$

The variation ratio of capacitor voltage v_C is

$$\rho = \frac{\Delta v_C/2}{V_C} = \frac{kI_2}{2fC\left[(k/(1-k))V_1 - ((RI_2)/(1-k)^2)\right]} \tag{14.223}$$

The variation ratio of inductor current i_{L1} is

$$\xi_1 = \frac{\Delta i_{L1}/2}{I_{L1}} = k\frac{V_1 - V_S - RI_1}{2fL_1 I_1} \tag{14.224}$$

The variation ratio of inductor current i_{D2} is

$$\zeta_{D2} = \xi_1 = \frac{\Delta i_{D2}/2}{I_{L1}} = k\frac{V_1 - V_S - RI_1}{2fL_1 I_1} \tag{14.225}$$

The variation ratio of inductor current i_{L2} is

$$\xi_2 = \frac{\Delta i_{L2}/2}{I_2} = \frac{k}{16f^2 CL_2} \tag{14.226}$$

If the diode current becomes zero before S_1 switch on again, the converter works in discontinuous region. The condition is

$$\zeta_{D2} = 1, \quad \text{i.e.} \quad k = \frac{2fL_1 I_1}{V_1 - V_S - RI_1} \tag{14.227}$$

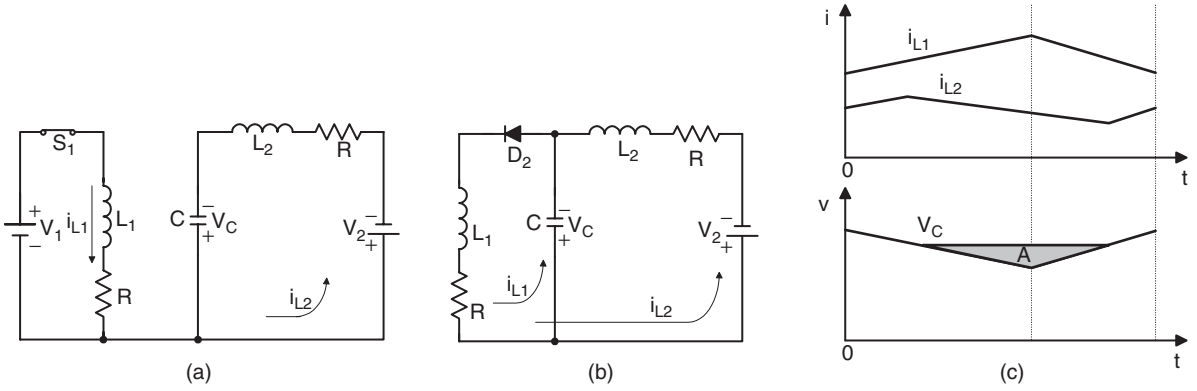

FIGURE 14.72 Mode C: (a) switch on; (b) switch off; and (c) waveforms.

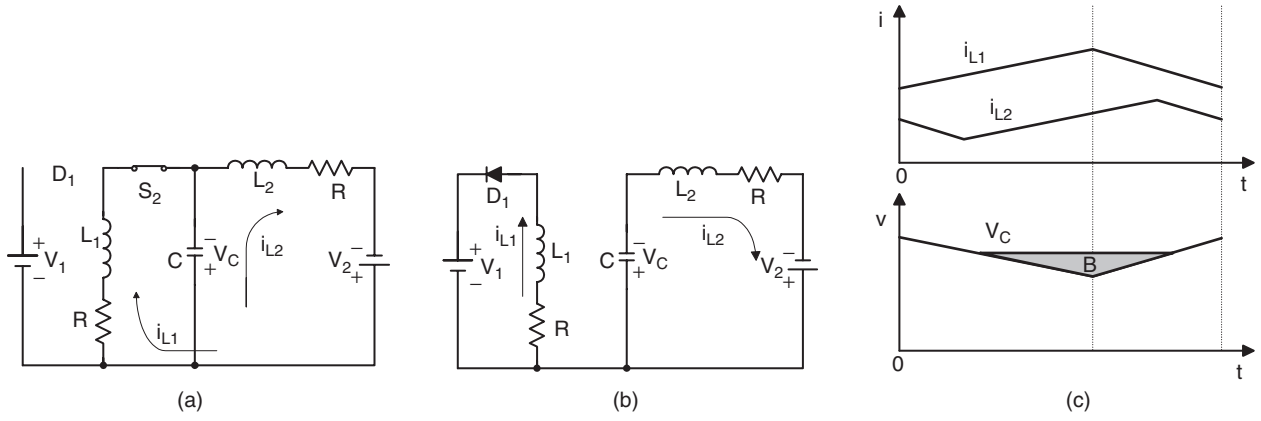

FIGURE 14.73 Mode D: (a) switch on; (b) switch off; and (c) waveforms.

Mode D: The equivalent circuits during switch-on and -off periods are shown in Figs. 14.73a and b. The typical output voltage and current waveforms are shown in Fig. 14.73c. We have the output current I_1 as

$$I_1 = \frac{1-k}{k} I_2 \tag{14.228}$$

and

$$I_1 = \frac{V_2 - (V_1 + V_S + V_D)((1-k)/k)}{R[(1/(k(1-k))) + (k/(1-k))]} \tag{14.229}$$

The minimum conduction duty k corresponding to $I_1 = 0$ is

$$k_{min} = \frac{V_1 + V_S + V_D}{V_1 + V_2 + V_S + V_D} \tag{14.230}$$

The power transfer efficiency is

$$\eta_D = \frac{P_O}{P_I} = \frac{V_1 I_1}{V_2 I_2} = \frac{1}{1 + ((V_S + V_D)/V_1) + (RI_1/V_1)[(1/(1-k)^2) + (k/(1-k))^2]} \tag{14.231}$$

The variation ratio of capacitor voltage v_C is

$$\rho = \frac{\Delta v_C/2}{V_C} = \frac{kI_1}{2fC\,[((1-k)/k)V_1 + ((RI_1)/(k(1-k)))]} \tag{14.232}$$

The variation ratio of inductor current i_{L1} is

$$\xi_1 = \frac{\Delta i_{L1}/2}{I_{L1}} = (1-k)\frac{V_2 - V_S - RI_2}{2fL_1 I_1} \tag{14.233}$$

And the variation ratio of inductor current i_{D1} is

$$\zeta_{D1} = \xi_1 = \frac{\Delta i_{D1}/2}{I_{L1}} = k\frac{V_2 - V_S - RI_2}{2fL_1 I_2} \tag{14.234}$$

The variation ratio of inductor current i_{L2} is

$$\xi_2 = \frac{\Delta i_{L2}/2}{I_2} = \frac{1-k}{16f^2 CL_2} \tag{14.235}$$

If the diode current becomes zero before S_2 switch on again, the converter works in discontinuous region. The condition is

$$\zeta_{D1} = 1, \quad \text{i.e.} \quad k = \frac{2fL_1 I_2}{V_2 - V_S - RI_2} \tag{14.236}$$

14.7.3 Four-quadrant DC/DC Luo-converter

Four-quadrant DC/DC Luo-converter is shown in Fig. 14.74, which consists of two switches with two passive diodes, two inductors, and one capacitor. The source voltage (V_1) and load voltage (V_2) are usually considered as constant voltages. The load can be a battery or motor back EMF. For example, the source voltage is 42 V and load voltage is ±14 V. There are four modes of operation:

1. Mode A (Quadrant I): electrical energy is transferred from source side V_1 to load side V_2;
2. Mode B (Quadrant II): electrical energy is transferred from load side V_2 to source side V_1;
3. Mode C (Quadrant III): electrical energy is transferred from source side V_1 to load side $-V_2$;
4. Mode D (Quadrant IV): electrical energy is transferred from load side $-V_2$ to source side V_1.

Each mode has two states: "on" and "off." Usually, each state is operating in different conduction duty k. The switches

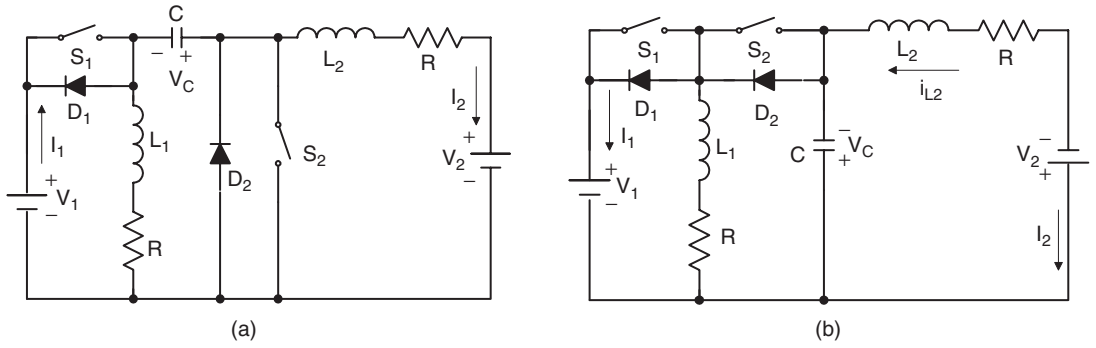

FIGURE 14.74 Four-quadrant operating Luo-converter: (a) circuit 1 and (b) circuit 2.

are the power MOSFET devices. The circuit 1 in Fig. 14.74 implements Modes A and B, and the circuit 2 in Fig. 14.74 implements Modes C and D. Circuits 1 and 2 can changeover by auxiliary switches (not in the figure).

Mode A: During state-**on** switch S_1 is closed, switch S_2 and diodes D_1 and D_2 are not conducted. In this case inductor currents i_{L1} and i_{L2} increase, and $i_1 = i_{L1} + i_{L2}$. During state-**off** switches S_1, S_2, and diode D_1 are off and diode D_2 is conducted. In this case current i_{L1} flows via diode D_2 to charge capacitor C, in the meantime current i_{L2} is kept to flow through load battery V_2. The free-wheeling diode current $i_{D2} = i_{L1} + i_{L2}$. Mode A implements the characteristics of the buck–boost conversion.

Mode B: During state-**on** switches S_2 is closed, switch S_1 and diodes D_1 and D_2 are not conducted. In this case inductor current i_{L2} increases by biased V_2, inductor current i_{L1} increases by biased V_C. Therefore capacitor voltage V_C reduces. During state-**off** switches S_1, S_2, and diode D_2 are not on, and only diode D_1 is on. In this case source current $i_1 = i_{L1} + i_{L2}$ which is a negative value to perform the regenerative operation. Inductor current i_{L2} flows through capacitor C, it is charged by current i_{L2}. After capacitor C, i_{L2} then flows through the source V_1. Inductor current i_{L1} flows through the source V_1 as well via diode D_1. Mode B implements the characteristics of the boost conversion.

Mode C: During state-**on** switch S_1 is closed, switch S_2 and diodes D_1 and D_2 are not conducted. In this case inductor currents i_{L1} and i_{L2} increase, and $i_1 = i_{L1}$. During state-**off** switches S_1, S_2, and diode D_1 are off and diode D_2 is conducted. In this case current i_{L1} flows via diode D_2 to charge capacitor C and the load battery V_2 via inductor L_2. The free-wheeling diode current $i_{D2} = i_{L1} = i_C + i_2$. Mode C implements the characteristics of the buck–boost conversion.

Mode D: During state-**on** switches S_2 is closed, switch S_1 and diodes D_1 and D_2 are not conducted. In this case inductor current i_{L1} increases by biased V_2, inductor current i_{L2} decreases by biased $(V_2 - V_C)$. Therefore capacitor voltage V_C reduces. Current $i_{L1} = i_{C-on} + i_2$. During state-**off** switches S_1, S_2, and diode D_2 are not on, and only diode D_1 is on. In this case source current $i_1 = i_{L1}$ which is a negative value to perform the regenerative operation. Inductor current i_2 flows through capacitor C that is charged by current i_2, i.e. $i_{C-off} = i_2$. Mode D implements the characteristics of the boost conversion.

Summary: The switch status is shown in Table 14.4.
The operation of all modes A, B, C, and D is same to the description in Sections 14.7.1 and 14.7.2.

14.8 Switched-capacitor Multi-quadrant Luo-converters

Switched-component converters are the third-generation converters. These converters are made of only inductor

TABLE 14.4 Switch's status (the blank status means OFF)

Switch or diode	Mode A (QI)		Mode B (QII)		Mode C (QIII)		Mode D (QIV)	
	State-on	State-off	State-on	State-off	State-on	State-off	State-on	State-off
Circuit	Circuit 1				Circuit 2			
S_1	ON				ON			
D_1				ON				ON
S_2			ON				ON	
D_2		ON				ON		

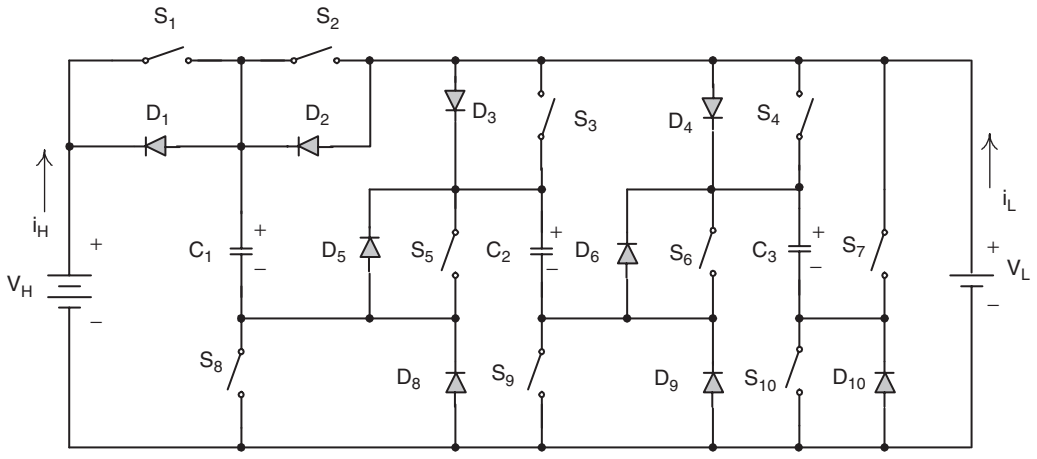

FIGURE 14.75 Two-quadrant switched-capacitor DC/DC Luo-converter.

or capacitors. They usually perform in the systems between two voltage sources: V_1 and V_2. Voltage source V_1 is proposed positive voltage and voltage V_2 is the load voltage that can be positive or negative. In the investigation both voltages are proposed constant voltage. Since V_1 and V_2 are constant values, so that voltage transfer gain is constant. Our interesting research will concentrate on the working current and the power transfer efficiency η. The resistance R of the capacitors and inductor has to be considered for the power transfer efficiency η calculation.

Reviewing the papers in the literature, we can find that almost of the papers investigating the switched-component converters are working in single-quadrant operation. Professor Luo and colleagues have developed this technique into multi-quadrant operation. We describe these in this and next sections.

Switched-capacitor multi-quadrant Luo-converters are the third-generation converters, and they are made of only capacitors. Because these converters implement voltage-lift and current-amplification techniques, they have the advantages of high power density, high power transfer efficiency, and low EMI. They have two modes:

- Two-quadrant switched-capacitor DC/DC Luo-converter;
- Four-quadrant switched-capacitor DC/DC Luo-converter.

The two-quadrant switched-capacitor DC/DC Luo-converter in forward operation has been derived for the energy transmission of a dual-voltage system in two-quadrant operation. The both, source and load voltages are positive polarity. It performs in the first-quadrant Q_I and the second-quadrant Q_{II} corresponding to the DC motor forward operation in motoring and regenerative braking states.

The four-quadrant switched-capacitor DC/DC Luo-converter has been derived for the energy transmission of a dual-voltage system in four-quadrant operation. The source voltage is positive and load voltage can be positive or negative polarity. It performs four-quadrant operation corresponding to the DC motor forward and reverse operation in motoring and regenerative braking states.

From the analysis and calculation, the conduction duty k does not affect the power transfer efficiency. It affects the input and output power in a small region. The maximum output power corresponds at $k = 0.5$.

14.8.1 Two-quadrant Switched-capacitor DC/DC Luo-converter

This converter is shown in Fig. 14.75. It consists of nine switches, seven diodes, and three capacitors. The high source voltage V_H and low load voltage V_L are usually considered as constant voltages, e.g. the source voltage is 48 V and load voltage is 14 V. There are two modes of operation:

- Mode A (Quadrant I): electrical energy is transferred from V_H side to V_L side;
- Mode B (Quadrant II): electrical energy is transferred from V_L side to V_H side.

Each mode has two states: "on" and "off." Usually, each state is operating in different conduction duty k. The switching period is T where $T = 1/f$, where f is the switching frequency. The switches are the power MOSFET devices. The parasitic resistance of all switches is r_S. The equivalent resistance of all capacitors is r_C and the equivalent voltage drop of all diodes is V_D. Usually we select the three capacitors having same capacitance $C = C_1 = C_2 = C_3$. Some reference data are useful: $r_S = 0.03\,\Omega$, $r_C = 0.02\,\Omega$, and $V_D = 0.5\,\text{V}$, $f = 5\,\text{kHz}$, and $C = 5000\,\mu\text{F}$. The switch's status is shown in Table 14.5.

For Mode A, state-**on** is shown in Fig. 14.76a: switches S_1 and S_{10} are closed and diodes D_5 and D_5 are conducted. Other switches and diodes are open. In this case capacitors C_1, C_2, and C_3 are charged via the circuit V_H–S_1–C_1–D_5–C_2–D_6–C_3–S_{10}, and the voltage across capacitors

TABLE 14.5 Switch's status (the blank status means OFF)

Switch or diode	Mode A		Mode B	
	State-on	State-off	State-on	State-off
S_1	ON			
D_1				ON
S_2,S_3,S_4		ON		
D_2,D_3,D_4			ON	
S_5,S_6,S_7				ON
D_5,D_6	ON			
S_8,S_9			ON	
S_{10}	ON		ON	
D_8,D_9,D_{10}		ON		

C_1, C_2, and C_3 is increasing. The equivalent circuit resistance is $R_{AN} = (2r_S + 3r_C) = 0.12\,\Omega$, and the voltage deduction is $2V_D = 1\,\text{V}$. State-**off** is shown in Fig. 14.76b: switches S_2, S_3, and S_4 are closed and diodes D_8, D_9, and D_{10} are conducted. Other switches and diodes are open. In this case capacitor C_1(C_2 and C_3) is discharged via the circuit S_2(S_3 and S_4)–V_L–D_8(D_9 and D_{10})–C_1(C_2 and C_3), and the voltage across capacitor C_1(C_2 and C_3) is decreasing. Mode A implements the **current-amplification technique**. The voltage and current waveforms are shown in Fig. 14.76c. All three capacitors are charged in series during state-on. The input current flows through three capacitors and the charges accumulated on the three capacitors should be the same. These three capacitors are discharged in parallel during state-off. Therefore, the output current is amplified by three times.

The variation of the voltage across capacitor C_1 is:

$$\Delta v_{C1} = \frac{k(V_H - 3V_{C1} - 2V_D)}{fCR_{AN}} = \frac{2.4k(1-k)(V_H - 3V_L - 5V_D)}{(2.4 + 0.6k)fCR_{AN}} \tag{14.237}$$

After calculation,

$$V_{C1} = \frac{k(V_H - 2V_D) + 2.4(1-k)(V_L + V_D)}{2.4 + 0.6k} \tag{14.238}$$

The average output current is

$$I_L = \frac{3}{T}\int_{kT}^{T} i_{C1}(t)dt \approx 3(1-k)\frac{V_{C1} - V_L - V_D}{R_{AF}} \tag{14.239}$$

The average input current is

$$I_H = \frac{1}{T}\int_{0}^{kT} i_{C1}(t)dt \approx k\frac{V_H - 3V_{C1} - 2V_D}{R_{AN}} \tag{14.240}$$

Therefore, we have $3I_H = I_L$.
Output power is

$$P_O = V_L I_L = 3(1-k)V_L\frac{V_{C1} - V_L - V_D}{R_{AF}} \tag{14.241}$$

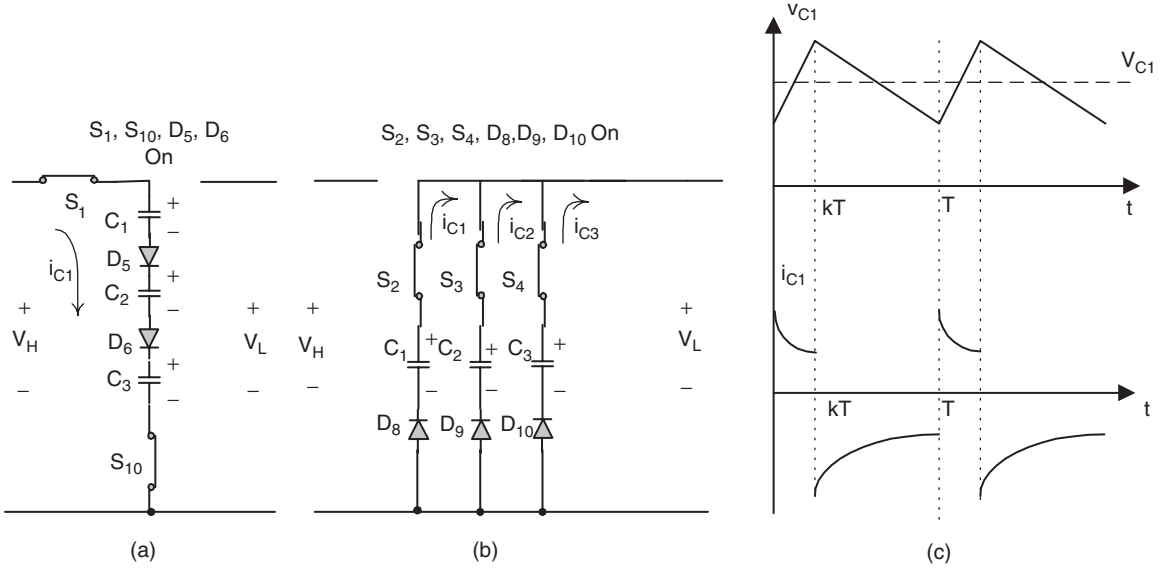

FIGURE 14.76 Mode A operation: (a) state-on; (b) state-off; and (c) voltage and current waveforms.

Input power

$$P_I = V_H I_H = kV_H \frac{V_H - 3V_{C1} - V_D}{R_{AN}} \tag{14.242}$$

The transfer efficiency is

$$\eta_A = \frac{P_O}{P_I} = \frac{1-k}{k}\frac{3V_L}{V_H}\frac{V_{C1} - V_L - V_D}{V_H - 3V_{C1} - V_D}\frac{R_{AN}}{R_{AF}} = \frac{3V_L}{V_H} \tag{14.243}$$

For Mode B, state-**on** is shown in Fig. 14.77a: switches S_8, S_9, and S_{10} are closed and diodes D_2, D_3, and D_4 are conducted. Other switches and diodes are off. In this case all three capacitors are charged via each circuit V_L–D_2(and D_3, D_4)–C_1(and C_2, C_3)–S_8(and S_9, S_{10}), and the voltage across three capacitors are increasing. The equivalent circuit resistance is $R_{BN} = r_S + r_C$ and the voltage deduction is V_D in each circuit. State-**off** is shown in Fig. 14.77b: switches S_5, S_6, and S_7 are closed and diode D_1 is on. Other switches and diodes are open. In this case all capacitors is discharged via the circuit V_L–S_7–C_3–S_6–C_2–S_5–C_1–D_1–V_H, and the voltage across all capacitors is decreasing. Mode B implements the **voltage-lift technique**. The voltage and current waveforms are shown in Fig. 14.77c. All three capacitors are charged in parallel during state-on. The input voltage is applied to the three capacitors symmetrically, so that the voltages across these three capacitors should be same. They are discharged in series during state-off. Therefore, the output voltage is lifted by three times.

The variation of the voltage across capacitor C is:

$$\Delta v_{C1} = \frac{k(1-k)[4(V_L - V_D) - V_H]}{fCR_{BN}} \tag{14.244}$$

After calculation

$$V_{C1} = k(V_L - V_D) + \frac{1-k}{3}(V_H - V_L + V_D) \tag{14.245}$$

The average input current is

$$I_L = \frac{1}{T}\left[3\int_0^{kT} i_{C1}(t)dt + \int_{kT}^{T} i_{C1}(t)dt\right]$$
$$\approx 3k\frac{V_L - V_{C1} - V_D}{R_{BN}} + (1-k)\frac{3V_{C1} + V_L - V_H - V_D}{R_{BF}} \tag{14.246}$$

The average output current is

$$I_H = \frac{1}{T}\int_{kT}^{T} i_{C1}(t)dt \approx (1-k)\frac{3V_{C1} + V_L - V_H - V_D}{R_{BF}} \tag{14.247}$$

From this formula, we have $4I_H = I_L$.
Input power is

$$P_I = V_L I_L$$
$$= V_L\left[3k\frac{V_L - V_C - V_D}{R_{BN}} + (1-k)\frac{3V_C + V_L - V_H - V_D}{R_{BF}}\right] \tag{14.248}$$

Output power is

$$P_O = V_H I_H = V_H(1-k)\frac{3V_C + V_L - V_H - V_D}{R_{BF}} \tag{14.249}$$

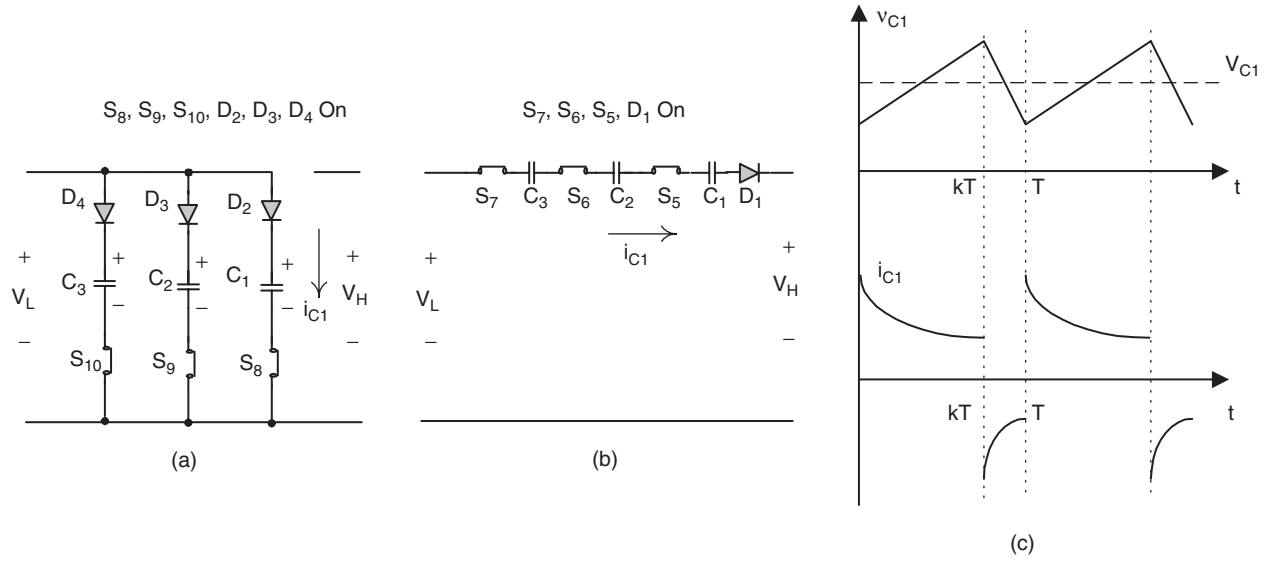

FIGURE 14.77 Mode B operation: (a) state-on; (b) state-off; and (c) voltage and current waveforms.

The efficiency is

$$\eta_B = \frac{P_O}{P_I} = \frac{V_H}{4V_L} \tag{14.250}$$

14.8.2 Four-quadrant Switched-capacitor DC/DC Luo-converter

Four-quadrant switched-capacitor DC/DC Luo-converter is shown in Fig. 14.78. Since it performs the *voltage-lift technique,* it has a simple structure with four-quadrant operation. This converter consists of eight switches and two capacitors. The source voltage V_1 and load voltage V_2 (e.g. a battery or DC motor back EMF) are usually constant voltages. In this paper they are supposed to be ± 21 V and ± 14 V. Capacitors C_1 and C_2 are same and $C_1 = C_2 = 2000\,\mu$F. The circuit equivalent resistance $R = 50\,\text{m}\Omega$. Therefore, there are four modes of operation for this converter:

1. Mode A: energy is converted from source to positive voltage load; the first-quadrant operation, Q_I;
2. Mode B: energy is converted from positive voltage load to source; the second-quadrant operation, Q_{II};
3. Mode C: energy is converted from source to negative voltage load; the third-quadrant operation, Q_{III};
4. Mode D: energy is converted from negative voltage load to source; the fourth-quadrant operation, Q_{IV}.

The first-quadrant (Mode A) is so called the forward motoring (Forw. Mot.) operation. V_1 and V_2 are positive, and I_1 and I_2 are positive as well. The second-quadrant (Mode B) is so called the forward regenerative (Forw. Reg.) braking operation. V_1 and V_2 are positive, and I_1 and I_2 are negative. The third-quadrant (Mode C) is so-called the reverse motoring (Rev. Mot.) operation. V_1 and I_1 are positive, and V_2 and I_2 are negative. The fourth-quadrant (Mode D) is so-called the reverse regenerative (Rev. Reg.) braking operation. V_1 and I_2 are positive, and I_1 and V_2 are negative.

Each mode has two conditions: $V_1 > V_2$ and $V_1 < V_2$ (or $|V_2|$ for Q_{III} and Q_{IV}). Each condition has two states: "on" and "off." Usually, each state is operating in various conduction duty k for different currents. As usual, the efficiency of all SC DC/DC converters is independent from the conduction duty cycle k. The switching period is T where $T = 1/f$. The switch status is shown in Table 14.6.

TABLE 14.6 Switch's status (mentioned switches are not open)

Quadrant No. and mode	Condition	State		Source side	Load side
		ON	OFF		
QI, Mode A	$V_1 > V_2$	$S_{1,4,6,8}$	$S_{2,4,6,8}$	V_1+	V_2+
Forw. Mot.	$V_1 < V_2$	$S_{1,4,6,8}$	$S_{2,4,7}$	I_1+	I_2+
QII, Mode B	$V_1 > V_2$	$S_{2,4,6,8}$	$S_{1,4,7}$	V_1+	V_2+
Forw. Reg.	$V_1 < V_2$	$S_{2,4,6,8}$	$S_{1,4,6,8}$	I_1-	I_2-
QIII, Mode C	$V_1 > \|V_2\|$	$S_{1,4,6,8}$	$S_{3,5,6,8}$	V_1+	V_2-
Rev. Mot.	$V_1 < \|V_2\|$	$S_{1,4,6,8}$	$S_{3,5,7}$	I_1+	I_2-
QIV Mode D	$V_1 > \|V_2\|$	$S_{3,5,6,8}$	$S_{1,4,7}$	V_1+	V_2-
Rev. Reg.	$V_1 < \|V_2\|$	$S_{3,5,6,8}$	$S_{1,4,6,8}$	I_1-	I_2+

As usual, the transfer efficiency only relies on the ratio of the source and load voltages, and it is independent on R, C, f, and k. We select $k = 0.5$ for our description. Other values for the reference are $f = 5\,\text{kHz}$, $V_1 = 21\,\text{V}$, $V_2 = 14\,\text{V}$, and total $C = 4000\,\mu\text{F}$, $R = 50\,\text{m}\Omega$.

For **Mode A1**, condition $V_1 > V_2$ is shown in Fig. 14.78a. Since $V_1 > V_2$, two capacitors C_1 and C_2 are connected in parallel. During switch-**on** state, switches S_1, S_4, S_6, and S_8 are closed and other switches are open. In this case, capacitors $C_1 /\!/ C_2$ are charged via the circuit V_1–S_1–$C_1 /\!/ C_2$–S_4, and the voltage across capacitors C_1 and C_2 is increasing. During switch-**off** state, switch S_2, S_4, S_6, and S_8 are closed and other switches are open. In this case capacitors $C_1 /\!/ C_2$ are discharged via the circuit S_2–V_2–S_4–$C_1 /\!/ C_2$, and the voltage across capacitors C_1 and C_2 is decreasing. Capacitors C_1 and C_2 transfer the energy from the source to the load.

The average capacitor voltage

$$V_C = kV_1 + (1-k)V_2 \tag{14.251}$$

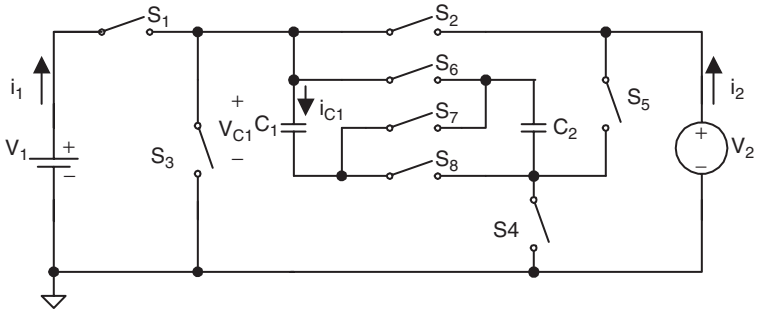

FIGURE 14.78 Four-quadrant sc DC/DC Luo-converter.

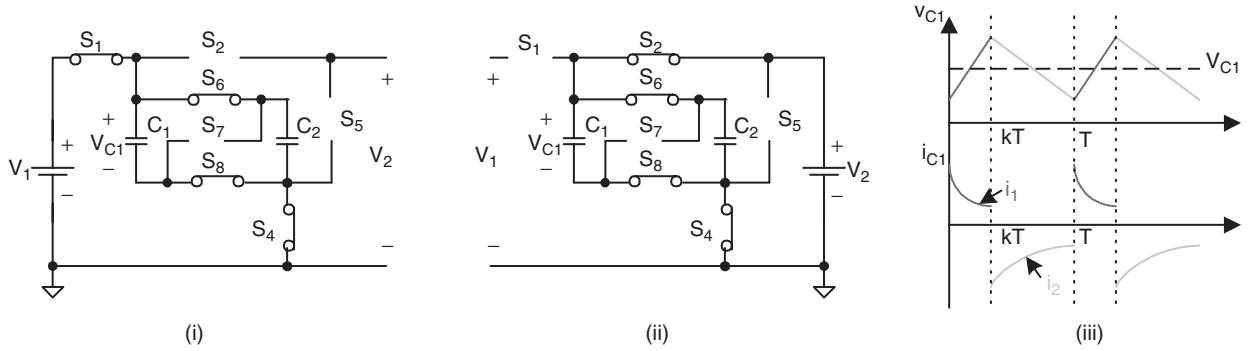

FIGURE 14.78a Mode A1 (QI): forward motoring with $V_1 > V_2$: (i) switch on: S_1, S_4, S_6, and S_8 on; (ii) switch off: S_2, S_4, S_6, and S_8, on; and (iii) waveforms.

The average current is

$$I_2 = \frac{1}{T}\int_{kT}^{T} i_C(t)dt \approx (1-k)\frac{V_C - V_2}{R} \tag{14.252}$$

and

$$I_1 = \frac{1}{T}\int_{0}^{kT} i_C(t)dt \approx k\frac{V_1 - V_C}{R} \tag{14.253}$$

The transfer efficiency is

$$\eta_{A1} = \frac{P_O}{P_I} = \frac{1-k}{k}\frac{V_2}{V_1}\frac{V_C - V_2}{V_1 - V_C} = \frac{V_2}{V_1} \tag{14.254}$$

For **Mode A2**, condition $V_1 < V_2$ is shown in Fig. 14.78b. Since $V_1 < V_2$, two capacitors C_1 and C_2 are connected in parallel during switch on and in series during switch off. This is so-called the *voltage-lift technique*. During switch-**on** state, switches S_1, S_4, S_6, and S_8 are closed and other switches are open. In this case, capacitors $C_1 /\!/ C_2$ are charged via the circuit V_1–S_1–$C_1 /\!/ C_2$–S_4, and the voltage across capacitors C_1 and C_2 is increasing. During switch-**off** state, switches S_2, S_4, and S_7 are closed and other switches are open. In this case, capacitors C_1 and C_2 are discharged via the circuit S_2–V_2–S_4–C_1–S_7–C_2, and the voltage across capacitor C_1 and C_2 is decreasing. Capacitors C_1 and C_2 transfer the energy from the source to the load.

The average capacitor voltage is

$$V_C = \frac{0.5V_1 + V_2}{2.5} = 11.2 \tag{14.255}$$

The average current is

$$I_2 = \frac{1}{T}\int_{kT}^{T} i_C(t)dt \approx (1-k)\frac{2V_C - V_2}{R} \tag{14.256}$$

and

$$I_1 = \frac{1}{T}\int_{0}^{kT} i_C(t)dt \approx k\frac{V_1 - V_C}{R} \tag{14.257}$$

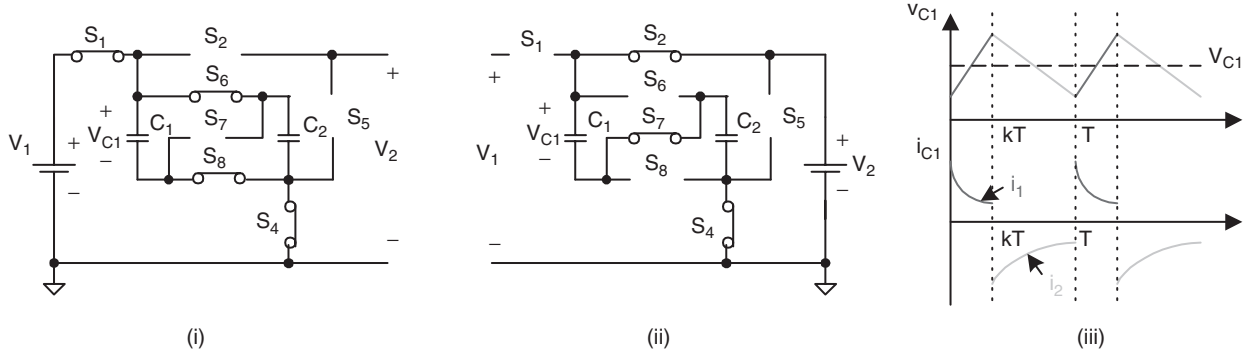

FIGURE 14.78b Mode A2 (QI): forward motoring with $V_1 < V_2$: (i) switch on: S_1, S_4, S_6, and S_8, on; (ii) switch off: S_2, S_4, and S_7, on; and (iii) waveforms.

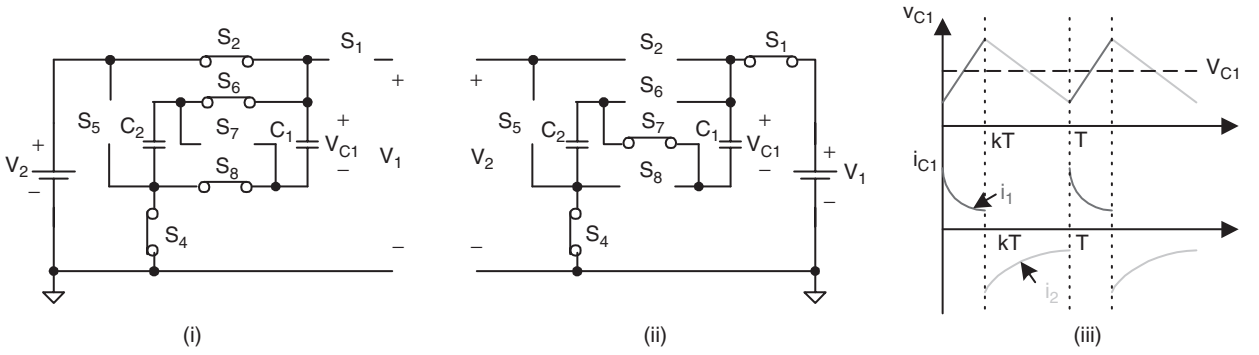

FIGURE 14.78c Mode B1 (QII): forward regenerative braking with $V_1 > V_2$: (i) switch on: S_2, S_4, S_6, and S_8, on; (ii) switch off; S_1, $S_4(S_5)$, and S_7 on; and (iii) waveforms.

The transfer efficiency is

$$\eta_{A2} = \frac{P_O}{P_I} = \frac{1-k}{k}\frac{V_2}{V_1}\frac{2V_C - V_2}{V_1 - V_C} = \frac{V_2}{2V_1} \tag{14.258}$$

For **Mode B1**, condition $V_1 > V_2$ is shown in Fig. 14.78c. Since $V_1 > V_2$, two capacitors C_1 and C_2 are connected in parallel during switch on and in series during switch off. The *voltage-lift technique* is applied. During switch-**on** state, switches S_2, S_4, S_6, and S_8 are closed. In this case, capacitors $C_1 /\!/ C_2$ are charged via the circuit V_2–S_2–$C_1 /\!/ C_2$–S_4, and the voltage across capacitors C_1 and C_2 is increasing. During switch-**off** state, switches S_1, S_4, and S_7 are closed. In this case, capacitors C_1 and C_2 are discharged via the circuit S_1–V_1–S_4–C_2–S_7–C_1, and the voltage across capacitor C_1 and C_2 is decreasing. Capacitors C_1 and C_2 transfer the energy from the load to the source. Therefore, we have $I_2 = 2I_1$.

The average capacitor voltage is

$$V_C = \frac{0.5V_2 + V_1}{2.5} = 11.2 \tag{14.259}$$

The average current is

$$I_1 = \frac{1}{T}\int_{kT}^{T} i_C(t)dt \approx (1-k)\frac{2V_C - V_1}{R} \tag{14.260}$$

and

$$I_2 = \frac{1}{T}\int_{0}^{kT} i_C(t)dt \approx k\frac{V_2 - V_C}{R} \tag{14.261}$$

The transfer efficiency is

$$\eta_{B1} = \frac{P_O}{P_I} = \frac{1-k}{k}\frac{V_1}{V_2}\frac{2V_C - V_1}{V_2 - V_C} = \frac{V_1}{2V_2} \tag{14.262}$$

For **Mode B2**, condition $V_1 < V_2$ is shown in Fig. 14.78d. Since $V_1 < V_2$, two capacitors C_1 and C_2 are connected in parallel. During switch-**on** state, switches S_2, S_4, S_6, and S_8 are closed. In this case, capacitors $C_1 /\!/ C_2$ are charged via the circuit V_2–S_2–$C_1 /\!/ C_2$–S_4, and the voltage across capacitors C_1 and C_2

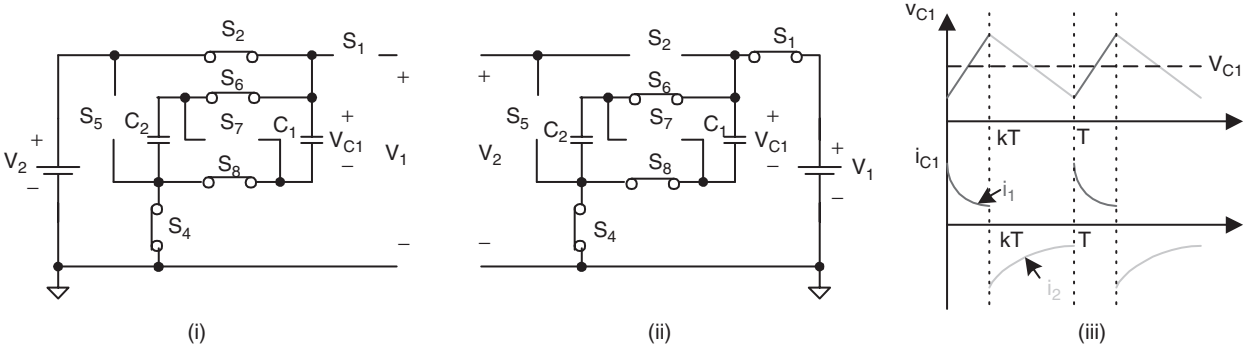

FIGURE 14.78d Mode B2 (QII): forward regenerative braking with $V_1 < V_2$: (i) switch on: S_2, S_4, S_6, and S_8, on; (ii) switch off: S_1, $S_4(S_5)$, S_6, and S_8 on; and (iii) waveforms.

is increasing. During switch-**off** state, switches S_1, S_4, S_6, and S_8 are closed. In this case capacitors $C_1 /\!/ C_2$ is discharged via the circuit S_1–V_1–S_4–$C_1 /\!/ C_2$, and the voltage across capacitors C_1 and C_2 is decreasing. Capacitors C_1 and C_2 transfer the energy from the load to the source. Therefore, we have $I_2 = I_1$.

The average capacitor voltage is

$$V_C = kV_2 + (1-k)V_1 \tag{14.263}$$

The average current is

$$I_1 = \frac{1}{T}\int_{kT}^{T} i_C(t)dt \approx (1-k)\frac{V_C - V_1}{R} \tag{14.264}$$

and

$$I_2 = \frac{1}{T}\int_{0}^{kT} i_C(t)dt \approx k\frac{V_2 - V_C}{R} \tag{14.265}$$

The transfer efficiency is

$$\eta_{B2} = \frac{P_O}{P_I} = \frac{1-k}{k}\frac{V_1}{V_2}\frac{V_C - V_1}{V_2 - V_C} = \frac{V_1}{V_2} \tag{14.266}$$

For **Mode C1**, condition $V_1 > |V_2|$ is shown in Fig. 14.78e. Since $V_1 > |V_2|$, two capacitors C_1 and C_2 are connected in parallel. During switch-**on** state, switches S_1, S_4, S_6, and S_8 are closed. In this case, capacitors $C_1 /\!/ C_2$ are charged via the circuit V_1–S_1–$C_1 /\!/ C_2$–S_4, and the voltage across capacitors C_1 and C_2 is increasing. During switch-**off** state, switches S_3, S_5, S_6, and S_8 are closed. Capacitors C_1 and C_2 are discharged via the circuit S_3–V_2–S_5–$C_1 /\!/ C_2$, and the voltage across capacitors C_1 and C_2 is decreasing. Capacitors C_1 and C_2 transfer the energy from the source to the load. We have $I_1 = I_2$.

The average capacitor voltage is

$$V_C = kV_1 + (1-k)|V_2| \tag{14.267}$$

The average current (absolute value) is

$$I_2 = \frac{1}{T}\int_{kT}^{T} i_C(t)dt \approx (1-k)\frac{V_C - |V_2|}{R} \tag{14.268}$$

and the average input current is

$$I_1 = \frac{1}{T}\int_{0}^{kT} i_C(t)dt \approx k\frac{V_1 - V_C}{R} \tag{14.269}$$

The transfer efficiency is

$$\eta_{C1} = \frac{P_O}{P_I} = \frac{1-k}{k}\frac{|V_2|}{V_1}\frac{V_C - |V_2|}{V_1 - V_C} = \frac{|V_2|}{V_1} \tag{14.270}$$

For **Mode C2**, condition $V_1 < |V_2|$ is shown in Fig. 14.78f. Since $V_1 < |V_2|$, two capacitors C_1 and C_2 are connected in parallel during switch on and in series during switch off, applying the *voltage-lift technique*. During switch-**on** state, switches S_1, S_4, S_6, and S_8, are closed. Capacitors C_1 and C_2 are charged via the circuit V_1–S_1–$C_1 /\!/ C_2$–S_4, and the voltage across capacitors C_1 and C_2 is increasing. During switch-**off** state, switches S_3, S_5, and S_7 are closed. Capacitors C_1 and C_2 is discharged via the circuit S_3–V_2–S_5–C_1–S_7–C_2, and the voltage across capacitor C_1 and C_2 is decreasing. Capacitors C_1 and C_2 transfer the energy from the source to the load. We have $I_1 = 2I_2$.

The average capacitor voltage is

$$V_C = \frac{0.5V_1 + |V_2|}{2.5} = 11.2 \tag{14.271}$$

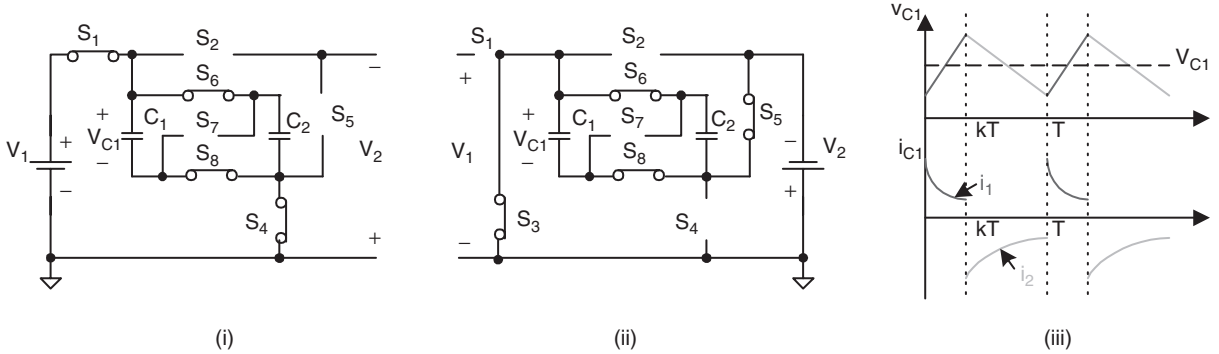

FIGURE 14.78e Mode C1 (QIII): reverse motoring with $V_1 > |V_2|$: (i) switch on: S_1, S_4, S_6, and S_8 on; (ii) switch off: S_3, S_5, S_6, and S_8 on; and (iii) waveforms.

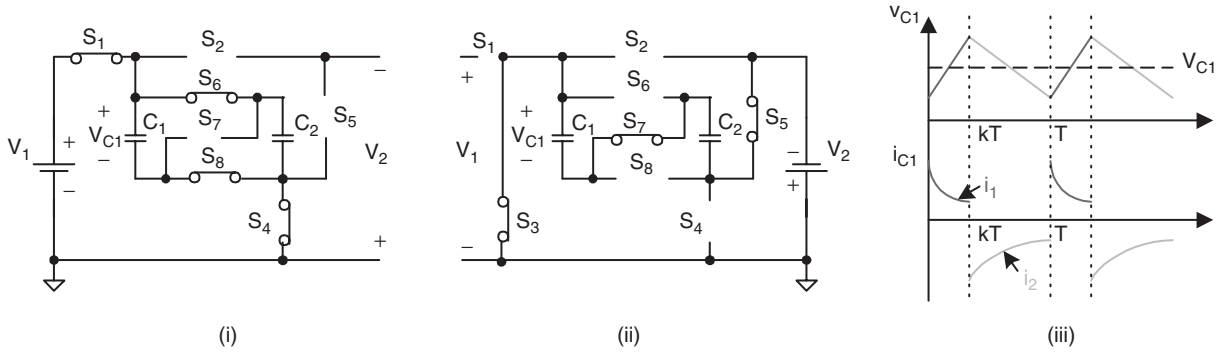

FIGURE 14.78f Mode C2 (QIII): reverse motoring with $V_1 < |V_2|$: (i) switch on: S_1, S_4, S_6, and S_8, on; (ii) switch off: S_3, S_5, and S_7, on; and (iii) waveforms.

The average currents are

$$I_2 = \frac{1}{T}\int_{kT}^{T} i_C(t)dt \approx (1-k)\frac{2V_C - |V_2|}{R} \tag{14.272}$$

and

$$I_1 = \frac{1}{T}\int_{0}^{kT} i_C(t)dt \approx k\frac{V_1 - V_C}{R} \tag{14.273}$$

The transfer efficiency is

$$\eta_{C2} = \frac{P_O}{P_I} = \frac{1-k}{k}\frac{|V_2|}{V_1}\frac{2V_C - |V_2|}{V_1 - V_C} = \frac{|V_2|}{2V_1} \tag{14.274}$$

For **Mode D1**, condition $V_1 > |V_2|$ is shown in Fig. 14.78g. Since $V_1 > |V_2|$, two capacitors C_1 and C_2 are connected in parallel during switch on and in series during switch off, applying the *voltage-lift technique*. During switch-**on** state, switches S_3, S_5, S_6, and S_8 are closed. In this case, capacitors $C_1 /\!/ C_2$ are charged via the circuit V_2–S_3–$C_1 /\!/ C_2$–S_5, and the voltage across capacitors C_1 and C_2 is increasing. During switch-**off** state, switches S_1, S_4, and S_7 are closed. Capacitors C_1 and C_2 are discharged via the circuit S_1–V_1–S_4–C_2–S_7–C_1, and the voltage across capacitor C_1 and C_2 is decreasing. Capacitors C_1 and C_2 transfer the energy from the load to the source. We have $I_2 = 2I_1$.

The average capacitor voltage is

$$V_C = \frac{0.5|V_2| + V_1}{2.5} = 11.2 \tag{14.275}$$

The average currents are

$$I_1 = \frac{1}{T}\int_{kT}^{T} i_C(t)dt \approx (1-k)\frac{2V_C - V_1}{R} \tag{14.276}$$

and

$$I_2 = \frac{1}{T}\int_{0}^{kT} i_C(t)dt \approx k\frac{|V_2| - V_C}{R} \tag{14.277}$$

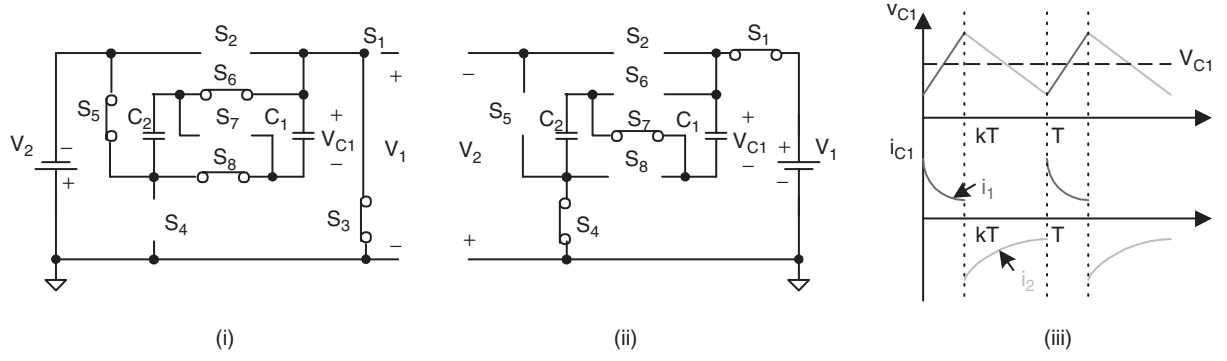

FIGURE 14.78g Mode D1 (QIV): reverse regenerative braking with $V_1 > |V_2|$: (i) switch on: S_3, S_4, S_6, and S_8, on; (ii) switch off: S_1, S_4, and S_7 on; and (iii) waveforms.

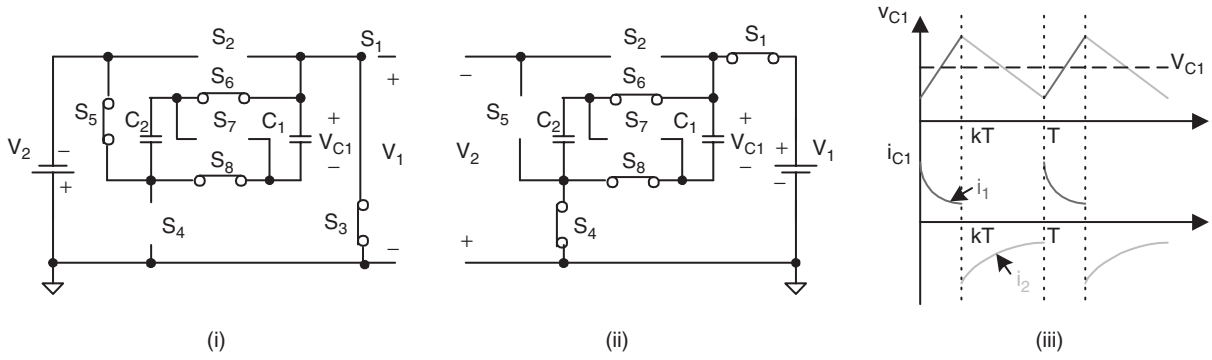

FIGURE 14.78h Mode D2 (QIV): reverse regenerative braking with $V_1 < |V_2|$: (i) switch on: S_3, S_5, S_6, and S_8, on; (ii) switch off: S_1, S_4, S_6, and S_8 on; and (iii) waveforms.

The transfer efficiency is

$$\eta_{D1} = \frac{P_O}{P_I} = \frac{1-k}{k}\frac{V_1}{|V_2|}\frac{2V_C - V_1}{|V_2| - V_C} = \frac{V_1}{2|V_2|} \tag{14.278}$$

For **Mode D2**, condition $V_1 < |V_2|$ is shown in Fig. 14.78h. Since $V_1 < |V_2|$, two capacitors C_1 and C_2 are connected in parallel. During switch-**on** state, switches S_3, S_5, S_6, and S_8 are closed. In this case, capacitors $C_1 /\!/ C_2$ are charged via the circuit V_2–S_3–$C_1 /\!/ C_2$–S_5, and the voltage across capacitors C_1 and C_2 is increasing. During switch-**off** state, switches S_1, S_4, S_6, and S_8 are closed. Capacitors C_1 and C_2 are discharged via the circuit S_1–V_1–S_4–$C_1 /\!/ C_2$, and the voltage across capacitors C_1 and C_2 is decreasing. Capacitors C_1 and C_2 transfer the energy from the load to the source. We have $I_2 = I_1$.

The average capacitor voltage is

$$V_C = k|V_2| + (1-k)V_1 \tag{14.279}$$

The average currents are

$$I_1 = \frac{1}{T}\int_{kT}^{T} i_C(t)dt \approx (1-k)\frac{V_C - V_1}{R} \tag{14.280}$$

and

$$I_2 = \frac{1}{T}\int_{0}^{kT} i_C(t)dt \approx k\frac{|V_2| - V_C}{R} \tag{14.281}$$

The transfer efficiency is

$$\eta_{D2} = \frac{P_O}{P_I} = \frac{1-k}{k}\frac{V_1}{|V_2|}\frac{V_C - V_1}{|V_2| - V_C} = \frac{V_1}{|V_2|} \tag{14.282}$$

14.9 Multiple-lift Push–Pull Switched-capacitor Luo-converters

Micro-power-consumption technique requires high power density DC/DC converters and power supply source. Voltage-lift (VL) technique is a popular method to apply in electronic circuit design. Since switched-capacitor can be integrated into power integrated circuit (IC) chip, its size is small. Combining switched-capacitor and VL techniques the DC/DC converters with small size, high power density, high voltage transfer gain, high power efficiency, and low EMI can be constructed. This section introduces a new series DC/DC converters – multiple-lift push–pull switched-capacitor DC/DC Luo-converters. There are two subseries:

- P/O multiple-lift (ML) push–pull (PP) switched-capacitor (SC) DC/DC Luo-converter;
- N/O multiple-lift push–pull switched-capacitor DC/DC Luo-converter.

14.9.1 P/O Multiple-lift Push–Pull Switched-capacitor DC/DC Luo-converter

P/O ML-PP SC DC/DC Luo-converters have several subseries:

- Main series;
- Additional series;
- Enhanced series;
- Re-enhanced series;
- Multiple-enhanced series.

We only introduce three circuits of main series and additional series in this section.

P/O ML-PP SC Luo-converter elementary circuit is shown in Fig. 14.79a. Its output voltage and current are

$$V_O = 2V_I$$

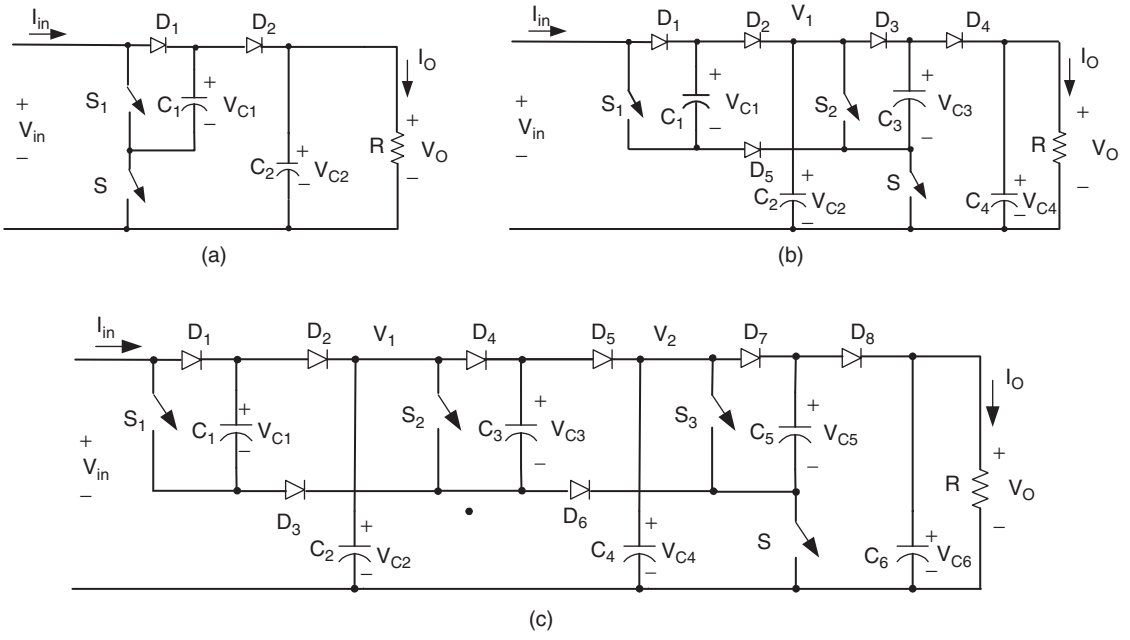

FIGURE 14.79 P/O ML-PP SC Luo-converter: (a) elemental; (b) re-lift; and (c) triple-lift circuits.

and

$$I_O = \frac{1}{2} I_I$$

The voltage transfer gain is

$$M_E = \frac{V_O}{V_I} = 2 \tag{14.283}$$

P/O ML-PP SC Luo-converter re-lift circuit is shown in Fig. 14.79b. Its output voltage and current are

$$V_O = 4V_I$$

and

$$I_O = \frac{1}{4} I_I$$

The voltage transfer gain is

$$M_R = 4 \tag{14.284}$$

P/O ML-PP SC Luo-converter triple-lift circuit is shown in Fig. 14.79c. Its output voltage and current are

$$V_O = 8V_I$$

and

$$I_O = \frac{1}{8} I_I$$

The voltage transfer gain is

$$M_T = 8 \tag{14.285}$$

P/O ML-PP SC Luo-converter additional circuit is shown in Fig. 14.80a. Its output voltage and current are

$$V_O = 3V_I$$

and

$$I_O = \frac{1}{3} I_I$$

The voltage transfer gain is

$$M_A = \frac{V_O}{V_I} = 3 \tag{14.286}$$

P/O ML-PP SC Luo-converter additional re-lift circuit is shown in Fig. 14.80b. Its output voltage and current are

$$V_O = 6V_I$$

and

$$I_O = \frac{1}{6} I_I$$

The voltage transfer gain is

$$M_{AR} = \frac{V_O}{V_I} = 6 \tag{14.287}$$

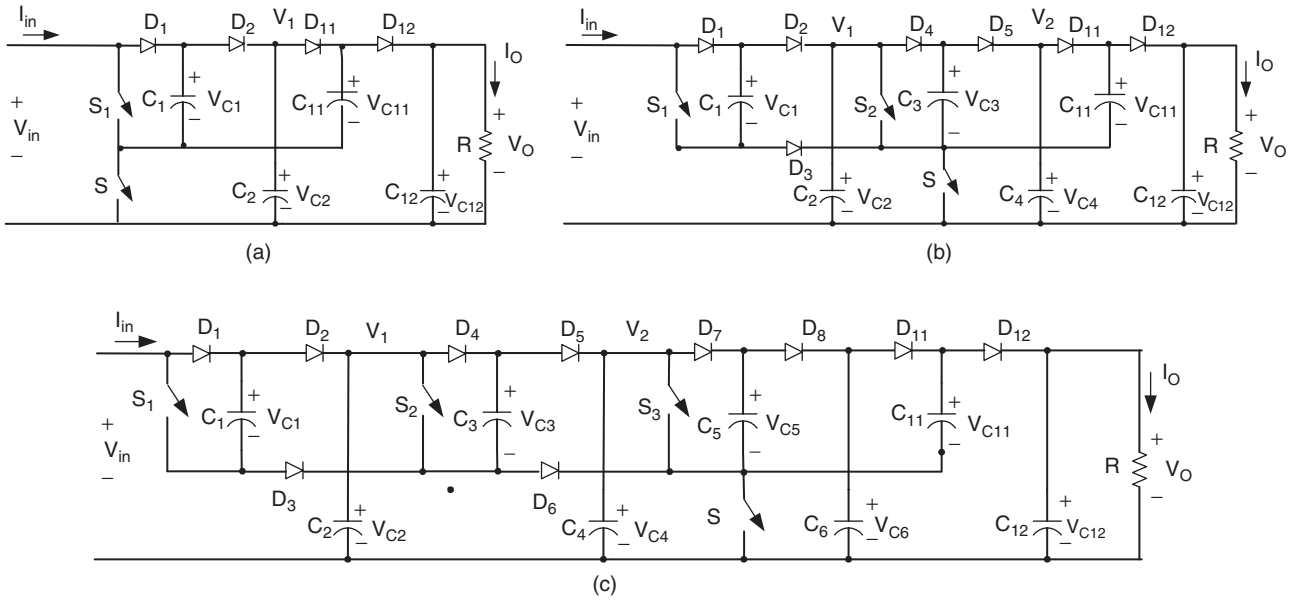

FIGURE 14.80 P/O ML-PP SC Luo-converter re-lift circuit: (a) additional; (b) re-lift; and (c) triple-lift circuits.

P/O ML-PP SC Luo-converter additional triple-lift circuit is shown in Fig. 14.80c. Its output voltage and current are

$$V_O = 12V_I$$

and

$$I_O = \frac{1}{12}I_I$$

The voltage transfer gain is

$$M_{AT} = \frac{V_O}{V_I} = 12 \tag{14.288}$$

14.9.2 N/O Multiple-lift Push–Pull Switched-capacitor DC/DC Luo-converter

N/O ML-PP SC DC/DC Luo-converters have several subseries:

- Main series;
- Additional series;
- Enhanced series;
- Re-enhanced series;
- Multiple-enhanced series.

We only introduce three circuits of main series and additional series in this section.

N/O ML-PP SC Luo-converter elementary circuit is shown in Fig. 14.81a. Its output voltage and current are

$$V_O = V_I$$

and

$$I_O = I_I$$

The voltage transfer gain is

$$M_E = \frac{V_O}{V_I} = 1 \tag{14.289}$$

N/O ML-PP SC Luo-converter re-lift circuit is shown in Fig. 14.81b. Its output voltage and current are

$$V_O = 3V_I$$

and

$$I_O = \frac{1}{3}I_I$$

The voltage transfer gain is

$$M_R = 3 \tag{14.290}$$

N/O ML-PP SC Luo-converter triple-lift circuit is shown in Fig. 14.81c. Its output voltage and current are

$$V_O = 7V_I$$

and

$$I_O = \frac{1}{7}I_I$$

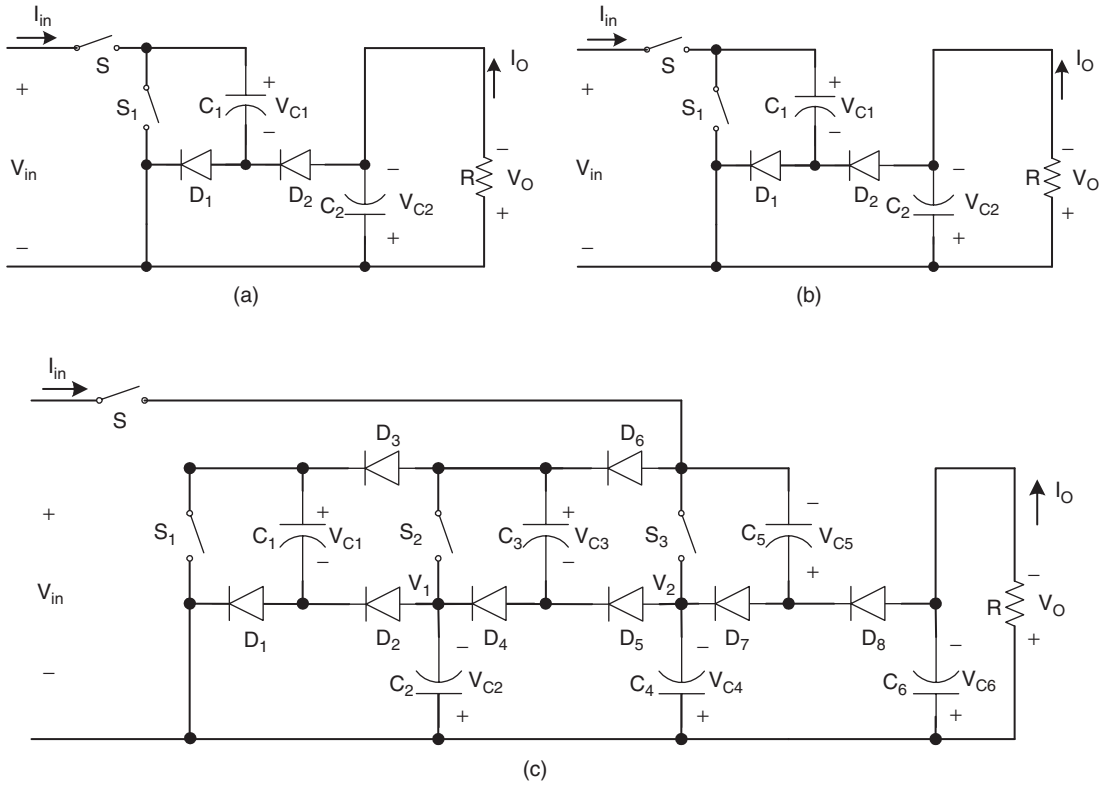

FIGURE 14.81 N/O ML-PP SC Luo-converter: (a) elemental; (b) re-lift; and (c) triple-lift circuits.

The voltage transfer gain is

$$M_T = 7 \tag{14.291}$$

N/O ML-PP SC Luo-converter additional circuit is shown in Fig. 14.82a. Its output voltage and current are

$$V_O = 2V_I$$

and

$$I_O = \frac{1}{2} I_I$$

The voltage transfer gain is

$$M_A = \frac{V_O}{V_I} = 2 \tag{14.292}$$

N/O ML-PP SC Luo-converter additional re-lift circuit is shown in Fig. 14.82b. Its output voltage and current are

$$V_O = 5V_I$$

and

$$I_O = \frac{1}{5} I_I$$

The voltage transfer gain is

$$M_{AR} = \frac{V_O}{V_I} = 5 \tag{14.293}$$

N/O ML-PP SC Luo-converter additional triple-lift circuit is shown in Fig. 14.82c. Its output voltage and current are

$$V_O = 11V_I$$

and

$$I_O = \frac{1}{11} I_I$$

The voltage transfer gain is

$$M_{AT} = \frac{V_O}{V_I} = 11 \tag{14.294}$$

14.10 Switched-inductor Multi-quadrant Operation Luo-converters

Switched-capacitor converters usually have many switches and capacitors, especially for the system with high ratio between

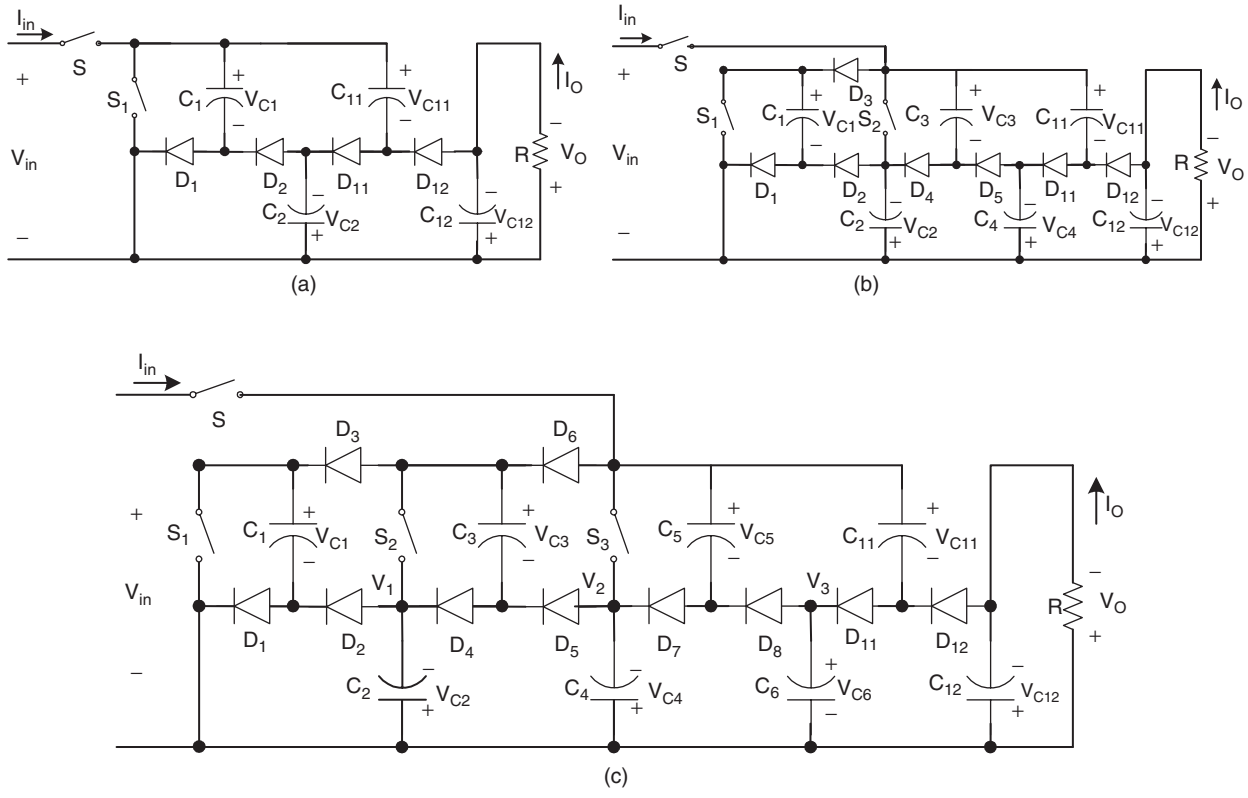

FIGURE 14.82 N/O ML-PP SC Luo-converter re-lift circuit: (a) additional; (b) re-lift; and (c) triple-lift circuits.

source and load voltages. Switched-inductor converter usually has only one inductor even if it works in single-, two-, and/or four-quadrant operation. Simplicity is the main advantage of all switched inductor converters.

Switched-inductor multi-quadrant Luo-converters are the third-generation converters, and they are made of only inductor. These converters have been derived from chopper circuits. They have three modes:

- Two-quadrant switched-inductor DC/DC Luo-converter in forward operation;
- Two-quadrant switched-inductor DC/DC Luo-converter in reverse operation;
- Four-quadrant switched-inductor DC/DC Luo-converter.

The two-quadrant switched-inductor DC/DC Luo-converter in forward operation has been derived for the energy transmission of a dual-voltage system. The both, source and load voltages are positive polarity. It performs in the first-quadrant Q_I and the second-quadrant Q_{II} corresponding to the DC motor forward operation in motoring and regenerative braking states.

The two-quadrant switched-inductor DC/DC Luo-converter in reverse operation has been derived for the energy transmission of a dual-voltage system. The source voltage is positive and load voltage is negative polarity. It performs in the third-quadrant Q_{III} and the fourth-quadrant Q_{IV} corresponding to the DC motor reverse operation in motoring and regenerative braking states.

The four-quadrant switched-inductor DC/DC Luo-converter has been derived for the energy transmission of a dual-voltage system. The source voltage is positive and load voltage can be positive or negative polarity. It performs four-quadrant operation corresponding to the DC motor forward and reverse operation in motoring and regenerative braking states.

14.10.1 Two-quadrant Switched-inductor DC/DC Luo-converter in Forward Operation

Forward operation (F) 2Q SI Luo-converter is shown in Fig. 14.83, and it consists of two switches with two passive diodes, two inductors, and one capacitor. The source voltage (V_1) and load voltage (V_2) are usually considered as constant voltages. The load can be a battery or motor back EMF. For example, the source voltage is 42 V and load voltage is +14 V. There are two modes of operation:

1. Mode A (QI): electrical energy is transferred from source side V_1 to load side V_2;

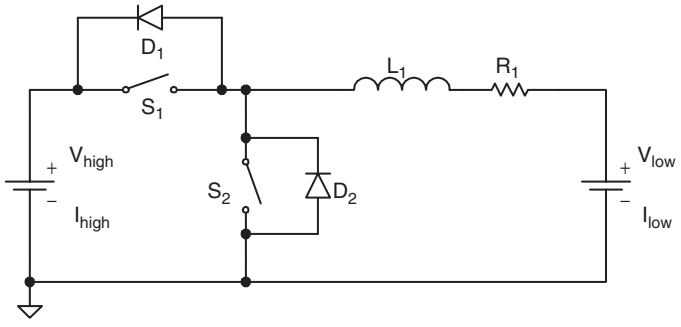

FIGURE 14.83 Switched-inductor QI and II DC/DC Luo-converter.

2. Mode B (QII): electrical energy is transferred from load side V_2 to source side V_1.

Mode A: The equivalent circuits during switch-on and -off periods are shown in Figs. 14.84a and b. The typical output voltage and current waveforms are shown in Fig. 14.84c.

We have the average inductor current I_L as

$$I_L = \frac{kV_1 - V_2}{R} \tag{14.295}$$

The variation ratio of the inductor current i_L is

$$\zeta = \frac{\Delta i_L/2}{I_L} = \frac{k(1-k)V_1}{kV_1 - V_2}\frac{R}{2fL} \tag{14.296}$$

The power transfer efficiency is

$$\eta_A = \frac{P_O}{P_I} = \frac{V_2}{kV_1} \tag{14.297}$$

The boundary between continuous and discontinuous regions is defined as

$$\zeta \geq 1 \quad \text{i.e.}$$

$$\frac{k(1-k)V_1}{kV_1 - V_2}\frac{R}{2fL} \geq 1 \quad \text{or} \quad k \leq \frac{V_2}{V_1} + k(1-k)\frac{R}{2fL} \tag{14.298}$$

Average inductor current I_L in discontinuous region is

$$I_L = \frac{V_1}{V_2 + RI_L}\frac{V_1 - V_2 - RI_L}{2fL}k^2 \tag{14.299}$$

The power transfer efficiency is

$$\eta_{A-dis} = \frac{P_O}{P_I} = \frac{V_2}{V_2 + RI_L} \quad \text{with} \quad k \leq \frac{V_2}{V_1} + k(1-k)\frac{R}{2fL} \tag{14.300}$$

Mode B: The equivalent circuits during switch-on and -off periods are shown in Figs. 14.85a and b. The typical output voltage and current waveforms are shown in Fig. 14.85c.

The average inductor current I_L is

$$I_L = \frac{V_2 - (1-k)V_1}{R} \tag{14.301}$$

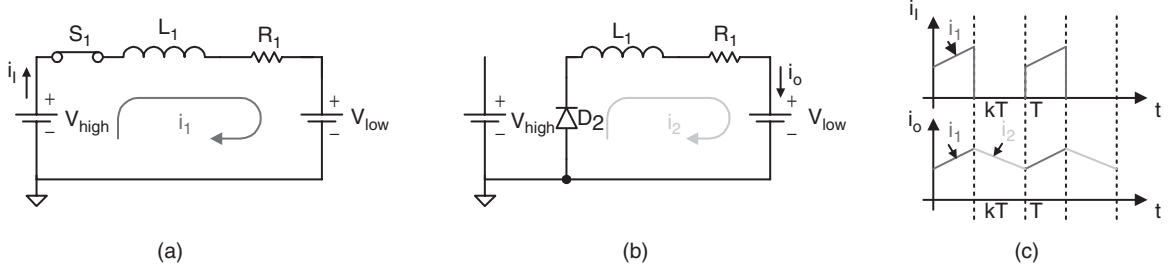

FIGURE 14.84 Mode A of F 2Q SI Luo-converter: (a) state-on: S_1 on; (b) state-off: D_2 on, S_1, off; and (c) input and output current waveforms.

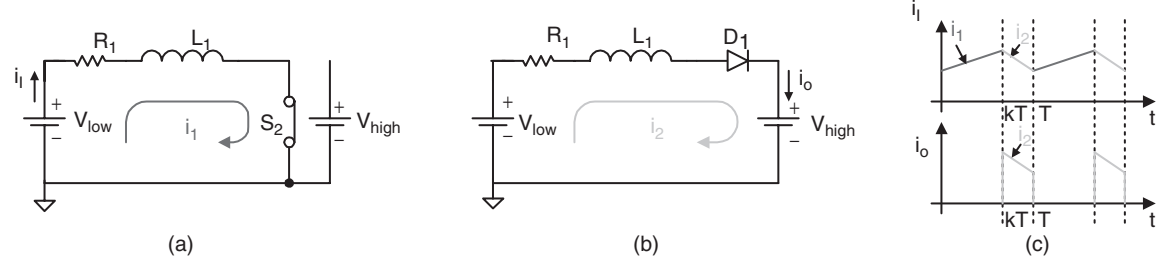

FIGURE 14.85 Mode B of F 2Q SI Luo-converter: (a) state-on: S_2 on; (b) state-off: D_1 on, S_2 off; and (c) input and output current waveforms.

The variation ratio of the inductor current i_L is

$$\zeta = \frac{\Delta i_L/2}{I_L} = \frac{k(1-k)V_1}{V_2-(1-k)V_1}\frac{R}{2fL} \tag{14.302}$$

The power transfer efficiency

$$\eta_B = \frac{P_O}{P_I} = \frac{(1-k)V_1}{V_2} \tag{14.303}$$

The boundary between continuous and discontinuous regions is defined as

$$\zeta \geq 1, \quad \text{i.e.}$$

$$\frac{k(1-k)V_1}{V_2-(1-k)V_1}\frac{R}{2fL} \geq 1 \quad \text{or} \quad k \leq \left(1-\frac{V_2}{V_1}\right)+k(1-k)\frac{R}{2fL} \tag{14.304}$$

Average inductor current I_L in discontinuous region is

$$I_L = \frac{V_1}{V_1 - V_2 + RI_L}\frac{V_2 - RI_L}{2fL}k^2 \tag{14.305}$$

The power transfer efficiency is

$$\eta_{B-dis} = \frac{P_O}{P_I} = \frac{V_2 - RI_L}{V_2}$$

$$\text{with} \quad k \leq \left(1-\frac{V_2}{V_1}\right)+k(1-k)\frac{R}{2fL} \tag{14.306}$$

14.10.2 Two-quadrant Switched-inductor DC/DC Luo-converter in Reverse Operation

Reverse operation (R) 2Q SI Luo-converter is shown in Fig. 14.86, and it consists of two switches with two passive diodes, two inductors, and one capacitor. The source voltage (V_1) and load voltage (V_2) are usually considered as constant voltages. The load can be a battery or motor back EMF. For example, the source voltage is 42 V and load voltage is −14 V. There are two modes of operation:

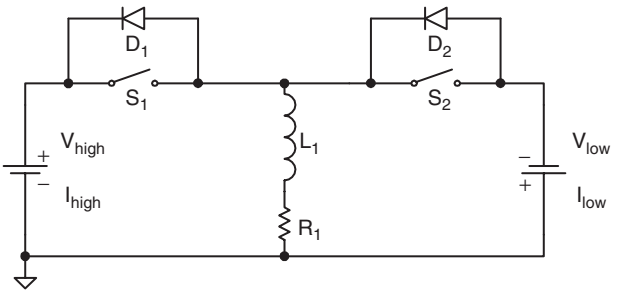

FIGURE 14.86 Switched-inductor QIII and IV DC/DC Luo-converter.

1. Mode C (QIII): electrical energy is transferred from source side V_1 to load side $-V_2$;
2. Mode D (QIV): electrical energy is transferred from load side $-V_2$ to source side V_1.

Mode C: The equivalent circuits during switch-on and -off periods are shown in Figs. 14.87a and b. The typical output voltage and current waveforms are shown in Fig. 14.87c.

We have the average inductor current I_L as

$$I_L = \frac{kV_1 - (1-k)V_2}{R} \tag{14.307}$$

The variation ratio of the inductor current i_L is

$$\zeta = \frac{\Delta i_L/2}{I_L} = \frac{k(1-k)(V_1+V_2)}{kV_1-(1-k)V_2}\frac{R}{2fL} \tag{14.308}$$

The power transfer efficiency is

$$\eta_C = \frac{P_O}{P_I} = \frac{(1-k)V_2}{kV_1} \tag{14.309}$$

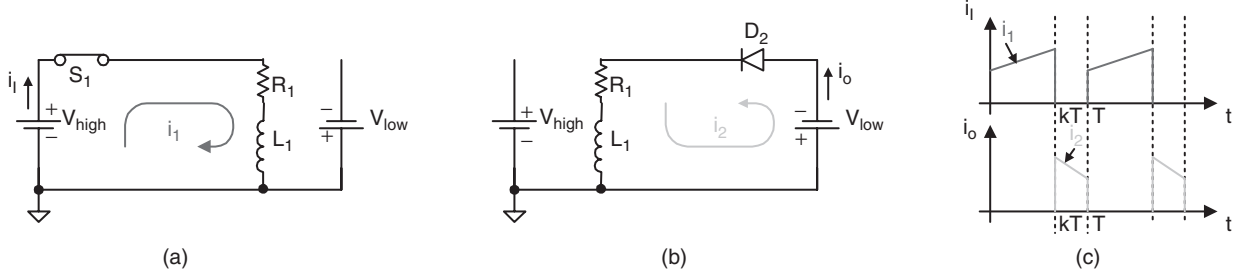

FIGURE 14.87 Mode C of F 2Q SI Luo-converter: (a) state-on; S_1 on; (b) state-off: D_2 on, S_1 off; and (c) input and output current waveforms.

The boundary between continuous and discontinuous regions is defined as

$$\zeta \geq 1, \quad \text{i.e.}$$

$$\frac{k(1-k)(V_1+V_2)}{kV_1-(1-k)V_2}\frac{R}{2fL} \geq 1 \quad \text{or} \quad k \leq \frac{V_2}{V_1+V_2}+k(1-k)\frac{R}{2fL} \tag{14.310}$$

Average inductor current I_L in discontinuous region is

$$I_L = \frac{V_1+V_2}{V_2+RI_L}\frac{V_1-RI_L}{2fL}k^2 \tag{14.311}$$

The power transfer efficiency is

$$\eta_{C-dis} = \frac{P_O}{P_I} = \frac{V_2}{V_1}\frac{V_1-RI_L}{V_2+RI_L}$$

$$\text{with} \quad k \leq \frac{V_2}{V_1+V_2}+k(1-k)\frac{R}{2fL} \tag{14.312}$$

Mode D: The equivalent circuits during switch-on and -off periods are shown in Figs. 14.88a and b. The typical output voltage and current waveforms are shown in Fig. 14.88c.

The average inductor current I_L is

$$I_L = \frac{kV_2-(1-k)V_1}{R} \tag{14.313}$$

The variation ratio of the inductor current i_L is

$$\zeta = \frac{\Delta i_L/2}{I_L} = \frac{k(1-k)(V_1+V_2)}{kV_2-(1-k)V_1}\frac{R}{2fL} \tag{14.314}$$

The power transfer efficiency is

$$\eta_D = \frac{P_O}{P_I} = \frac{(1-k)V_1}{kV_2} \tag{14.315}$$

The boundary between continuous and discontinuous regions is defined as

$$\zeta \geq 1, \quad \text{i.e.}$$

$$\frac{k(1-k)(V_1+V_2)}{kV_2-(1-k)V_1}\frac{R}{2fL} \geq 1 \quad \text{or} \quad k \leq \frac{V_1}{V_1+V_2}+k(1-k)\frac{R}{2fL} \tag{14.316}$$

Average inductor current I_L in discontinuous region is

$$I_L = \int_0^{t_4} = \frac{V_1+V_2}{V_1+RI_L}\frac{V_2-RI_L}{2fL}k^2 \tag{14.317}$$

The power transfer efficiency is

$$\eta_{D-dis} = \frac{P_O}{P_I} = \frac{V_1}{V_2}\frac{V_2-RI_L}{V_1+RI_L}$$

$$\text{with} \quad k \leq \frac{V_1}{V_1+V_2}+k(1-k)\frac{R}{2fL} \tag{14.318}$$

14.10.3 Four-quadrant Switched-inductor DC/DC Luo-converter

Switched-inductor DC/DC converters successfully overcome the disadvantage of switched-capacitor converters. Usually, only one inductor is required for each converter with one- or two- or four-quadrant operation, no matter how large the difference between the input and output voltage is. Therefore, switched-inductor converter has very simple topology and circuit. Consequently, it has high power density. This paper introduces a *switched-inductor four-quadrant DC/DC Luo-converter*.

This converter, shown in Fig. 14.89, consists of three switches, two diodes, and only one inductor *L*. The source voltage V_1 and load voltage V_2 (e.g. a battery or DC motor back EMF) are usually constant voltages. *R* is the equivalent resistance of the circuit, it is usually small. In this paper, $V_1 > |V_2|$,

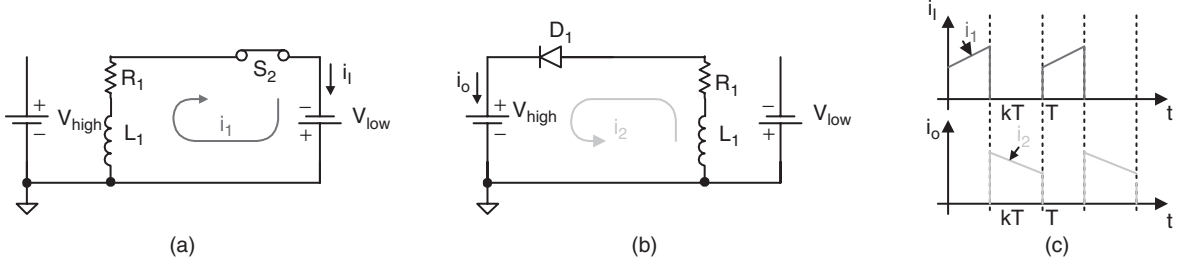

FIGURE 14.88 Mode D of F 2Q SI Luo-converter: (a) state-on: S_2 on; (b) state-off: D_1 on, S_2 off; and (c) input and output waveforms.

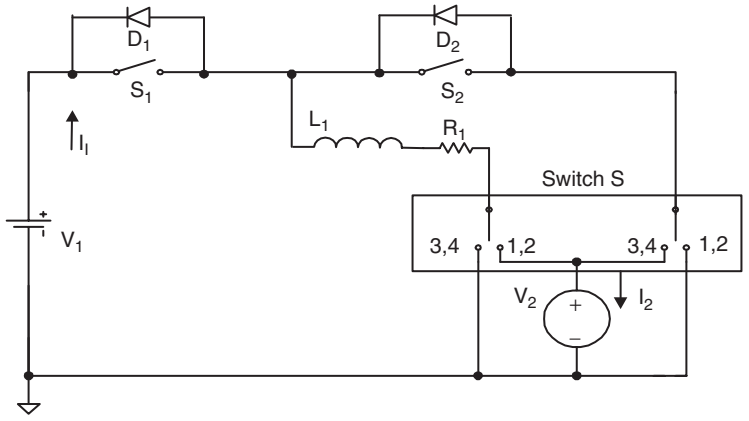

FIGURE 14.89 Four-quadrant switched-inductor DC/DC Luo-converter.

they are supposed as +42 V and ±14 V, respectively. Therefore, there are four-quadrants (modes) of operation:

1. Mode A: energy is transferred from source to positive voltage load; the first-quadrant operation, Q_I;
2. Mode B: energy is transferred from positive voltage load to source; the second-quadrant operation, Q_{II};
3. Mode C: energy is transferred from source to negative voltage load; the third-quadrant operation, Q_{III};
4. Mode C: energy is transferred from negative voltage load to source; the fourth-quadrant operation, Q_{IV}.

The first-quadrant is so-called the forward motoring (Forw. Mot.) operation. V_1 and V_2 are positive, and I_1 and I_2 are positive as well. The second-quadrant is so-called the forward regenerative (Forw. Reg.) braking operation. V_1 and V_2 are positive, and I_1 and I_2 are negative. The third-quadrant is so-called the reverse motoring (Rev. Mot.) operation. V_1 and I_1 are positive, and V_2 and I_2 are negative. The fourth-quadrant is so-called the reverse regenerative (Rev. Reg.) braking operation. V_1 and I_2 are positive, and I_1 and V_2 are negative. Each mode has two states: "on" and "off." Usually, each state is operating in different conduction duty k. The switching period is T, where $T = 1/f$. The switch status is shown in Table 14.7.

Mode A is shown in Fig. 14.84. During switch-**on** state, switch S_1 is closed. In this case the source voltage V_1 supplies the load V_2 and inductor L, inductor current i_L increases.

TABLE 14.7 Switch's status (mentioned switches are not off)

Q no.	State	S_1	D_1	S_2	D_2	S_3	Source	Load
Q_I, Mode A	ON	ON				ON 1/2	V_1+	V_2+
Forw. Mot.	OFF				ON	ON 1/2	I_1+	I_2+
Q_{II}, Mode B	ON			ON		ON 1/2	V_1+	V_2+
Forw. Reg.	OFF		ON			ON 1/2	I_1-	I_2-
Q_{III}, Mode C	ON	ON				ON 3/4	V_1+	V_2-
Rev. Mot.	OFF				ON	ON 3/4	I_1+	I_2-
Q_{IV}, Mode D	ON			ON		ON 3/4	V_1+	V_2-
Rev. Reg.	OFF		ON			ON 3/4	I_1-	I_2+

During switch-**off** state, diode D_2 is on. In this case current i_L flows through the load V_2 via the free-wheeling diode D_2, and it decreases.

Mode B is shown in Fig. 14.85. During switch-**on** state, switch S_2 is closed. In this case the load voltage V_2 supplies the inductor L, inductor current i_L increases. During switch-**off** state, diode D_1 is on, current i_L flows through the source V_1 and load V_2 via the diode D_1, and it decreases.

Mode C is shown in Fig. 14.87. During switch-**on** state, switch S_1 is closed. The source voltage V_1 supplies the inductor L, inductor current i_L increases. During switch-**off** state, diode D_2 is on. Current i_L flows through the load V_2 via the free-wheeling diode D_2, and it decreases.

Mode D is shown in Fig. 14.88. During switch-**on** state, switch S_2 is closed. The load voltage V_2 supplies the inductor L, inductor current i_L increases. During switch-**off** state, diode D_1 is on. Current i_L flows through the source V_1 via the diode D_1, and it decreases.

All description of the Modes A, B, C, and D is same as in Sections 14.10.1 and 14.10.2.

14.11 Multi-quadrant ZCS Quasi-resonant Luo-converters

Soft-switching converters are the fourth-generation converters. These converters are made of only inductor or capacitors. They usually perform in the systems between two voltage sources: V_1 and V_2. Voltage source V_1 is proposed positive voltage and voltage V_2 is the load voltage that can be positive or negative. In the investigation, both voltages are proposed constant voltage. Since V_1 and V_2 are constant value, the voltage transfer gain is constant. Our interesting research will concentrate on the working current and the power transfer efficiency η. The resistance R of the inductor has to be considered for the power transfer efficiency η calculation.

Reviewing the papers in the literature, we can find that most of the papers investigating the switched-component converters

are working in single-quadrant operation. Professor Luo and colleagues have developed this technique into multi-quadrant operation. We describe these in this section and the next sections.

Multi-quadrant ZCS quasi-resonant Luo-converters are the fourth-generation converters. Because these converters implement ZCS technique, they have the advantages of high power density, high power transfer efficiency, low EMI, and reasonable EMC. They have three modes:

- Two-quadrant ZCS quasi-resonant DC/DC Luo-converter in forward operation;
- Two-quadrant ZCS quasi-resonant DC/DC Luo-converter in reverse operation;
- Four-quadrant ZCS quasi-resonant DC/DC Luo-converter.

The two-quadrant ZCS quasi-resonant DC/DC Luo-converter in forward operation is derived for the energy transmission of a dual-voltage system. Both, the source and load voltages are positive polarity. It performs in the first-quadrant Q_I and the second-quadrant Q_{II} corresponding to the DC motor forward operation in motoring and regenerative braking states.

The two-quadrant ZCS quasi-resonant DC/DC Luo-converter in reverse operation is derived for the energy transmission of a dual-voltage system. The source voltage is positive and load voltage is negative polarity. It performs in the third-quadrant Q_{III} and the fourth-quadrant Q_{IV} corresponding to the DC motor reverse operation in motoring and regenerative braking states.

The four-quadrant ZCS quasi-resonant DC/DC Luo-converter is derived for the energy transmission of a dual-voltage system. The source voltage is positive, and load voltage can be positive or negative polarity. It performs four-quadrant operation corresponding to the DC motor forward and reverse operation in motoring and regenerative braking states.

14.11.1 Two-quadrant ZCS Quasi-resonant Luo-converter in Forward Operation

Since both voltages are low, this converter is designed as a ZCS quasi-resonant converter (ZCS-QRC). It is shown in Fig. 14.90. This converter consists of one main inductor L and two switches with their auxiliary components. A switch S_a is used for two-quadrant operation. Assuming the main inductance is sufficiently large, the current i_L is constant. The source voltage V_1 and load voltage V_2 are usually constant, $V_1 = 42\,\text{V}$ and $V_2 = 14\,\text{V}$. There are two modes of operation:

1. Mode A (Quadrant I): electrical energy is transferred from V_1 side to V_2 side, switch S_a links to D_2;
2. Mode B (Quadrant II): electrical energy is transferred from V_2 side to V_1 side, switch S_a links to D_1.

Each mode has two states: "on" and "off." The switch status of each state is shown in Table 14.8.

TABLE 14.8 Switch's status (the blank status means off)

Switch or diode	Mode A (QI)		Mode B (QII)	
	State-on	State-off	State-on	State-off
S_1	ON			
D_1				ON
S_2			ON	
D_2		ON		

Mode A is a ZCS buck converter. The equivalent circuit, current, and voltage waveforms are shown in Fig. 14.91. There are four time regions for the switching on and off period. The conduction duty cycle is $k = (t_1 + t_2)$ when the input current

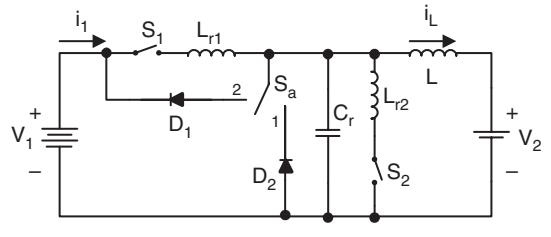

FIGURE 14.90 Two-quadrant (QI+QII) DC/DC ZCS quasi-resonant Luo-converter.

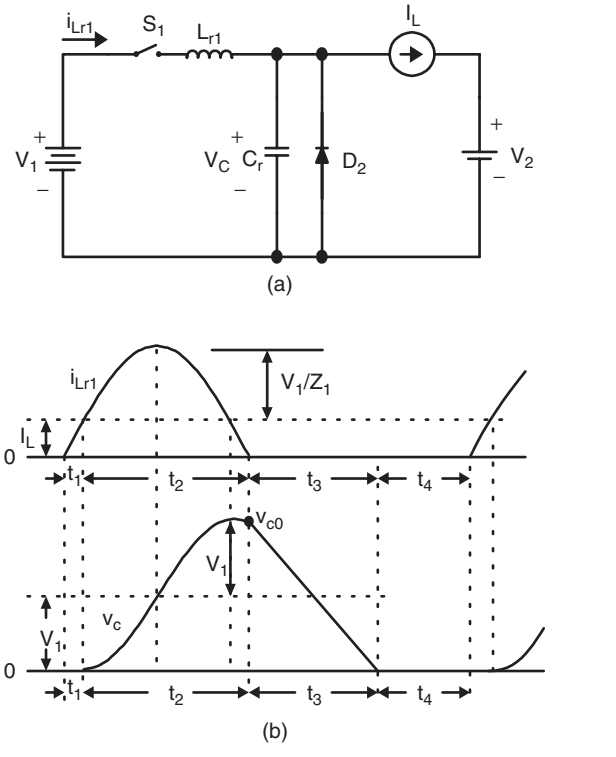

FIGURE 14.91 Mode A operation: (a) equivalent circuit and (b) waveforms.

flows through the switch S_1 and inductor L. The whole period is $T = (t_1 + t_2 + t_3 + t_4)$. Some formulas are listed below

$$\omega_1 = \frac{1}{\sqrt{L_{r1}C_r}}; \quad Z_1 = \sqrt{\frac{L_{r1}}{C_r}}; \quad i_{1-peak} = I_L + \frac{V_1}{Z_1} \tag{14.319}$$

$$t_1 = \frac{I_L L_{r1}}{V_1}; \quad \alpha_1 = \sin^{-1}\left(\frac{I_L Z_1}{V_1}\right) \tag{14.320}$$

$$t_2 = \frac{1}{\omega_1}(\pi + \alpha_1); \quad v_{CO} = V_1(1 + \cos\alpha_1) \tag{14.321}$$

$$t_3 = \frac{v_{CO}C_r}{I_L}; \quad \frac{I_L V_2}{V_1} = \frac{t_1 + t_2}{T}\left(I_L + \frac{V_1}{Z_1}\frac{\cos\alpha_1}{\pi/2 + \alpha_1}\right) \tag{14.322}$$

$$t_4 = \frac{V_1(t_1 + t_2)}{V_2 I_L}\left(I_L + \frac{V_1}{Z_1}\frac{\cos\alpha_1}{\pi/2 + \alpha_1}\right) - (t_1 + t_2 + t_3); \tag{14.323}$$

$$k = \frac{t_1 + t_2}{t_1 + t_2 + t_3 + t_4}; \quad T = t_1 + t_2 + t_3 + t_4; \quad f = 1/T \tag{14.324}$$

Mode B is a ZCS boost converter. The equivalent circuit, current, and voltage waveforms are shown in Fig. 14.92. There are four time regions for the switching on and off period. The conduction duty cycle is $k = (t_1 + t_2)$, but the output current only flows through the source V_1 in the period t_4. The whole period is $T = (t_1 + t_2 + t_3 + t_4)$. Some formulas are listed below

$$\omega_2 = \frac{1}{\sqrt{L_{r2}C_r}}; \quad Z_2 = \sqrt{\frac{L_{r2}}{C_r}}; \quad i_{2-peak} = I_L + \frac{V_1}{Z_2} \tag{14.325}$$

$$t_1 = \frac{I_L L_{r2}}{V_1}; \quad \alpha_2 = \sin^{-1}\left(\frac{I_L Z_2}{V_1}\right) \tag{14.326}$$

$$t_2 = \frac{1}{\omega_2}(\pi + \alpha_2); \quad v_{CO} = -V_1\cos\alpha_2 \tag{14.327}$$

$$t_3 = \frac{(V_1 - v_{CO})C_r}{I_L}; \quad \frac{I_L V_2}{V_1} = \frac{t_4}{T}I_L \tag{14.328}$$

$$\frac{V_2}{V_1} = \frac{t_4}{T} = \frac{t_4}{t_1 + t_2 + t_3 + t_4}; \quad t_4 = \frac{t_1 + t_2 + t_3}{(V_1/V_2) - 1} \tag{14.329}$$

$$k = \frac{t_1 + t_2}{t_1 + t_2 + t_3 + t_4}; \quad T = t_1 + t_2 + t_3 + t_4; \quad f = 1/T \tag{14.330}$$

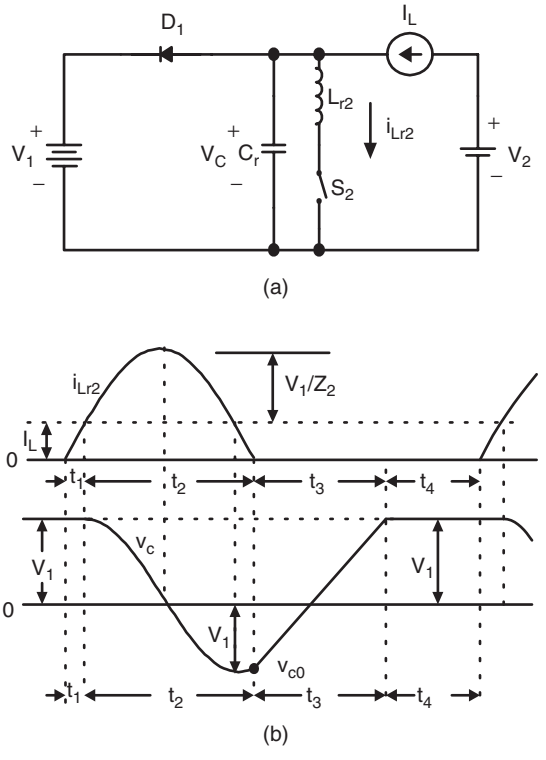

FIGURE 14.92 Mode B operation: (a) equivalent circuit and (b) waveforms.

14.11.2 Two-quadrant ZCS Quasi-resonant Luo-converter in Reverse Operation

Two-quadrant ZCS quasi-resonant Luo-converter in reverse operation is shown in Fig. 14.93. It is a new soft-switching technique with two-quadrant operation, which effectively reduces the power losses and largely increases the power transfer efficiency. It consists of one main inductor L and two switches with their auxiliary components. A switch S_a is used for two-quadrant operation. Assuming the main inductance L is sufficiently large, the current i_L is constant. The source voltage V_1 and load voltage V_2 are usually constant, e.g. $V_1 = 42\,\text{V}$ and $V_2 = -28\,\text{V}$. There are two modes of operation:

1. Mode C (Quadrant III): electrical energy is transferred from V_1 side to $-V_2$ side, switch S_a links to D_2;
2. Mode D (Quadrant IV): electrical energy is transferred from $-V_2$ side to V_1 side, switch S_a links to D_1.

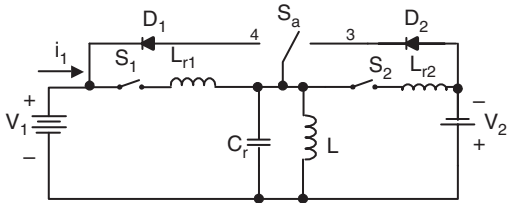

FIGURE 14.93 Two-quadrant (QIII+IV) DC/DC ZCS quasi-resonant Luo-converter.

Each mode has two states: "on" and "off." The switch status of each state is shown in Table 14.9.

Mode C is a ZCS buck–boost converter. The equivalent circuit, current, and voltage waveforms are shown in Fig. 14.94. There are four time regions for the switching on and off period. The conduction duty cycle is $kT = (t_1 + t_2)$ when the input current flows through the switch S_1 and the main inductor L. The whole period is $T = (t_1 + t_2 + t_3 + t_4)$. Some formulas are listed below

$$\omega_1 = \frac{1}{\sqrt{L_{r1}C_r}}; \quad Z_1 = \sqrt{\frac{L_{r1}}{C_r}}; \quad i_{1-peak} = I_L + \frac{V_1}{Z_1} \tag{14.331}$$

TABLE 14.9 Switch's status (the blank status means off)

Switch or diode	Mode C (QIII)		Mode D (QIV)	
	State-on	State-off	State-on	State-off
S_1	ON			
D_1				ON
S_2			ON	
D_2		ON		

$$t_1 = \frac{I_L L_{r1}}{V_1 + V_2}; \quad \alpha_1 = \sin^{-1}\left(\frac{I_L Z_1}{V_1 + V_2}\right) \tag{14.332}$$

$$t_2 = \frac{1}{\omega_1}(\pi + \alpha_1); \quad v_{CO} = (V_1 - V_2) + V_1 \sin(\pi/2 + \alpha_1) = V_1(1 + \cos\alpha_1) - V_2 \tag{14.333}$$

$$t_3 = \frac{(v_{CO} + V_2)C_r}{I_L} = \frac{V_1(1 + \cos\alpha_1)C_r}{I_L};$$

$$I_1 = \frac{t_1 + t_2}{T}\left(I_L + \frac{V_1 + V_2}{Z_1}\frac{\cos\alpha_1}{\pi/2 + \alpha_1}\right); \quad I_2 = \frac{t_4}{T}I_L \tag{14.334}$$

$$t_4 = \frac{V_1(t_1 + t_2)}{V_2 I_L}\left(I_L + \frac{V_1 + V_2}{Z_1}\frac{\cos\alpha_1}{\pi/2 + \alpha_1}\right) \tag{14.335}$$

$$k = \frac{t_1 + t_2}{t_1 + t_2 + t_3 + t_4}; \quad T = t_1 + t_2 + t_3 + t_4; \quad f = 1/T \tag{14.336}$$

Mode D is a cross ZCS buck–boost converter. The equivalent circuit, current, and voltage waveforms are shown in Fig. 14.95. There are four time regions for the switching on and off period. The conduction duty cycle is $kT = (t_1 + t_2)$, but the output current only flows through the source V_1 in

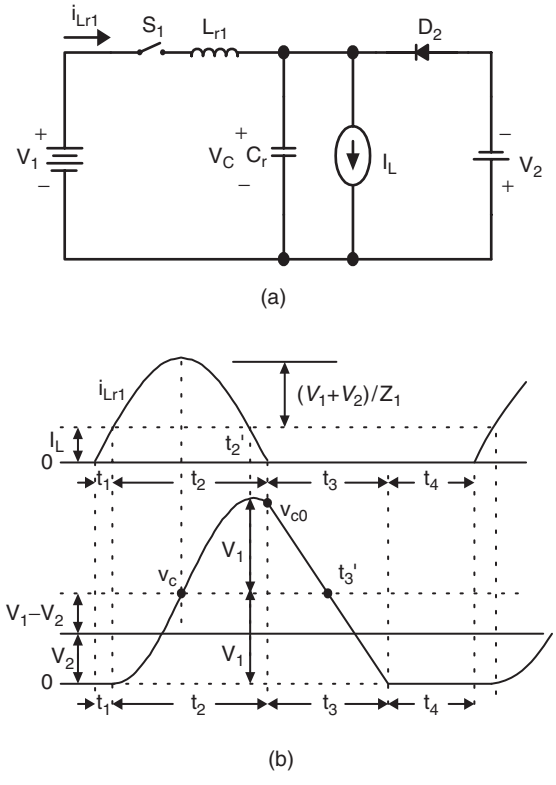

FIGURE 14.94 Mode C operation: (a) equivalent circuit and (b) waveforms.

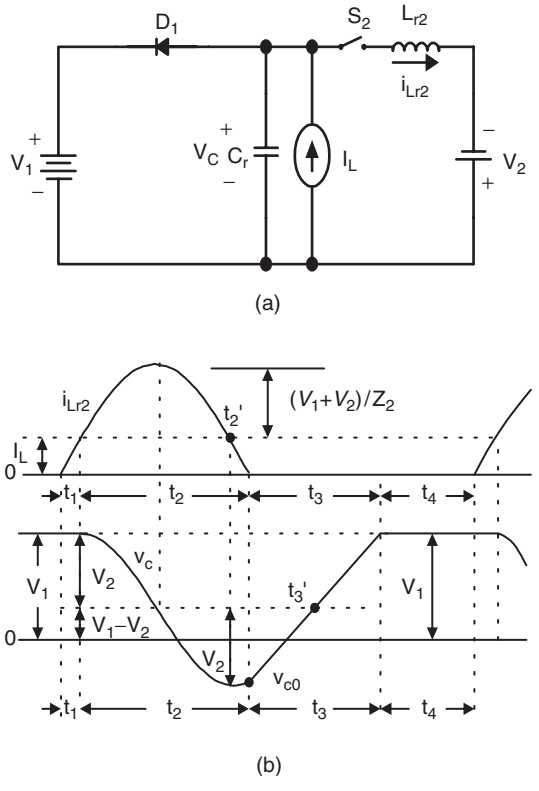

FIGURE 14.95 Mode D operation: (a) equivalent circuit and (b) waveforms.

the period t_4. The whole period is $T = (t_1 + t_2 + t_3 + t_4)$. Some formulas are listed below

$$\omega_2 = \frac{1}{\sqrt{L_{r2}C_r}}; \quad Z_2 = \sqrt{\frac{L_{r2}}{C_r}}; \quad i_{2-peak} = I_L + \frac{V_2}{Z_2} \tag{14.337}$$

$$t_1 = \frac{I_L L_{r2}}{V_1 + V_2}; \quad \alpha_2 = \sin^{-1}\left(\frac{I_L Z_2}{V_2 + V_2}\right) \tag{14.338}$$

$$t_2 = \frac{1}{\omega_2}(\pi + \alpha_2); \quad v_{CO} = (V_1 - V_2) - V_2\sin(\pi/2 + \alpha_2)$$
$$= V_1 - V_2(1 + \cos\alpha_2) \tag{14.339}$$

$$t_3 = \frac{(V_1 - v_{CO})C_r}{I_L} = \frac{V_2(1 + \cos\alpha_2)C_r}{I_L};$$
$$I_2 = \frac{t_1 + t_2}{T}\left(I_L + \frac{V_1 + V_2}{Z_2}\frac{\cos\alpha_2}{\pi/2 + \alpha_2}\right); \quad I_1 = \frac{t_4}{T}I_L \tag{14.340}$$

$$t_4 = \frac{V_2(t_1 + t_2)}{V_1 I_L}\left(I_L + \frac{V_1 + V_2}{Z_2}\frac{\cos\alpha_2}{\pi/2 + \alpha_2}\right) \tag{14.341}$$

$$k = \frac{t_1 + t_2}{t_1 + t_2 + t_3 + t_4}; \quad T = t_1 + t_2 + t_3 + t_4; \quad f = 1/T \tag{14.342}$$

14.11.3 Four-quadrant ZCS Quasi-resonant Luo-converter

Four-quadrant ZCS quasi-resonant Luo-converter is shown in Fig. 14.96. Circuit 1 implements the operation in quadrants I and II, circuit 2 implements the operation in quadrants III and IV. Circuit 1 and 2 can be converted to each other by auxiliary switch. Each circuit consists of one main inductor L and two switches. A switch S_a is used for four-quadrant operation. Assuming that the main inductance L is sufficiently large, the current i_L remains constant. The source and load voltages are usually constant, e.g. $V_1 = 42\,\text{V}$ and $V_2 = \pm 28\,\text{V}$ [7–9]. There are four modes of operation:

1. Mode A (Quadrant I): electrical energy is transferred from V_1 side to V_2 side, switch S_a links to D_2;
2. Mode B (Quadrant II): electrical energy is transferred from V_2 side to V_1 side, switch S_a links to D_1;
3. Mode C (Quadrant III): electrical energy is transferred from V_1 side to $-V_2$ side, switch S_a links to D_2;
4. Mode D (Quadrant IV): electrical energy is transferred from $-V_2$ side to V_1 side, switch S_a links to D_1.

Each mode has two states: "on" and "off." The switch status of each state is shown in Table 14.10.

The operation of Mode A, B, C, and D is same as in the previous Sections 14.11.1 and 14.11.2.

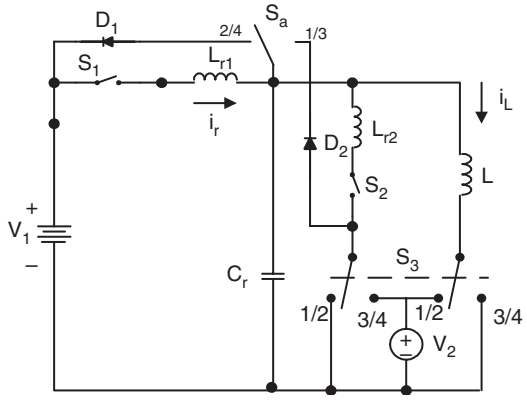

FIGURE 14.96 Four-quadrant DC/DC ZCS quasi-resonant Luo-converter.

14.12 Multi-quadrant ZVS Quasi-resonant Luo-converters

Multi-quadrant ZVS quasi-resonant Luo-converters are the fourth-generation converters. Because these converters implement ZCS technique, they have the advantages of high power density, high power transfer efficiency, low EMI, and reasonable EMC. They have three modes:

- Two-quadrant ZVS quasi-resonant DC/DC Luo-converter in forward operation;
- Two-quadrant ZVS quasi-resonant DC/DC Luo-converter in reverse operation;
- Four-quadrant ZVS quasi-resonant DC/DC Luo-converter.

The two-quadrant ZVS quasi-resonant DC/DC Luo-converter in forward operation is derived for the energy transmission of a dual-voltage system. Both, the source and load voltages are positive polarity. It performs in the first-quadrant Q_I and the second-quadrant Q_{II} corresponding to the DC motor forward operation in motoring and regenerative braking states.

The two-quadrant ZVS quasi-resonant DC/DC Luo-converter in reverse operation is derived for the energy transmission of a dual-voltage system. The source voltage is positive and load voltage is negative polarity. It performs in the third-quadrant Q_{III} and the fourth-quadrant Q_{IV} corresponding to the DC motor reverse operation in motoring and regenerative braking states.

The four-quadrant ZVS quasi-resonant DC/DC Luo-converter is derived for the energy transmission of a dual-voltage system. The source voltage is positive, and load voltage can be positive or negative polarity. It performs four-quadrant operation corresponding to the DC motor forward and reverse operation in motoring and regenerative braking states.

TABLE 14.10 Switch's status (the blank status means off)

Circuit//switch or diode	Mode A (QI)		Mode B (QII)		Mode C (QIII)		Mode D (QIV)	
	State-on	State-off	State-on	State-off	State-on	State-off	State-on	State-off
Circuit	Circuit 1				Circuit 2			
S_1	ON				ON			
D_1				ON				ON
S_2			ON				ON	
D_2		ON				ON		

14.12.1 Two-quadrant ZVS Quasi-resonant DC/DC Luo-converter in Forward Operation

Two-quadrant ZVS quasi-resonant Luo-converter in forward operation is shown in Fig. 14.97. It consists of one main inductor L and two switches with their auxiliary components.

Assuming the main inductance L is sufficiently large, the current i_L is constant. The source voltage V_1 and load voltage V_2 are usually constant, e.g. $V_1 = 42\,\text{V}$ and $V_2 = 14\,\text{V}$. There are two modes of operation:

1. Mode A (Quadrant I): electrical energy is transferred from V_1 side to V_2 side;
2. Mode B (Quadrant II): electrical energy is transferred from V_2 side to V_1 side.

Each mode has two states: "on" and "off." The switch status of each state is shown in Table 14.11.

Mode A is a ZVS buck converter shown in Fig. 14.98. There are four time regions for the switching on and off period.

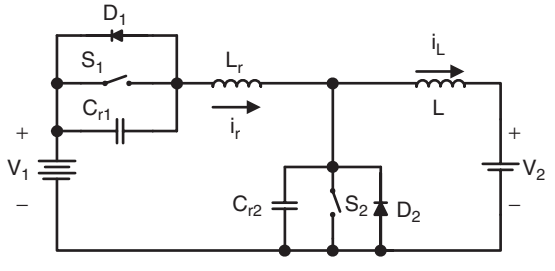

FIGURE 14.97 Two-quadrant (QI+QII) DC/DC ZVS quasi-resonant Luo-converter.

TABLE 14.11 Switch's status (the blank status means off)

Switch	Mode A (QI)		Mode B (QII)	
	State-on	State-off	State-on	State-off
S_1	ON			
D_1				ON
S_2			ON	
D_2		ON		

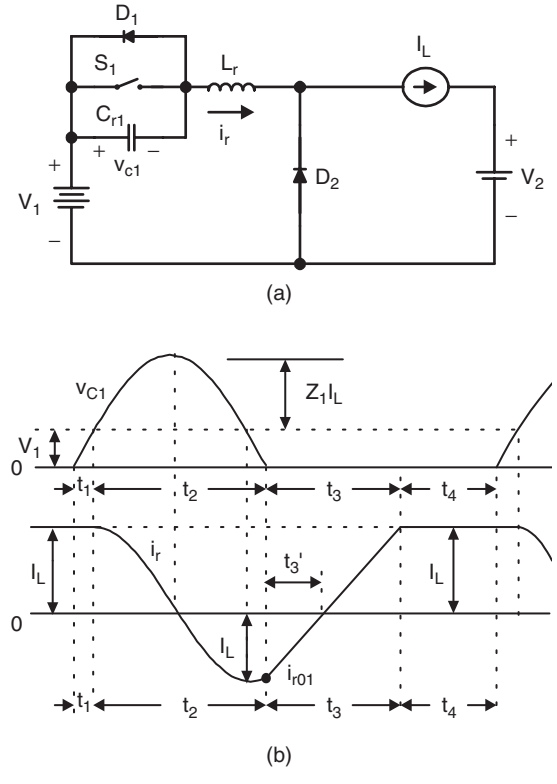

FIGURE 14.98 Mode A operation: (a) equivalent circuit and (b) waveforms.

The conduction duty cycle is $kT = (t_3 + t_4)$ when the input current flows through the switch S_1 and the main inductor L. The whole period is $T = (t_1 + t_2 + t_3 + t_4)$. Some relevant formulas are listed below

$$\omega_1 = \frac{1}{\sqrt{L_r C_{r1}}}; \quad Z_1 = \sqrt{\frac{L_r}{C_{r1}}}; \quad v_{c1-peak} = V_1 + Z_1 I_L \tag{14.343}$$

$$t_1 = \frac{V_1 C_{r1}}{I_L}; \quad \alpha_1 = \sin^{-1}\left(\frac{V_1}{Z_1 I_L}\right) \tag{14.344}$$

$$t_2 = \frac{1}{\omega_1}(\pi + \alpha_1); \quad i_{rO1} = -I_L \cos\alpha_1 \tag{14.345}$$

$$t_3=\frac{(I_L-i_{rO1})L_r}{V_1};\quad I_1=\frac{I_LV_2}{V_1}=\frac{1}{T}\int_{t_3}^{t_4} i_r\,dt\approx\frac{1}{T}(I_Lt_4)=\frac{t_4}{T}I_L \tag{14.346}$$

$$t_4=\frac{t_1+t_2+t_3}{(V_1/V_2)-1} \tag{14.347}$$

$$k=\frac{t_3+t_4}{t_1+t_2+t_3+t_4};\quad T=t_1+t_2+t_3+t_4;\quad f=1/T \tag{14.348}$$

Mode B is a ZVS boost converter shown in Fig. 14.99. There are four time regions for the switching on and off period. The conduction duty cycle is $kT=(t_3+t_4)$, but the output current only flows through the source V_1 in the period (t_1+t_2). The whole period is $T=(t_1+t_2+t_3+t_4)$. Some relevant formulas are listed below

$$\omega_2=\frac{1}{\sqrt{L_rC_{r2}}};\quad Z_2=\sqrt{\frac{L_r}{C_{r2}}};\quad v_{C2-peak}=V_1+Z_2I_L \tag{14.349}$$

$$t_1=\frac{V_1C_{r2}}{I_L};\quad \alpha_2=\sin^{-1}\left(\frac{V_1}{Z_2I_L}\right) \tag{14.350}$$

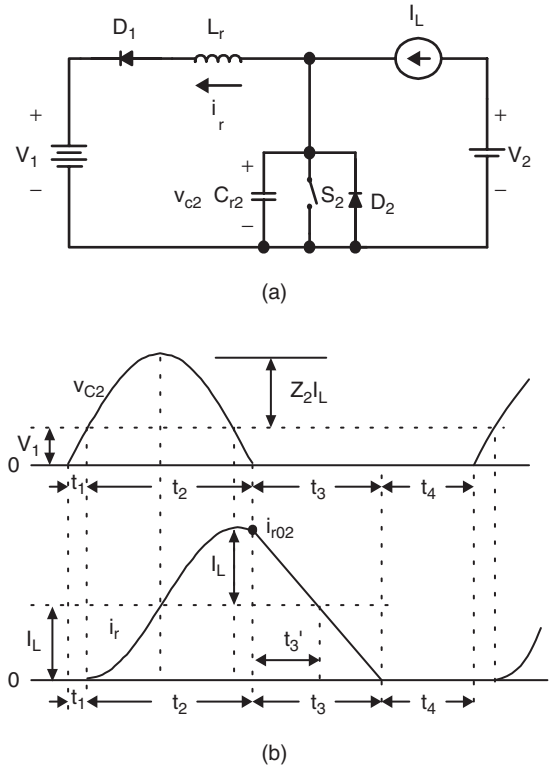

FIGURE 14.99 Mode B operation: (a) equivalent circuit and (b) waveforms.

$$t_2=\frac{1}{\omega_2}(\pi+\alpha_2);\quad i_{rO2}=I_L(1+\cos\alpha_2) \tag{14.351}$$

$$t_3=\frac{i_{rO2}L_r}{V_1};$$

$$I_1=\frac{I_LV_2}{V_1}=\frac{1}{T}\int_{t_1}^{t_3} i_r\,dt\approx\frac{1}{T}\big[I_L\big(t_2+t_3\big)\big]=\frac{t_2+t_3}{T}I_L;$$

$$\text{or}\quad \frac{V_2}{V_1}=\frac{1}{T}(t_2+t_3)=\frac{t_2+t_3}{t_1+t_2+t_3+t_4} \tag{14.352}$$

$$t_4=\left(\frac{V_1}{V_2}-1\right)(t_2+t_3)-t_1; \tag{14.353}$$

$$k=\frac{t_3+t_4}{t_1+t_2+t_3+t_4};\quad T=t_1+t_2+t_3+t_4;\quad f=1/T \tag{14.354}$$

14.12.2 Two-quadrant ZVS Quasi-resonant DC/DC Luo-converter in Reverse Operation

Two-quadrant ZVS quasi-resonant Luo-converter in reverse operation is shown in Fig. 14.100. It consists of one main inductor L and two switches with their auxiliary components. Assuming the main inductance L is sufficiently large, the current i_L is constant. The source voltage V_1 and load voltage V_2 are usually constant, e.g. $V_1=+42\,\text{V}$ and $V_2=-28\,\text{V}$. There are two modes of operation:

1. Mode C (Quadrant III): electrical energy is transferred from V_1 side to $-V_2$ side;
2. Mode D (Quadrant IV): electrical energy is transferred from $-V_2$ side to V_1 side.

Each mode has two states: "on" and "off." The switch status of each state is shown in Table 14.12.

Mode C is a ZVS buck–boost converter shown in Fig. 14.101. There are four time regions for the switching on and off period. The conduction duty cycle is $kT=(t_3+t_4)$ when the input current flows through the switch S_1 and the main inductor L. The whole period is $T=(t_1+t_2+t_3+t_4)$.

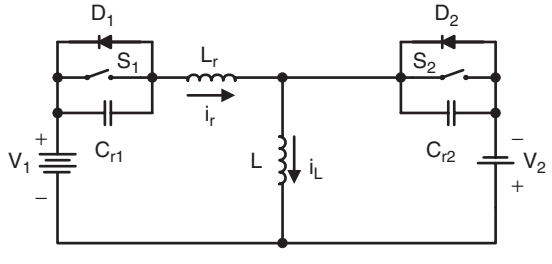

FIGURE 14.100 Two-quadrant (QIII+IV) DC/DC ZVS quasi-resonant Luo-converter.

TABLE 14.12 Switch's status (the blank status means off)

Switch	Mode C (QIII)		Mode D (QIV)	
	State-on	State-off	State-on	State-off
S_1	ON			
D_1				ON
S_2			ON	
D_2		ON		

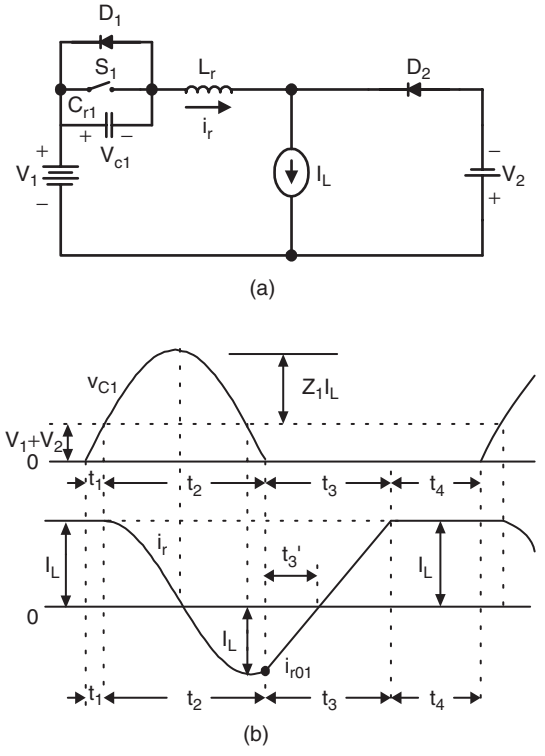

FIGURE 14.101 Mode C operation: (a) equivalent circuit and (b) waveforms.

Some formulas are listed below

$$\omega_1=\frac{1}{\sqrt{L_r C_{r1}}};\quad Z_1=\sqrt{\frac{L_r}{C_{r1}}};\quad v_{c1-peak}=V_1+V_2+Z_1 I_L \tag{14.355}$$

$$t_1=\frac{(V_1+V_2)C_{r1}}{I_L};\quad \alpha_1=\sin^{-1}\left(\frac{V_1+V_2}{Z_1 I_L}\right) \tag{14.356}$$

$$t_2=\frac{1}{\omega_1}(\pi+\alpha_1);\quad i_{rO1}=-I_L\sin(\pi/2+\alpha_1) \tag{14.357}$$

$$t_3=\frac{(I_L-i_{rO1})L_r}{V_1+V_2}=\frac{I_L(1+\cos\alpha_1)L_r}{V_1+V_2};$$

$$I_1=\frac{I_L V_2}{V_1}=\frac{1}{T}\int_{t_3}^{t_4} i_r\,dt\approx\frac{1}{T}(I_L t_4)=\frac{t_4}{T}I_L \tag{14.358}$$

$$t_4=\frac{t_1+t_2+t_3}{(V_1/V_2)-1};\quad I_2=\frac{1}{T}\int_{t_1}^{t_3}(I_L-i_r)\,dt\approx\frac{t_1+t_2+t_3}{T}I_L \tag{14.359}$$

$$k=\frac{t_3+t_4}{t_1+t_2+t_3+t_4};\quad T=t_1+t_2+t_3+t_4;\quad f=1/T \tag{14.360}$$

Mode D is a cross ZVS buck–boost converter shown in Fig. 14.102. There are four time regions for the switching on and off period. The conduction duty cycle is $kT = (t_3 + t_4)$, but the output current only flows through the source V_1 in the period $(t_1 + t_2)$. The whole period is $T = (t_1 + t_2 + t_3 + t_4)$. Some formulae are listed below

$$\omega_2=\frac{1}{\sqrt{L_r C_{r2}}};\quad Z_2=\sqrt{\frac{L_r}{C_{r2}}};\quad v_{C2-peak}=V_1+V_2+Z_2 I_L \tag{14.361}$$

$$t_1=\frac{(V_1+V_2)C_{r2}}{I_L};\quad \alpha_2=\sin^{-1}\left(\frac{V_1+V_2}{Z_2 I_L}\right) \tag{14.362}$$

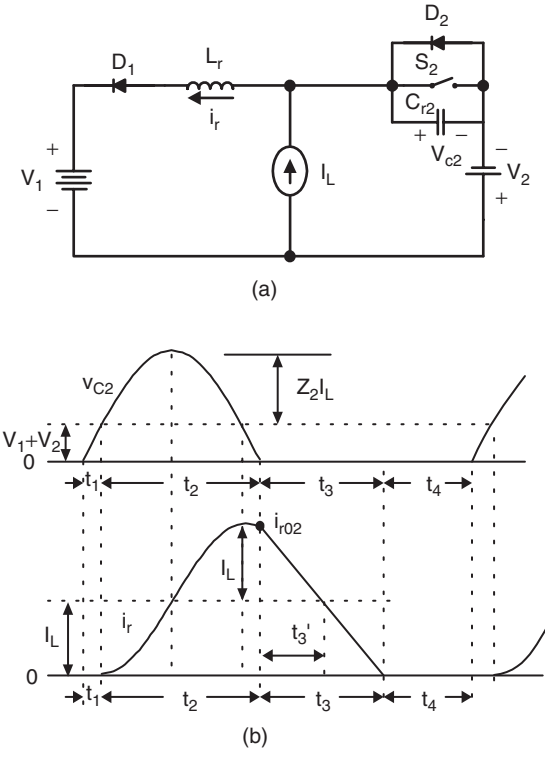

FIGURE 14.102 Mode D operation: (a) equivalent circuit and (b) waveforms.

$$t_2 = \frac{1}{\omega_2}(\pi + \alpha_2); \quad i_{rO2} = I_L[1 + \sin(\pi/2 + \alpha_2)] \quad (14.363)$$

$$t_3 = \frac{i_{rO2}L_r}{V_1 + V_2} = \frac{I_L(1 + \cos\alpha_2)L_r}{V_1 + V_2};$$

$$I_1 = \frac{1}{T}\int_{t_1}^{t_3} i_r dt \approx \frac{t_1 + t_2 + t_3}{T} I_L;$$

$$I_2 = \frac{1}{T}\int_{t_3}^{t_4} i_r dt \approx \frac{1}{T}(I_L t_4) = \frac{t_4}{T} I_L;$$

$$\frac{V_2}{V_1} = \frac{1}{T}(t_1 + t_2 + t_3) = \frac{t_1 + t_2 + t_3}{t_1 + t_2 + t_3 + t_4} \quad (14.364)$$

$$t_4 = \left(\frac{V_1}{V_2} - 1\right)(t_1 + t_2 + t_3) \quad (14.365)$$

$$k = \frac{t_3 + t_4}{t_1 + t_2 + t_3 + t_4}; \quad T = t_1 + t_2 + t_3 + t_4; \quad f = 1/T \quad (14.366)$$

14.12.3 Four-quadrant ZVS Quasi-resonant DC/DC Luo-converter

Four-quadrant ZVS quasi-resonant Luo-converter is shown in Fig. 14.103. Circuit 1 implements the operation in quadrants I and II, circuit 2 implements the operation in quadrants III and IV. Circuit 1 and 2 can be converted to each other by auxiliary switch. Each circuit consists of one main inductor L and two switches. Assuming that the main inductance L is sufficiently large, the current i_L is constant. The source and load voltages are usually constant, e.g. $V_1 = 42\,\text{V}$ and $V_2 = \pm 28\,\text{V}$. There are four modes of operation:

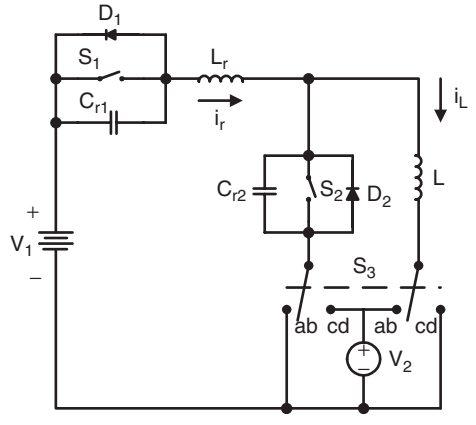

FIGURE 14.103 Four-quadrant DC/DC ZVS quasi-resonant Luo-converter.

- Mode A (Quadrant I): electrical energy is transferred from V_1 side to V_2 side;
- Mode B (Quadrant II): electrical energy is transferred from V_2 side to V_1 side;
- Mode C (Quadrant III): electrical energy is transferred from V_1 side to $-V_2$ side;
- Mode D (Quadrant IV): electrical energy is transferred from $-V_2$ side to V_1 side.

Each mode has two states: "on" and "off." The switch status of each state is shown in Table 14.13.

The description of Modes A, B, C, and D is same as in the previous Sections 14.12.1 and 14.12.2.

14.13 Synchronous-rectifier DC/DC Luo-converters

Synchronous-rectifier (SR) DC/DC converters are called the fifth-generation converters. The development of the microelectronics and computer science requires the power supplies with low output voltage and strong current. Traditional diode bridge rectifiers are not available for this requirement. Soft-switching technique can be applied in SR DC/DC converters. We have created few converters with very low voltage (5 V, 3.3 V, and 1.8 ~ 1.5 V) and strong current (30 A, 60 A up to 200 A) and high power transfer efficiency (86%, 90% up to 93%). In this section, few new circuits, different from the ordinary SR DC/DC converters, are introduced:

- Flat transformer synchronous-rectifier DC/DC Luo-converter;
- Double current synchronous-rectifier DC/DC Luo-converter with active clamp circuit;
- Zero-current-switching synchronous-rectifier DC/DC Luo-converter;
- Zero-voltage-switching synchronous-rectifier DC/DC Luo-converter.

14.13.1 Flat Transformer Synchronous-rectifier DC/DC Luo-converter

Flat transformer **SR DC/DC Luo-converter** is shown in Fig. 14.104. The switches S_1, S_2, and S_3 are the low-resistance MOSFET devices with very low resistance R_S (7–8 mΩ). Since we use a flat transformer, the leakage inductance L_m and resistance R_L are small. Other parameters are $C = 1\,\mu\text{F}$, $L_m = 1\,\text{nH}$, $R_L = 2\,\text{m}\Omega$, $L = 5\,\mu\text{H}$, $C_O = 10\,\mu\text{F}$. The input voltage is $V_1 = 30\,\text{VDC}$ and output voltage is V_2, the output current is I_O. The transformer term's ratio is $N = 12:1$. The repeating period is $T = 1/f$ and conduction duty is k. There are four working modes.

TABLE 14.13 Switch's status (the blank status means off)

Circuit//switch or diode	Mode A (QI)		Mode B (QII)		Mode C (QIII)		Mode D (QIV)	
	State-on	State-off	State-on	State-off	State-on	State-off	State-on	State-off
Circuit	Circuit 1				Circuit 2			
S_1	ON				ON			
D_1				ON				ON
S_2			ON				ON	
D_2		ON				ON		

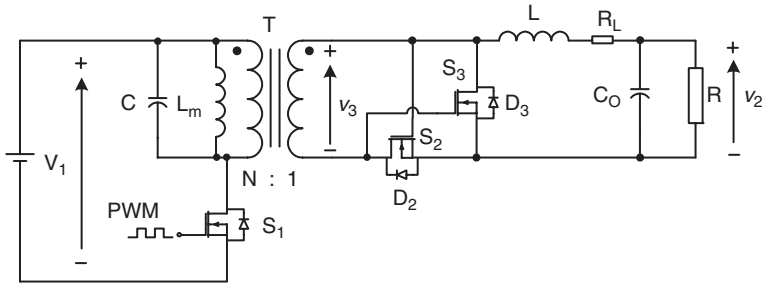

FIGURE 14.104 Flat transformer SR Luo-converter.

The natural resonant frequency is

$$\omega = \frac{1}{\sqrt{L_m C}} \tag{14.367}$$

The intervals are

$$t_1 = \frac{L_m}{V_1}\frac{I_O}{N}; \quad t_2 \approx kT; \tag{14.368}$$

$$t_3 = \sqrt{L_m C}\left[\frac{\pi}{2} + \frac{V_1}{\sqrt{V_1^2 + \frac{L_m}{C}\left(\frac{I_O}{N}\right)^2}}\right]; \quad t_4 \approx (1-k)T \tag{14.369}$$

Average output voltage V_2 and input current I_1 are

$$V_2 = \frac{kV_1}{N} - \left(R_L + R_S + \frac{L_m}{TN^2}\right) I_O; \quad I_1 = k\frac{I_O}{N} \tag{14.370}$$

The power transfer efficiency is

$$\eta = \frac{V_2 I_O}{V_1 I_1} = 1 - \frac{R_L + R_S + (L_m/TN^2)}{kV_1/N} I_O \tag{14.371}$$

When we set the frequency $f = 150$–$200\,\text{kHz}$, we obtained the $V_2 = 1.8\,\text{V}$, $N = 12$, $I_O = 0$–30 A, Volume $= 2.5\,\text{in}^3$. The average power transfer efficiency is 92.3% and the maximum power density (PD) is $21.6\,\text{W/in}^3$.

14.13.2 Double Current SR DC/DC Luo-converter with Active Clamp Circuit

The converter in Fig. 14.104 resembles a half-wave rectifier. **Double current (DC) SR DC/DC Luo-converter** with active clamp circuit is shown in Fig. 14.105. The switches S_1–S_4 are the low-resistance MOSFET devices with very low resistance R_S (7–8 mΩ). Since S_3 and S_4 plus L_1 and L_2 form a double current circuit and S_2 plus C is the active clamp circuit, this converter resembles a full-wave rectifier and obtains strong output current. Other parameters are $C = 1\,\mu\text{F}$, $L_m = 1\,\text{nH}$, $R_L = 2\,\text{m}\Omega$, $L = 5\,\mu\text{H}$, $C_O = 10\,\mu\text{F}$. The input voltage is $V_1 = 30\,\text{VDC}$ and output voltage is V_2, the output current is I_O. The transformer term's ratio is $N = 12:1$. The repeating period is $T = 1/f$ and conduction duty is k. There are four working modes.

The natural resonant frequency is

$$\omega = \frac{1}{\sqrt{L_m C}}; \quad V_C = \frac{k}{1-k} V_1 \tag{14.372}$$

The interval of t_1 is

$$t_1 = \frac{L_m}{V_1}\frac{I_O}{N}; \quad t_2 \approx kT; \tag{14.373}$$

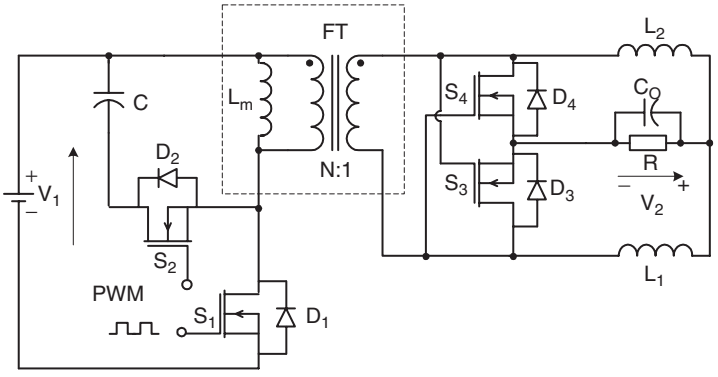

FIGURE 14.105 Double current SR Luo-converter.

$$t_3 = \sqrt{L_m C}\left[\frac{\pi}{2} + \frac{V_1}{\sqrt{V_1^2 + \frac{L_m}{C}\left(\frac{I_O}{N}\right)^2}}\right]; \quad t_4 \approx (1-k)T \tag{14.374}$$

Average output voltage V_2 and input current I_1 are

$$V_2 = \frac{kV_1}{N} - \left(R_L + R_S + \frac{L_m}{TN^2}\right) I_O; \quad I_1 = k\frac{I_O}{N} \tag{14.375}$$

The power transfer efficiency

$$\eta = \frac{V_2 I_O}{V_1 I_1} = 1 - \frac{R_L + R_S + (L_m/TN^2)}{kV_1/N} I_O \tag{14.376}$$

When we set the frequency $f = 200$–$250\,\text{kHz}$, we obtained the $V_2 = 1.8\,\text{V}$, $N = 12$, $I_O = 0$–$35\,\text{A}$, Volume $= 2.5\,\text{in}^3$. The average power transfer efficiency is 94% and the maximum power density (PD) is $25\,\text{W/in}^3$.

14.13.3 Zero-current-switching Synchronous-rectifier DC/DC Luo-converter

Since the power loss across the main switch S_1 is high in **DC SR DC/DC Luo-converter**, we designed **ZCS SR DC/DC Luo-converter** shown in Fig. 14.106. This converter is based on the **DC SR DC/DC Luo-converter** plus ZCS technique. It employs a double core flat transformer.

The ZCS resonant frequency is

$$\omega_r = \frac{1}{\sqrt{L_r C_r}} \tag{14.377}$$

The normalized impedance is

$$Z_r = \sqrt{\frac{L_r}{C_r}} \quad \text{and} \quad \alpha = \sin^{-1}\left(\frac{I_1 Z_r}{V_1}\right) \tag{14.378}$$

The intervals are

$$t_1 = \frac{I_1 L_r}{V_1}; \quad t_2 = \frac{1}{\omega_r}(\pi + \alpha); \tag{14.379}$$

$$t_3 = \frac{V_1(1+\cos\alpha)C_r}{I_1};$$

$$t_4 = \frac{V_1(t_1+t_2)}{V_2 I_1}\left(I_L + \frac{V_1}{Z_r}\frac{\cos\alpha}{\pi/2+\alpha}\right) - (t_1+t_2+t_3) \tag{14.380}$$

Average output voltage V_2 and input current I_1 are

$$V_2 = \frac{kV_1}{N} - \left(R_L + R_S + \frac{L_m}{TN^2}\right) I_O; \quad I_1 = k\frac{I_O}{N} \tag{14.381}$$

The power transfer efficiency

$$\eta = \frac{V_2 I_O}{V_1 I_1} = 1 - \frac{R_L + R_S + (L_m/TN^2)}{kV_1/N} I_O \tag{14.382}$$

When we set the $V_1 = 60\,\text{V}$ and frequency $f = 200$–$250\,\text{kHz}$, we obtained the $V_2 = 1.8\,\text{V}$, $N = 12$, $I_O = 0$–$60\,\text{A}$, Volume $= 4\,\text{in}^3$. The average power transfer efficiency is 94.5% and the maximum power density (PD) is $27\,\text{W/in}^3$.

14.13.4 Zero-voltage-switching Synchronous-rectifier DC/DC Luo-converter

ZVS SR DC/DC Luo-converter is shown in Fig. 14.107. This converter is based on the **DC SR DC/DC Luo-converter** plus ZVS technique. It employs a double core flat transformer.

The ZVS resonant frequency is

$$\omega_r = \frac{1}{\sqrt{L_r C_r}} \tag{14.383}$$

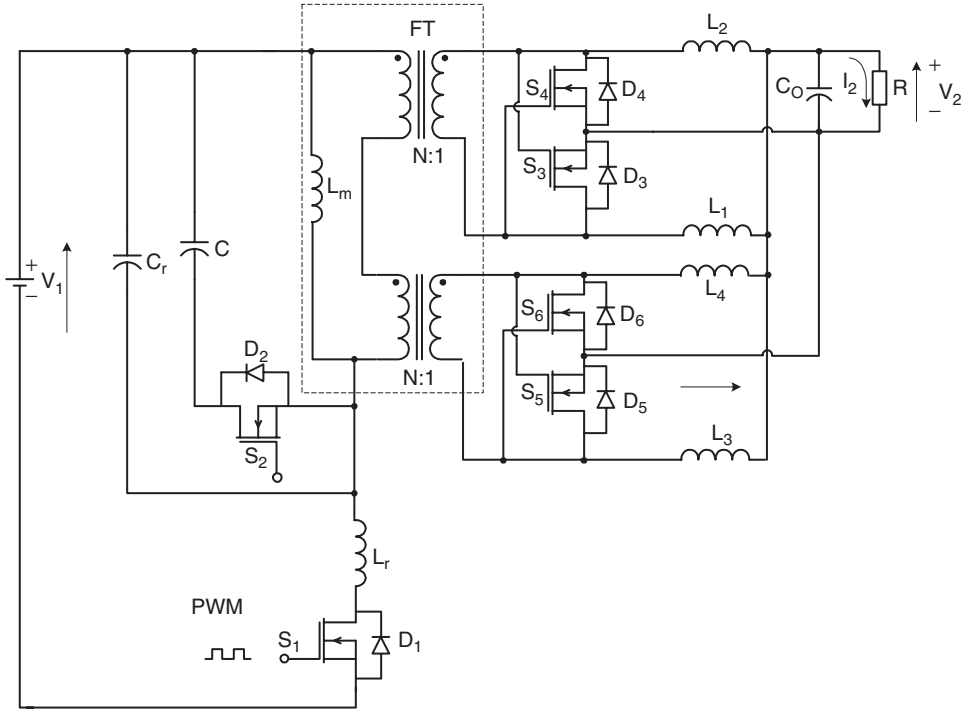

FIGURE 14.106 ZCS DC SR Luo-converter.

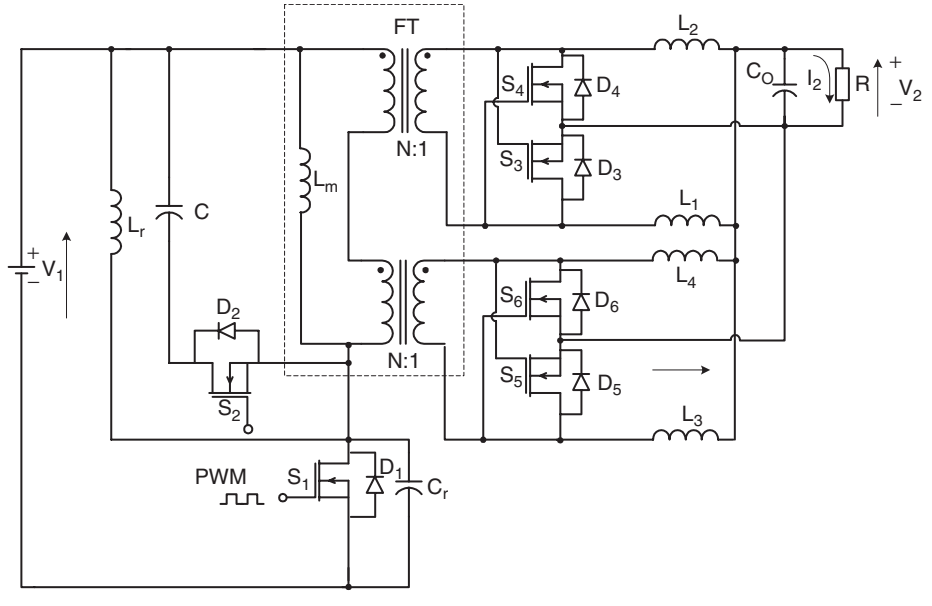

FIGURE 14.107 ZVS DC SR Luo-converter.

The normalized impedance is

$$Z_r = \sqrt{\frac{L_r}{C_r}}; \quad \alpha = \sin^{-1}\left(\frac{V_1}{Z_r I_1}\right) \tag{14.384}$$

The intervals are

$$t_1 = \frac{V_1 C_r}{I_1}; \quad t_2 = \frac{1}{\omega_r}(\pi + \alpha); \tag{14.385}$$

$$t_3 = \frac{I_1(1+\cos\alpha)L_r}{V_1}; \quad t_4 = \frac{t_1 + t_2 + t_3}{(V_1/V_2) - 1} \tag{14.386}$$

Average output voltage V_2 and input current I_1 are

$$V_2 = \frac{kV_1}{N} - \left(R_L + R_S + \frac{L_m}{TN^2}\right) I_O; \quad I_1 = k\frac{I_O}{N} \tag{14.387}$$

The power transfer efficiency

$$\eta = \frac{V_2 I_O}{V_1 I_1} = 1 - \frac{R_L + R_S + (L_m/TN^2)}{kV_1/N} I_O \tag{14.388}$$

When we set the $V_1 = 60$ V and frequency $f = 200$–250 kHz, we obtained the $V_2 = 1.8$ V, $N = 12$, $I_O = 0$–60 A, Volume $= 4$ in^3. The average power transfer efficiency is 94.5% and the maximum power density (PD) is 27 W/in^3.

14.14 Multiple-element Resonant Power Converters

Multiple energy-storage elements resonant power converters (x-Element RPC) are the sixth-generation converters. According to the transferring, power becomes higher and higher, traditional methods are hardly satisfied to deliver large power from source to final actuators with high efficiency. In order to reduce the power losses during the conversion process the sixth-generation converters – multiple energy-storage elements resonant power converters (x-Element RPC) – are created. They can be sorted into two main groups:

- DC/DC resonant converters;
- DC/AC resonant inverters.

Both groups converters consist of multiple energy-storage elements: two elements, three elements, or four elements. These energy-storage elements are passive parts: inductors and capacitors. They can be connected in series or parallel in various methods. In full statistics, the circuits of the multiple energy-storage elements converters are:

- 8 topologies of 2-element RPC;
- 38 topologies of 3-element RPC;
- 98 topologies of 4-element ($2L$-$2C$) RPC.

How to investigate the large quantity converters is a vital task. This problem was addressed in the last decade of last century. Unfortunately, much attention was not paid to it. This generation converters were not well discussed, only limited number of papers was published in the literature.

14.14.1 Two Energy-storage Elements Resonant Power Converters

The 8 topologies of 2-element RPC are shown in Fig. 14.108. These topologies have simple circuit structure and least components. Consequently, they can transfer the power from source to end-users with higher power efficiency and lower power losses.

Usually, the 2-Element RPC has very narrow response frequency bands, which is defined as the frequency width between the two half-power points. The working point must be selected in the vicinity of the natural resonant frequency $\omega_0 = 1/\sqrt{LC}$. Another drawback is that the transferred waveform is usually not a perfect sinusoidal, i.e. the output waveform THD is not zero.

Since total power losses are mainly contributed by the power losses across the main switches. As resonant conversion technique, the 2-Element RPC has high power transferring efficiency.

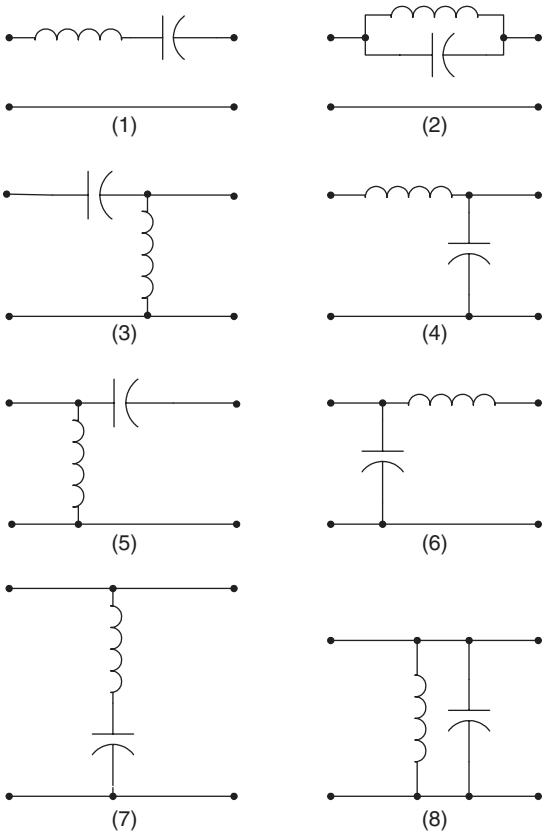

FIGURE 14.108 8 topologies of 2-element RPC.

14.14.2 Three Energy-storage Elements Resonant Power Converters

The 38 topologies of 3-element RPC are shown in Fig. 14.109. These topologies have one more component when compared to the 2-element RPC topologies. Consequently, they can transfer the power from source to end-users with higher lower power and lower power transfer efficiency.

Usually, the 3-element RPC has a much wider response frequency bands, which is defined as the frequency width between the two half-power points. If the circuit is a low-pass filter, the frequency bands can cover the frequency range from 0 to the natural resonant frequency $\omega_0 = 1/\sqrt{LC}$. The working point can be selected from a much wider frequency width which is lower than the natural resonant frequency $\omega_0 = 1/\sqrt{LC}$.

Another advantage, better than the 2-element RPC topologies, is that the transferred waveform can usually be a perfect sinusoidal, i.e. the output waveform THD is nearly zero. As well-known, mono-frequency waveform transferring operation has very low EMI.

14.14.3 Four Energy-storage Elements Resonant Power Converters

The 98 topologies of 4-element (2L-2C) RPC are shown in Fig. 14.110. If no restriction such as $2L$-$2C$ for 4-element RPC,

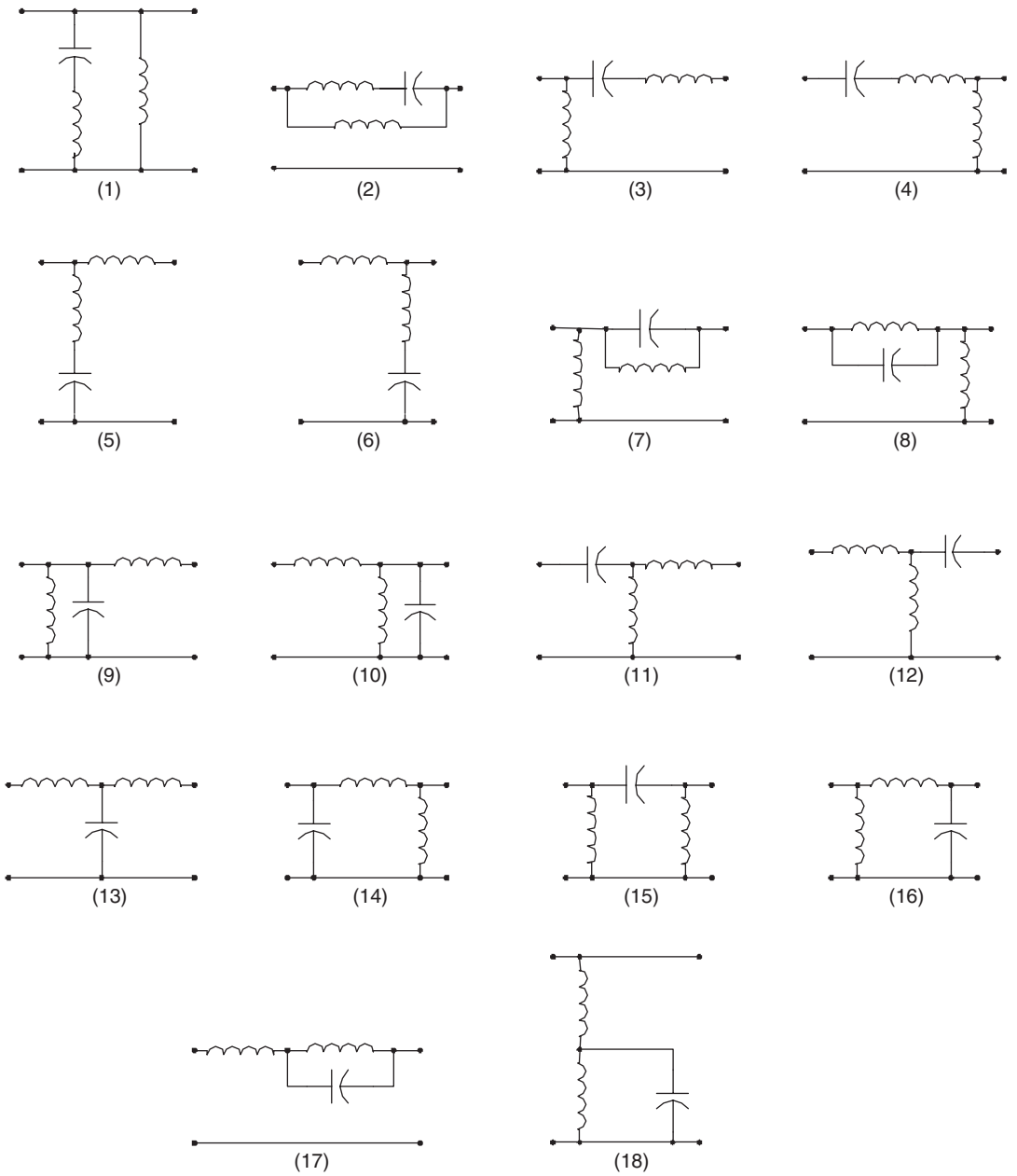

FIGURE 14.109 38 topologies of 3-element RPC.

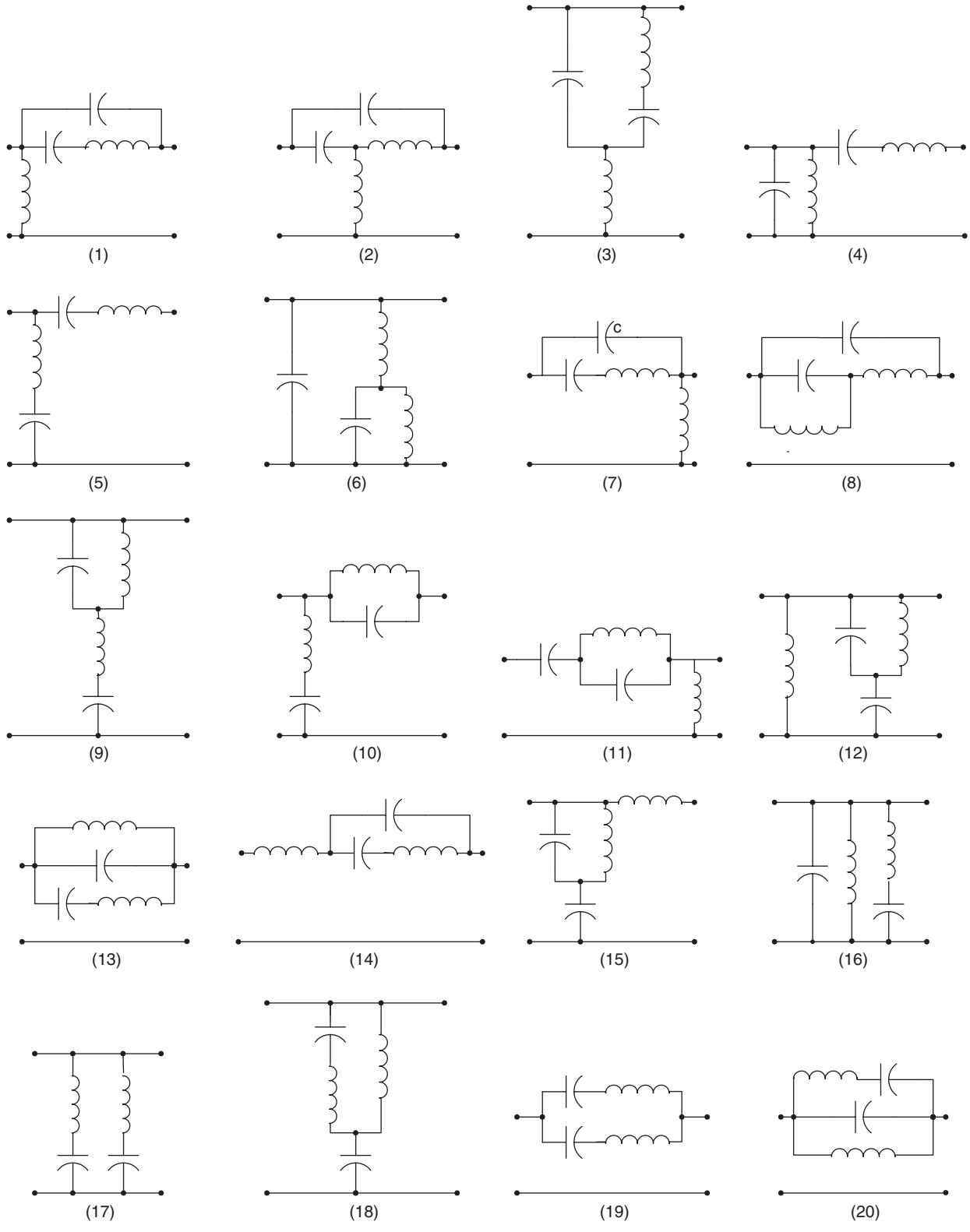

FIGURE 14.110 98 topologies of 4-element RPC.

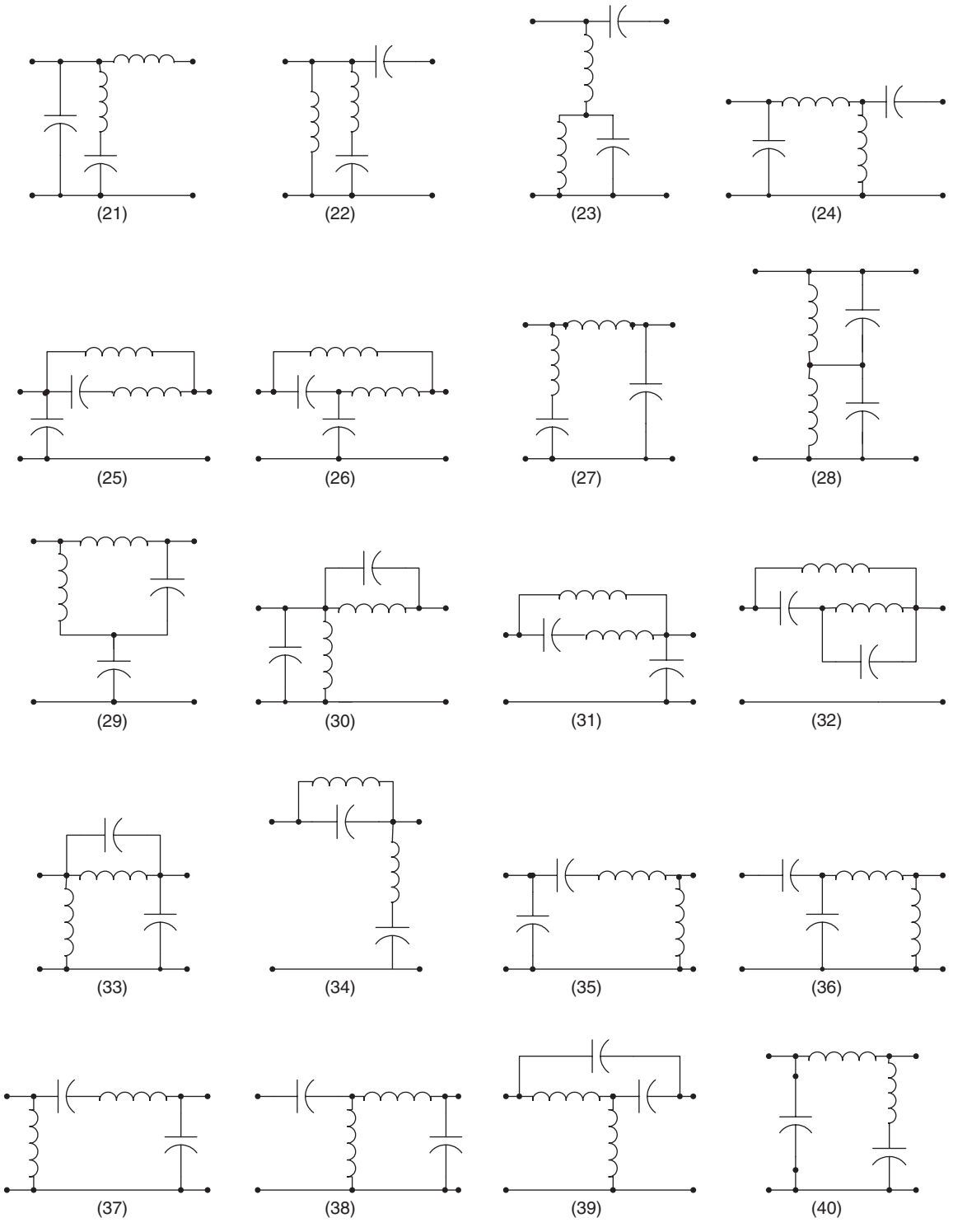

FIGURE 14.110 *continued.*

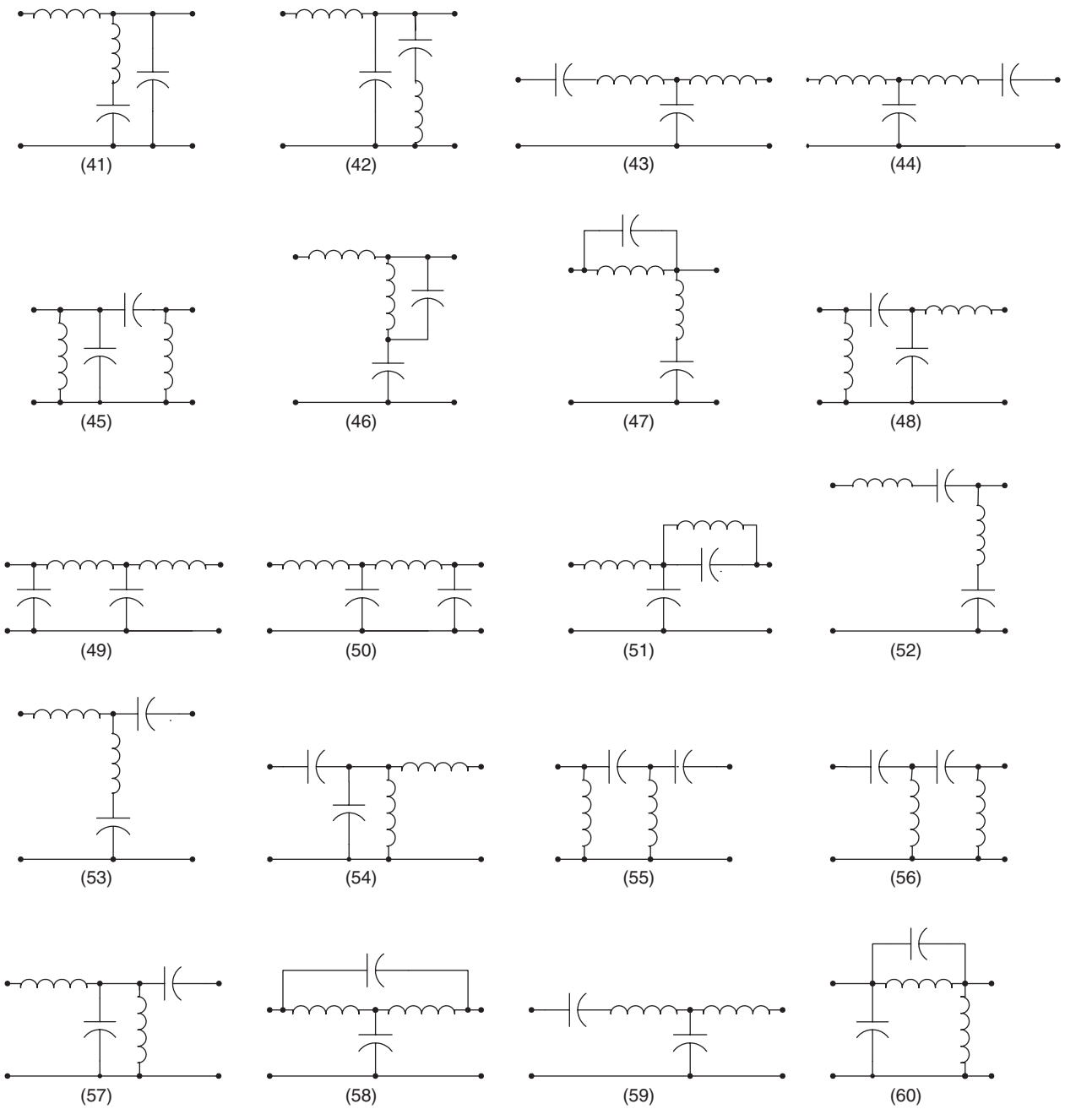

FIGURE 14.110 *continued.*

the number of the topologies of 4-element RPC can be much larger. Although these topologies have comparably complex circuit structure, they can still transfer the power from source to end-users with higher power efficiency and lower power losses.

Usually, the 4-element RPC has a wide response frequency bands, which is defined as the frequency width between the two half-power points. If the circuit is a low-pass filter, the frequency bands can cover the frequency range from 0 to the high half-power point which is definitely higher that the natural resonant frequency $\omega_0 = 1/\sqrt{LC}$. The working point can be selected from a wide area across (lower and higher than) the natural resonant frequency $\omega_0 = 1/\sqrt{LC}$. Another advantage is that the transferred waveform is usually a perfect sinusoidal, i.e. the output waveform THD is very close to zero. As well-known, mono-frequency-waveform

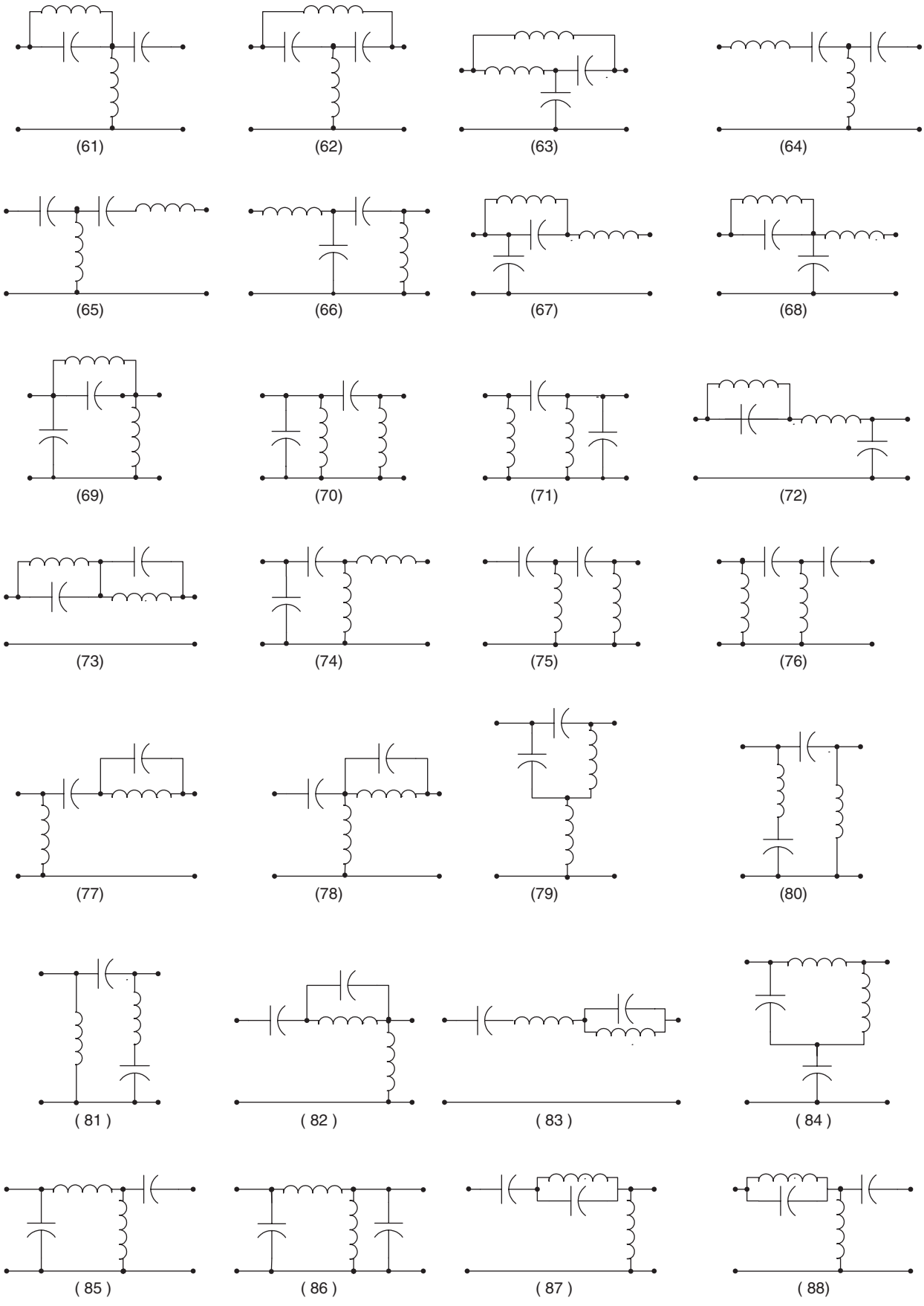

FIGURE 14.110 *continued.*

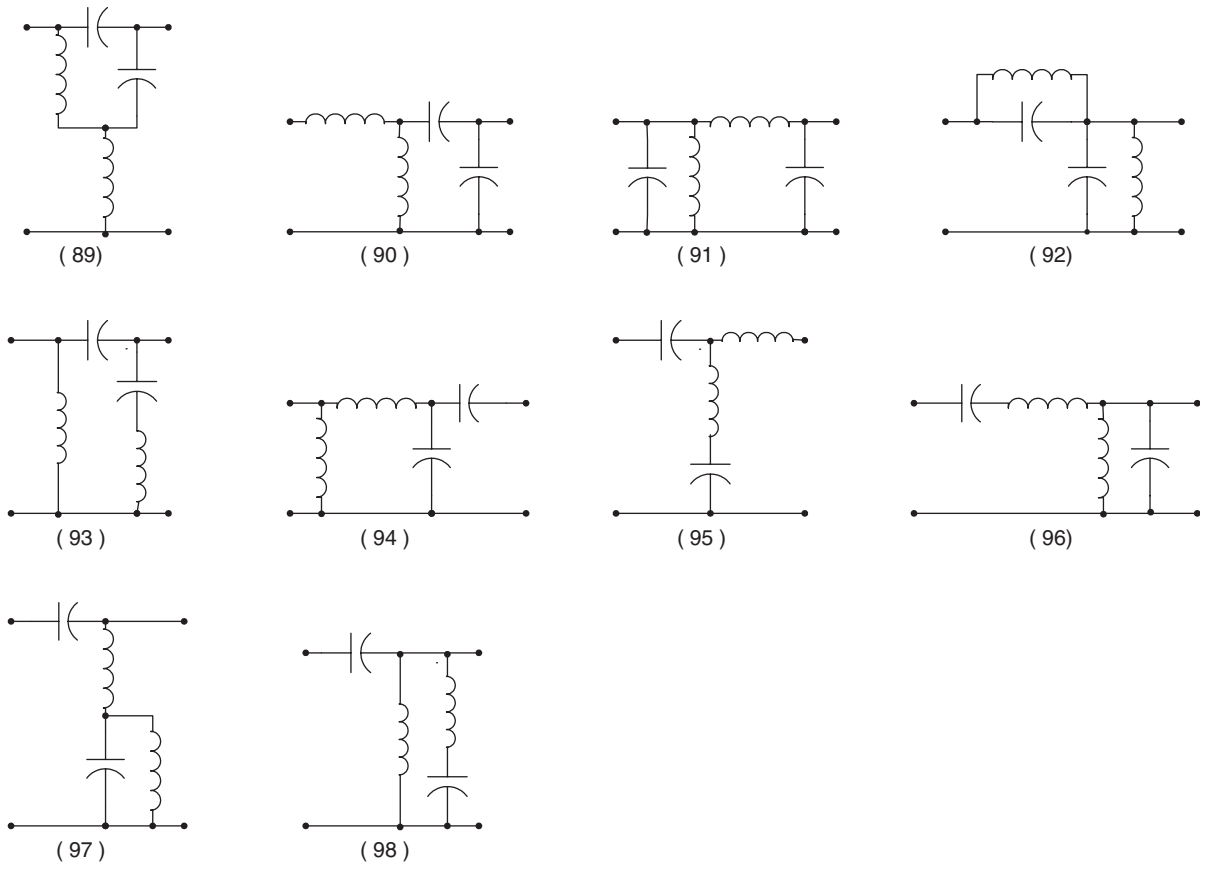

FIGURE 14.110 *continued.*

transferring operation has very low EMI and reasonable EMS and EMC.

14.14.4 Bipolar Current and Voltage Sources

Depending on different applications, resonant network can be low-pass filter, high-pass filter, or band-pass filter. For large power transferring, low-pass filter is usually employed. In this case, inductors are arranged in series arms and capacitors are arranged in shunt arms. If the first component is inductor, only voltage source can be applied since inductor current is continuous. Vice versa, if the first component is capacitor, only current source can be applied since capacitor voltage is continuous.

14.14.4.1 Bipolar Voltage Source

A bipolar voltage source using single voltage source is shown in Fig. 14.111. Since only voltage source is applied, there are four switches applied alternatively switching on or off to supply positive and negative voltage to the network. In the figure, the load is a resistance *R*.

The circuit of this voltage source is likely a four-quadrant operational chopper. The conduction duty cycle for each switch is 50%. For safety reason, the particular circuitry design has to consider some small gap between the turn-over (commutation) operation to avoid the short-circuit incidence.

The repeating frequency is theoretically not restricted. For industrial applications, the operating frequency is usually arranged in the range between 10 kHz and 5 MHz, depending on the application conditions.

14.14.4.2 Bipolar Current Source

A bipolar current voltage source using single voltage sources is shown in Fig. 14.112. To obtain stable current, the voltage source is connected in series by a large inductor. There are four switches applied alternatively switching on or off to supply positive and negative current to the network. In the figure, the load is a resistance *R*.

The circuit of this current source is likely a two-quadrant operational chopper. The conduction duty cycle for each

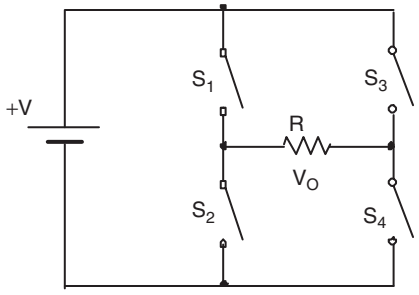

FIGURE 14.111 A bipolar voltage source using single voltage source.

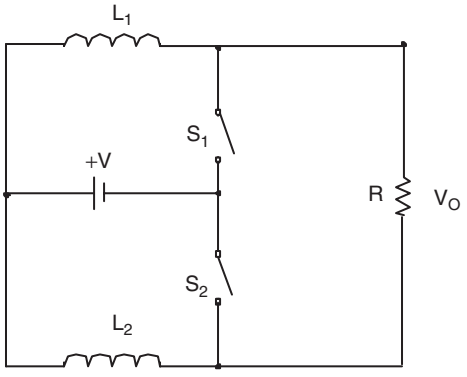

FIGURE 14.112 A bipolar current voltage source using single voltage source.

switch is 50%. For safety reason, the particular circuitry design has to consider some small gap between the turn-over (commutation) operation to avoid the short-circuit incidence.

The repeating frequency is theoretically not restricted. For industrial applications, the operating frequency is usually arranged in the range between 10 kHz and 5 MHz, depending on the application conditions.

14.15 Gate Control Luo-resonator

Luo-resonator is shown in Fig. 14.113. It generates the PWM pulse train to drive the static switch S. Luo-resonator is a high efficiency and simple structure circuit with easily adjusting frequency f and conduction duty k. It consists of three operational amplifiers (**OA**) named OA1-3 and auxiliary. These three 741-type OA's are integrated in a chip TL074 (which contains four OA's). Two potentiometers are applied to adjust the frequency f and conduction duty k. The voltage waveforms are shown in Fig. 14.114.

Type-741 OA can work at the power supply $\pm 3 - \pm 18$ V that are marked $V+$, G, and $V-$ with $|V-| = V+$. OA2 in Fig. 14.113 acts as the integration operation, its output V_C is a triangle waveform with regulated frequency $f = 1/T$ controlled by potentiometer R_4. OA1 acts as a resonant operation, its output V_B is a square-waveform with the frequency f. OA3 acts as a comparator, its output V_D is a square-waveform pulse train with regulated conduction duty k controlled by R_7.

Firstly, assuming the voltage $V_B = V+$ at $t = 0$ and feeds positively back to OA1 via R_2. This causes the OA1's output voltage maintained at $V_B = V+$. In the meantime, V_B inputs to OA2 via R_4, the output voltage V_C of OA2, therefore, decreases towards $V-$ with the slope $1/R_4C$. Voltage V_C feeds negatively back to OA1 via R_3. Voltage V_A at point A changes from $(mV+)$ to 0 in the period of $2mR_4C$. Usually, R_3 is set slightly smaller than R_2, the ratio is defined as $m = R_3/R_2$. Thus, voltage V_A intends towards negative. It causes the OA1's output voltage $V_B = V-$ at $t = 2mR_4C$ and voltage V_A jumps to $mV-$. Vice versa, the voltage $V_B = V-$ at $t = 2mR_4C$ and feeds positively back to OA1 via R_2. This causes the OA1's output voltage maintained at $V_B = V-$. In the meantime, V_B inputs to OA2 via R_4, the output voltage V_C of OA2, therefore, increases towards $V+$ with the slope $1/R_4C$. Voltage V_C feeds negatively back to OA1 via R_3. Voltage V_A at point A changes from $(mV-)$ to 0 in the period of $2mR_4C$. Thus, voltage V_A intends towards positive. It causes the OA1's output voltage $V_B = V+$ at $t = 4mR_4C$ and voltage V_A jumps to $mV+$.

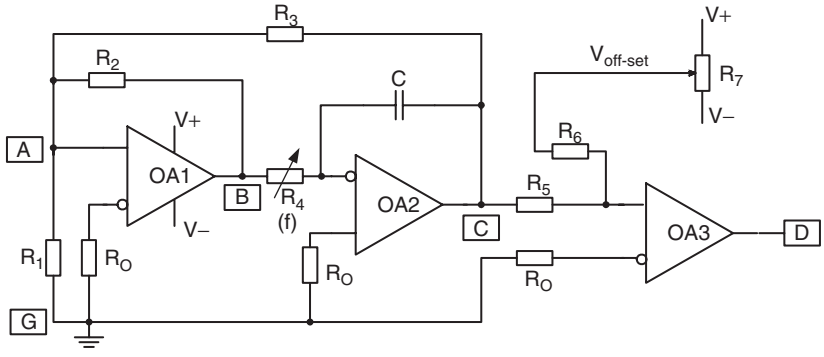

FIGURE 14.113 Luo-resonator.

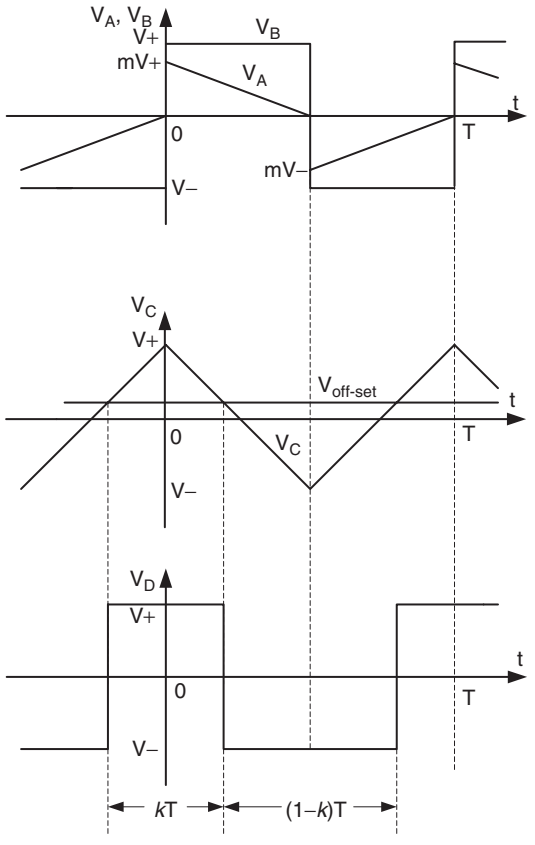

FIGURE 14.114 Voltage waveforms of Luo-resonator.

Then V_C inputs to OA3 and compares with shift signal $V_{off\text{-}set}$ regulated by the potentiometer R_7 via R_6. When $V_{off\text{-}set} = 0$, OA3 yields its output voltage V_D as a pulse train with conduction duty $k = 0.5$. Positive $V_{off\text{-}set}$ shifts the zero-cross point of voltage V_C downwards, hence, OA3 yields its output voltage V_D as a pulse train with conduction duty $k > 0.5$. Vice versa, negative $V_{off\text{-}set}$ shifts the zero-cross point of voltage V_C upwards, hence, OA3 yields its output voltage V_D as a pulse train with conduction duty $k < 0.5$ as shown in Fig. 14.114. Conduction duty k is controlled by $V_{off\text{-}set}$ via the potentiometer R_7.

The calculation formulas are

$$m = \frac{R_3}{R_2} \tag{14.389}$$

$$f = \frac{1}{4mR_4C} \tag{14.390}$$

$$k = 0.5 + \frac{R_5 V_{off\text{-}set}}{2R_6 V+} \tag{14.391}$$

This PWM pulse train V_D is applied to the DC/DC converter switch such as a transistor, MOSFET, or IGBT via a coupling circuit.

A design example: A Luo-resonator was designed as shown in Fig. 14.113 with the component values of $R_0 = 10\,\text{k}\Omega$; $R_1 = R_2 = R_5 = 100\,\text{k}\Omega$, $R_3 = R_6 = 95\,\text{k}\Omega$; $R_4 = 510\,\Omega$–$5.1\,\text{k}\Omega$ $R_7 = 20\,\text{k}\Omega$; and $C = 5.1\,\text{nF}$. The results are $m = 0.95$, frequency $f = 10$–$100\,\text{kHz}$ and conduction duty $k = 0$–1.0.

14.16 Applications

The DC/DC conversion technique has been rapidly developed and has been widely applied in industrial applications and computer peripheral equipment. Three examples are listed below:

- 5000 V insulation test bench;
- MIT 42/14 V DC/DC converter;
- IBM 1.8 V/200 A power supply.

14.16.1 5000 V Insulation Test Bench

Insulation test bench is the necessary equipment for semiconductor manufacturing organizations. An adjustable DC voltage power supply is the heart of this equipment. Traditional method to obtain the adjustable high DC voltage is a diode rectifier via a setting up transformer. It is costly and larger in size with poor efficiency.

Using a positive output super-lift Luo-converter triple-lift circuit, which is shown in Fig. 14.115. This circuit is small, effective, and low cost. The output voltage can be determined by

$$V_O = \left(\frac{2-k}{1-k}\right)^3 V_{in} \tag{14.392}$$

The conduction duty cycle k is only adjusted in the range 0–0.8 to carry out the output voltage in the range of 192–5184 V.

The experimental results are listed in Table 14.14. The measured data verified the advantages of this power supply.

14.16.2 MIT 42/14 V–3 KW DC/DC Converter

MIT 42/14 V–3 KW DC/DC converter was requested to transfer 3 kW energy between two battery sources with 42 and 14 V. The circuit diagram is shown in Fig. 14.116. This is a two-quadrant zero-voltage-switching (ZVS) quasi-resonant-converter (QRC). The current in low voltage side can be up to 250 A. This is a typical low voltage strong current converter. It is easier to carry out by ZVS-QRC.

This converter consists of two sources V_1 and V_2, one main inductor L, two main switches S_1 and S_2, two reverse-paralleled

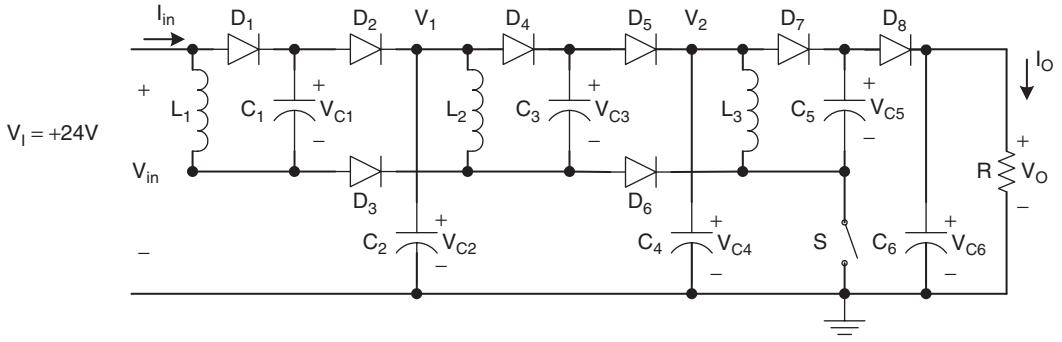

FIGURE 14.115 5000 V Insulation test bench.

TABLE 14.14 The experimental results of the 5000 V test bench

Conduction duty, k	0	0.1	0.2	0.3	0.4	0.5	0.6	0.7	0.8	0.82
Output voltage V_O (V)	192	226	273	244	455	648	1029	1953	5184	6760

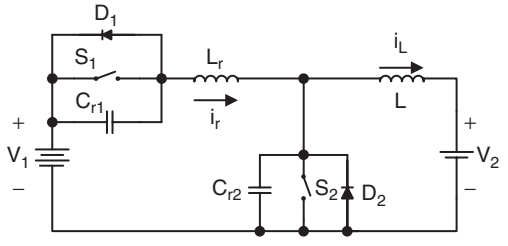

FIGURE 14.116 MIT 42/14 V-3 kW DC/DC converter.

diodes D_1 and D_2, one resonant inductor L_r and two resonant capacitors C_{r1} and C_{r2}. The working condition is selected

$$V_1 = 42\,\text{V}; \quad V_2 = 14\,\text{V}$$

$$L = 470\,\mu\text{H}; \quad C_{r1} = C_{r2} = C_r = 1\,\mu\text{F}$$

$$L_r = \begin{cases} 1\,\mu\text{H} & \textit{normal operation} \\ 9\,\mu\text{H} & \textit{low current operation} \end{cases}$$

Therefore,

$$\omega_O = \frac{1}{\sqrt{L_r C_r}} = 10^6\,\text{rad/s} \tag{14.393}$$

$$Z_O = \sqrt{\frac{L_r}{C_r}} = 1\,\Omega \text{ (normal operation)} \tag{14.394}$$

$$\alpha = \sin^{-1}\frac{V_1}{Z_O I_2} \tag{14.395}$$

It is easy to keep the quasi-resonance when the working current $I_2 > 50\,\text{A}$. If the working current is too low, the resonant inductor will take large value to guarantee the quasi-resonance state. This converter performs two-quadrant operation:

- Mode A (Quadrant I): energy transferred from V_1 side to V_2 side;
- Mode B (Quadrant II): energy transferred from V_2 side to V_1 side.

Assuming the working current is $I_2 = 100\,\text{A}$ and the converter works in Mode A, following calculations are obtained

$$\omega_O = \frac{1}{\sqrt{L_r C_r}} = 10^6\,\text{rad/s}$$

$$Z_O = \sqrt{\frac{L_r}{C_r}} = 1\,\Omega$$

$$\alpha = \sin^{-1}\frac{V_1}{Z_O I_2} = 24.83^\circ \tag{14.396}$$

$$t_1 = \frac{V_1 C_r}{I_2} = 0.42\,\mu\text{s} \tag{14.397}$$

$$t_2 = \frac{\pi + \alpha}{\omega_O} = 3.58\,\mu\text{s} \tag{14.398}$$

$$t_3 = \frac{1 + \cos\alpha}{V_1} I_2 L_r = \frac{1 + 0.908}{42} 100 \times 10^{-6} = 4.54\,\mu\text{s} \tag{14.399}$$

$$t_4 = \frac{t_1 + t_2 + t_3}{V_1/V_2 - 1} = \frac{0.42 + 3.58 + 4.54}{2} = 4.27\,\mu\text{s} \tag{14.400}$$

TABLE 14.15 The experimental test results of MIT 42V/14 converter (with the condition: $L_r = 1\,\mu\text{H}$, $C_{r1} = C_{r2} = 1\,\mu\text{F}$)

Mode	f(kHz)	I_1 (A)	I_2 (A)	I_L (A)	P_1 (W)	P_2 (W)	η (%)	PD (W/in^3)
A	78	77.1	220	220	3239	3080	95.1	23.40
A	80	78.3	220	220	3287	3080	93.7	23.58
A	82	81	220	220	3403	3080	90.5	24.01
B	68	220	69.9	220	3080	2939	95.3	22.28
B	70	220	68.3	220	3080	2871	93.2	22.04
B	72	220	66.6	220	3080	2797	90.8	21.77

$$T = t_1 + t_2 + t_3 + t_4 = 0.42 + 3.58 + 4.54 + 4.27 = 12.81\,\mu\text{s} \tag{14.401}$$

$$f = \frac{1}{T} = \frac{1}{12.81} = 78.06\ \text{kHz} \tag{14.402}$$

$$k = \frac{t_3 + t_4}{T} = \frac{4.54 + 4.27}{12.81} = 0.688 \tag{14.403}$$

The volume of this converter is 270 in^3. The experimental test results in full power 3 kW are listed in Table 14.15. From the tested data, a high power density 22.85 W/in^3 and a high efficiency 93% are obtained. Because of soft-switching operation, the EMI is low and EMS and EMC are reasonable.

14.16.3 IBM 1.8 V/200 A Power Supply

This equipment is suitable for IBM new generation computer with power supply 1.8 V/200 A. This is a ZCS SR DC/DC Luo-converter, and is shown in Fig. 14.117. This converter is based on the double-current synchronous-rectifier DC/DC converter plus ZCS technique. It employs a hixaploid-core flat-transformer with the turns ratio $N = 1/12$. It has six-unit ZCS synchronous-rectifier double-current DC/DC converter. The six primary coils are connected in series, and six secondary circuits are connected in parallel. Each unit has particular input voltage V_{in} to be about 33 V, and can offer 1.8 V/35 A individually. Total output current is 210 A. The equivalent primary full current is $I_1 = 14.5$ A and equivalent primary load voltage is $V_2 = 200$ V. The ZCS natural resonant frequency is

$$\omega_O = \frac{1}{\sqrt{L_r C_r}} \tag{14.404}$$

$$Z_O = \sqrt{\frac{L_r}{C_r}} \tag{14.405}$$

$$\alpha = \sin^{-1}\frac{Z_O I_1}{V_1} \tag{14.406}$$

The main power supply is from public utility board (PUB) via a diode rectifier. Therefore V_1 is nearly 200 V, and the each unit input voltage V_{in} is about 33 V. Other calculation formulas are

$$t_1 = \frac{I_1 L_r}{V_1} \tag{14.407}$$

$$t_2 = \frac{\pi + \alpha}{\omega_O} \tag{14.408}$$

$$t_3 = \frac{1 + \cos\alpha}{I_1} V_1 C_r \tag{14.409}$$

$$t_4 = \frac{V_1(t_1 + t_2)}{I_1 V_2}\left(I_1 + \frac{V}{Z_O}\frac{\cos\alpha}{\pi/2 + \alpha}\right) - (t_1 + t_2 + t_3) \tag{14.410}$$

$$T = t_1 + t_2 + t_3 + t_4 \tag{14.411}$$

$$f = \frac{1}{T} \tag{14.412}$$

$$k = \frac{t_1 + t_2}{T} \tag{14.413}$$

Real output voltage and input current are

$$V_O = kNV_1 - \left(R_L + R_S + \frac{L_m}{T}N^2\right) I_O \tag{14.414}$$

$$I_{in} = kNI_O \tag{14.415}$$

The efficiency is

$$\eta = \frac{V_O I_O}{V_{in} I_{in}} = 1 - \frac{R_L + R_S + (L_m/T)N^2}{kNV_{in}} I_O \tag{14.416}$$

The commercial unit of this power supply works in voltage closed loop control with inner current closed loop to keep the output voltage constant. Applying frequency is arranged in the band of 200–250 kHz. Whole volume of the power supply is 14 in^3. The transfer efficiency is about 88–92% and power density is about 25.7 W/in^3.

14.17 Energy Factor and Mathematical Modeling for Power DC/DC Converters

We have well discussed the various DC/DC converters operating in steady state in previous sections. We will investigate the transient process of DC/DC converters. Furthermore, we define a series of new parameters such as energy factor (*EF*) and so on to establish the mathematical modeling of all power DC/DC converters.

Energy storage in power DC/DC converters has been paid attention long time ago. Unfortunately, there is no clear

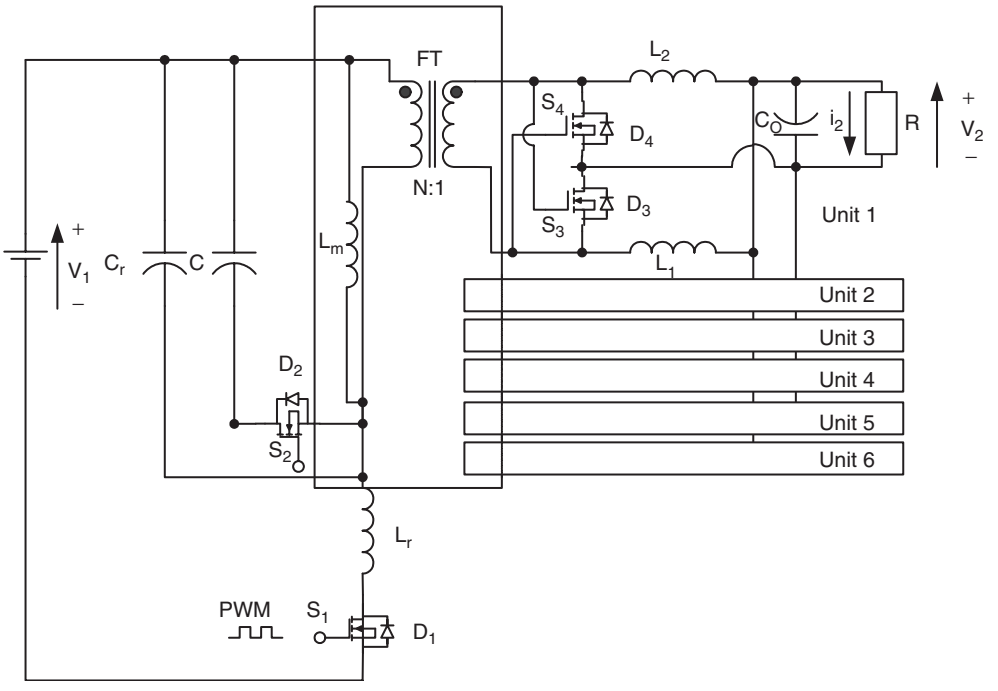

FIGURE 14.117 IBM 1.8 V/200 A power supply.

concept to describe the phenomena and reveal the relationship between the stored energy and the characteristics of power DC/DC converters. We have theoretically defined a new concept – energy factor (*EF*) and researched the relations between ***EF*** and the mathematical modeling of power DC/DC converters. Energy factor is a new concept in power electronics and conversion technology, which thoroughly differs from the traditional concepts such as power factor (*PF*), power transfer efficiency (η), total harmonic distortion (*THD*), and ripple factor (*RF*). Energy factor and the other sub-sequential parameters can illustrate the system stability, reference response, and interference recovery. This investigation is very helpful for system design and DC/DC converters characteristics foreseeing.

14.17.1 Pumping Energy (*PE*)

All power DC/DC converters have pumping circuit to transfer the energy from the source to some energy storage passive elements, e.g. inductors and capacitors. The ***PE*** is used to count the input energy in a switching period T. Its calculation formula is

$$PE = \int_0^T P_{in}(t)dt = \int_0^T V_1 i_1(t)dt = V_1 I_1 T \qquad (14.417)$$

where

$$I_1 = \int_0^T i_1(t)dt$$

is the average value of the input current if the input voltage V_1 is constant. Usually the input average current I_1 depends on the conduction duty cycle.

14.17.2 Stored Energy (*SE*)

The stored energy in an inductor is

$$W_L = \frac{1}{2}LI_L^2 \qquad (14.418)$$

The stored energy across a capacitor is

$$W_C = \frac{1}{2}CV_C^2 \qquad (14.419)$$

Therefore, if there are n_L inductors and n_C capacitors the total stored energy in a DC/DC converter is

$$SE = \sum_{j=1}^{n_L} W_{Lj} + \sum_{j=1}^{n_C} W_{Cj} \qquad (14.420)$$

Capacitor–inductor stored energy ratio (*CIR*) – Most power DC/DC converters consist of inductors and capacitors.

Therefore, we can define the capacitor–inductor stored energy ratio (***CIR***).

$$CIR = \frac{\sum_{j=1}^{n_C} W_{Cj}}{\sum_{j=1}^{n_L} W_{Lj}} \tag{14.421}$$

Energy losses (*EL*) – Usually, most analysis applied in DC/DC converters is assuming no power losses, i.e. the input power is equal to the output power, $P_{in} = P_O$ or $V_1 I_1 = V_2 I_2$, so that pumping energy is equal to output energy in a period, T.

Particularly, power losses always exist during the conversion process. They are caused by the resistance of the connection cables, resistance of the inductor and capacitor wire, and power losses across the semiconductor devices (diode, IGBT, MOSFET, and so on). We can sort them as the resistance power losses P_r, passive element power losses P_e, and device power losses P_d. The total power losses are P_{loss}.

$$P_{loss} = P_r + P_e + P_d$$

and

$$P_{in} = P_O + P_{loss} = P_O + P_e + P_e + P_d = V_2 I_2 + P_e + P_e + P_d$$

Therefore,

$$EL = P_{loss} \times T = (P_r + P_e + P_d)T$$

The energy losses (***EL***) is in a period T,

$$EL = \int_0^T P_{loss} dt = P_{loss} T \tag{14.422}$$

14.17.3 Energy Factor (*EF*)

As described in previous section the input energy in a period T is the pumping energy $PE = P_{in} \times T = V_{in} I_{in} \times T$. We now define the ***EF***, that is the ratio of the *SE* over the pumping energy

$$EF = \frac{SE}{PE} = \frac{SE}{V_1 I_1 T} = \frac{\sum_{j=1}^{m} W_{Lj} + \sum_{j=1}^{n} W_{Cj}}{V_1 I_1 T} \tag{14.423}$$

Energy factor is a very important factor of a power DC/DC converter. It is usually independent from the conduction duty cycle k, and proportional to the switching frequency f (inversely proportional to the period T) since the pumping energy PE is proportional to the switching period T.

14.17.4 Time Constant τ and Damping Time Constant τ_d

The **time constant τ** of a power DC/DC converter is a new concept to describe the transient process of a DC/DC converter. If no power losses in the converter, it is defined

$$\tau = \frac{2T \times EF}{1 + CIR} \left(1 + CIR \frac{1 - \eta}{\eta}\right) \tag{14.424}$$

The **damping time constant τ_d** of a power DC/DC converter is new concept to describe the transient process of a DC/DC converter. If no power losses, it is defined

$$\tau_d = \frac{2T \times EF}{1 + CIR} \frac{CIR}{\eta + CIR(1 - \eta)} \tag{14.425}$$

The **time constants ratio ξ** of a power DC/DC converter is new concept to describe the transient process of a DC/DC converter. If no power losses, it is defined

$$\xi = \frac{\tau_d}{\tau} = \frac{CIR}{\eta \left(1 + CIR \frac{1-\eta}{\eta}\right)^2} \tag{14.426}$$

14.17.5 Mathematical Modeling for Power DC/DC Converters

The mathematical modeling for all power DC/DC converters is

$$G(s) = \frac{M}{1 + s\tau + s^2 \tau \tau_d} \tag{14.427}$$

where M is the voltage transfer gain: $M = V_O / V_{in}$, τ is the time constant in Eq. (14.424), τ_d the damping time constant in Eq. (14.425), $\tau_d = \xi\tau$. Using this mathematical model of power DC/DC converters, it is significantly easy to describe the characteristics of power DC/DC converters. In order to verify this theory, few converters are investigated to demonstrate the characteristics of power DC/DC converters and applications of the theory.

14.17.6 Buck Converter with Small Energy Losses (r_L= 1.5 Ω)

A buck converter shown in Fig. 14.118 has the components values: $V_1 = 40\,\text{V}$, $L = 250\,\mu\text{H}$ with resistance $r_L = 1.5\,\Omega$, $C = 60\,\mu\text{F}$, $R = 10\,\Omega$, the switching frequency $f = 20\,\text{kHz}$ ($T = 1/f = 50\,\mu\text{s}$) and conduction duty cycle $k = 0.4$. This converter is stable and works in CCM.

Therefore, we have got the voltage transfer gain $M = 0.35$, i.e. $V_2 = V_C = MV_1 = 0.35 \times 40 = 14\,\text{V}$. $I_L = I_2 = 1.4\,\text{A}$, $P_{loss} = I_L^2 \times r_L = 1.4^2 \times 1.5 = 2.94\,\text{W}$, and $I_1 = 0.564\,\text{A}$. The parameter EF and others are listed below

$$PE = V_1 I_1 T = 40 \times 0.564 \times 50\,\mu = 1.128\,\text{mJ};$$

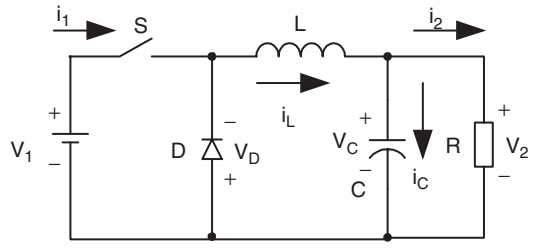

FIGURE 14.118 A buck converter.

$$W_L = \frac{1}{2}LI_L^2 = 0.5 \times 250\,\mu \times 1.4^2 = 0.245 \text{ mJ}$$

$$W_C = \frac{1}{2}CV_C^2 = 0.5 \times 60\,\mu \times 14^2 = 5.88 \text{ mJ};$$

$$SE = W_L + W_C = 0.245 + 5.88 = 6.125 \text{ mJ}$$

$$EF = \frac{SE}{PE} = \frac{6.125}{1.128} = 5.43; \quad CIR = \frac{W_C}{W_L} = \frac{5.88}{0.245} = 24$$

$$EL = P_{loss} \times T = 2.94 \times 50 = 0.147 \text{ mJ};$$

$$\eta = \frac{P_O}{P_O + P_{loss}} = 0.87$$

$$\tau = \frac{2T \times EF}{1 + CIR}(1 + CIR\frac{1-\eta}{\eta}) = 99.6\ \mu\text{s};$$

$$\tau_d = \frac{2T \times EF}{1 + CIR}\frac{CIR}{\eta + CIR(1-\eta)} = 130.6\ \mu\text{s};$$

$$\xi = \frac{\tau_d}{\tau} = \frac{CIR}{\eta\left(1 + CIR\frac{1-\eta}{\eta}\right)^2} = 1.31 \gg 0.25$$

By cybernetic theory, since the damping time constant τ_d is larger than the time constant τ, the corresponding ratio ξ is $1.31 \gg 0.25$. The output voltage has heavy oscillation with high overshot. The corresponding transfer function is

$$G(s) = \frac{M}{1 + s\tau + s^2\tau\tau_d} = \frac{M/\tau\tau_d}{(s + s_1)(s + s_2)} \tag{14.428}$$

where

$$s_1 = \sigma + j\omega \quad \text{and} \quad s_2 = \sigma - j\omega$$

with

$$\sigma = \frac{1}{2\tau_d} = \frac{1}{261.2\,\mu s} = 3833 \text{ Hz}$$

and

$$\omega = \frac{\sqrt{4\tau\tau_d - \tau^2}}{2\tau\tau_d} = \frac{\sqrt{52{,}031 - 9920}}{26{,}015.5} = \frac{205.2}{26{,}015.5\,\mu} = 7888 \text{ rad/s}$$

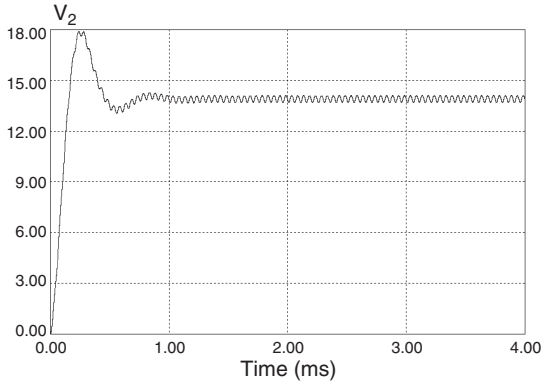

FIGURE 14.119 Buck converter unit-step response.

The unit-step function response is

$$v_2(t) = 14\left[1 - e^{-(t/0.000261)}(\cos 7888t - 0.486 \sin 7888t)\right] \text{ V} \tag{14.429}$$

The unit-step function response (transient process) has oscillation progress with damping factor σ and frequency ω. The simulation result is shown in Fig. 14.119.

The impulse interference response is

$$\Delta v_2(t) = 0.975Ue^{-(t/0.000261)} \sin 7888t$$

where U is the interference signal. The impulse response (interference recovery process) has oscillation progress with damping factor σ and frequency ω. The simulation result is shown in Fig. 14.120.

In order to verify the analysis, calculation and simulation results, we constructed a test rig with same conditions. The corresponding experimental results are shown in Figs. 14.121 and 14.122.

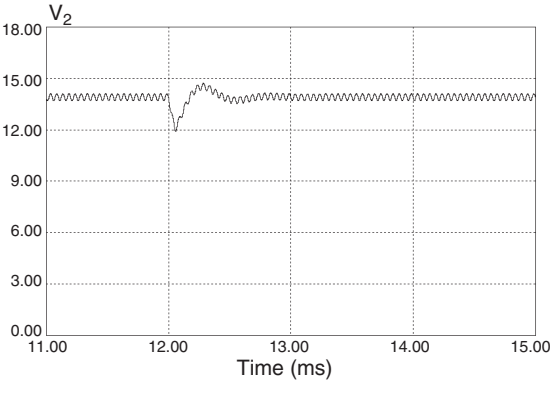

FIGURE 14.120 Buck converter impulse response.

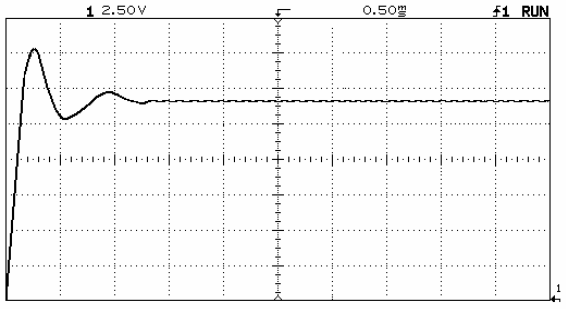

FIGURE 14.121 Unit-step response (test).

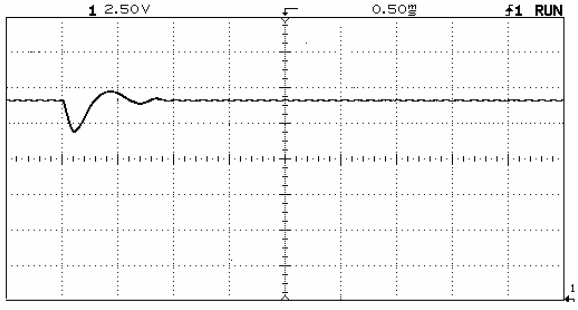

FIGURE 14.122 Impulse response (test).

14.17.7 A Super-lift Luo-converter in CCM

Figure 14.123 shows a super-lift Luo-converter with the conduction duty $k = 0.5$. The components values are $V_1 = 20\,\text{V}$, $f = 50\,\text{kHz}$ ($T = 20\,\mu\text{s}$), $L = 100\,\mu\text{H}$ with resistance $r_L = 0.12\,\Omega$, $C_1 = 2500\,\mu\text{F}$, $C_2 = 800\,\mu\text{F}$, and $R = 10\,\Omega$. This converter is stable and works in CCM.

Therefore, we have got the voltage transfer gain $M = 2.863$, i.e. the output voltage $V_2 = V_{C2} = 57.25\,\text{V}$. $V_{C1} = V_1 = 20\,\text{V}$, $I_1 = 14.145\,\text{A}$, $I_2 = 5.725\,\text{A}$, $I_L = 11.45\,\text{A}$, and $P_{loss} = I_L^2 \times r_L = 11.45^2 \times 0.12 = 15.73\,\text{W}$. The parameter EF and others are listed below

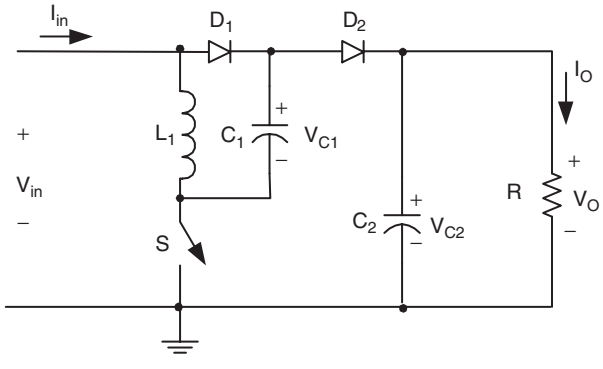

FIGURE 14.123 A super-lift Luo-converter.

$$PE = V_1 I_1 T = 20 \times 17.175 \times 20\,\mu = 6.87\ \text{mJ};$$

$$W_L = \frac{1}{2} L I_L^2 = 0.5 \times 100\,\mu \times 11.45^2 = 6.555\ \text{mJ};$$

$$W_{C1} = \frac{1}{2} C_1 V_{C1}^2 = 0.5 \times 2500\,\mu \times 20^2 = 500\ \text{mJ};$$

$$W_{C2} = \frac{1}{2} C_2 V_{C2}^2 = 0.5 \times 800\,\mu \times 57.25^2 = 1311\ \text{mJ}$$

$$SE = W_L + W_{C1} + W_{C2} = 6.555 + 500 + 1311 = 1817.6\ \text{mJ};$$

$$EF = \frac{SE}{PE} = \frac{1817.6}{6.87} = 264.6;$$

$$CIR = \frac{W_{C1} + W_{C2}}{W_L} = \frac{1811}{6.555} = 276.3$$

$$EL = P_{loss} T = 15.73 \times 20 = 0.3146\ \text{mJ};$$

$$\eta = \frac{P_O}{P_O + P_{loss}} = \frac{327.76}{343.49} = 0.9542$$

$$\tau = \frac{2T \times EF}{1 + CIR}\left(1 + CIR\frac{1-\eta}{\eta}\right)$$

$$= \frac{40\,\mu \times 264.6 \times 13.26}{277.3} = 506\,\mu\text{s}$$

$$\tau_d = \frac{2T \times EF}{1 + CIR}\frac{CIR}{\eta + CIR(1-\eta)}$$

$$= \frac{40 \times 264.6 \times 20.3}{277.3} = 775\ \mu\text{s}$$

By cybernetic theory, since the damping time constant τ_d is much larger than the time constant τ, the corresponding ratio $\xi = 775/506 = 1.53 \gg 0.25$. The output voltage has heavy oscillation with high overshot. The transfer function of this converter has two poles ($-s_1$ and $-s_2$) that are located in the left-hand half plane (LHHP).

$$G(s) = \frac{M}{1 + s\tau + s^2\tau\tau_d} = \frac{M/\tau\tau_d}{(s + s_1)(s + s_2)} \qquad (14.430)$$

where

$$s_1 = \sigma + j\omega \quad \text{and} \quad s_2 = \sigma - j\omega$$

with

$$\sigma = \frac{1}{2\tau_d} = \frac{1}{1.55\,\text{ms}} = 645\ \text{Hz}$$

$$\omega = \frac{\sqrt{4\tau\tau_d - \tau^2}}{2\tau\tau_d} = \frac{\sqrt{16,86,400 - 2,95,936}}{8,43,200}$$

$$= \frac{1197.2}{8,43,200\,\mu} = 1398\ \text{rad/s}$$

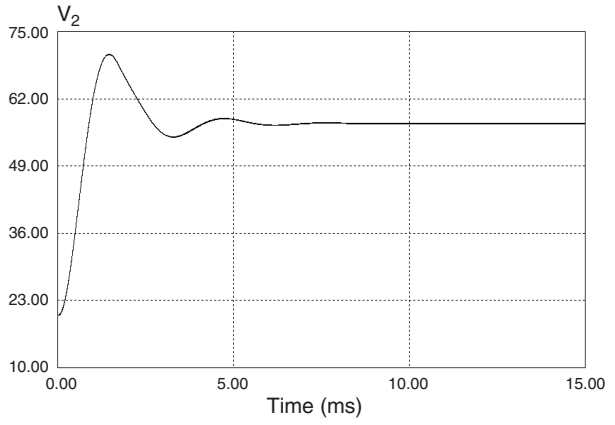

FIGURE 14.124 SL Luo-converter unit-step response.

The unit-step function response is

$$v_2(t) = 57.25\left[1 - e^{-(t/0.00155)}(\cos 1398t - 0.461 \sin 1398t)\right] \text{V}$$

The unit-step function response (transient process) has oscillation progress with damping factor σ and frequency ω. The simulation is shown in Fig. 14.124.

The impulse interference response is

$$\Delta v_2(t) = 0.923 U e^{-(t/0.00155)} \sin 1398t$$

where U is the interference signal. The impulse response (interference recovery process) has oscillation progress with damping factor σ and frequency ω, and is shown in Fig. 14.125.

In order to verify the analysis, calculation and simulation results, we constructed a test rig with same conditions. The corresponding test results are shown in Figs. 14.126 and 14.127.

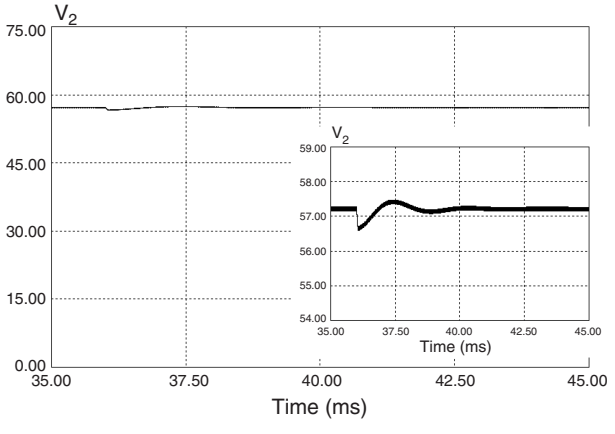

FIGURE 14.125 SL Luo-converter impulse response.

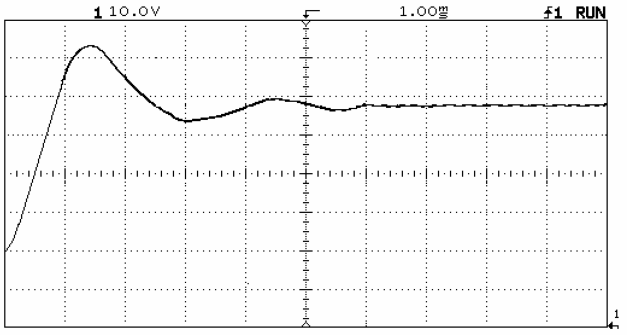

FIGURE 14.126 SL Luo-converter unit-step response (test).

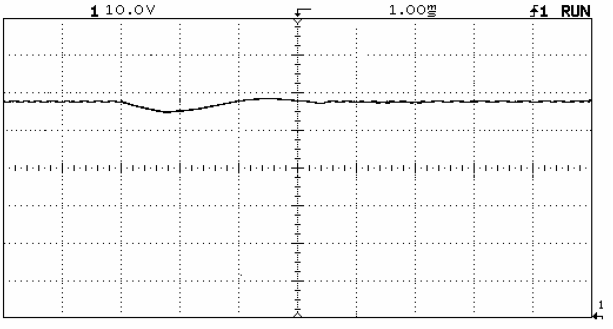

FIGURE 14.127 SL Luo-converter impulse response (test).

Further Reading

1. Luo F. L. and Ye H. "Advanced DC/DC Converters" **CRC Press LLC**, Boca Raton, Florida 07030, USA, 2004. **ISBN: 0-8493-1956-0**.
2. Luo F. L., Ye H., and Rashid M. H. "Digital Power Electronics and Applications" **Elsevier Academic Press**, Burlington, Massachusetts 01803, USA, June 2005. **ISBN: 0-1208-8757-6**.
3. Luo F. L. and Ye H. "Essential DC/DC Converters" **Taylor and Francis Group LLC**, Boca Raton, Florida 07030, USA, October 2005. **ISBN: 0-8493-7238-0**.
4. Luo F. L. "Positive Output Luo-Converters, Voltage Lift Technique" **IEE Proceedings on Electric Power Applications**, Vol. 146, No. 4, July 1999, pp. 415–432.
5. Luo F. L. "Negative Output Luo–Converters, Voltage Lift Technique" **IEE Proceedings on Electric Power Applications**, Vol. 146, No. 2, July 1999, pp. 208–224.
6. Luo F. L. "Double Output Luo–Converters, Advanced Voltage Lift Technique" **IEE Proceedings on Electric Power Applications**, Vol. 147, No. 6, November 2000, pp. 618–633.
7. Luo F. L. "Re–Lift Converter: Design, Test, Simulation and Stability Analysis" **IEE Proceedings on Electric Power Applications**, Vol. 145, No. 4, July 1998, pp. 315–325.
8. Luo F. L., Ye H., and Rashid M. H. "Chapter 14: DC/DC Conversion Techniques and Nine Series Luo–Converters" of "Power Electronics Handbook" (Edited by M. H. Rashid) **Academic Press**, San Diego, USA, August 2001, pp. 335–406. **ISBN: 0-12-581650-2**.
9. Rashid M. H. "Power Electronics: Circuits, Devices and Applications" Second edition, **Prentice-Hall**, USA, 1993.

10. Mohan N., Undeland T. M., and Robbins W. P. "Power Electronics: Converters, Applications and Design" **John Wiley & Sons**, New York, 1995.
11. Severns R. P. and Bloom G. "Modern DC-to-DC Switchmode Power Converter Circuits" **Van Nostrand Reinhold Company**, New York, 1985.
12. Kularatna N. "Power Electronics Design Handbook" **John Wiley & Sons**, New York, 1985.
13. Luo F. L. and Ye H. "Advanced Multi-Quadrant Operation DC/DC Converters" **Taylor and Francis Group LLC**, Boca Raton, Florida 07030, USA, June 2005. **ISBN: 0-8493-7239-9**.
14. Luo F. L. "Neural Network Control for Synchronous Rectifier DC/DC Converter" **Proceedings of the International Conference ICARCV'2000**, Singapore, 5–8 December 2000 (CD ROM).
15. Luo F. L., Ye H., and Rashid M. H. "Two-Quadrant DC/DC ZCS Quasi-Resonant Luo-Converter" **Proceedings of the IEEE International Conference IPEMC'2000**, Beijing, China, 15–18 August 2000, pp. 272–277.
16. Luo F. L., Ye H., and Rashid M. H. "Two-Quadrant DC/DC ZVS Quasi-Resonant Luo-Converter" **Proceedings of the IEEE International Conference IPEMC'2000**, Beijing, China, 15–18 August 2000, pp. 1132–1137.
17. Luo F. L. "Negative Output Luo–Converters – Voltage Lift Technique" **Proceedings of the Second World Energy System International Conference WES'98**, Toronto, Canada, 19–22 May 1998, pp. 253–260.
18. Luo F. L. and Ye H. "Ultra-Lift Luo-Converter" **IEE-EPA Proceedings**, Vol. 152, No. 1, January 2005, pp. 27–32.
19. Luo F. L. and Ye H. "Positive Output Cascade Boost Converters" **IEE-EPA Proceedings**, Vol. 151, No. 5, September 2004, pp. 590–606.
20. Luo F. L. and Ye H. "Positive Output Multiple-Lift Push-Pull Switched-Capacitor Luo-Converters" **IEEE-Transactions on Industrial Electronics**, Vol. 51, No. 3, June 2004, pp. 594–602.
21. Luo F. L. and Ye H. "Negative Output Super-Lift Converters" **IEEE-Transactions on Power Electronics**, Vol. 18, No. 5, September 2003, pp. 1113–1121.
22. Luo F. L. and Ye H. "Positive Output Super-Lift Converters" **IEEE-Transactions on Power Electronics**, Vol. 18, No. 1, January 2003, pp. 105–113.
23. Luo F. L. and Ye H. "Investigation and Verification of a Cascade Double Γ-CL Current Source Resonant Inverter" **IEE-EPA Proceedings**, Vol. 149, No. 5, September 2002, pp. 369–378.
24. Luo F., Ye H., and Rashid M. H. "Multiple Quadrant Operation Luo-Converters" **IEE-EPA Proceedings**, Vol. 149, No. 1, January 2002, pp. 9–18.
25. Luo F. L. "Six Self-Lift DC/DC Converters: Voltage Lift Technique" **IEEE-Transactions on Industrial Electronics**, Vol. 48, No. 6, December 2001, pp. 1268–1272.
26. Luo F. L. "Seven Self-Lift DC/DC Converters: Voltage Lift Technique" **IEE-EPA Proceedings**, Vol. 148, No. 4, July 2001, pp. 329–338.
27. Luo F. L., Ye H., and Rashid M. H. "Four-Quadrant Operating Luo-Converters" **Proceedings of the IEEE International Conference PESC'2000**, Galway, Ireland, 18–23 June 2000, pp. 1047–1052.
28. Luo F. L. "42/14 V Two-Quadrant DC/DC Soft-Switching Converter" **Proceedings of the IEEE International Conference PESC'2000**, Galway, Ireland, 18–23 June 2000, pp. 143–148.
29. Luo F. L. and Ye H. "Two-Quadrant Switched Capacitor Converter" **Proceedings of the 13th Chinese Power Supply Society IAS Annual Meeting**, Shenzhen, China, 15–18 November 1999, pp. 164–168.
30. Luo F. L. and Ye H. "Four-Quadrant Switched Capacitor Converter" **Proceedings of the 13th Chinese Power Supply Society IAS Annual Meeting**, Shenzhen, China, 15–18 November 1999, pp. 513–518.
31. Luo F. L., Ye H., and Rashid M. H. "Switched Capacitor Four-Quadrant Luo-Converter" **Proceedings of the IEEE-IAS Annual Meeting**, **IAS'99**, Phoenix, Arizona, USA, 3–7 October 1999, pp. 1653–1660.
32. Luo F. L., Ye H., and Rashid M. H. "Switched Inductor Four-Quadrant Luo-Converter" **Proceedings of the IEEE-IAS Annual Meeting**, **IAS'99**, Phoenix, Arizona, USA, 3–7 October 1999, pp. 1631–1638.
33. Luo F. L. "Four-Quadrant DC/DC ZCS Quasi-Resonant Luo-Converter" Accepted for publication by IEE International Conference IPEC'2001, Singapore, 14–19 May 2001.
34. Luo F. L. "Four-Quadrant DC/DC ZVS Quasi-Resonant Luo-Converter" Accepted for publication by IEE International Conference IPEC'2001, Singapore, 14–19 May 2001.
35. Gao Y. and Luo F. L. "Theoretical Analysis on performance of a 5V/12V Push-Pull Switched Capacitor DC/DC Converter" Accepted for publication by IEE International Conference IPEC'2001, Singapore, 14–19 May 2001.
36. Luo F. L. and Chua L. M. "Fuzzy Logic Control for Synchronous Rectifier DC/DC Converter" **Proceedings of the IASTED International Conference ASC'2000**, Banff, Alberta, Canada, 24–26 July 2000, pp. 24–28.
37. Luo F. L. "Luo-Converters – Voltage Lift Technique" **Proceedings of the IEEE Power Electronics Special Conference IEEE-PESC'98**, Fukuoka, Japan, 14–22 May 1998, pp. 1483–1489.
38. Luo F. L. "Luo-Converters, A Series of New DC-DC Step-Up (Boost) Conversion Circuits" **Proceedings of the IEEE International Conference PEDS'97**, 26–29 May 1997, Singapore, pp. 882–888.
39. Luo F. L. "Re-Lift Circuit, A New DC-DC Step-Up (Boost) Converter" **IEE – Electronics Letters**, Vol. 33, No. 1, 2 January 1997, pp. 5–7.
40. Luo F. L., Lee W. C., and Lee G. B., "Self-Lift Circuit, A New DC-DC Converter" **Proceedings of the 3rd National Undergraduate Research Programme (NURP), Congress 97**, Singapore, 13 September 1997, pp. 31–36.
41. Luo F. L. "DSP-Controlled PWM L-Converter Used for PM DC Motor Drives" **Proceedings of the IEEE International Conference SISCTA'97**, Singapore, 29–30 July 1997, pp. 98–102.
42. Luo F. L. "Luo-Converters, New DC-DC Step-Up Converters" **Proceedings of the IEE International Conference ISIC-97**, Singapore, 10–12 September 1997, pp. 227–230.
43. Luo F. L. and Ye H. "Synchronous and Resonant DC/DC Conversion Technology, Energy Factor and Mathematical Modeling" **Taylor and Francis Group LLC**, Boca Raton, Florida 07030, USA, October 2005. **ISBN: 0-8493-7237-2**.
44. Luo F. L. and Ye H. "Chapter 11 (32): D/A and A/D Converters" of Volume 2 of "Electrical Engineering Handbook" (Edited by R. C. Dorf) Third edition, **CRC Press LLC**, Boca Raton, Florida 07030, USA, September 2004. **ISBN: 0-8493-7339-5 (0-8493-2774-0)**.
45. Maksimovic D. and Cuk S. "A General Approach to Synthesis and Analysis of Quasi-Resonant Converters" **IEEE Transactions on PE**, Vol. 6, No. 1, January 1991, pp. 127–140.

46. Middlebrook R. D. and Cuk S. "Advances in Switched-Mode Power Conversion" Vols. I and II, **TESLAco**, Pasadena, CA, 1981.
47. Liu Y. and Sen P. C., "New Class-E DC-DC Converter Topologies with Constant Switching Frequency" **IEEE-IA Transactions**, Vol. 32, No. 4, July/August 1996, pp. 961–969.
48. Redl R., Molnar B., and Sokal N. O. "Class-E Resonant DC-DC Power Converters: Analysis of Operations, and Experimental Results at 1.5 MHz" **IEEE Transactions, Power Electronics**, Vol. 1, April 1986, pp. 111–119.
49. Kazimierczuk M. K. and Bui X. T. "Class-E DC-DC Converters with an Inductive Impedance Inverter" **IEEE Transactions, Power Electronics**, Vol. 4, July 1989, pp. 124–135.
50. Massey R. P. and Snyder E. C. "High Voltage Single-Ended DC-DC Converter" **IEEE PESC, 1977 Record**, pp. 156–159
51. Jozwik J. J. and Kazimerczuk M. K. "Dual Sepic PWM Switching-Mode DC/DC Power Converter" **IEEE Transactions on Industrial Electronics**, Vol. 36, No. 1, 1989, pp. 64–70.
52. Martins D. C. "Application of the Zeta Converter in Switch-Mode Power Supplies" **Proc. of IEEE APEC'93, USA**, pp. 214–220.
53. Kassakian J. G., Wolf H-C., Miller J. M. and Hurton C. J. "Automotive electrical systems, circa 2005" **IEEE Spectrum**, August 1996, pp. 22–27.
54. Wang J., Dunford W. G., and Mauch K. "Some Novel Four-Quadrant DC-DC Converters" **Proc. Of IEEE-PESC'98**, Fukuoka, Japan, pp. 1475–1482.
55. Luo F. L. "Double Output Luo-Converters" **Proceedings of the IEE International Conference IPEC'99**, Singapore, 24–26 May 1999, pp. 647–652.
56. Ye H. and Luo F. L. "Luo-Converters, A Series of New DC-DC Step-Up Conversion Circuits" **International Journal <Power Supply Technologies and Applications>**, Vol. 1, No. 1, April 1998, Xi'an, China, pp. 30–39.
57. Ye H. and Luo F. L. "Advanced Voltage Lift Technique – Negative Output Luo-Converters" **International Journal <Power Supply Technologies and Applications>**, Vol. 1, No. 3, August 1998, Xi'an, China, pp. 152–168.
58. Luo F. L. "Negative Output Luo-Converters – Voltage Lift Technique" **Proceedings of the Second world energy system International Conference WES'98**, Toronto, Canada, 19–22 May 1998, pp. 253–260.
59. Luo F. L. "Luo-Converters – Voltage Lift Technique" **Proceedings of the IEEE Power Electronics Special Conference IEEE-PESC'98**, Fukuoka, Japan, 14–22 May 1998, pp. 1483–1489.
60. Luo F. L. and Ye H. "Two-Quadrant DC/DC Converter with Switched Capacitors" **Proceedings of the International Conference IPEC'99**, Singapore, 24–26 May 1999, pp. 641–646.
61. Midgley D. and Sigger M. "Switched-capacitors in power control" **IEE Proc.**, Vol. 121, July 1974, pp. 703–704.
62. Cheong S. V., Chung H., and Ioinovici A. "Inductorless DC-DC Converter with high Power Density" **IEEE Trans. on Industrial Electronics**, Vol. 41, No. 2, April 1994, pp. 208–215.
63. Midgley D. and Sigger M. "Switched-capacitors in power control" **IEE Proc.**, Vol. 121, July 1974, pp. 703–704.
64. Chung H., Hui S. Y. R., and Tang S. C. "A low-profile Switched-capacitor-based DC/DC Converter" **Proc. of AUPEC'97**, October 1997, pp. 73–78.
65. Ngo K. D. T. and Webster R. "Steady-state Analysis and Design of a Switched-Capacitor DC-DC Converter" **IEEE Transactions on ANES**, Vol. 30, No. 1, January 1994, pp. 92–101.
66. Harris W. S. and Ngo K. D. T. "Power Switched-Capacitor DC-DC Converter: Analysis and Design" **IEEE Transactions on ANES**, Vol. 33, No. 2, April 1997, pp. 386–395.
67. Tse C. K., Wong S. C., and Chow M. H. L. "On Lossless Switched-Capacitor Power Converters" **IEEE Trans. on PE**, Vol. 10, No. 3, May 1995, pp. 286–291.
68. Luo F. L. and Ye H. "Energy Factor and Mathematical Modeling for Power DC/DC Converters" **IEE-EPA Proceedings**, Vol. 152, No. 2, March 2005, pp. 191–198.
69. Mak O. C., Wong Y. C., and Ioinovici A. "Step-up DC Power Supply Based on a Switched-capacitor Circuit" **IEEE Trans. on IE**, Vol. 42, No. 1, February 1995, pp. 90–97.
70. Mak O. C. and Ioinovici A. "Switched-capacitor Inverter with High Power Density and Enhanced Regulation Capability" **IEEE Trans. on CAS-I**, Vol. 45, No. 4, April 1998, pp. 336–347.
71. Luo F. L. and Ye H. "Switched Inductor Two-Quadrant DC/DC Converter with Fuzzy Logic Control" **Proceedings of IEEE International Conference PEDS'99**, Hong Kong, 26–29 July 1999, pp. 773–778.
72. Luo F. L. and Ye H. "Switched Inductor Two-Quadrant DC/DC Converter with Neural Network Control" **Proceedings of IEEE International Conference PEDS'99**, Hong Kong, 26–29 July 1999, pp. 1114–1119.
73. Liu K. H. and Lee F. C. "Resonant Switches – A Unified Approach to Improved Performances of Switching Converters," **International Telecommunications Energy Conference (INTELEC) Proc.**, New Orleans, LA, USA, 4–7 November 1984, pp. 344–351.
74. Liu K. H. and Lee F. C. "Zero-Voltage Switching Techniques in DC/DC Converter Circuits" **Power Electronics Specialist's Conf. (PESC) Record**, June 1986, Vancouver, Canada, pp. 58, 70.
75. Martinez Z. R. and Ray B. "Didirectional DC/DC Power Conversion Using Constant-Frequency Multi-Resonant Topology," **Applied Power Electronics Conf. (APEC) Proc.**, Orlando, FL, USA, 13–14 February 1994, pp. 991–997.
76. Pong M. H., Ho W. C., and Poon N. K. "Soft Switching Converter with Power Limiting Feature" **IEE-EPA Proceedings**, Vol. 146, No. 1, January 1999, pp. 95–102.
77. Gu W. J. and Harada K. "A Novel Self-Excited Forward DC-DC Converter with Zero-Voltage-Switched Resonant Transitions using a Saturable Core" **IEEE-PE Transactions**, Vol. 10, No. 2, March 1995, pp. 131–141.
78. Cho J. G., Sabate J. A., Hua G., and Lee F. C. "Zero-Voltage and Zero-Current-Switching Full Bridge PWM Converter for High Power Applications" **IEEE-PE Transactions**, Vol. 11, No. 4, July 1996, pp. 622–628.
79. Poon N. K. and Pong M. H. "Computer Aided Design of a Crossing Current Resonant Converter (XCRC)" **Proceedings of IECON'94**, Bologna, Italy, 5–9 September 1994, pp. 135–140.
80. Kassakian J. G., Schlecht M. F., and Verghese G. C. "Principles of Power Electronics" **Addison-Wesley**, New York, 1991, p. 214.